IN VITRO AND *IN VIVO* ELUCIDATION OF THE ROLE OF miRNAS IN THE APOPTOTIC PROPERTIES OF *BCL-XL*-SILENCED HUMAN LUNG ADENOCARCINOMA CELLS

NORAHAYU BINTI OTHMAN

FACULTY OF SCIENCE
UNIVERSITY OF MALAYA
KUALA LUMPUR

2017

IN VITRO AND *IN VIVO* ELUCIDATION OF THE ROLE OF miRNAS IN THE APOPTOTIC PROPERTIES OF *BCL-XL*-SILENCED HUMAN LUNG ADENOCARCINOMA CELLS

NORAHAYU BINTI OTHMAN

THESIS SUBMITTED IN FULFILMENT OF THE REQUIREMENTS FOR THE DEGREE OF DOCTOR OF PHILOSOPHY

INSTITUTE OF BIOLOGICAL SCIENCES
FACULTY OF SCIENCE
UNIVERSITY OF MALAYA
KUALA LUMPUR

2017

UNIVERSITY OF MALAYA

ORIGINAL LITERARY WORK DECLARATION

Name of Candidate: Norahayu Binti Othman

Matric No: SHC120082

Name of Degree: Doctor of Philosophy

Title of Project Paper/Research Report/Dissertation/Thesis ("this Work"): "*In vitro* and *in vivo* elucidation of the role of miRNAs in the apoptotic properties of *BCL-XL*-silenced human lung adenocarcinoma cells"

Field of Study: Molecular Oncology

I do solemnly and sincerely declare that:

(1) I am the sole author/writer of this Work;
(2) This Work is original;
(3) Any use of any work in which copyright exists was done by way of fair dealing and for permitted purposes and any excerpt or extract from, or reference to or reproduction of any copyright work has been disclosed expressly and sufficiently and the title of the Work and its authorship have been acknowledged in this Work;
(4) I do not have any actual knowledge nor do I ought reasonably to know that the making of this work constitutes an infringement of any copyright work;
(5) I hereby assign all and every rights in the copyright to this Work to the University of Malaya ("UM"), who henceforth shall be owner of the copyright in this Work and that any reproduction or use in any form or by any means whatsoever is prohibited without the written consent of UM having been first had and obtained;
(6) I am fully aware that if in the course of making this Work I have infringed any copyright whether intentionally or otherwise, I may be subject to legal action or any other action as may be determined by UM.

Candidate's Signature Date:

Subscribed and solemnly declared before,

Witness's Signature Date:

Name: Professor Dr. Noor Hasima Nagoor

Designation: Professor

ABSTRACT

Anti-apoptotic BCL-XL is frequently overexpressed in non-small cell lung cancer, leading to inhibition of apoptosis and poor prognosis. MicroRNAs play a role in regulating apoptosis and cell survival during tumourigenesis, with cancer cells showing perturbed expression of miRNAs. The aim of this study was to determine the biological effects of miRNA dysregulation on non-small cell lung cancer, and the molecular mechanisms by which apoptosis is regulated. Overexpression and knockdown studies were performed via transfection of miRNA mimics and inhibitors and cell death was detected using the annexin V-FITC detection kit and caspase 3/7 activity assay. Cell cycle analysis was also performed to determine the role candidate miRNAs play in cell growth. Results indicated that overexpression of miR-608 and down-regulation of miR-361-5p induced cell death in A549 and SK-LU-1 cells. Gene target prediction analysis implicated various signaling pathways as targets of *BCL-XL* induced miRNA alterations. Luciferase reporter assay identified *AKT2* and *SMAD2* as direct targets of miR-608 and miR-361-5p, respectively, and suppression of its protein levels were validated using Western blot. To elucidate the role and importance of these miRNAs *in vivo*, labeled tumour cells were injected into the yolk sac of zebrafish embryos and immunostained using monoclonal antibodies to detect the cleaved, active form of caspase 3. In conclusion, *BCL-XL* silencing in A549 and SK-LU-1 cells leads to the occurrence of apoptosis through the dysregulation of miR-608 and miR-361-5p, thus providing a platform for anti-sense gene therapy whereby miRNA expression can be exploited to increase the apoptotic properties in lung adenocarcinoma cells.

ABSTRAK

BCL-XL merupakan protein anti-apoptotik yang kerap dijumpai dalam kanser paru-paru yang menyebabkan perencatan apoptosis serta prognosis yang kurang baik. MicroRNAs (miRNAs) memainkan peranan dalam mengawal selia apoptosis dan kehidupan sel semasa tumorigenesis, dimana sel-sel kanser menunjukkan ungkapan miRNA terganggu. Tujuan kajian ini adalah untuk menentukan perubahan dalam ungkapan miRNA dalam sel-sel paru-paru adenokarsinoma, dan menentukan mekanisme molekul yang meregulasikan apoptosis. Kajian peningkatan dan perencatan ekspresi miRNA dilaksanakan melalui transfeksi miRNA mimik dan perencat, dan kematian sel dibuktikan menggunakan kit pengesanan annexin V-FITC dan cerakin aktiviti "caspase" 3/7. Analisis kitaran sel juga dilakukan untuk menentu peranan yang dimainkan oleh calon miRNA ini dalam dalam pertumbuhan sel. Keputusan menunjukkan bahawa peningkatan miR-608 dan perencatan miR-361-5p menyebabkan kematian sel-sel A549 dan SK-LU-1. Analisis ramalan sasaran gen membabitkan pelbagai laluan isyarat sebagai sasaran dari penginduksian perubahan miRNA oleh *BCL-XL*. Assay pelapor luciferase menunjukkan bahawa *AKT2* dan *SMAD2* adalah sasaran langsung untuk miR-608 dan miR-361-5p, masing-masing, dimana penindasan tahap protin AKT dan SMAD2 disahkan dengan menggunakan pemendapan Western. Untuk menjelaskan peranan miRNAs ini *in vivo*, sel-sel tumor berlabel telah disuntik ke dalam kantung kuning telur embrio zebrafish dan telah di "immunostain" menggunakan antibodi monoklonal untuk mengesahkan pembentukan "caspase" 3 aktif yang tersisih. Kesimpulannya, pelenyapan *BCL-XL* dalam sel-sel A549 dan SK-LU-1 menyebabkan apoptosis melalui perubahan ekspresi miR-608 dan miR-361-5p. Keputusan ini menyediakan platform untuk terapi gen "anti-sense" di mana ekspresi miRNA boleh dieksploitasi untuk meningkatkan ciri-ciri apoptosis dalam sel-sel paru-paru adenokarsinoma.

ACKNOWLEDGEMENTS

The completion of this project would not have been possible without the support of many people, who in one way or another has contributed and extended valuable assistance in the preparation and completion of this study. First and foremost, I would like to thank my project supervisor, Prof. Dr. Noor Hasima Nagoor, without whom the completion of this project would not be possible. I am grateful for her invaluable knowledge, and continuous guidance and support throughout the duration of this project.

My sincere gratitude goes to all members of the Cancer Research Lab for the numerous brainstorming sessions and endless support. I would also like to acknowledge Dr. Suzita Mohd. Noor for her valuable advice and training during the commencement of my *in vivo* study, as well as Puan Norlida Hussain and Puan Juraina Abdul Jamil for their technical assistance at the Institute of Biological Sciences (ISB) Central Lab and Tropical Infectious Diseases Research & Education Centre (TIDREC), respectively.

I would also like to thank University of Malaya for their utmost generosity for the scholarship I received, as well as for financing this project through the High Impact Research Grant (HIR) (UM.C/625/1/HIR/MOE/CHAN/016) and the Postgraduate Research Grant (PPP) (PG019-2016A).

Finally I would like to express my love and gratitude to my beloved family and friends for their patience and endless support throughout the duration of my studies. Thank you for keeping me motivated, the completion of this PhD would not have been possible without all of you. Most importantly, I would like to thank GOD, for all the blessings, patience, and strength to keep pushing forward. Thank You.

TABLE OF CONTENTS

LIST OF FIGURES

LIST OF TABLES

LIST OF SYMBOLS AND ABBREVIATIONS

α	:	Alpha
β	:	Beta
Δ	:	Delta
κ	:	Kappa
≈	:	Approximately
°	:	Degree
°C	:	Degree Celsius
<	:	Less than
≤	:	Less than or equal to
>	:	More than
≥	:	More than or equal to
+	:	Anode
−	:	Cathode
×	:	(i) Multiplication (ii) Times
#	:	Number
%	:	Percentage
±	:	Plus-minus
× *g*	:	Times gravity
µg	:	Microgram
µL	:	Microlitre
µm	:	Micrometer
µM	:	Micromolar
µS	:	Microseconds

3’	:	End of the molecule which terminates in a 3’ phosphate group
3’UTR	:	3’-untranslated region
5’	:	End of the molecule which terminates in a 5’ phosphate group
®	:	Registered
™	:	Trademark
(v/v)	:	Volume per Volume
(w/v)	:	Weight per Volume
$A_{260/230}$	:	Ratio of absorbance at 260 nm to absorbance at 230 nm
$A_{260/280}$	:	Ratio of absorbance at 260 nm to absorbance at 280 nm
AAALAC	:	Association for Assessment and Accreditation of Laboratory Animal Care
Ago2	:	Argonaute protein
AIF	:	Apoptosis inducing factor
AKT2	:	V-Akt murine thymoma viral oncogene homolog 2
ALL	:	Acute lymphoblastic leukemia
AML	:	Acute myeloid leukemia
AP-1	:	Activator protein 1
Apaf-1	:	Apoptosis protease-activating factor 1
APC	:	Adenomatous polyposis coli
APS	:	Ammonium persulfate
ARID1A	:	AT-rich interaction domain 1A
ASK	:	Apoptosis signal-regulating kinase group
ATF-2	:	Activating transcription factor 2
BAD	:	Bcl-2-associated agonist of cell death
BAK	:	Bcl-2 antagonist/killer
BAX	:	Bcl-2-associated protein X

BCA	:	Bicinchoninic acid
BCL-2	:	B-cell lymphoma-2
BCL-B	:	Bcl-2-like protein 10
BCL-W	:	Bcl-2-like protein 2
BCL-XL	:	B-cell lymphoma extra large
BFL-1	:	Bcl-2 related protein A1
BH	:	Bcl-2 homology
BID	:	BH3-interacting domain death agonist
BIM	:	Bcl-2-interacting mediator of cell death
BRAF	:	B-Raf proto-oncogene, serine/threonine kinase
BSA	:	Bovine serum albumin
c-Fos	:	Fos proto-oncogene, AP-1 transcription factor subunit
c-Jun	:	Jun proto-oncogene, AP-1 transcription factor subunit
c-Myc	:	v-Myc avian myelocytomatosis viral oncogene homolog
$CaCl_2$	:	Calcium chloride
CARIF	:	Cancer Research Initiative Foundation
CCD	:	Charged couple device
CCDC6	:	Coiled-coil domain containing 6
CCND2	:	Cyclin D2
CDC25A	:	Cell division cycle 25A
CDC42	:	Cell division cycle 42
CDE	:	Cell cycle-regulated repressor element
CDH1	:	E-cadherin
CDK	:	Cyclin dependent kinase
CDKI	:	Cyclin dependent kinase inhibitor
cDNA	:	Complementary DNA

CDX2	:	Caudal type homeobox 2
CER I	:	Cytoplasmic Extraction Reagent I
CER II	:	Cytoplasmic Extraction Reagents II
CHR	:	Cell cycle gene homology region
CLC	:	Cell lysis buffer
cm	:	Centimeter
CO_2	:	Carbon dioxide
Co-Smad	:	Common-mediator Smad
CSF1	:	Colony stimulating factor 1
CWC	:	Column wash solution
CXCR6	:	C-X-C chemokine receptor type 6
DAPK	:	Death associated protein kinase
DAVID	:	Database for annotation, visualization and integrated discovery
DDR2	:	Discoidin domain receptor 2
DED	:	Death effector domain
DEPC	:	Diethyl pyrocarbonate
DGCR8	:	DiGeorge syndrome critical region 8
dH_2O	:	Distilled H_2O
DIABLO	:	Direct inhibitor of apoptosis protein (IAP)-binding protein with low PI
Dill	:	1,1'-Dioctadecyl-3,3,3',3'-Tetramethylindocarbocyanine Perchlorate
DISC	:	Death inducing signaling complex
Dkk-1	:	Dickkopf WNT signaling pathway inhibitor 1
DLBCL	:	Diffuse large B-cell lymphoma
DMSO	:	Dimethyl sulfoxide
DNA	:	Deoxyribonucleic acid

DPBS	:	Dulbecco's phosphate-buffered saline
Dpf	:	Days post-fertilization
Dsh	:	Disheveled
DTT	:	Dithiothreitol
E2F	:	Retinoblastoma-associated protein
EBB	:	Elution buffer
EDTA	:	Ethylenediaminetetraacetic acid
EGF	:	Epidermal growth factor
EGFR	:	Epidermal growth factor receptor
EMT	:	Epithelial-to-mesenchymal
EPO	:	Erythropoietin
ERB	:	Endotoxin removal wash
ERK	:	Extracellular signal–regulated kinases
ESCC	:	Esophageal squamous cell carcinoma
Ets	:	Erythroblastosis virus E26 (v-Ets) oncogene homolog
FADD	:	Fas-associated death domains
FasL	:	Fas ligand
FBS	:	Fetal bovine serum
FDA	:	Food and Drug Administration
FGFR1	:	Fibroblast growth factor receptor 1
FITC	:	Fluorescein isothiocyanate
FKHR	:	Forkhead
FLIP	:	FLICE (FADD-like IL-1β-converting enzyme)-inhibitory protein
FOM	:	Faculty of Medicine
FZD8	:	Frizzled-8
GADD45	:	Growth arrest and DNA damage inducible alpha

GEF	:	Guanine nucleotide exchange factor
GM-CSF	:	Granulocyte macrophage-colony stimulating factor
GSK-3β	:	Glycogen synthase-kinase-3-beta
h	:	Hours
H_2O	:	Water
HCl	:	Hydrogen chloride
HER2	:	v-Erb-B2 avian erythroblastic leukemia viral oncogene homolog 2
HER4	:	v-Erb-B2 avian erythroblastic leukemia viral oncogene homolog 4
HMGA2	:	High mobility group AT-hook 2
hPa	:	Hectopascal
HPC	:	Hypopharynx cancer
Hpf	:	Hours post-fertilization
Hpi	:	Hours post-injection
HRP	:	Horseradish peroxidase
HtrA2	:	High temperature requirement protein A
IACUC	:	Institutional Care of Use Committee
IARC	:	International Agency for Research on Cancer
IDH	:	Isocitrate dehydrogenase
IEX-1	:	Immediately early gene X-1
IGF	:	Insulin-like growth factor
IgG	:	Immunoglobulin G
IκB	:	Inhibitor of NFκB
IKK	:	Inhibitor of NFκB (IκB) kinase
IMS	:	Intermembrane space
JNK	:	c-Jun N-terminal kinase
kb	:	Kilobase

KCl	:	Potassium chloride
kDa	:	Kilodalton
KH_2PO_4	:	Potassium dihydrogen phosphate
KRAS	:	v-K-ras2 Kirsten rat sarcoma viral oncogene homolog
L	:	Liter
LB	:	Lysogeny broth
LNA	:	Locked nucleic acid
LOH	:	Loss of heterozygosity
mA	:	Milliampere
MAP2K	:	MAP kinase
MAP3K	:	MAPK kinase kinase
MAPK	:	Mitogen-activated protein kinase
MCC	:	Merkel cell carcinoma
MCL-1	:	Induced myeloid leukemia cell differentiation protein
MCV	:	Merkel cell polyomavirus
MDM2	:	Mouse double minute 2 homolog
MEK	:	MAP kinase
MEKK	:	Mitogen-activated protein kinase kinase kinase 1, E3 ubiquitin protein ligase group
MEM	:	Minimum essential medium
MeOH	:	Methanol
MET	:	Hepatocyte growth factor receptor
mg	:	Milligram
$MgCl_2$	:	Magnesium chloride
MIF	:	Macrophage migration inhibitory factor
Min	:	Minutes

MiRNA	:	MicroRNA
ml	:	Milliliter
MLK	:	Mixed lineage kinase
mm	:	Millimeter
MOMP	:	Mitochondrial outer membrane permeabilization
MTT	:	3-(4,5-dimethylthiazol-2-yl)-2,5-diphenltetrazolium bromide
Na_2HPO_4	:	Disodium hydrogen phosphate
NAA10	:	N-a-acetyltransferase 10 protein
NaCl	:	Sodium chloride
NaOH	:	Sodium hydroxide
NCBI	:	National Center for Biotechnology Information
NER	:	Nuclear extraction reagent
NFAT	:	Nuclear factor of activated T cells
NFκB	:	Nuclear factor of light polypeptide gene enhancer in B cells
nm	:	Nanometer
nM	:	Nanomolar
NSC	:	Neutralization Solution
NSCLC	:	Non-small cell lung cancer
OD_{260}	:	Optical density at 260 nm
OD_{280}	:	Optical density at 280 nm
OSCC	:	Oral squamous cell carcinoma
OTA	:	Oral tongue adenocarcinoma
OTSCC	:	Oral tongue squamous cell carcinoma
p16/CDKN2A	:	Cyclin-dependent kinase inhibitor 2A, multiple tumor suppressor 1
p21	:	Cyclin dependent kinase inhibitor 1A
p53	:	Tumor protein p53

PARP	:	Poly (ADP-ribose) polymerase
PBS	:	Phosphate buffered saline
PBST	:	PBS with Tween 20
P_c	:	Compensation pressure
PCR	:	Polymerase chain reaction
PDCD4	:	Programmed cell death protein 4
PDGF	:	Platelet-derived growth factor
PDGFR	:	Platelet derived growth factor receptor
PDK1	:	3-phosphoinositide-dependent protein kinase-1
PDT	:	PBST with Triton X and DMSO
PFA	:	Paraformaldehyde
pg	:	Picogram
PH	:	Plekstrin homology
pH	:	Potential of hydrogen
P_i	:	Injection pressure
PI	:	Propidium iodide
PI3K/AKT	:	Phosphatidylinositol 3-kinase/protein kinase B
PIK3CA	:	Phosphatidylinositol-4,5-bisphosphate 3-kinase catalytic subunit alpha
PIP_2	:	Phosphatidylinositol-3,4-biphosphase
PKB	:	Protein kinase B
PORC	:	Porcupine
Pre-miRNA	:	Precursor miRNA
Pri-miRNA	:	Primary miRNA
PS	:	Phosphatidylserine
PTU	:	1-phenyl 2-thiourea

PTEN	:	Phosphatase and tensin homolog
qPCR	:	Quantitative polymerase chain reaction
qRT-PCR	:	Quantitative reverse transcription polymerase chain reaction
R-Smads	:	Receptor-regulated Smad
Rac1	:	Ras-related C3 botulinum toxin substrate 1
Rb	:	Retinoblastoma
RIN	:	RNA integrity number
RISC	:	RNA-induced silencing complex
RNA	:	Ribonucleic acid
RPM	:	Rotations per minute
RPMI-1640	:	Roswell Park Memorial Institute 1640 medium
RT-PCR	:	Reverse transcription polymerase chain reaction
RT-qPCR	:	Reverse transcription-quantitative real-time polymerase chain reaction
RUNX3	:	Runt related transcription factor 3
SAPK	:	Stress-activated protein kinases
SCC	:	Squamous cell carcinoma
SCLC	:	Small cell lung cancer
SD	:	Standard deviation
SDS	:	Sodium dodecyl sulfate
SDS-PAGE	:	Sodium dodecyl sulphate polyacrylamide gel electrophoresis
Sec	:	Seconds
Ser112	:	Serine-112
Ser136	:	Serine-136
Ser166	:	Serine-166
Ser184	:	Serine-184

Ser186	:	Serine-186
siRNA	:	Short interfering RNA
siRNA NC	:	Scrambled negative control siRNA
Smac	:	Second mitochondria derived activator of caspase
SMAD2	:	Mothers Against Decapentaplegic Homolog 2
SND1	:	Staphylococcal nuclease domain containing-1
SNPs	:	Single nucleotide polymorphisms
STAT6	:	Signal transducer and activator of transcription 6
TAE	:	Tris base/ acetic acid/ EDTA
TAK1	:	Transforming growth factor-beta activated kinase 1
tBID	:	Truncated BID
TBS	:	Tris-buffered saline
TBST	:	Tris-buffered saline with Tween20
TCF-4	:	Transcription factor 4
Tcf/Lef	:	T-cell factor/lymphocyte enhancer factor
TE	:	Tris/EDTA
TEMED	:	Tetramethyl-ethylenediamine
TGF-βRI	:	Transforming growth factor, beta-receptor I
TGF-βRII	:	Transforming growth factor, beta-receptor II
TGFβ	:	Transforming growth factor, beta
TGS	:	Tris/Glycine/SDS
Thr18	:	Threonine-18
Thr125	:	Threonine-125
Thr163	:	Threonine-163
Thr308	:	Threonine-308
t_i	:	Injection time

TIEG1	:	TGF-beta early-response gene
TIMP3	:	Tissue inhibitor of metalloproteinases 3
TNF	:	Tumour necrosis factor
TNFR1	:	Tumour necrosis factor receptor 1
TPM1	:	Tropomyosin 1
TRADD	:	TNF receptor-associated death domain
TRAIL	:	TNF-related apoptosis-inducing ligand
TRAILR1	:	TNF-related apoptosis-inducing ligand, receptor 1
TRAIL-R2	:	TRAIL receptor 2
TRBP	:	Transactivating response RNA-binding protein
Tris-HCl	:	Tris hydrochloride
VEGF	:	Vascular endothelial growth factor
VIM	:	Vimentin
WIF-1	:	WNT inhibitory factor 1
WNT	:	Wingless-type MMTV integration site family
XIAP	:	X-linked inhibitor of apoptosis protein
Y22	:	Tyrosine 22
ZEB	:	Zinc finger E-box-binding homeobox

LIST OF APPENDICES

CHAPTER 1: INTRODUCTION

The most common cancer worldwide, remains to be lung cancer (Ferlay *et al.*, 2013). In Malaysia, lung cancer led to the most cancer deaths in the country in 2012, making up 19.1% of total cancer deaths, with adenocarcinoma being the most common cell type (Ferlay *et al.*, 2012). When possible, the most effective option for treatment of lung cancer is surgical resection (Molina *et al.*, 2008). As a majority of lung cancer patients are diagnosed at an advanced or metastatic stage of disease, the most favorable form of treatment is chemotherapy and/or simultaneous administration of radiation and chemotherapy (Pfister *et al.*, 2004). However, even with treatment, the 5-year survival rate in lung cancer remains to be very low at only 17.7% (Howlader, 2017a), with late stage diagnosis and high incidence of drug resistance being the main contributors to low survival rates.

Apoptosis plays a crucial role in the development and maintenance of multicellular organisms through the elimination of cells that are damaged, aged or autoimmune (Sorenson, 2004). Cancer cells have the ability to disrupt the balance between pro- and anti-apoptotic factors, thereby making evasion of apoptosis an important hallmark of tumour progression. The B-cell lymphocyte 2 (BCL-2) family of proteins are the central regulators of apoptosis (Daniel & Smythe, 2004). Studies have demonstrated that anomalous patterns of BCL-2 expression was found in a wide variety of human cancers (Hockenbery *et al.*, 1991). However, studies conducted on non-small cell lung cancer (NSCLC), which accounts for the majority of lung cancer cases (Liam *et al.*, 2006), have shown that the expression of BCL-2 is either very low or even absent (Daniel & Smythe, 2004). Instead, the expression of B-cell lymphocyte xL (BCL-XL), the other major prototype of the anti-apoptotic *BCL-2* gene, is shown to be overexpressed in NSCLC (Soini *et al.*, 1999). BCL-XL over-expression counteracts the pro-apoptotic

functions of Bcl-2 associated X protein (BAX) and Bcl-2 associated death promoter (BAD) through the inhibition of their translocation from the cytosol to the mitochondria. Apoptosis is thereby obstructed through the maintenance of the permeability status or stabilization of the outer mitochondrial membrane, which in turn prevents the release of cytochrome c and pro-caspase 9 activation (Gottlieb *et al.*, 2000).

MicroRNAs (miRNAs) are a subset of non-coding RNAs of about 19 to 23 nucleotides long which regulate gene expression post-transcriptionally via inhibition of mRNA translation through the direct binding of particular targets sites in the 3'-untranslated region (3'UTR), or by stimulation of target mRNA degradation through cleavage (Bartel, 2004). Individual miRNAs are able to regulate the expression of multiple genes; correspondingly a single target can be modulated my many miRNAs (Lewis *et al.*, 2005). These regulatory elements play a role in a wide range of biological processes including apoptosis (Mott *et al.*, 2007). A disturbed miRNA function or altered miRNA expression has been reported to disorganize cellular processions and may eventually contribute to human diseases, including cancer (Calin *et al.*, 2004a). MiRNAs have the ability to influence the development of cancer through the manipulation of the apoptotic process (Jovanovic & Hengartner, 2006; Lima *et al.*, 2011). The expression of miRNAs can be either up-regulated or down-regulated, and studies have demonstrated that dysregulated miRNAs can act as oncogenes or tumour suppressor genes in lung cancers (Volinia *et al.*, 2006; Son, 2009).

In my Masters project, miRNA microarrays were utilized to determine the expression of miRNA dysregulated in response to *BCL-XL* silencing in A549 cells and to determine their involvement in regulation of apoptosis. A total of ten miRNAs were found to be significantly differentially expressed when compared between siRNA-transfected and non-transfected cells. These miRNAs were found to have putative gene targets in

various signal transduction pathways including the PI3K/AKT, WNT, TGF-β and ERK pathways.

The expression of miRNAs has frequently been identified to be dysregulated in cancers, however, due to non-specific binding properties of each individual miRNAs, their specific functions remain to be unclear. This study is an extension of my Masters project, with validation of the expression of the dysregulated miRNAs in a second lung adenocarcinoma cell line, SK-LU-1. As the characteristics of A549 and SK-LU-1 cells are similar, it is hypothesized that the biological effects, as well as regulation of miRNA expression, in response to anti-apoptotic BCL-XL, in these two cell lines, will be comparable. As miRNA studies continue to be developed, it is crucial to obtain an in-depth understanding of miRNA biogenesis and function, as it will certainly affect the improvement of miRNA-based therapies. Therefore, further analysis will be performed on the candidate miRNAs to determine their biological functions. Animal studies using zebrafish embryos will then be performed to determine the *in vivo* effects of miRNA regulation on apoptosis.

Objectives

1) To determine the change in expression of miRNAs in lung adenocarcinoma cancer cells regulated by the anti-apoptotic protein BCL-XL
2) To predict and identify the targets of selected candidate miRNAs dysregulated in lung adenocarcinoma cells.
3) To identify experimentally validated miRNA gene targets through overexpression or silencing studies on candidate miRNA.
4) To investigate and determine the effects of miRNA regulation on downstream mRNA and protein expression.
5) To observe the effects of candidate miRNA on *in vivo* regulation of apoptosis.

CHAPTER 2: LITERATURE REVIEW

2.1 Cancer

Cancer is a genetic disease that is characterized by the transformation of normal cells to a neoplastic state. This progression is enabled through the acquisition of various hallmark capabilities that allows cells to become tumourigenic and ultimately malignant, as illustrated in Figure 2.1 (Hanahan & Weinberg, 2011). These distinctive and complementary capabilities that facilitate tumour growth and metastatic dissemination include sustaining proliferative signaling, evasion of growth suppressors, avoidance of immune destruction, enabling replicative immortality, tumour-promoting inflammation, activation of invasion and metastasis, inducing angiogenesis, resistance to cell death, deregulation of cellular energetics, and genome instability and mutation (Hanahan & Weinberg, 2011).

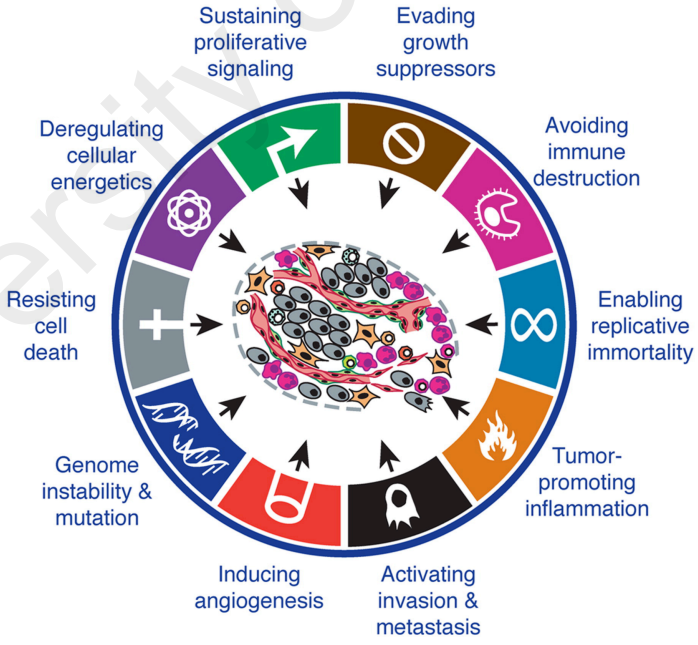

Figure 2.1: The hallmarks of cancer (Reproduced from Cell, Vol. 144, Hanahan & Weinberg, Hallmarks of Cancer: The Next Generation, 646-674, 2011, with permission from Elsevier).

2.1.1 Cancer statistics

According to GLOCOBAN, a Windows based software which provides access to global cancer incidence and mortality rates, there are about 14.1 million new cancer cases (within 5 years of diagnosis), 8.2 million cancer deaths and 32.6 million people living with cancer in 2012 worldwide (Ferlay *et al.*, 2013). Lung cancer remains to be the most common cancer worldwide, in both sexes combined, with an estimated 1.8 million new cases in 2012 (12.9% of the total cancer cases), followed by breast cancer (1.67 million new cases in 2012) and colorectum cancer (746,000 new cases in men and 614,000 new cases in females) (Ferlay *et al.*, 2013). As highlighted in Figure 2.2, the most common cancer site for males, in Malaysia, in the year 2012, was lung (17.9% incidence) followed by colorectum (14.1% incidence) and prostate (6.5). In females, the most common cancer site was breast (28.0% incidence), with cervix uteri (11.1% incidence) and colorectum (10.2% incidence) followed by lung (6.0% incidence) (Ferlay *et al.*, 2012).

Lung cancer led to the most cancer deaths worldwide with 1,098,606 deaths in males and females combined, accounting for 23.6% of the total deaths caused by cancer (Ferlay *et al.*, 2012). Similarly, in Malaysia, lung cancer led to the most cancer deaths in the country in 2012, making up 19.1% of total cancer deaths, followed by breast cancer (11.9% of total cancer deaths) and colorectum cancer (10.6% of total cancer deaths) (Ferlay *et al.*, 2012).

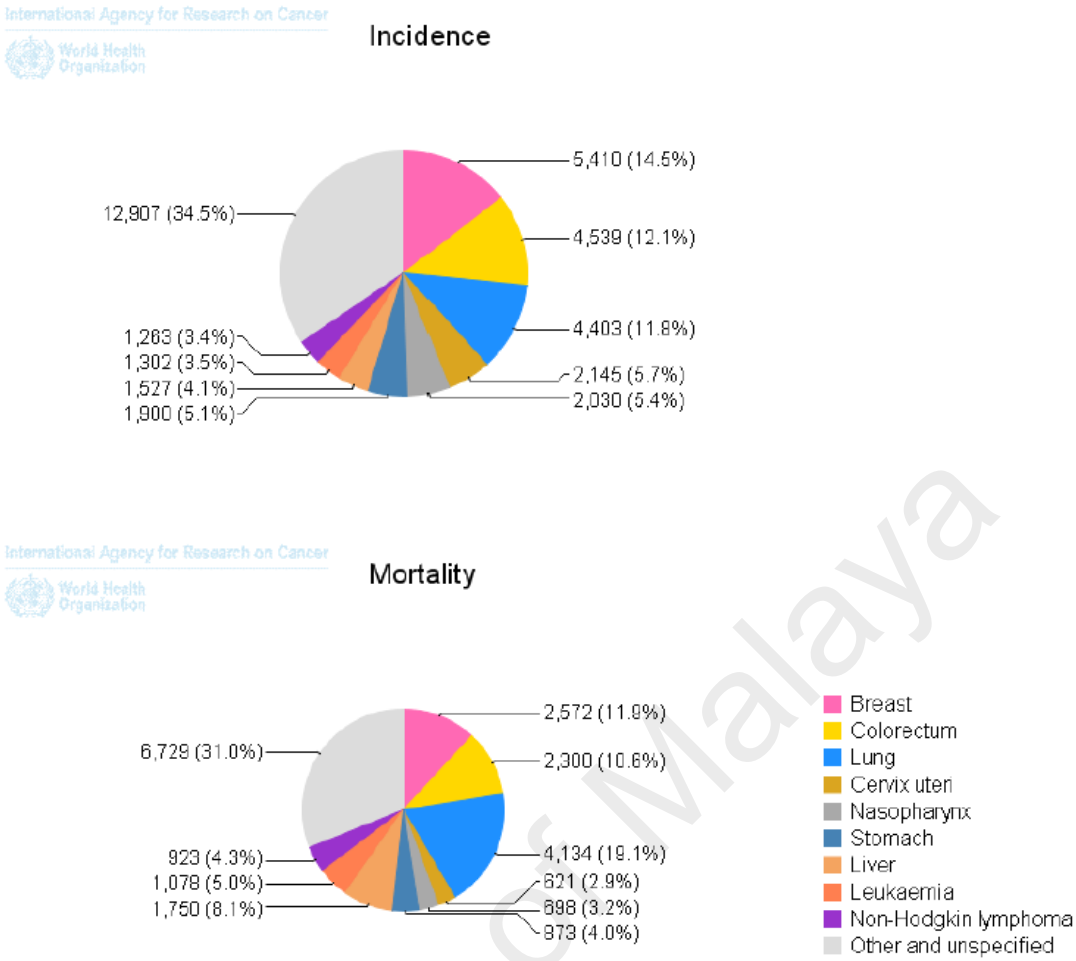

Figure 2.2: Malaysian population's incidence and mortality of cancers in males and females combined, in 2012 (Reproduced with permission from Ferlay *et al*. GLOBOCAN 2012 v1.0, Cancer Incidence and Mortality Worldwide: IARC CancerBase No. 11 [Internet]. Lyon, France: International Agency for Research on Cancer; 2013. Available from: http://globocan.iarc.fr, accessed May 26, 2017).

2.2 Lung cancer

Lung cancer is characterized by uncontrolled cell growth in the tissues of the lungs (Howlader, 2017a), and can be categorized into two main groups: small cell lung cancer (SCLC) and non-small cell lung cancer (NSCLC). SCLC accounts for about 15% of lung cancer cases and is a highly malignant tumour, while NSCLC makes up the remaining 85% of cases and can be further grouped into 3 major pathologic subtypes: adenocarcinoma, squamous cell carcinoma and large cell carcinoma (Dela Cruz *et al.*, 2011). Adenocarcinoma is the most common NSCLC subtype accounting for 38.5% of all lung cancer cases, while squamous cell carcinoma accounts for 20.0% and large cell carcinoma 2.9% (Howlader, 2017b).

2.2.1 Etiology of lung cancer

There are various factors that may increase the risk of lung cancer, and they can be grouped into two broad categories: factors inherent to the individual (intrinsic factors) and factors extraneous to the individual (extrinsic or environmental factors) (Ruano-Ravina *et al.*, 2003). Intrinsic factors include genetic susceptibility, family history of cancer, gender, race, age, and previous respiratory diseases, whereas the extrinsic factors include use of tobacco, diet and obesity, occupational and environmental air pollution (Ruano-Ravina *et al.*, 2003; Dela Cruz *et al.*, 2011).

The use of tobacco remains to be the principal risk factor for lung cancer. Tobacco smoke was suspected to be linked to lung cancer as early as the 1920's, and a case-control study was published in 1940 in Germany that reported for the first time that tobacco use was the single most important source of increase in lung cancer incidence (Müller, 1940). Today, tobacco smoking accounts for approximately 90% of male lung cancer deaths and 75-80% of female lung cancer deaths in the United States (Shopland, 1995). Due to the complexity of tobacco smoke there is still some unknowns regarding the mechanism by which it causes lung cancer. However, to date, among the multiple components of tobacco smoke, at least 50 carcinogens have been identified by the International Agency for Research on Cancer (IARC) (Hoffmann & Hoffmann, 1997). Polycyclic aromatic hydrocarbons and nicotine-derived nitroso-aminoketone are the most well known carcinogens found in tobacco smoke, and they have been reported to lead to genetic mutations through DNA adduct formation (Hecht, 1999).

While all subtypes of lung cancer are associated with tobacco smoking, the strongest association is with SCLC and squamous cell carcinoma. In contrast adenocarcinoma is more common in non-smokers, which refers to those who have never smoked in their lifetime or those who have smoked less than 100 cigarettes in their lifetime (Gabrielson, 2006; Sun *et al.*, 2007). The principal key risk factors in non-smokers include secondhand smoke, radon exposure, environmental exposures, history of lung disease, and genetic factors (Samet *et al.*, 2009).

Familial aggregation of lung cancer has been observed frequently in the past 60 years. This implies a hereditary base to the development of this disease (Sellers & Yang, 2002). For example, Bailey-Wilson and colleagues reported the first association of familial lung cancer to a region on chromosome 6q23-25 in 2004 (Bailey-Wilson *et al.*, 2004). A history of smoking in addition to this inheritance was found to be associated with a three-fold increase risk for lung cancer (Bailey-Wilson *et al.*, 2004). Studies have also demonstrated that carriers of TP53 germline sequence variations who also smoked was found to be three times more likely to develop lung cancer than carriers who do not smoke (Hwang *et al.*, 2003). Furthermore, T790M sequence variation in germline epidermal growth factor (EGF) was reported in a family with multiple cases of NSCLC (Li & Hemminki, 2004). Therefore, it is clear that susceptibility to lung cancer is determined in part by host genetic factors. These findings could thus be utilized for the design of early detection and treatment of lung cancers in patients with inherited cancer predisposition.

2.2.2 Pathogenesis of lung cancer

Development of lung cancer occurs through a multi-step process that involves the acquisition of numerous genetic and epigenetic changes, especially the activation of growth promoting pathways and silencing of tumour suppressor pathways (Fong *et al.*, 1999). Genetic and epigenetic changes would in turn cause dysregulation of molecular signal transduction pathways, which can regulate cell proliferation, differentiation and apoptosis, directly or indirectly (Kitamura *et al.*, 2008). The stimulation of growth promoting oncogenes can arise through gene amplification, point mutations or structural rearrangements that lead to uncontrolled signaling (Fong *et al.*, 1999). Growth promoting protein such as V-Ki-ras2 Kirsten rat sarcoma viral oncogene homolog (KRAS) is found to be frequently activated by point mutations in approximately 20% of lung adenocarcinomas but rarely exhibited in SCLCs (Rodenhuis & Slebos, 1992; Riely *et al.*, 2008; Schmid *et al.*, 2009). Constitutive activation of KRAS may result in inappropriate extended signaling for continued cell division (Richardson & Johnson, 1993).

Mutation in the activation of the epidermal growth factor receptor (*EGFR*) is also observed in NSCLC cells, most frequently in lung adenocarcinoma, although they may also be seen in squamous cell carcinomas (Kosaka *et al.*, 2004; Shigematsu *et al.*, 2005; Ohtsuka *et al.*, 2007). Mutations of *EGFR* in NSCLC normally appear in the first four exons of the tyrosine kinase domain, most frequently exon 19 frame deletions (Tam *et al.*, 2006). *EGFR* plays a role in the regulation of various oncogenic processes including cell proliferation, survival, differentiation, neovascularization, invasion, and metastasis (Yarden & Sliwkowski, 2001), and a mutant *EGFR* has been reported to have enhanced tyrosine kinase activity (Sordella *et al.*, 2004). Other, less common, somatic mutations have also been reported in other *EGFR* pathway genes including v-Erb-B2 avian erythroblastic leukemia viral oncogene homolog 2 (*HER2*) (Shigematsu *et al.*, 2005)

and homolog 4 (*HER4*) (Soung *et al.*, 2006), B-Raf proto-oncogene, serine/threonine kinase (*BRAF*) (Naoki *et al.*, 2002) and phosphatidylinositol-4,5-bisphosphate 3-kinase catalytic subunit alpha (*PIK3CA*) (Samuels *et al.*, 2004; Yamamoto *et al.*, 2008).

Inactivation of tumour suppressor p53 is the most significant genetic abnormality in lung cancer occurring in approximately 90% of SCLC and 50% of NSCLC (Takahashi *et al.*, 1989; Greenblatt *et al.*, 1994; Bennett *et al.*, 1999), usually through missense mutations within the DNA-binding domain (D'Amico *et al.*, 1992). In response to DNA damage, p53 maintains genomic integrity through regulation of downstream genes including cyclin dependent kinase inhibitor 1A (*p21*), mouse double minute 2 homolog (*MDM2*), growth arrest and DNA damage inducible alpha (*GADD45*) and BCL2 associated X, apoptosis regulator (*BAX*), to help regulate the G_1/S cell cycle transition, G_2/M DNA damage checkpoint and apoptosis (Fong *et al.*, 1999). Therefore, a dysregulation of p53 expression in lung cancer will allow for continued survival of genetically damaged cells, thus leading to accumulation of numerous mutations and consequent evolution of cancer cells (Fong *et al.*, 1999).

Other alterations that occurs in lung cancer is the inactivation of tumour suppressor genes, such as, retinoblastoma (*Rb*) (Kaye, 2002; Wikman & Kettunen, 2006), phosphatase and tensin homolog (*PTEN*) (Marsit *et al.*, 2005; Jin *et al.*, 2010) and cyclin-dependent kinase inhibitor 2A, multiple tumor suppressor 1 (*p16/CDKN2A*) (Otterson *et al.*, 1994; Brambilla *et al.*, 1999), as well as, amplification of oncogenes, such as, fibroblast growth factor receptor 1 (*FGFR1*) (Dutt *et al.*, 2011; Tran *et al.*, 2013), discoidin domain receptor 2 (*DDR2*) (Hammerman *et al.*, 2011), retinoblastoma-associated protein 1 (*E2F*) (Eymin *et al.*, 2001; Cooper *et al.*, 2006) and v-Myc avian myelocytomatosis viral oncogene homolog (c-*MYC*) (Johnson *et al.*, 1987; Johnson *et al.*, 1996). Therefore, the identification of genetic alterations in lung cancer that lead to stimulation or inactivation of oncogenes and tumour suppressor genes, respectively, can potentially offer further opportunities in development of therapeutics.

2.2.3 Treatment of lung cancer

When possible, the most reliable and successful option for cure of lung cancer patients is surgical resection (Molina *et al.*, 2008). Lobectomy, in which the entire lobe that contains the tumour is removed, is the most common surgical procedure. Patients who cannot tolerate an extensive procedure normally undergo limited resections, such as, wedge resections, though they are associated with an increased risk of local recurrence. In cases of extensive disease, a total pneumonectomy (removal of an entire lung) may be required (Ginsberg *et al.*, 1983). However, as almost 70% of patients are diagnosed at an advanced or metastatic stage of disease, the most beneficial form of treatment becomes chemotherapy and/or simultaneous administration of radiation and chemotherapy (Pfister *et al.*, 2004). Even with treatment, the 5-year survival rate for lung cancer is very low at 17.7% (Howlader *et al.*, 2017b), with late stage diagnosis and high incidence of drug resistance being the main contributors to low survival rates.

With an increase in comprehension of the biology of cancer, abundant potential therapeutic strategies has been revealed, including the targeting of signal transduction and angiogenesis pathways known to be dysregulated in lung cancer. Targeted therapy drugs are often used in combination with chemotherapy drugs. For example, EGFR is overexpressed in 40-80% of NSCLC patients, and its overexpression is correlated with poor prognosis (Mendelsohn & Baselga, 2003). The first targeted therapy for lung cancer to be registered and approved by the Food and Drug Administration (FDA) was gefitinib, an EGFR inhibitor (Kris *et al.*, 2003). However, findings from two phase 3 randomized trials of gefitinib comparing daily dosage of 250 mg of the drug versus placebo did not show a survival benefit (Thatcher *et al.*, 2005). Another EGFR inhibitor, erlotinib, has been approved by FDA for patients with locally advanced or metastatic NSCLC who have not responded to previous rounds of therapy (Shepherd *et al.*, 2004). The rate of response to erlotinib in comparison with placebo was found to be statistically significant at 8.9% with a average survival rate of 6.7 months (Shepherd *et al.*, 2004). In another trial, bevacizumab, which targets vascular endothelial growth factor (*VEGF*) in combination with chemotherapy, was found to significantly increase survival rates for patients with advanced non-squamous NSCLC and was thus approved by FDA in 2005 (Sandler *et al.*, 2005).

2.3 Apoptosis

Apoptosis is programmed cell death that plays an essential role in normal development and tissue homeostasis through the elimination of damaged, aged or autoimmune cells (Kerr *et al.*, 1972). The process of apoptosis, regulated by intracellular and/or extracellular signals, is characterized by morphological hallmarks, which include chromatin condensation, nuclear fragmentation, cell shrinkage, membrane blebbing, and the formation of apoptotic bodies (Nicholson, 1999; Hengartner, 2000). Proper apoptotic signaling is crucial for maintaining the balance

between cell survival and cell death, thus dysregulation of apoptosis can contribute to human diseases, including cancer (Reed, 1999). Apoptosis evasion is a prominent hallmark of cancer and the mechanism by which this can occur includes disruption of the balance between pro-apoptotic and anti-apoptotic proteins, decreased caspase function, and compromised signaling of death receptors (Hanahan & Weinberg, 2000). Therefore, current cancer therapies, such as, chemotherapy, gamma-irradiation, immunotherapy or targeted gene therapy largely exercises their anti-tumour effect by stimulating apoptosis in cancer cells (Makin & Dive, 2001; Fulda & Debatin, 2004).

2.3.1 Caspase cascade

Apoptosis is primarily executed by a group of enzymes called caspases (cysteinyl aspartate-specific proteases), which belong to the cysteine protease family (Thornberry & Lazebnik, 1998; Li & Yuan, 2008). Caspases are sub-classified based on their mechanism of action and are either initiator caspases (caspase 8 and 9) or effector caspases (caspase 3, 6, and 7) (McIlwain *et al.*, 2013). Upon receiving pro-apoptotic signals, initiator caspases, which exists as inactive pro-caspase monomers, are recruited to oligomeric complexes by activating adaptor proteins, which stimulates dimerization (Muzio *et al.*, 1998; Degterev *et al.*, 2003). Dimerization enables the autocatalytic cleavage of caspase monomers into a p20 and p10 heterotetramer, resulting in stabilization of the dimer (Muzio *et al.*, 1998). In turn, the activated initiator caspases will activate effector caspases, to cleave downstream key proteins to induce biochemical and morphological changes specific to apoptotic cells (Degterev *et al.*, 2003; Luthi & Martin, 2007; Pop & Salvesen, 2009). This caspase cascade can be activated by either the intrinsic (or mitochondrial) or the extrinsic (or death receptor) pathways of apoptosis (Figure 2.3). These two pathways will ultimately merge to a common pathway termed the execution phase of apoptosis (Orrenius *et al.*, 2003; Elmore, 2007).

2.3.2 Intrinsic (mitochondrial) pathway

The intrinsic pathway of apoptosis is activated by various stress stimuli including UV radiation, gamma radiation, growth-factor deprivation, DNA damage, and activation of oncogenic factors (Kroemer, 2002; Green & Kroemer, 2004). Multiple intracellular components will recognize these stressors and convey the message to the mitochondria, resulting in mitochondrial outer membrane permeability (MOMP) (Zou *et al.*, 1999; Garrido *et al.*, 2006). Disruption of the outer mitochondrial membrane will result in the diffusion of various proteins normally found in the mitochondrial intermembrane space (Grimson *et al.,* 2007) into the cytosol, such as, cytochrome c, second mitochondria derived activator of caspase (SMAC)/ direct inhibitor of apoptosis protein (IAP)-binding protein with low PI (DIABLO), Omi/High temperature requirement protein A (HTRA2), apoptosis inducing factor (AIF), and endonuclease G (Cande *et al.*, 2004; Saelens *et al.*, 2004; Kroemer *et al.*, 2007). Cytochrome c will form a complex with apoptosis protease-activating factor 1 (APAF-1) and dATP, to result in the dimerization and subsequent activation of pro-caspase 9 (Li *et al.*, 1997; Pop *et al.*, 2006). Caspase 9, an initiator caspase, in turn activates effector caspases that cleave multiple cellular proteins (Singh, 2007). At the same time, SMAC/DIABLO and OMI/HTRA2 enhances the activation of caspases through the alleviation of the inhibitor effects of IAPs (Saelens *et al.*, 2004; Garrido *et al.*, 2006). The central regulators of the mitochondrial pathway are a group of proteins that belong to the BCL-2 family.

Dysregulation of the intrinsic pathway has been reported in lung cancer. For example, decreased expression of Apaf-1 has been detected in NSCLC tumours in comparison to normal lung, whereas expression of pro-caspase 9 and 3 were found to be up-regulated in the absence of apoptosis (Yang *et al.*, 2003; Krepela *et al.*, 2006). There is mounting evidence that tumour cells also express higher levels of IAPs, signifying

that increased expression of IAPs thwarted the high basal caspase activity in tumour cells (Yang *et al.*, 2003).

2.3.2.1 BCL-2 family members

B-cell lymphoma-2 (BCL-2) was the first protein of this family to be identified, and it is encoded by the *BCL-2* gene found in human B-cell lymphomas with the t(14;18) chromosomal translocation (Tsujimoto *et al.*, 1984). This family of proteins is made up of pro-apoptotic and anti-apoptotic members that play a crucial role in the regulation of apoptosis by mediating permeability of the mitochondrial membrane, and they can be divided into three sub-groups based on their function and the presence of shared blocks of sequence homology, termed BCL-2 homology (BH) (Table 2.1) (Danial, 2007; Giam *et al.*, 2008). The first group is the anti-apoptotic multi-domain proteins, which counteract the process of apoptosis by sequestering pro-apoptotic family members (Hata *et al.*, 2015). This group is made up of BCL-2, B cell lymphoma extra large (BCL-XL), induced myeloid leukemia cell differentiation protein (MCL-1), BCL-2-like protein 2 (BCL-W), BCL-2 related protein A1 (BFL-1), and BCL-2-like protein 10 (BCL-B). The second group is the pro-apoptotic BH-3-only proteins, which share only a single block of sequence homology, the BH3 block. Members of this group include BCL-2-interacting mediator of cell death (BIM), BH3-interacting domain death agonist (BID) (Sevilla *et al.,* 2001), and BCL-2-associated agonist of cell death (BAD), amongst others (Hata *et al.*, 2015). Members of the third group are the pro-apoptotic multi-domain proteins, and some examples include BCL-2-associated protein X (BAX) and BCL-2 antagonist/killer (BAK) (Hata *et al.*, 2015).

In response to cellular stress, pro-apoptotic proteins, such as, BAX and BAK are dephosphorylated and cleaved leading to their translocation from the cytoplasm to the mitochondria. Oligomerization of BAX and BAK will be induced and the oligomers will subsequently be inserted into the mitochondrial outer membrane for the release of cytochrome c and activation of caspases to induce cell death (Debatin, 2004; Green & Kroemer, 2004). Furthermore, BH3-proteins, such as, BIM and BID, function by directly or indirectly activating pro-apoptotic BAX and BAK to induce apoptosis (Delbridge & Strasser, 2015). The balance between pro- and anti-apoptotic BCL-2 family members is crucial for cellular apoptotic homeostasis and abnormalities in BCL-2 family proteins have been observed in various human cancers, including lung cancer (Daniel & Smythe, 2004).

Table 2.1: Functional categories of the BCL-2 family of proteins

Anti-apoptotic proteins	Pro-apoptotic proteins	BH-3 only proteins
BCL-2	BAX	BID
BCL-XL	BAK	BIM
MCL-1	BOK/MTC	PUMA
BCL-W		NOXA
BFL-1		BAD
BCL-B		BMF
		HRK
		BIK

(Reproduced from Seminars in Thoracic and Cardiovascular Surgery, Vol. 16, Daniel & Smythe, The Role of Bcl-2 Family Members in Non-Small Cell Lung Cancer, 19-27, 2004, with permission from Elsevier).

2.3.2.2 BCL-2 family members expression in lung cancer

Overexpression of anti-apoptotic BCL-2 and BCL-XL is a prominent mechanism of apoptosis dysregulation in various cancers including acute lymphoblastic leukemia (ALL), acute myeloid leukemia (AML), diffuse large B-cell lymphoma (DLBCL), glioblastoma, melanoma, as well as prostate and lung cancers (Campana *et al.*, 1993; Colombel *et al.*, 1993; Ramsay *et al.*, 1995; Kitagawa *et al.*, 1996; Deininger *et al.*, 1999; Venditti *et al.*, 2004; Abramson & Shipp, 2005; Reed, 2008). Increased expression of BCL-2 is often correlated with poor prognosis, recurrence, and resistance to cancer therapeutics (Granville *et al.*, 1999; Pellecchia & Reed, 2004).

In lung cancer, overexpression of BCL-2 is more frequently overexpressed in SCLC and squamous cell carcinoma than in adenocarcinoma (Pezzella *et al.*, 1993). Furthermore, loss of BCL-2 expression has been reported to be associated with an increase in angiogenesis and cell migration (Koukourakis *et al.*, 1997; Koukourakis *et al.*, 1999), thus suggesting that BCL-2 expression may be required for survival of premalignant cells and some malignant cells, however as the tumour develops metastatic potential it may be less prone to undergo apoptosis, resulting in inhibition of BCL-2 (Kim *et al.*, 1998; Koty *et al.*, 2002).

While BCL-2 expression is less significant in lung adenocarcinoma, the expression of BCL-XL is frequently overexpressed in these tumours (Reeve *et al.*, 1996; Groeger *et al.*, 2004; Sanchez-Ceja *et al.*, 2006). BCL-XL has the ability to neutralize the pro-apoptotic functions of BAX and BAD through prevention of its translocation from the cytosol to the mitochondria. This will prevent initiation of apoptosis by maintaining the stability of the outer mitochondrial membrane, thus preventing release of cytochrome c and ensuing activation of pro-caspase 9 (Gottlieb *et al.*, 2000; Grad *et al.*, 2000). Pro-apoptotic BAD is normally phosphorylated at a number of serine residues allowing it to

be sequestered by the cytosolic scaffold protein 14-3-3. Upon receiving an apoptotic signal, BAD will be dephosphorylated and bind to BCL-XL leading to inactivation of BCL-XL's pro-survival function (Zha *et al.*, 1996). However, when BCL-XL is present in large quantities it will have a greater affinity for BAD than 14-3-3, thus sequestering BAD to the mitochondria, leaving excess uncomplexed BCL-XL to perform its pro-survival functions (Cheng *et al.*, 2001; Jeong *et al.*, 2004).

2.3.3 Extrinsic (death receptor) pathway

The extrinsic pathway of apoptosis is initiated at the plasma membrane upon stimulation of the death receptors, which include the tumour necrosis factor (TNF) receptor 1 (TNFR1), FAS (APO-1, CD95), TNF-related apoptosis-inducing ligand (TRAIL) receptor 1 (TRAILR1, DR4), and TRAIL receptor 2 (TRAIL-R2, DR5) (Hengartner, 2001; Jin & El-Deiry, 2005; Guicciardi & Gores, 2009). Upon receiving extracellular cues, the cytoplasmic domains of the death receptors recruits death domain-containing adaptor proteins, such as, TNF receptor-associated death domain (TRADD) and Fas-associated death domain (FADD), which then interacts with pro-caspase 8 via the death effector domain (DED), resulting in the formation of a complex known as the death inducing signaling complex (DISC) (Kischkel *et al.*, 1995). The formation of DISC in turn initiates the assembly and activation of initiator caspase 8, which can transmit the apoptosis signal through direct cleavage and activation of downstream effector caspases, such as, caspase 3, 6 and 7 (Figure 2.3) (Scaffidi *et al.*, 1998; Fulda, 2009). Alternatively, activated caspase 8 can induce mitochondrial damage through the cleavage of the BH3-only protein BID to generate truncated BID (tBID) (Li *et al.*, 1998; Garrido *et al.*, 2006).

Studies have shown that TRAIL receptors, TRAIL-R1 and -R2, are located on chromosome 8p, a region of frequent loss of heterozygosity (LOH) in tumours, including lung carcinomas (LeBlanc & Ashkenazi, 2003). Somatic mutations of TRAIL-R2 can be found in approximately 10% of NSCLC patients, with the mutations reported to be located in the death domain region (Lee *et al.*, 1999). However, whether these mutations influence patient response to therapy or overall survival remains to be examined. Furthermore, loss of pro-caspase 8, FAS-L, FAS-R and TRAIL-R have all been reported in SCLC (Joseph *et al.*, 1999; Hopkins-Donaldson *et al.*, 2003), and expression of decoy receptor 3 (DCR3), which competitively binds Fas ligand (FASL) to interfere with FAS-induced apoptosis has been found to be genetically overexpressed in lung carcinoma (Pitti *et al.*, 1998; Shen *et al.*, 2005).

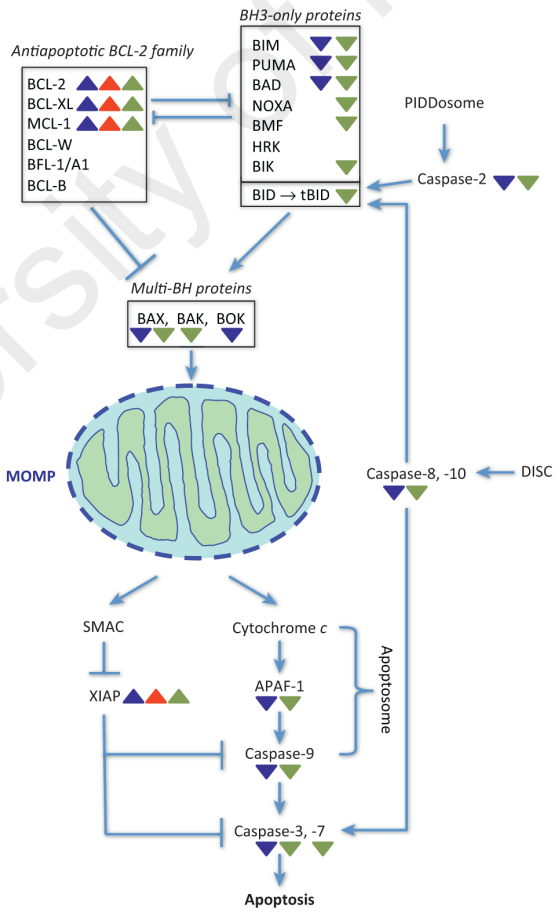

Figure 2.3: Extrinsic and intrinsic pathways of apoptosis (Reproduced from Trends in Cell Biology, Vol. 23, Fernald & Kurokawa, Evading Apoptosis in Cancer, 620-633, 2013, with permission from Elsevier).

2.3.4 Transforming growth factor, beta (TGF-β) signaling pathway

The TGF-β signaling pathway controls a critical network of signals that regulate cellular growth, differentiation, migration, adhesion, and cell death (Massagué, 1998). Signaling is initiated when the TGF-β ligand binds to the cell surface type II serine/threonine kinase receptor, also known as the transforming growth factor, beta-receptor II (TGF-βRII). This will be followed by an interaction and phosphorylation of a glycine/serine rich domain within transforming growth factor, beta-receptor I (TGF-βRI) to form an activated multimeric ligand-receptor complex (Massagué, 1998; Shi & Massagué, 2003). The activated TGF-βRI in turn propagates the signal by phosphorylating receptor-regulated Smad proteins (R-Smads) that consist of SMAD2 and SMAD3 proteins. R-Smads will undergo homotrimerization and form heteromeric complexes with common-mediator Smad (Co-Smad), SMAD4 (Massagué, 1998). This complex will be translocated into the nucleus and in cooperation with other transcription factors, regulate the transcription of target genes (Shi & Massagué, 2003; Gatza *et al.*, 2010).

TGF-β regulates the transcription of cell cycle regulators, thus functioning as a tumour suppressor through inhibition of cell cycle (Alexandrow & Moses, 1995). Cell cycle arrest is mediated by TGF-β through up-regulation of cyclin dependent kinase inhibitor proteins (CDKI), p15 and p21 (Hu *et al.*, 1999; Feng *et al.*, 2000). The p15 protein binds to CDK4 and CDK6 subunits to inactivate their catalytic activity and subsequently inhibits the cyclin D-CDK4/6 complex formation, whereas p21 blocks both cyclin D-CDK4/6 and cyclin E/CDK2 formation during the G_1-S phase of cell cycle (Hannon & Beach, 1994; Sherr & Roberts, 1999), thus inhibiting cell cycle progression. In addition to activating cell cycle inhibitors, TGF-β also suppresses mitogenic factors that stimulate cell growth, such as, v-MYC avian myelocytomatosis viral oncogene homolog (c-MYC) (Warner *et al.*, 1999; Feng *et al.*, 2002).

As depicted in Figure 2.4, TGF-β also has the ability to mediate the induction of apoptosis; however activation of apoptosis by TGF-β is variable depending on the cell and tissue type (Schuster & Krieglstein, 2002). For example, in human gastric SNU-620 cell line, TGF-β induces apoptosis via the Fas death receptor pathway and can subsequently activate caspase 8 via Bid cleavage (Kim *et al.*, 2004). Smad induced factors, such as, TGF-β early-response gene (TIEG1) and the death associated protein kinase (DAPK) have also been reported to be related to TGF-β mediated apoptosis (Tachibana *et al.*, 1997; Jang *et al.*, 2002). Expression of TIEG1 and DAPK are increased in response to TGF-β treatment, with TIEG1 inducing cell cycle arrest and enhancing TGF-β mediated apoptosis (Bender *et al.*, 2004). On the other hand, DAPK is directly activated by TGF-β via the SMAD2, SMAD3, and SMAD4 transcription factors, and in turn sensitizes cells to TGF-β dependent apoptosis (Jang *et al.*, 2002).

Alterations in TGF-β signaling have been associated with numerous human diseases, including cancer (Massague & Wotton, 2000; Jeon & Jen, 2010). TGF-β ligands along with downstream elements, including the receptors and SMAD proteins, are all essential in suppressing primary tumorigenesis in many tissues types (Markowitz & Roberts, 1996). However, many cancers have also been reported to use the TGF-β pathway to their advantage. As the tumour progresses, mutations are amassed and disturbs the suppressive effects of TGF-β (Miyazono *et al.*, 2003). For example, a marked increase in TGF-β ligand is frequently observed in lung cancer and is associated with advanced stages of malignancy and metastasis and with decreased survival (Jakowlew, 2008). Therefore, depending upon the context of the tumour microenvironment, TGF-β can function as either a tumour suppressor or a tumour promoter.

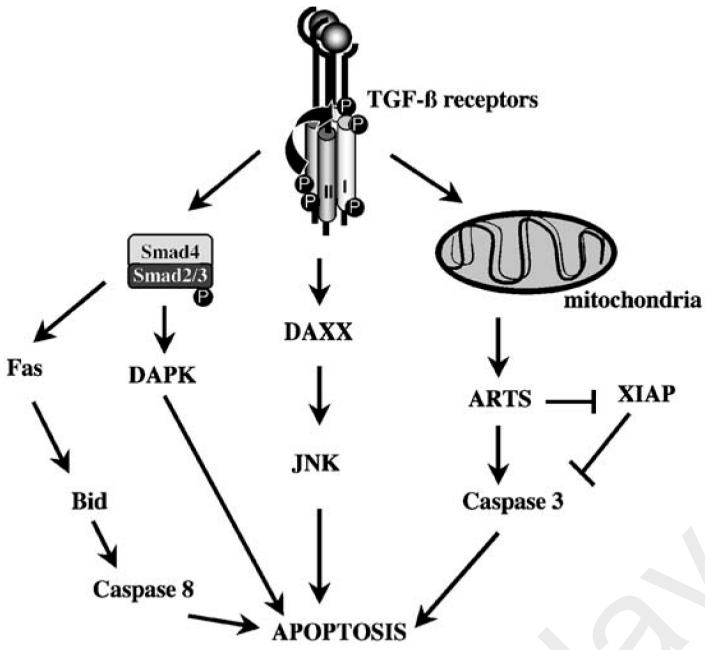

Figure 2.4: TGF-β induced apoptotic pathway (Reproduced from Cytokines in the Genesis and Treatment of Cancer, Bonine-Summers *et al.*, Transforming Growth Factor-β and Cancer, 91-111, 2007, with permission from Humana Press).

2.3.5 Phosphatidylinositol 3-Kinase (PI3K)/Protein kinase B (AKT) signaling pathway

The PI3K/AKT signaling pathway affects a vast assortment of intracellular events that can directly or indirectly influence cell apoptosis (Duronio, 2008). PI3K phosphorylates phosphatidylinositol-3,4-biphosphase (PtdIns(3,4)P2) (PIP_2) to generate PIP_3 (Vivanco & Sawyers, 2002). The PIP_3 ligands will in turn mediate their cellular effects through the recruitment of plekstrin homology (PH) containing proteins to the inner surface of the cell membrane (Lemmon & Ferguson, 2000). One of the key kinases activated downstream of PI3K at the plasma membrane is 3-phosphoinositide-dependent protein kinase-1 (PDK1) (Alessi *et al.*, 1997).

A central event for PI3K-dependent cell survival is the phosphorylation of a serine/threonine kinase, AKT, the cellular homologue of the retroviral oncogene v-Akt, also known as protein kinase B (PKB), at the threonine-308 (Thr308) region by PDK-1 in the presence of PIP_3 (Vivanco & Sawyers, 2002; Mora *et al.*, 2004). AKT will relocalize from the cytoplasm to signaling complexes located at the plasma membrane.

Signaling of AKT plays an important role in processes critical to tumourigenesis, including inhibition of apoptosis, aberrant cell proliferation, promotion of angiogenesis, and tumour cell invasiveness (summarized in Figure 2.5) (Testa & Bellacosa, 2001).

Activation of AKT plays a crucial role in cell survival by inhibiting apoptotic pathways. For example, AKT phosphorylates BAD, a pro-apoptotic member of the BCL-2 family of proteins, at serine-136 (Ser136) leading to inactivation of BAD activity by promoting its association with cytosolic 14-3-3 proteins (del Peso *et al.*, 1997; Blume-Jensen *et al.*, 1998). This localizes BAD to the cytosol and inhibits its interaction with anti-apoptotic BCL-2 and BCL-XL, thus deactivating its pro-apoptotic activity (Zha *et al.*, 1996). Another member of the BCL-2 family protein regulated by AKT is the pro-apoptotic BAX, which is a key regulator of mitochondrial permeability leading to apoptosis. AKT phosphorylates BAX at serine-184 (Ser184), suppressing BAX-mediated cell death (Gardai *et al.*, 2004).

Another set of substrates targeted by AKT is the forkhead transcription factors (FKHR) (Brunet *et al.*, 1999; Tang *et al.*, 1999). Phosphorylation by AKT will lead to binding of FKHR to 14-3-3 proteins, leading to sequestration and degradation in the cytoplasm (Brunet *et al.*, 1999). Thus in the event of AKT loss, FKHR will be dephosphorylated and translocated to the nucleus where they can induce an increase in numerous regulators of cell death, including the FAS death receptor ligand, as well as the pro-apoptotic BIM, and the cell cycle inhibitor $p27^{Kip1}$ (Biggs *et al.*, 1999; Guo *et al.*, 1999; Kops *et al.*, 1999; Nakae *et al.*, 1999; Rena *et al.*, 1999; Tang *et al.*, 1999).

NFκB (nuclear factor of light polypeptide gene enhancer in B cells), an important regulator of numerous anti-apoptotic and pro-apoptotic genes, is indirectly affected by AKT signaling (Vivanco & Sawyers, 2002). AKT regulates NFκB through the activation of IKK (IκB kinase) α, which together with IKKβ phosphorylates inhibitor of NFκB (IκB), leading to its ubiquitination and degradation (Ozes *et al.*, 1999; Romashkova & Makarov, 1999; Karin & Ben-Neriah, 2000). Degradation of IκB will allow for the release of NFκB from the cytoplasm into the nucleus, and regulation of its target genes, which includes BCL-2, BCL-XL, and the inhibitor of caspase 8, FLIP (FLICE (FADD (Fas-associated death domain)-like IL-1β-converting enzyme)-inhibitory protein) (Chen *et al.*, 2000; Kreuz *et al.*, 2001; Sevilla *et al.*, 2001).

Another pathway influenced by PI3K/AKT signaling is regulation of the tumour suppressor P53 (Vivanco & Sawyers, 2002; Duronio, 2008). p53 regulates apoptosis through various mechanisms including the up-regulation of pro-apoptotic proteins, such as, BAX and PUMA (Wu & Deng, 2002; Roos & Kaina, 2006). Negative regulation of p53 occurs via a molecule called murine double minute 2 (MDM2), which can move into the nucleus to promote the ubiquitination and consequent degradation of p53. Reports have shown that AKT can mediate the phosphorylation of MDM2 at serine-166 (Ser166) and serine-186 (Ser186), which in turn allows the translocation of MDM2 from the cytoplasm into the nucleus (Mayo & Donner, 2001).

AKT plays a role in various components of the cell-death process, and studies have shown that aberrant expression of AKT can significantly influence human malignancy (Testa & Bellacosa, 2001). Expression of AKT has been demonstrated to be up-regulated in various tumour types including ovarian, breast, prostate, pancreatic, gastric, and lung cancer (Staal, 1987; Bellacosa *et al.*, 1995; Edlind & Hsieh, 2014; Baer *et al.*, 2015). In lung cancer, amplification of AKT has been associated with resistance to

chemotherapy, radiation, and tyrosine kinase inhibitors (Brognard *et al.*, 2001; Hill & Hemmings, 2002; Janmaat *et al.*, 2003).

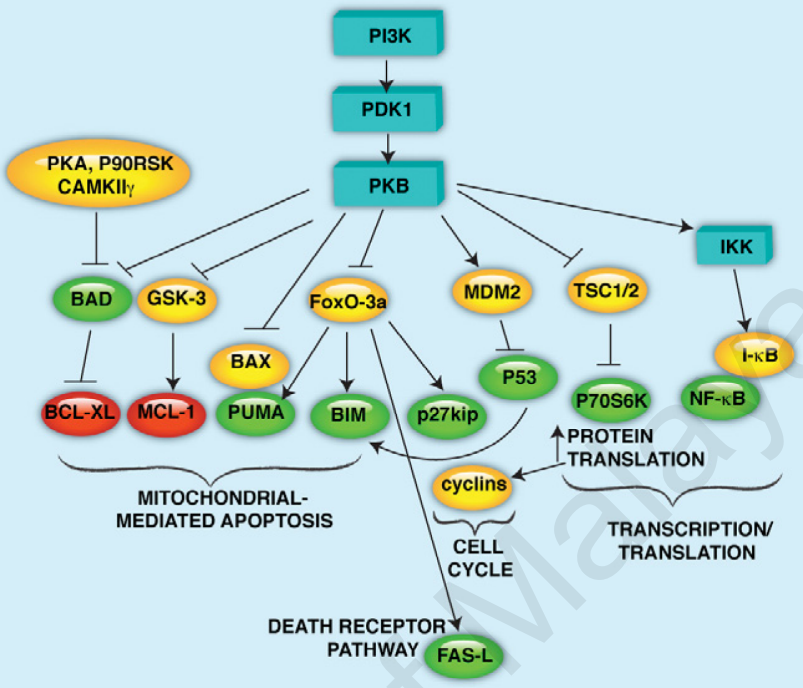

Figure 2.5: Target substrates of PI3K/AKT whose pro-apoptotic activities are suppressed by phosphorylation (Reproduced from Biochemical Journal, Vol. 415, Duronio, The Life of a Cell: Apoptosis Regulation by the PI3K/PKB Pathway, 333-344, 2008, with permission from Portland Press).

2.3.6 Mitogen-activated protein kinase (MAPK) signaling pathway

Mitogen-activated protein kinases (MAPKs) are serine-threonine kinases that control numerous cellular activities including proliferation, differentiation, apoptosis, survival, inflammation, transformation, and innate immunity (Platanias, 2003; Torii *et al.*, 2006; Turjanski *et al.*, 2007; Arthur & Ley, 2013; Peti & Page, 2013). This signaling cascade is activated by various extracellular and intracellular stimuli, such as, peptide growth factors, cytokines, hormones, and cellular stresses including oxidative stress and endoplasmic reticulum stress (Kim & Choi, 2010). The MAPK family is made up of three subfamilies: the extracellular signal-regulated kinase (ERK; ERK1 and ERK2), c-Jun N-terminal kinase (JNK; JNK1, JNK2, and JNK3), and the p38-MAP kinase (α, β, δ and γ) (Figure 2.6) (Schaeffer & Weber, 1999; Raman *et al.*, 2007). Each MAPK signaling cascade consists of at least three components: a MAPK kinase kinase

(MAP3K), a MAPK kinase (MAP2K), and a MAPK (Chang & Karin, 2001; Plotnikov *et al.*, 2011). Within each tier of the cascade, one or more kinase component will phosphorylate and activate components in the next tier, eventually leading to the phosphorylation of target regulatory molecules by the activated MAPK (Figure 2.6) (Raman *et al.*, 2007).

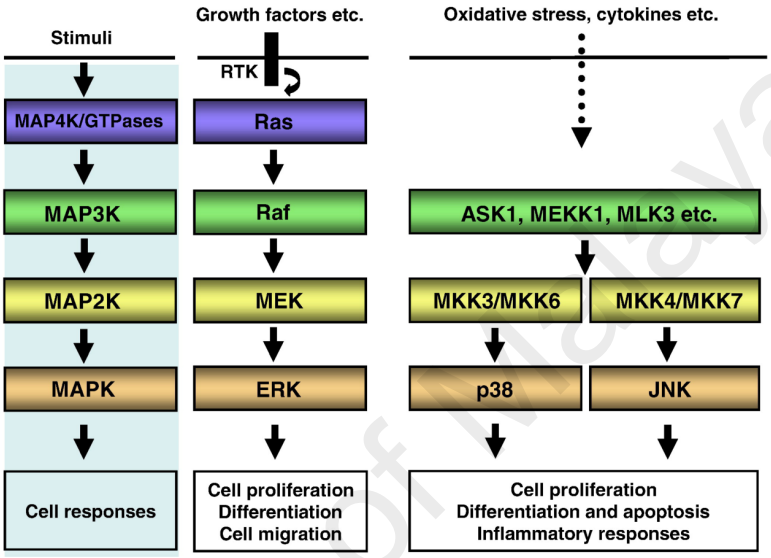

Figure 2.6: Mitogen-activated protein kinase (MAPK) signaling pathways (Reproduced from Biochimica et Biophysica Acta, Vol. 1802, Kim & Choi, Pathological Roles of MAPK Signaling Pathways in Human Diseases, 396-405, 2010, with permission from Elsevier).

2.3.6.1 ERK1/2 cascade

The best characterized MAPK pathway is the ERK cascade, and there are two ERK isoforms that are ubiquitously expressed, ERK1 (p42) and ERK2 (p33), that are 83% identical (Boulton *et al.*, 1991). The ERK cascade is initially activated by mitogenic stimuli, such as, epidermal growth factor (EGF) or platelet-derived growth factor (PDGF). Binding of the growth factors to its cell surface receptor tyrosine kinase, will induce dimerization and autophosphorylation of the receptor (Mercer & D'Armiento, 2006). This in turn will activate guanine nucleotide exchange factors (GEFs) such as Son of Sevenless (SOS), which facilitates the activation of GTPase Ras (Dhillon *et al.*, 2007; Plotnikov *et al.*, 2011). Ras-GTP will activate the MAP3K tier of the cascade, the

Raf isoforms (RAF-1, A-RAF, B-RAF), which mediates phosphorylation of the dual-specificity MAP kinase-1 and -2 (MEKs), MEK1/2 (Malumbres & Barbacid, 2003; Mercer & D'Armiento, 2006). MEK1/2 will in turn phosphorylate ERK1/2 allowing the activated ERK to execute its function through a large number of downstream molecules.

Activation of ERK1/2 can promote cell survival through the inhibition of apoptosis at stages upstream, downstream or unrelated to changes in the mitochondrial membrane potential and release of cytochrome c (Erhardt *et al.*, 1999; Qiao *et al.*, 2001). For example, ERK1/2 can inhibit the activation of caspase 8, cleavage of Bid and loss of mitochondrial membrane potential through the stimulation of FAS/CD95, TNF, and TRAIL receptors (Holmstrom *et al.*, 2000; Tran *et al.*, 2001; Shonai *et al.*, 2002). ERK1/2 can also stimulate cell survival by boosting the activation of anti-apoptotic molecules, such as, MCL-1, an anti-apoptotic member of the BCL-2 family, which is phosphorylated by ERK1/2 at threonine-163 (Thr163) (Domina *et al.*, 2004). Furthermore, IEX-1 (immediately early gene X-1) can be phosphorylated at threonine-18 (Thr18) by ERK/1/2 and prevents cell death by inhibiting the release of cytochrome c from the mitochondria (Garcia *et al.*, 2002). Reports have also concluded that caspase 9 can be regulated by ERK1/2 by phosphorylation at threonine-125 (Thr125) to inhibit caspase 9 processing and subsequent activation of caspase 3 (Allan *et al.*, 2003). ERK1/2 is also able to phosphorylate and activate various transcription factors including TCF-member ELK-1, c-FOS (Fos proto-oncogene, AP-1 transcription factor subunit), p53, ETS1/2 (avian erythroblastosis virus E26 (v-ETS) oncogene homolog) and c-JUN (JUN proto-oncogene, AP-1 transcription factor subunit), all of which are important for the initiation and regulation of cell proliferation and oncogenic transformation (Gille *et al.*, 1992; Milne *et al.*, 1994; Yang *et al.*, 1996; Murphy *et al.*, 2002; Morton *et al.*, 2003).

Studies have also reported an association between the dysregulation of the ERK pathway and tumourigenesis. The incidence of cancer has been positively correlated with an increased activation of RAS, increased ERK1/2 activity, or binding of DNA by ERK1/2 transcription factor targets in both *in vitro* and *in vivo* studies (Sebolt-Leopold *et al.*, 1999; Vicent *et al.*, 2004; Han *et al.*, 2005; Mercer & D'Armiento, 2006).

2.3.6.2 JNK/SAPK cascade

The JNK-family kinases, also known as stress-activated protein kinases (SAPK), is initiated by numerous stimuli, including growth factors, cytokines, and cellular stresses, such as, genotoxic, osmotic, hypoxic, or oxidative stress (Hibi *et al.*, 1993; Cano *et al.*, 1994; Westwick *et al.*, 1994). The activated stimuli will transmit their signal to GTPases, such as, cell division cycle 42 (CDC42) and Ras-related C3 botulinum toxin substrate 1 (RAC1) which induces the activation of the MAP3K level kinases (Plotnikov *et al.*, 2011), which includes members of the mitogen-activated protein kinase kinase kinase 1, E3 ubiquitin protein ligase group (MEKK1-4), apoptosis signal-regulating kinase group (ASK1 and ASK2), mixed lineage kinase (MLK1, MLK2, MLK3, DLK, and LZK), and transforming growth factor-β activated kinase 1 (TAK1) (Davis, 2000). The signal will then be transmitted further by phosphorylation of the kinases at the MAPKK level, MEK4 (MKK4) and MEK7 (MKK7). MKK4 and MKK7 will in turn activate the components at the MAPK level, JNK (JNK1-3) via dual phosphorylation of the Thr-Pro-Tyr motif (Davis, 2000; Fleming *et al.*, 2000).

Activated JNK can control various transcription factors, such as, c-JUN, c-FOS, ATF-2 (activating transcription factor 2), p53, ELK, and NFAT (nuclear factor of activated T cells) (Johnson & Nakamura, 2007; Raman *et al.*, 2007). These phosphorylated targets would in turn regulate transcription of many genes thus mediating numerous cellular processes including apoptosis, immunological effects, neuronal activity, and insulin signaling (Dhanasekaran & Reddy, 2008; Haeusgen *et al.*, 2009; Rincon & Davis, 2009). In regards to apoptosis, JNK can phosphorylate and inhibit the activity of cytoplasmic substrates including the anti-apoptotic proteins BCL-2 and BCL-XL, to produce a change in mitochondrial membrane potential and subsequent release of cytochrome c and activation of caspase 3 (Fan *et al.*, 2000; Basu & Haldar, 2003). Furthermore, the phosphorylation of c-JUN and ATF-2 resulted in activation of activator protein 1 (AP-1) and increased expression of pro-apoptotic genes, *FasL* and *Fas*, to initiate activation of caspase 8 (Fan & Chambers, 2001; Tang *et al.*, 2012).

2.3.6.3 p38 cascade

Similar to the JNK pathway, the p38 cascade is also induced by stress related stimuli (heat shock, changes in osmolarity, ultraviolet, oxygen radicals and hypoxic state) and various growth factors including granulocyte macrophage-colony stimulating factor (GM-CSF), colony stimulating factor 1 (CSF1), erythropoietin (EPO), insulin-like growth factor (IGF), VEGF, and PDGF (Foltz *et al.*, 1997; Pyne & Pyne, 1997; Rousseau *et al.*, 1997; Cheng & Feldman, 1998). Activated receptors will transmit the signals via adaptor proteins, small GTPases, MAP4Ks and MAP3Ks, similar to those functioning in the JNK cascade, such as, ASK and TAK1 (Plotnikov *et al.*, 2011). Following that, MAP3Ks will phosphorylate and activate the MAP2K components, which are made up of the MKK3 and MKK6 (Brancho *et al.*, 2003). Activated MKK3 and MKK6 will in turn activate the four isoforms at the MAPK tier of the cascade,

p38α, p38β, p38δ, and p38γ. Upon activation, p38 proteins will translocate from the cytosol to the nucleus to mediate cellular responses via downstream transcription factors (Plotnikov *et al.*, 2011).

The p38 cascade plays a critical role in the control of immunological effects, cell cycle checkpoint, and apoptosis (Huang *et al.*, 2009; Thornton & Rincon, 2009). Therefore, a dysregulation of the p38 has been implicated in tumourigenesis. Studies have shown that p38 functions as a tumour suppressor through the down-regulation of Ras-dependent and independent transformation, invasion and also by inducing apoptosis (Plotnikov *et al.*, 2011). For example, activation of p38 leads to rapid dephosphorylation of MEK1/2 and subsequent apoptosis (Li *et al.*, 2003). Furthermore, p38 can mediate TNF-induced BCL-XL phosphorylation, however the exact mechanism by which this occurs is still unknown (Grethe *et al.*, 2004). p38 has also been implicated indirectly through increasing or decreasing BAD phosphorylation at serine-112 (Ser112) (She *et al.*, 2002; Grethe & Porn-Ares, 2006).

2.3.7 Wingless-type MMTV integration site family (WNT) signaling pathway

WNT signaling plays a crucial role in development as it acts as a regulator of embryonic cell patterning, proliferation, differentiation, cell survival, and apoptosis (Pećina-Šlaus, 2010). WNT signaling can be classified as canonical and non-canonical, whereby the canonical pathway is responsible for prevention of β-catenin degradation (Widelitz, 2005). When WNT signaling is absent, β-catenin is linked with a cytoplasmic complex made up of the glycogen synthase kinase 3-beta (GSK3-β), adenomatous polyposis coli protein (APC), and axin (Su *et al.*, 1993; Sakanaka *et al.*, 1998). GSK3-β phosphorylates β-catenin at the NH_2-terminal region and induces its degradation through the ubiquitin-proteasome pathway (Kitagawa *et al.*, 1999; Winston *et al.*, 1999).

As depicted in Figure 2.7, when WNT signaling is activated, WNT ligands bind to receptors of the Frizzled (FZD) family on the cell surface. In turn, FZD receptors activates the intracellular protein, Disheveled, to inhibit the multiprotein GSK3-β /APC/AXIN complex thus allowing β-catenin to escape from phosphorylation and accumulate in the cytoplasm (Barth *et al.*, 1997; Rubinfeld *et al.*, 1997). β-catenin can then translocate to the nucleus to form a complex with members of the T-cell factor/lymphocyte enhancer factor (TCF/LEF) family of transcription factors to activate various target genes including *c-MYC*, *CCND1*, *BIRC5*, and *MMP* (Roose & Clevers, 1999; Tapia *et al.*, 2006). Therefore, a constitutively activated WNT pathway can lead to cancer.

Reports have demonstrated that the WNT signaling pathway can regulate apoptosis through a variety of mechanisms. The tumour suppressor protein, APC, can play a role in regulation of apoptosis depending on whether it is present as a full length (wild type) or truncated (mutant) protein. Expression of the wild type APC induces apoptosis, whereas overexpression of the mutant truncated protein maintains an anti-apoptotic mode of action (Brocardo & Henderson, 2008). The mutated truncated APC protein is frequently found in cancers and is it has been reported that mutant APC can bind to Bcl-2 proteins to increase their levels in the mitochondria, resulting in increased cell survival (Brocardo & Henderson, 2008). However, the exact mechanism by which this occurs is still unclear.

Another well-researched WNT protein, WNT1, has also been associated with the control of apoptosis. WNT1 inhibits apoptosis through the prevention of cytochrome c release from the mitochondria and inhibition of the subsequent activation of caspase 9. WNT1 is frequently overexpressed in NSCLC, and its overexpression results in increased resistance to therapies that mediate apoptosis (Chen *et al.*, 2001; Li *et al.*,

2006). Other WNT-pathway components including frizzled-8 (FZD8), disheveled (DSH), porcupine (PORC), and transcription factor 4 (TCF-4) are also frequently overexpressed in NSCLC, and is associated with poor prognosis (Xu *et al.*, 2007; Wei *et al.*, 2008; Bartling *et al.*, 2010; Bravo *et al.*, 2013). Furthermore, down-regulation of WNT inhibitors, such as axin, WNT inhibitory factor 1 (WIF-1), dickkopf WNT signaling pathway inhibitor 1(DKK-1), runt related transcription factor 3 (RUNX3), and caudal type homeobox 2 (CDX2), amongst others, is also common is NSCLC cell lines and may be associated with high stage, dedifferentiation, and poor prognosis (Licchesi *et al.*, 2008; Liu *et al.*, 2012; Na *et al.*, 2012).

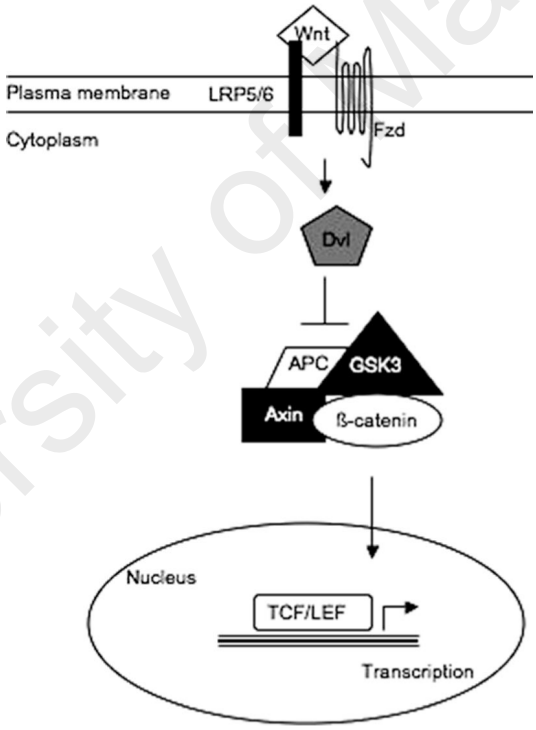

Figure 2.7: Canonical WNT/β-catenin signaling pathway (Reproduced from Journal of Thoracic Oncology, Vol. 2, Tennis *et al*., Role of the WNT Signaling Pathway and Lung Cancer, 889-892, 2001, with permission from Elsevier).

2.4 MicroRNA (miRNA)

MiRNAs were first discovered in the *Caenorhabdotis elegans* (*C. elegans*) worm by Ambros and colleagues in 1993 (Lee *et al.*, 1993). They discovered that a 22-nucleotide transcript of *lin-4*, a repressor of *lin-14* that controls the timing of *C. elegans* larval development, did not code for a protein. Instead it was observed that *lin-4* produces two small RNAs of about 22 and 62 nucleotides in length. The authors determined that the shorter lin-4 RNA had anti-sense complementarity to multiple sites in the 3'-untranslated region (3'UTR) of *lin-14* which led the authors to hypothesize that lin-4 inhibits the translation of *lin-14* through interaction with these 3'UTR elements (Lee *et al.*, 1993; Wightman *et al.*, 1993). Seven years later, in 2000, the evolutionarily conserved let-7 miRNA of *C. elegans* was determined to also regulate the expression of downstream genes through partial complementarity between the miRNA and its target 3'UTR (Reinhart *et al.*, 2000). These discoveries led to the characterization of numerous large-scale cDNA libraries enriched for small miRNAs, which in turn led to the identification of other miRNAs from plants, *C. elegans*, *Drosophila*, and mammals (Lagos-Quintana *et al.*, 2001).

MiRNAs are a subset of non-coding RNAs of about 19 to 23 nucleotides long which regulate gene expression post-transcriptionally through the inhibition of mRNA translation, via direct binding to specific target sites in their 3'UTR regions, or inducement of target mRNA degradation through cleavage (Bartel, 2004). MiRNAs target approximately 60% of human protein-coding genes (Friedman *et al.*, 2009). These regulatory elements play a role in a wide range of biological processes including cell proliferation (Hayashita *et al.*, 2005), differentiation (Shivdasani, 2006), and apoptosis (Mott *et al.*, 2007).

2.4.1 MiRNA biogenesis

MiRNA genes can be found embedded within intergenic and intragenic (in introns and exons) regions of both protein-coding and non-coding transcripts, and are therefore co-transcribed with the gene in which they reside (Rodriguez *et al.*, 2004). As demonstrated in Figure 2.8, miRNAs are initially transcribed by RNA polymerase II to form a primary miRNA (pri-miRNA) that can measure up to several thousands of nucleotides and contain stem-loop structures with single stranded RNA extensions at both ends. Pri-miRNA also contains a 5' 7-methylguanosine cap structures and are polyadenylated at their 3'end (Lee *et al.*, 2003; Cai *et al.*, 2004; Borchert *et al.*, 2006). The hairpin structures are recognized and the maturation process will begin with the nuclear cleavage of pri-miRNA by a 650 kDA microprocessor complex made up of RNase III endonuclease Drosha and the double-stranded RNA-binding protein DiGeorge syndrome critical region 8 (DGCR8) (Lee *et al.*, 2003; Han *et al.*, 2004).

The resulting precursor miRNA (pre-miRNA), a ~65 nucleotide RNA hairpin intermediate with two nucleotide 3'overhang, will be bound by the nuclear export factor Exportin 5 and transported from the nucleus to the cytoplasm (Lee *et al.*, 2002; Lund *et al.*, 2004). In the cytoplasm, the terminal loop of the the pre-miRNA will be cleaved by a second RNase endonuclease Dicer, with its dsRNA binding partner, the human immunodeficiency virus transactivating response RNA-binding protein (TRBP), to generate a double stranded RNA duplex that is made up of both the mature miRNA strand and its complementary strand (Chendrimada *et al.*, 2005; Haase *et al.*, 2005). TBRP will then recruit the argonaute protein (AGO2), to form the RNA-induced silencing complex (RISC) (Chendrimada *et al.*, 2005). The strand of the duplex that has the lowest thermodynamic stability at its 5'end is selected as the guide strand, which then functions to direct RISC to the 3'UTR of target mRNA based on sequence

complementarity. The passenger strand of the duplex will be degraded and removed from the RISC complex (Schwarz *et al.*, 2003; Matranga *et al.*, 2005).

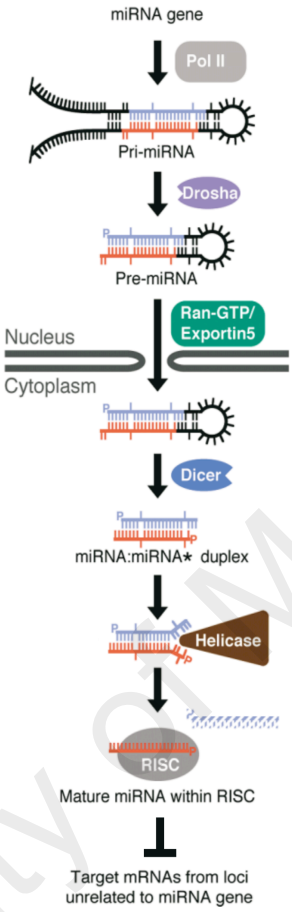

Figure 2.8: Biogenesis of miRNAs (Reproduced from Cell, Vol. 116, Bartel, MicroRNAs: Genomics, Biogenesis, Mechanism, and Function, 281-297, 2004, with permission from Elsevier).

2.4.2 MiRNA mode of action

Mature miRNA incorporated in the RISC will target mRNA based upon Watson-Crick base-pairing between the 3'UTR of the target and the seed region (residues 2-8 at the 5' end) of the miRNA guide strand (Lee *et al.*, 1993; Lewis *et al.*, 2003; Brennecke *et al.*, 2005). Therefore, a single miRNA is able to control the expression of hundreds of mRNA targets, and each mRNA may be regulated by multiple miRNAs.

The gene silencing mechanism that is employed depends upon the degree and nature of complementary sites between the target and guide miRNA (Bartel, 2004). In the case of multiple complementary sites with partial base-pairing in each site, translational inhibition of the mRNA will occur, whereas AGO2 endonuclease cleavage of target mRNA will occur in situations of perfect base-pairing (Bartel, 2004; Yekta *et al.*, 2004).

The two silencing mechanisms; mRNA cleavage and mRNA translational repression can be defined as slicer-dependent and slicer-independent silencing, respectively, with slicer activity referring to endonuclease cleavage of mRNA by AGO2 (Sheth & Parker, 2003; Meister *et al.*, 2004; Brengues *et al.*, 2005). In the slicer-dependent silencing mechanism, mRNA can be degraded by one of two processes, both beginning with the removal of the poly (A) tail through deadenylation of the mRNA (Parker & Song, 2004; Valencia-Sanchez *et al.*, 2006). Degradation can then occur via exosome or decapping by the enzymes DCP1 and DCP2, which performs 5'-to-3' degradation through the exoribonuclease XRN1P (Coller & Parker, 2004; Valencia-Sanchez *et al.*, 2006). For slicer-independent silencing mechanism, the multiple complementary sites of partial base-pairing induces the creation of bulges in the RNA duplex, thus inhibiting the slicer activity of AGO2 (Valencia-Sanchez *et al.*, 2006). Furthermore, mRNA targeted by miRNA can be relocated and separated into P-bodies, which are small cytoplasmic protein spheroid domains, for temporary storage and/or decay sites (Brengues *et al.*, 2005; Liu *et al.*, 2005a; Liu *et al.*, 2005b). The reduction in the amount of target mRNA is the principal result of this molecular event.

2.4.3 MiRNA and lung cancer

As miRNAs play a vital role in a variety of biological processes including differentiation, cell proliferation, development, and apoptosis, a disturbed miRNA function or altered miRNA expression may disorganize cellular processes and eventually cause or contribute to disease, including cancer (Wiemer, 2007). Studies have reported that miRNA genes reside in genomic regions that are involved in cancers, including minimal regions of loss of heterozygosity (LOH), minimal regions of amplification, or breakpoint cluster regions (Calin *et al.*, 2004b). MiRNAs can be either up-regulated or down-regulated in human cancers, with those whose expressions are increased are considered oncogenic miRNAs, or oncomiRs, while miRNAs that are down-regulated are considered tumour suppressor genes (Zhang *et al.*, 2007). Overexpression of miRNAs may result from deregulation of transcription factors, amplification or demethylation of CpG islands in the promoter regions of the gene (Croce, 2008). On the other hand, down-regulation of miRNAs may be due to deletions, epigenetic silencing, or loss of transcription factor expression (Ruan *et al.*, 2009).

In lung cancer, there are a number of miRNAs implicated in the development and progression of this disease (Table 2.2). For example, miR-21 is an oncomiR up-regulated in lung cancer that functions to inhibit the expression of phosphatase and tensin homolog (PTEN), programmed cell death protein 4 (PDCD4) and tropomyosin 1 (TPM1) to promote cell proliferation, migration, and inhibition of apoptosis (Zhu *et al.*, 2008; Zhang *et al.*, 2010b; Bhatti *et al.*, 2011). The miR-17-92 polycistronic cluster (miR-17-3p, miR-17-5p, miR-18a, miR-19a, miR-20a, miR-19b, miR-92-1) is also overexpressed in lung cancer, particularly in SCLC, and functions as oncomiRs to promote cancer progression and cell proliferation (Hayashita *et al.*, 2005; Matsubara *et al.*, 2007; Osada & Takahashi, 2011). Another well documented oncomiR is miR-221/222, which is overexpressed in lung cancer to inhibit apoptosis and promote cell

migration through the down-regulation of PTEN and tissue inhibitor of metalloproteinases 3 (TIMP3) (Garofalo *et al.*, 2009).

Tumour suppressor miRNAs that are frequently down-regulated in lung cancer includes the let-7 family, miR-34 family, and miR-200 family. The let-7 family negatively regulates numerous oncogenes involved in cell proliferation and cell cycle regulation, including *RAS*, *MYC*, *HMGA2* (high mobility group AT-hook 2), *CDC25A* (cell division cycle 25A), *CDK6* and *CCND2* (cyclin D2) (Johnson *et al.*, 2005; Johnson *et al.*, 2007; Kumar *et al.*, 2007; Lee & Dutta, 2007). Meanwhile, the miR-34 family (miR-34a, miR-34b, miR-34c), also down-regulated in lung cancer, controls cell proliferation via inhibition of *MET* (hepatocyte growth factor receptor), *BCL2*, *PDGFR-α* and *PDGFR-β* (platelet derived growth factor receptor). Another tumour suppressor down-regulated in lung cancer is the miR-200 family (miR-200a, miR-200b, miR-200c, and miR-429), which regulates the induction of epithelial-mesenchymal transition (EMT) via regulation of *ZEB* (zinc finger E-box-binding homeobox) transcription factors (ZEB1 and ZEB2), CDH1 (E-cadherin), and *VIM* (vimentin) (Ceppi *et al.*, 2010; Takeyama *et al.*, 2010).

Table 2.2: Principal microRNAs involved in the development or progression of lung cancer

MicroRNAs	Gene Targets	Biological Processes
Tumor suppressor microRNAs with down-regulation in lung cancer		
let-7 family	RAS, HMGA2, CDK6, CCND2, MYC, DICER1	(i) Cell proliferation (RAS, MYC, HMGA2) (ii) Cell cycle regulation (CDK6, CCND2) (iii) microRNA maturation (DICER1)
miR-34 family	BCL2, PDGFRA, PDGFRB	TRAIL-induced cell death and cell proliferation
miR-200 family	ZEB1, ZEB2, E-cadherin (CDH1), vimentin (VIM)	Promotion of EMT and metastasis
Oncogenic microRNAs with up-regulation in lung cancer		
miR-21	PTEN, PDCD4, TPM1	Apoptosis, cell proliferation, and migration
miR-17-92 cluster	miR-17-92 cluster E2F1, PTEN, HIF1A	Cell proliferation and carcinogenesis
miR-221/222	miR-221/222 PTEN, TIMP3	Apoptosis and cell migration

(Reproduced from Journal of Clinical Medicine, Vol. 5, Inamura & Ishikawa, MicroRNA in Lung Cancer: Novel Biomarkers and Potential Tools for Treatment, 36, 2016, licensed under CC BY 4.0).

The expression of miRNAs has also been associated with prognosis and survival of lung cancer patients. Studies have reported that a lower let-7 expression and a higher expression of miR-155 in lung cancer in comparison to normal lung tissue were associated with poor prognosis in NSCLC patients (Takamizawa *et al.*, 2004; Yanaihara *et al.*, 2006). In 2008, a five-miRNA signature (let-71, miR-221, miR-137, and miR-182*) was able to predict a poor overall and disease-free survival rates for lung cancer patients with high-risk scores in this miRNA signature (Yu *et al.*, 2008). High expression of miR-146b has been associated with poor overall survival in squamous cell lung cancer patients (Raponi *et al.*, 2009), whereby high expression of miR-16 is associated with better survival in lung cancer patients (Wang *et al.*, 2013b). Furthermore, overexpression of miR-519c has been correlated with better prognosis, while low levels of miR-34a is associated with relapse in lung cancer patients (Cha *et al.*, 2010; Wiggins *et al.*, 2010).

Reports have also suggested that miRNA expression can be utilized to classify stages and subtypes of lung cancers. For instance, miR-205 is a useful marker to differentiate SCC from non-SCC NSCLCs with a sensitivity of 96% and specificity of 90% (Lebanony *et al.*, 2009). Meanwhile, detection of miR-21, miR-486, miR-375 and miR-200b in sputum samples, in combination, is one of the best predictors of lung adenocarcinoma with 81% sensitivity and 92% specificity (Yu *et al.*, 2010). Furthermore, detection of miR-21 expression along with detection of four protein-coding genes (XPO1, BRCA1, HIF1A, and DLC1) was able to independently classify stage 1 adenocarcinomas into two groups with different survival rates (Robles *et al.*, 2015).

2.4.4 MiRNA and apoptosis

Dysregulation of programmed cell death is a significant hallmark of tumour development and progression, and various studies have shown that miRNAs influence development of cancer through regulation of the apoptotic process (Jovanovic & Hengartner, 2006; Wang & Lee, 2009; Li *et al.*, 2012a; Othman & Nagoor, 2014). As mentioned previously in section 2.3, the events that culminate in the activation of caspases can be categorized into the extrinsic and intrinsic pathways. The extrinsic pathway is activated through the binding of appropriate ligands to death receptors, and evidence has shown that these molecules are targets of various miRNAs, summarized in Figure 2.9. For example, miR-19a, a member of the miR-17-92 cluster, which is often overexpressed in lung cancers, targets TNF-α receptors to inhibit apoptosis (Liu *et al.*, 2011). On the other hand, miR-34a, miR-34c, and miR-212 are all down-regulated in NSCLC and ectopic expression of these miRNAs increases TRAIL-induced cell death to inhibit tumourigenesis (Incoronato *et al.*, 2010; Garofalo *et al.*, 2013). Lung cancer however, has also developed resistance to TRAIL-induced apoptosis through miRNA dependent mechanisms, such as, increased expression of miR-494a, miR-221, and miR-

222, which impair TRAIL-induced apoptosis. Therefore, blocking of these miRNAs through anti-miR transfection resulted in TRAIL-sensitivity in NSCLC (Garofalo *et al.*, 2008; Romano *et al.*, 2012).

The intrinsic pathway is characterized by cytochrome c release as a result of the permeability of the outer mitochondrial membrane, which is controlled by the presence of pro- and anti-apoptotic members of the BCL-2 family of proteins. There are numerous miRNAs that have been reported to regulate the expression of various BCL-2 family members (Figure 2.9). Anti-apoptotic *BCL-2* is targeted by miR-503, miR-181b, miR-200b/c-429 cluster, miR-497, and miR-7, whose expressions are all down-regulated in NSCLC cells. Ectopic expression of these miRNAs has been shown to lead to a significant reduction of *Bcl-2* to induce apoptosis (Zhu *et al.*, 2010; Xiong *et al.*, 2011; Zhu *et al.*, 2012a; Zhu *et al.*, 2012b; Qiu *et al.*, 2013). *BCL-XL*, another anti-apoptotic member, is targeted by let-7c (Cui *et al.*, 2013), whereas miR-125b and miR-335 suppresses anti-apoptotic *BCL-W* (Gong *et al.*, 2013; Wang *et al.*, 2013a). Pro-apoptotic members of the BCL-2 family has also been demonstrated to be targeted by miRNAs up-regulated in NSCLC cells, such as, *PUMA* which is targeted by miR-221/222 (Zhang *et al.*, 2010a), *BIM* which is targeted by miR-494, miR-17, miR-30b, mR-30c, miR-221, miR-103, and miR-203 (Dai *et al.*, 2011; Garofalo *et al.*, 2011; Romano *et al.*, 2012), and *BMF* and *NOXA* which are targets of miR-197 (Fiori *et al.*, 2014).

In lung cancer, another component of the intrinsic pathway targeted by miRNAs include *APAF-1*, which is a target of up-regulated miR-21 and miR-155 (Figure 2.9) (Kim *et al.*, 2009; Zang *et al.*, 2012; Fiori *et al.*, 2014). Furthermore, BAX oligomerization, mitochondrial transmembrane potential dissipation, and the proteolytic maturation of caspase 9 and caspase 3 have been reported to be modulated by pre-miR-181a and pre-miR-630 in A549 lung adenocarcinoma cell line (Galluzzi *et al.*, 2010)

Studies have shown that miRNAs are also able to interfere with apoptosis in lung cancer through regulation of the expression and activation of effector caspases. In A549 lung cancer cells, ectopic expression of miR-1 and miR-15a-3p enhances the activation of caspase 3 and caspase 7 (Nasser *et al.*, 2008). On the other hand, inhibition of miR-133a/b and miR-361-3p was able to activate caspase 3 and caspase 7 in 95D lung cancer cells (Du *et al.*, 2013). Furthermore, overexpression of miR-192 was able to inhibit cell viability in both *in vitro* and *in vivo* lung cancer studies (Feng *et al.*, 2011).

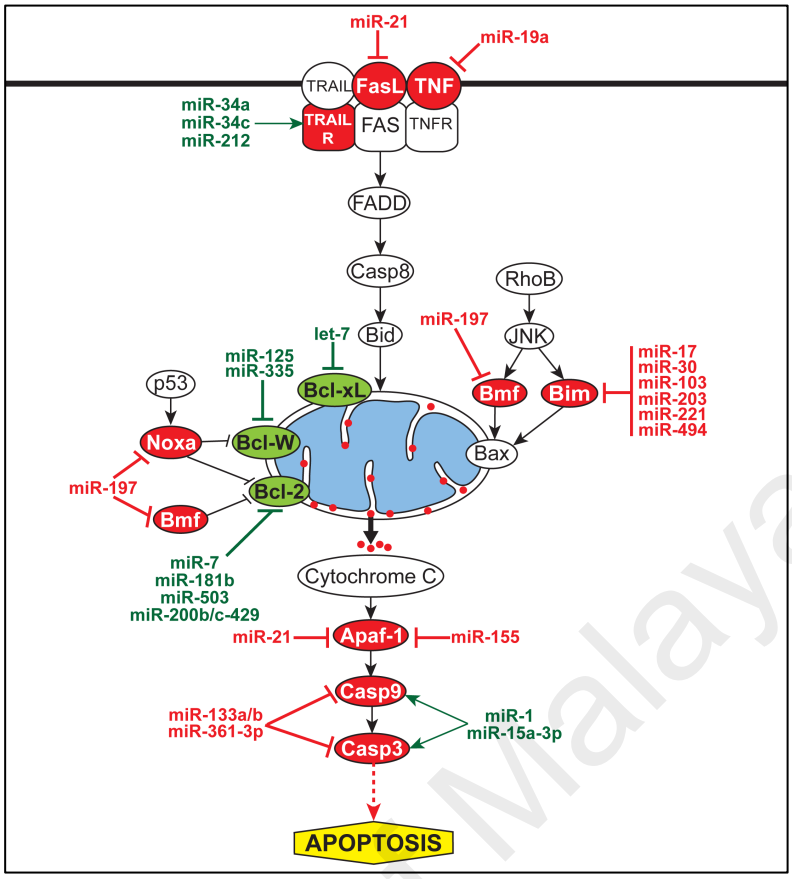

Figure 2.9: Scheme depicting up- and down-regulated miRNAs in lung cancer and the roles they play in apoptosis (Reproduced from Biomed Research International, Vol. 2014, Othman & Nagoor, 2014, The Role of MicroRNAs in the Regulation of Apoptosis in Lung Cancer and its Application in Cancer Treatment, Article ID 318030, with permission from Hindawi).

2.4.5 MiRNA in cancer treatment

The targeting of miRNAs as a therapeutic tool is very promising for applications in cancer medicine. The short sequences of mature miRNA have proven to be advantageous as they are almost always completely conserved across multiple vertebrate species. This makes them easy targets therapeutically, while also allowing the same miRNA-modulating compound to be used in preclinical efficacy and safety studies as well as in clinical trials (van Rooij & Kauppinen, 2014). Furthermore, as miRNAs typically have multiple targets within the same signaling pathway, this may potentiate the efficacy of miRNA-based treatments, as they are able to modulate entire pathways in a disease state (van Rooij & Kauppinen, 2014; Pichler & Calin, 2015). In general, there are two approaches employed in the development of miRNA-based

therapies: (i) restoration of tumour suppressor miRNA to reverse the loss of miRNA function using synthetic double-stranded miRNA mimics or viral vector-based overexpression and (ii) down-regulation of oncogenic miRNAs through the administration of chemically-modified anti-sense nucleotides (anti-miR/ antagomiR or miRNA inhibitors) (Figure 2.10) (Krutzfeldt *et al.*, 2005; Taylor & Schiemann, 2014).

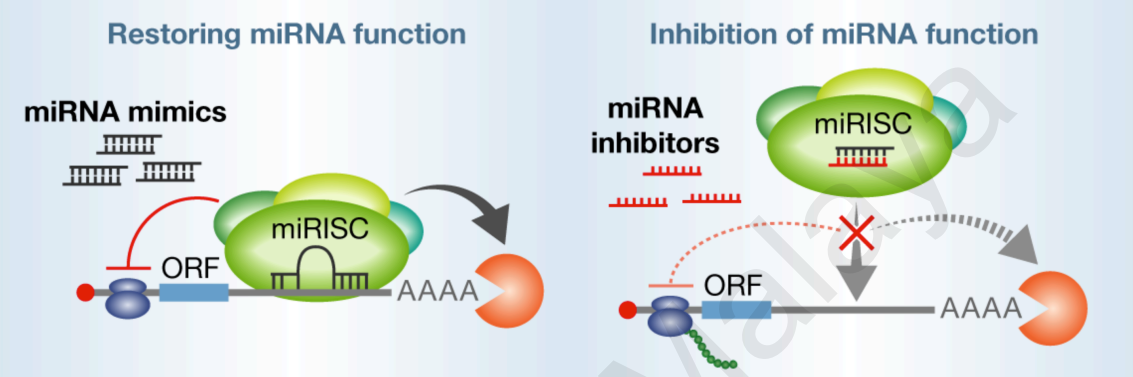

Figure 2.10: Modulation of miRNA activity by miRNA mimics and anti-miR oligonucleotides (Reproduced from EMBO Molecular Medicine, Vol. 6, van Rooij & Kauppinen, Development of MicroRNA Therapeutics is Coming of Age, 851-864, 2014, licensed under CC BY 3.0).

2.4.5.1 MiRNA mimics

Utilization of miRNA mimics, also termed miRNA replacement therapy, allows for the exploitation of tumour suppressors as it reintroduces lost or down-regulated miRNAs in cancer cells, to reactivate pathways that are necessary for normal cellular welfare (Bader *et al.*, 2010). MiRNA mimics are double stranded, with the strand identical to the miRNA of interest called the guide (anti-sense) strand, while the opposite strand is called the passenger (sense) strand. This passenger strand is less stable and is linked to a molecule, such as, cholesterol, to boost cellular uptake as well as chemical modifications to prevent RISC uptake (Chen *et al.*, 2008; Garzon *et al.*, 2010; Bader *et al.*, 2011; Thorsen *et al.*, 2012). MiRNA mimics can be delivered systemically using technologies already available for therapeutic siRNAs. Furthermore, reports have suggested that miRNAs will be well tolerated in normal tissues as they

have the same sequence as endogenous miRNAs and will therefore target the same set of genes, thus eliminating non-specific off target effects (Bader *et al.*, 2010).

Based on reports of its strong *in vitro* tumour-suppressive effects, miR-34, which is frequently silenced in lung cancer, has been a focus for clinical trials. MiR-34 mimics, using a lipid-based delivery vehicle distributed locally or systemically, was able to block tumour growth in mouse models of NSCLC (Wiggins *et al.*, 2010). The anti-oncogenic effects observed were accompanied by an increase of miR-34 expression in tumour tissues along with down-regulation of its direct targets (Wiggins *et al.*, 2010). In 2013, MiRNA Therapeutics announced that a liposome-formulated miR-34 mimic-based drug, called MRX34, was going to enter phase 1 study for patients with primary liver cancer or metastatic cancer with liver involvement, thus becoming the first miRNA mimic to advance into the clinical phase (Bouchie, 2013).

Another tumour suppressor miRNA of interest was let-7, which is frequently down-regulated in lung cancer. Studies have shown that intranasal administration of let-7 mimics induced a significant reduction in tumour growth in lung cancer xenograft models (Esquela-Kerscher *et al.*, 2008; Kumar *et al.*, 2008; Trang *et al.*, 2010; Trang *et al.*, 2011). This suggests that let-7 replacement therapy may have potential as a therapeutic treatment in humans. Other prospective miRNAs for therapeutic lung cancer treatment include miR-7, miR-29b, miR-34a, miR-145, miR-150, and miR-200c (Table 2.3).

2.4.5.2 MiRNA inhibitors

Mature miRNAs can be inhibited by anti-sense nucleotides (antagomiRs), thereby inducing their degradation or inhibition of their function. AntagomiRs are single stranded oligonucleotides that have miRNA complementary sequences with chemically modified backbones to enhance thermal stability, binding affinity, and specificity (Meister *et al.*, 2004). Addition of 2'-O-methyl-group or locked nucleic acid (LNA) constructs have been shown to improve miRNA stability and affinity towards endogenous miRNA, and sequesters them to prevent processing by RISC (Krutzfeldt *et al.*, 2005).

An example of an antagomiR used in lung cancer studies is anti-miR-150 expression vector (PR-ASO-150) (Table 2.3). A study demonstrated that PR-ASO-150 was able to inhibit A549 lung cancer cell proliferation and induce apoptosis *in vitro*. Furthermore, administration of PR-ASO-150 intratumourally into lung tumour xenografts in nude mice led to inhibition of tumour growth (Li *et al.*, 2012c).

Table 2.3: Pre-clinical miRNA-based therapeutic strategies for lung cancer

miRNA	Administration	Modulation Strategy	Delivery Technology	References
let-7	Intravenous	Replacement	Neutral liposomes	(Trang *et al.*, 2011)
	Intranasal	Replacement	Adenoviruses	(Esquela-Kerscher *et al.*, 2008)
	Intratracheal	Replacement	Lentiviruses	(Kumar *et al.*, 2008)
miR-200c	Intravenous	Replacement	Liposomes (NOV340)	(Cortez *et al.*, 2014)
miR-29b	Intravenous	Replacement	Cationic liposomes	(Wu *et al.*, 2013b)
miR-145	Intratumoral	Replacement	PEI	(Chiou *et al.*, 2012)
miR-150	Intratumoral	Inhibition	Cationic liposomes	(Li *et al.*, 2012c)
miR-7	Intratumoral	Replacement	Cationic liposomes	(Rai *et al.*, 2011)
miR-34a	Intratumoral	Replacement	Neutral liposomes	(Wiggins *et al.*, 2010)

(Reproduced from International Journal of Molecular Sciences, Vol. 16, Fujita *et al.*, Development of Small RNA Delivery Systems for Lung Cancer Therapy, 5254-5270, 2015, licensed under CC BY 4.0).

CHAPTER 3: MATERIALS AND METHODS

3.1 Cell lines

3.1.1 Cell lines and culture conditions

Human lung adenocarcinoma cell lines A549 (Cancer Research Initiative Foundation (CARIF), Sime Darby Medical Centre, Malaysia) and SK-LU-1 (AseaCyte Sdn. Bhd., Malaysia) were cultured in Roswell Park Memorial Institute 1640 medium (RPMI-1640) (Hyclone, GE Healthcare Life Sciences, USA) and minimum essential medium (MEM) α (Gibco, USA), respectively. Both culture mediums were supplemented with 10% (v/v) heat inactivated fetal bovine serum (FBS) (JR Scientific Inc., USA). Cells were grown as a monolayer and maintained in a carbon dioxide (CO_2) incubator (Memmert, Germany) with high relative humidity (95.0%), stable temperature (37°C), controlled CO_2 levels (5.0%) and controlled pH (7.2 – 7.4).

3.1.2 Sub-culturing cell line monolayers: harvesting a cell monolayer

The cell lines were split every two to three days, or when 80.0 – 90.0% confluency was achieved on the culture flask surface. Spent culture medium was removed and discarded using a serological pipette. The cell monolayer was rinsed with sterile autoclaved 1 × phosphate buffered saline (1 × PBS) to remove any residual serum that could inactivate trypsin activity. PBS was removed and discarded using a serological pipette. 3.0 ml of dissociating agent, 0.25% trypsin (Sigma-Aldrich, USA) ethylenediaminetetraacetic acid (EDTA) (Thermo Fisher Scientific, USA), was added to the culture flask. The culture flask was incubated in 37°C in the CO_2 incubator for approximately 10 min to allow the cells to detach from the bottom of the flask. The progress of cell detachment was checked every 5 min using an inverted fluorescence microscope (Nikon, Japan). Once cells were detached, equal volume of culture medium was added to the culture flask to inactivate trypsin activity and the suspension was transferred to a labeled 15.0 ml Falcon tube and centrifuged for 5 min at 1,500 RPM

using the Eppendorf Centrifuge 5702 (Eppendorf, Germany). The supernatant in the tube was discarded and the cell pellet was resuspended in fresh culture medium. The cell suspension was either collected for counting or divided into prepared culture flasks for routine maintenance of cell lines. For routine maintenance of cell lines, 2.0 ml of cell suspension was transferred to a new T-25 cm^2 culture flask with 3.0 ml of fresh culture medium and stored at 37°C in the CO_2 incubator.

3.1.3 Cell counting

A dye exclusion viability assay using a haemocytometer was used to determine the number of cells present in a specific population. Cell suspension was gently mixed and 20.0 µL of the suspension was aliquoted into a 1.5 ml microcentrifuge tube and 20.0 µL of 0.08% tryphan blue stain (Sigma-Aldrich, USA) was added to this aliquot and mixed well. The tube was left to stand for about 3 min, after which 10.0 µL of the mixture was removed and loaded on to a clean haemocytometer (Resistance, Germany) chamber to be counted. The counting was conducted under the inverted microscope at 100× magnification. Dead cells appeared blue, while viable cells appeared as unstained bright spheres. The number of cells in each of the four square grid corners was counted and the average number of cells was obtained. Each square grid represents 0.1 mm^3 or 10^{-4} ml volume, and the concentration of cells was determined according to the following formula, with a dilution factor of two.

$$\text{Cell Concentration (cell/ml)} = \left(\frac{\text{Avg. Number of Cells Counted}}{\text{Volume Counted (ml)}}\right) \times \text{Dilution Factor}$$

3.2 *BCL-XL* silencing via short interfering RNA (siRNA) transfection

Silencing of the *BCL-XL* gene was performed using the Stealth RNAi™ siRNA Duplex Oligunucleotides (Invitrogen, USA) (Table 3.1), according to a modified version of the manufacturer's protocol. One day prior to transfection, 1.5×10^5 cells were plated in 2.0 ml of appropriate medium in a 6-well plate (SPL Life Sciences, Korea). For each transfection sample, a Stealth RNAi™ -Lipofectamine™ 2000 complex was prepared as follows: 1.25 µL of 20.0 µM of Stealth RNAi™ oligonucleotide was diluted in 250.0 µL of Opti-MEM® I Reduced Serum Medium (Invitrogen, USA) to prepare the final concentration of 100.0 nM, and mixed gently (Tube 1). 5.0 µL of Lipofectamine™ 2000 Transfection Reagent (Invitrogen, USA) was diluted in 250.0 µL of Opti-MEM® I Reduced Serum Medium and mixed gently (Tube 2). Both solutions were left to incubate for 15 min at room temperature. After incubation, contents of Tube 1 and Tube 2 were combined and mixed gently. The combined solution was incubated for 15 min at room temperature to allow complexes to form. The complex was then added to the 6-well plate containing cells and 1.5 ml culture medium. The plate was mixed gently by rocking back and forth, and the cells incubated at 37°C in a humidified CO_2 incubator for 24 h. The same procedure was carried out with the Stealth RNAi™ siRNA Negative Control Low GC (Invitrogen, USA), Stealth RNAi™ siRNA Negative Control High GC (Invitrogen, USA), as well as the BLOCK-iT™ Alexa Fluor® Red Fluorescent Oligo (Invitrogen, USA). At 24 h post-transfection, total RNA was extracted using the miRNeasy® Mini Kit to determine the silencing efficiency of the siRNAs.

Table 3.1: Stealth RNAi™ siRNA Duplex Oligonucleotides used for transfection

Name	Sequence
siRNA 1	UCA CUA AAC UGA CUC CAG CUG UAU C
siRNA 2	AUG GGU UGC CAU UGA UGG CAC UGG G
siRNA 3	AUC ACC UCC CGG GCA UCC AAA CUG C

3.3 Total RNA extraction

3.3.1 Guanidinium isothiocyanate acidic phenol extraction using TRIzol® Reagent (Invitrogen, USA)

Transfected cells were harvested by trypsinization and centrifugation and cell pellet was resuspended in 1.0 ml of TRIzol® reagent. The cell lysate was passed through a pipette several times. The homogenized sample was transferred to a 1.5 ml microcentrifuge tube and incubated for 5 min at room temperature to allow for complete dissociation of nucleoprotein complexes. 0.2 ml chloroform (J.T. Baker, USA) was added and the tubes capped securely. The tubes were shaken vigorously by hand for 15 sec and incubated at room temperature for 3 min. The tubes were then centrifuged at 12,000 × *g* for 10 min at 4°C in the Sorvall Legend Micro17R (Thermo Fisher Scientific, USA) refrigerated centrifuge. Following centrifugation, the mixture separated into a lower red phenol-chloroform phase, an interphase, and a colorless upper aqueous phase. RNA remains exclusively in the aqueous phase. The volume of the aqueous phase was about 60.0% of the volume of TRIzol® reagent used for homogenization.

The aqueous phase was transferred to a fresh tube. The RNA was precipitated from the aqueous phase by mixing with 0.5 ml isopropanol (Merck, Germany). The samples were incubated at room temperature for 10 min and then centrifuged at 12,000 × *g* for 10 min at 4°C. The supernatant was removed and the pellet washed once with 1.0 ml of 75.0% ethanol (J.T. Baker, USA). The sample was mixed by vortexing and then centrifuged at 7,500 × *g* for 5 min at 4°C.

After centrifugation, the supernatant was removed and the RNA pellet was air-dried for about 5-10 min. The RNA samples were dissolved in nuclease-free water (Qiagen, Germany) by passing the solution a few times through a pipette tip, and incubated for 10 min in the water bath incubator (Memmert, Germany) at 58°C.

3.3.2 Silica membrane column-based extraction using miRNeasy® Mini Kit (Qiagen, USA)

Transfected cells were harvested by trypsinization and centrifugation and cell pellet was resuspended in 700.0 µL QIAzol Lysis Reagent (Qiagen, USA). The sample was transferred to a centrifuge tube and homogenized by passing through a pipette several times and vortexed vigorously for 15 sec. The homogenate was incubated at room temperature for 5 min, 140.0 µL chloroform was added and the tube capped securely. The tube was shaken vigorously for 15 sec and left to incubate at room temperature for 2-3 min. The tube was then centrifuged for 15 min at 12,000 × *g* at 4°C. The upper aqueous phase was transferred to a new collection tube and 1.5 volumes (≈ 525.0 µL) of 100.0% ethanol was added and mixed thoroughly by pipetting. 700.0 µL of sample was pipetted, including any precipitate, into an RNeasy® Mini column (Qiagen, USA) in a 2.0 ml collection tube. The tube was centrifuged at 8,000 × *g* for 15 sec, and the flow-through was discarded. This step was repeated for the remainder of the sample. 700.0 µL Buffer RWT (Qiagen, USA) was added to the RNeasy® Mini column and centrifuged for 15 sec at 8,000 × *g* and the flow-through discarded. 500.0 µL Buffer RPE (Qiagen, USA) was pipetted onto the RNeasy® Mini column and centrifuged at 8,000 × *g* and the flow-through discarded. Another 500.0 µL Buffer RPE was added to the RNeasy® Mini column and then centrifuged for 2 min at 8,000 × *g*. The RNeasy® Mini column was placed into a new 2.0 ml collection tube and centrifuged at full speed for 1 min to further dry the membrane. The RNeasy® Mini column was transferred to a new 1.5 ml collection tube and 30.0-50.0 µL RNase-free water was pipetted directly

onto the RNeasy® Mini column membrane. The tube was centrifuged for 1 min at 8,000 × *g* to elute the RNA.

3.4 RNA quantitation and quality check

3.4.1 Quantitation of RNA using NanoDrop 2000 (Thermo Fisher Scientific, USA)

The concentration and purification of extracted RNA was analyzed using the NanoDrop 2000. When the arm was open 1.0 µL of distilled water was pipetted directly on the pedestal and used as a blank. When the measurement was complete, the surfaces were wiped with a lint-free KimWipe before going on to the next sample. The RNA concentration, OD_{260}, OD_{280}, $A_{260/280}$, and $A_{260/230}$ ratio of the samples were measured.

3.4.2 Determination of RNA integrity using Agilent 2200 TapeStation System (Agilent Technologies, Germany)

The quality of extracted RNA was analyzed using the Agilent 2200 TapeStation. 4.0 µL R6K sample buffer was mixed with 1.0 µL RNA sample. The samples were denatured by heating at 72°C for 3 min. The samples were then placed on ice for 2 min and briefly centrifuged to allow the contents to collect in the base of the tubes. The Agilent 2200 TapeStation software was launched and the samples, ScreenTape R6K and loading tips were loaded into the Agilent 2200 TapeStation. The required samples were selected on the controller software and the RNA concentration (ng/µL) and RNA integrity number (RIN value) of the samples was measured.

3.5 Quantification of *BCL-XL* expression using quantitative reverse transcription polymerase chain reaction (qRT-PCR)

3.5.1 Reverse transcription polymerase chain reaction (RT-PCR)

First strand cDNA was synthesized for use in qRT-PCR using the SuperScript III First-Strand Synthesis SuperMix (Invitrogen, USA). The following kit components (Table 3.2) were combined on ice. For multiple reactions, a master mix without RNA was prepared.

Table 3.2: Kit components used to prepare cDNA samples

Component	Volume
2× RT Reaction Mix	10 µL
RT Enzyme Mix	2 µL
RNA (up to 1 µg)	χ µL
DEPC treated water	to 20 µL

The tube contents were gently mixed and incubated at room temperature for 10 min. The tubes were then incubated at 50°C for 30 min, and the reaction terminated at 85°C for 5 min. The tubes were chilled on ice and 1.0 µL of *Escherichia coli* (*E. coli*) RNAse H was added and the tubes incubated at 37°C for 20 min. The cDNA was then used in qPCR.

3.5.2 Quantitative polymerase chain reaction (qPCR)

The Platinum® SYBR® Green qPCR SuperMix-UDG with ROX (Invitrogen, USA) was used to carry out qPCR. The primers used for qPCR was purchased from First Base Laboratories Sdn Bhd, Malaysia (Table 3.3). For each qPCR reaction the following components were added to a 0.2 ml microcentrifuge tube. The volumes for a single 50 µL reaction are listed in Table 3.4. For multiple reactions, a master mix of common components was prepared and the appropriate volume added to each tube, and the unique reaction components (eg. template) was then added.

Table 3.3: Oligonucleotides used for qPCR determination of *BCL-XL* expression

Name	Sequence	Length
BCL-XL Forward	5'-CGT GGA AAG CGT AGA CAA GGA – 3'	21
BCL-XL Reverse	5' –ATT CAG GTA AGT GGC CAT CCA A– 3'	22
β-actin Forward	5' –AAG CCA CCC CAC TTC TCT CTA A– 3'	22
β-actin Reverse	5' –ACC TCC CCT GTG TGG ACT TG– 3'	20

Table 3.4: Kit components used to prepare qPCR samples

Component	Volume
Platinum® SYBR® Green qPCR SuperMix-UDG with ROX	25 µL
Forward primer, 10 µM	1 µL
Reverse primer, 10 µM	1 µL
Template (cDNA generated from 10 pg to 1 µg of total RNA)	≤ 10 µL
DEPC-treated water	to 50 µL

The reaction tubes were capped and gently mixed. The reactions were then placed into a preheated real-time instrument, the CFX96™ Real-Time PCR Detection System (Bio-Rad Laboratories, USA), and programmed as described in Table 3.5.

Table 3.5: Real-time PCR instrument conditions

50°C for 2 minutes hold (UDG incubation)
90°C for 2 minutes
40 cycles of: 95°C, 15 seconds 60°C, 30 seconds
Melting curve analysis

3.6 Protein expression analysis

3.6.1 Protein isolation using NE-PER® Nuclear and Cytoplasmic Extraction Kit (Pierce, USA)

NE-PER® Nuclear and Cytoplasmic Extraction Kit was used to extract the cytoplasmic protein from the whole cell lysate. This kit contains three reagents, Cytoplasmic Extraction Reagent I (CER I), Cytoplasmic Extraction Reagents II (CER II) and Nuclear Extraction Reagent (NER). 1 × Halt™ Protease (Thermo Fisher Scientific, USA) and 1 × Phosphatase inhibitor cocktails (Thermo Fisher Scientific, USA) were freshly prepared and added to CER I and NER in 1:1,000 dilution to prevent

proteolysis and dephosphorylation.

Cells were harvested by trypsinization and centrifugation, the supernatant in the tube was discarded and the pellet resuspended in 100.0 µL ice cold CER I and vortexed vigorously for 15 sec to fully resuspend the pellet. The tube was then incubated on ice for 10 min. 5.5 µL of ice cold CER II was added to the tube and vortexed for 5 sec. The tubes were incubated on ice for 1 min and then vortexed again for 5 sec. The tubes were then centrifuged at 16,000 × *g* for 5 min using the Sorvall Legend Micro 17R refrigerated centrifuge and the supernatant containing the cytoplasmic extract was transferred to a new pre-chilled tube. The protein solution was used immediately for western blotting, otherwise the solubilized proteins was stored at -20°C and the heating, centrifugation steps performed at the time of use.

3.6.2 Protein concentration quantification using Pierce® bicinchoninic acid (BCA) protein assay kit (Thermo Fisher Scientific, USA)

The Pierce BCA Protein Assay Kit was used to determine the protein concentration of extracted protein samples. Table 3.6 was used to prepare a set of protein standards. The contents of one Albumin Standard (BSA) ampule were diluted into several clean microcentrifuge tubes. Final BSA concentrations of 2,000, 1,500, 1,000, 750, 500, 250, 125, and 25 µg/ml were used to create a standard curve. This allows for the determination of the unknown sample's concentration.

A BCA working reagent was prepared by mixing 50 parts of BCA Reagent A with 1 part of BCA Reagent B (50:1, Reagent A: Reagent B). 10.0 µL blank, standards and samples were diluted with 200.0 µL of working reagent and mixed thoroughly in a microcentrifuge tube. The tubes were incubated at 37°C for 30 min. The tubes were cooled to room temperature and absorbance was measured at 562 nm using the NanoDrop 2000. After obtaining the sample's concentration, samples were normalized

to the same concentration with nuclease free water. All samples were kept at -20°C freezer until further use.

Table 3.6: Preparation of diluted albumin (BSA) standards

Vial	Volume of Diluent (µL)	Volume and Source of BSA (µL)	Final BSA Concentration (µg/ml)
A	0	300 of Stock	2,500
B	125	375 of Stock	1,500
C	325	325 of Stock	1,000
D	175	175 of vial B dilution	750
E	325	325 of vial C dilution	500
F	325	325 of vial E dilution	250
G	325	325 of vial F dilution	125
H	400	100 of vial G dilution	25
I	400	0	0 = Blank

3.6.3 Protein sample preparation

Antibodies typically recognize a small portion of the protein of interest (epitope), and this domain may reside within the three dimensional conformation of the protein. To enable access of the antibody to this portion it is necessary to denature the protein. Lane Marker Reducing Sample Buffer (5×) (Thermo Fisher Scientific, USA) contains dithiothreitol (DTT) as a reducing agent to reduce disulphide bridges within tertiary protein structures to produce primary protein structures. The sample buffer also contains sodium dodecyl sulfate (SDS), which binds to the polypeptides to form complexes with fairly constant negative charge to mass ratios. The electrophoretic migration rate through the gel is therefore determined only by the size of the complexes.

First, cytoplasmic protein samples and the Lane Marker Reducing Sample Buffer (5×) were equilibrated to room temperature. Cytoplasmic protein concentrations were diluted using distilled H_2O (dH_2O) to a final concentration of 1.0 µg/ml. A final volume of 20.0 µL of cytoplasmic protein samples was mixed with 5.0 µL sample buffer. These mixtures were vortexed before boiling for 5 min at 95°C using a thermal cycler, and then cooled to room temperature.

3.6.4 Sodium dodecyl sulphate polyacrylamide gel electrophoresis (SDS-PAGE)

SDS-PAGE is a technique for separating proteins according to their molecular weight. The separation of protein molecules within a gel is determined by relative size of the pores formed within the gel. 12.0% resolving gel was used to separate proteins ranging from 14 – 70 kDa. 4.0% stacking gel and 12.0% resolving gel was prepared by mixing together the reagents listed in Table 3.7. Freshly prepared 10.0% (w/v) ammonium persulfate (APS) was added last to the mixture to initiate gel polymerization. Bromophenol blue, an anionic small molecule, was added to the stacking gel and functioned as a tracking dye, which monitored the migration front of the proteins.

18.0 cm × 16.0 cm, with 1.0 mm thickness glass plates (Bio-Rad, USA) were aligned and clipped to the casting tray (Bio-Rad, USA). The resolving gel was prepared and loaded until 75.0% of the glass was filled. The remaining resolving gel solution was kept in a tube rack as an indicator of complete gel polymerization, which takes approximately 30 min. Immediately after adding the resolving gel, 0.1% (v/v) SDS was added gently on top of the resolving gel to prevent oxidization and dehydration of the gel, which can slow down the polymerization process. After polymerization was complete, 0.1% SDS solution was rinsed out by tilting the casting tray and blotting out the solution with Kim-wipes.

The desired volume of 10.0% APS was added into the stacking solution. The solution was mixed well and added immediately to the cast above the resolving gel. The stacking solution was ensured to completely fill 100.0% of the glass plate until it overflows. A 10-well gel comb with a 1.0 mm thickness was inserted at an angle to prevent formation of air bubbles. The remaining stacking gel solution was kept in a tube rack as an indicator of complete polymerization (approximately 30 min).

Table 3.7: Reagents for preparation of stacking resolving gel for SDS-PAGE

Reagent	Stacking Gel (4.0%) (µL)	Resolving Gel (12.0%) (µL)
40% Acrylamide (Promega, USA)	500	4,500
0.5M Tris-HCl (pH 6.8)	1,260	-
1.5M Tris-HCl (pH 8.8)	-	3,750
10% SDS	50	150
Distilled H_2O (dH_2O)	3,150	6,517.5
Tetramethyl-ethylenediamine (TEMED) (Acros, USA)	5	7.5
10% (w/v) Fresh Ammonium Persulfate (APS)	25	75
Bromophenol Blue (Fisher Scientific, USA)	10	-
Total Volume	**5,000**	**15,000**

3.6.5 Protein sample loading and running the gel

The glass plates were transferred to the Mini PROTEAN Tetra System (Bio-Rad, USA) and placed in the holder facing each other. The space between the gels was filled fully with 1 × Tris/Glycine/SDS (TGS) running buffer. The comb was gently removed and the wells were flushed with TGS buffer to allow the wells to form properly and to rinse off traces of unpolymerized gel. The tank was filled with sufficient amount of buffer according to the number of gels being run. 5.0 µL of biotinylated protein ladder (Cell Signaling Technology, USA) was loaded into the first well (Protein ladder sizes are listed in Appendix B). 20.0 µL of protein samples pre-mixed with sample buffer was then added to subsequent wells. Gels were run at 110 volts with 400 mA until the sample front reached the resolving gel (approximately 15 min), followed by 150 volts with 400 mA until the end of the gel. Power supply was provided by the Power Pack (Bio-Rad, USA).

3.6.6 Western blot electrotransfer

The 2.0 µm nitrocellulose membrane (Bio-Rad, USA) and the extra thick blot paper (Bio-Rad, USA) were cut to the same size as the gel or slightly larger than the gel. The membrane and filter papers were soaked in transfer buffer made up of 1 × TGS with 20% (v/v) methanol (Merck, Germany), for 10 min. Once the SDS-PAGE has finished

running, the glass was removed from the tank carefully. The upper glass was removed using a plastic spatula. Using a delicate task wiper, the stacking gel was carefully torn away from the resolving gel. The glass plate was then inverted over the transfer buffer and lifted so that the surface tension will peel the gel from the glass plate. The gel was soaked in transfer buffer for at least 10 min. The "transfer sandwich" was then placed in the Trans-Blot SD Semi-Dry Transfer Cell (Bio-Rad, USA). Each layer of the sandwich was rolled out to ensure no air bubbles were formed. Transfer of proteins from gel to membrane was run at 50 mA at 25 volts for 90 min using the MP-2AP Power Supply (Major Science, Taiwan).

Transfer sandwich:

Cathode (–)

Blot paper

PAGE gel

Nitrocellulose membrane

Blot paper

Anode (+)

After transferring, the membrane was stained with 0.1% (w/v) Ponceau S (Sigma Aldrich, USA) for 30 sec to check the efficiency of proteins transferred. After observation, the membrane was washed twice with dH_2O by shaking slowly on the Reciprocal Shaker MS-RC (Major Science, Taiwan) for 2 min each. The membrane was then blocked for 1 h at room temperature with agitation in blocking buffer containing 5.0% (w/v) non-fat skim milk powder (Merck, Germany), 0.05% (v/v) Tween 20 (Promega, USA) in 1 × tris-buffered saline (TBS), to prevent non-specific binding of the primary and secondary antibodies to the membrane.

The blocked membrane was washed with TBS with Tween 20 (TBST) buffer three times, 5 min each. The membrane was then incubated in primary antibody at appropriate dilution in 10.0 ml primary antibody dilution buffer for 1 h at room temperature with gentle agitation, followed by 4°C overnight. The following day the membrane was incubated at room temperature for 1 h with gentle agitation. The membrane was then washed three times with 1 × TBST, 5 min each wash. Antibody concentration was determined according to manufacturer's protocol as mentioned in Table 3.8.

The membrane bound with primary antibody was then probed with anti-rabbit IgG HRP-linked antibody (Cell Signaling Technology, USA) and anti-biotin HRP-linked antibody (Cell Signaling Technology, USA) at a dilution of 1:1:1000 in appropriate secondary antibody dilution buffer, for 1 h at room temperature with gentle agitation (Table 3.8). The membranes were then washed three times with 1 × TBST buffer for 5 min with agitation, followed by a single wash with 1× TBS buffer for 5 min, with agitation.

Table 3.8: Antibodies dilution buffer and dilution ratio

Antibody	Dilution Buffer	Dilution
GAPDH (14C10) Rabbit mAb	5% w/v BSA, 1×TBS, 0.1% Tween 20	1:10,000
BCL-XL (54H6) Rabbit mAb	5% w/v nonfat dry milk, 1×TBS, 0.1% Tween 20	1:1,000
AKT (pan) (C67E7) Rabbit mAb	5% w/v BSA, 1×TBS, 0.1% Tween 20	1:1,000
SMAD2 (86F7) Rabbit mAb	5% w/v nonfat dry milk, 1×TBS, 0.1% Tween 20	1:1,000
Anti-rabbit IgG, HRP-linked	5% w/v BSA, 1×TBS, 0.1% Tween 20	1:1,000
Anti-biotin, HRP-linked	5% w/v BSA, 1×TBS, 0.1% Tween 20	1:1,000

3.6.7 Exposure of membrane using charged couple device (CCD) camera

Western Bright Quantum (Advansta, USA) is a high-sensitivity substrate that reacts with horseradish peroxidase (HRP) conjugated to the secondary antibodies on the membrane by releasing chemiluminescence signal. The kit utilized contained two solutions and the working solution was prepared by mixing equal parts of each component. The membrane was incubated in the working solution for 2 min and the excess substrate on the membrane was blotted away. Bands were then visualized under a CCD camera using a chemiluminescent imaging system, the Fusion FX7 system (Vilber Lourmat, France) and quantified using the ImageJ v1.48 Analyst software (National Institutes of Health, USA) with band intensities normalized to GAPDH.

3.7 3-(4,5-dimethylthiazol-2-yl)-2,5-diphenltetrazolium bromide (MTT) cell viability assay

Cells were harvested by trypsinization and centrifugation, and then re-suspended with appropriate culture medium. Using a dye exclusion viability assay, viable cells were counted and 1.0×10^4 cells in 100 μL of medium were plated in triplicates onto a 96-well microtiter plate (Thermo Fisher Scientific, USA). The plate was incubated at 37°C overnight in a CO_2 incubator to allow for cell attachment to the well surface. Commencement of siRNA transfection was carried out at 100.0 nM at various incubation periods (12 h, 24 h and 48 h). Wells containing Stealth RNAi™ siRNA Negative Control Low GC were used as negative controls and solvent controls using Opti-MEM® I Reduced Serum Medium and Lipofectamine™ 2000 Transfection Reagent were conducted to ensure that decrease in cell viability was not solvent induced. Wells containing cells at descending concentrations (10,000 cells, 5,000 cells, 2,500 cells, 1,250 cells and 0 cells) via a serial dilution was used to construct standard curves for quantification purposes.

Following incubation, 20.0 µL MTT reagent (5.0 mg/ml) (Calbiochem, USA) was added to each well and incubated in the dark at 37°C for 1 h. Periodically cells were viewed under an inverted microscope for the presence of purple formazon crystals at the bottom of each well. When the purple formazon crystals were clearly visible under the microscope, the media containing MTT reagent was aspirated and 200.0 µL of dimethyl sulfoxide (DMSO) (Merck, Germany) was added to dissolve the purple formazon precipitates. After a few minutes at room temperature, to allow for the complete color stabilization of the formazon compound, results were obtained using a microtiter plate reader (Tecan Sunrise®, Switzerland) at 570 nM absorbance wavelength and 650 nM reference wavelength. The results were then quantified using the Magellan Version 6.3 (Tecan, Switzerland) software.

3.8 Annexin V-FITC apoptosis detection assay

The FITC annexin V apoptosis detection kit (BD Biosciences, USA) was used to quantitatively determine the percentage of cells within the population that are actively undergoing apoptosis. The kit was made up of three components: 10 × Annexin V Binding Buffer, FITC Annexin V and Propidium Iodide (PI) Staining Solution.

At 72 h post-transfection media from the wells was transferred to a 15 ml Falcon tube and placed on ice. This media contains cells that have become detached from the wells during the cell death process. The remaining adherent living cells in the wells was then gently washed with 1.0 ml 1 × PBS. 1.0 ml 0.25% trypsin EDTA was added and the plate incubated for 5 min at 37°C or until the cells appear to be detached when evaluated under the microscope. 1.0 ml appropriate media, containing 10.0% FBS, was added to deactivate trypsin. Cells were then resuspended in the culture medium that was previously transferred into the Falcon tube and centrifuged at 1,500 RPM for 10 min. The supernatant was discarded and 500.0 µL of cold PBS was added and the tube

centrifuged at 3,263 RPM for 5 min.

PBS was removed from the tubes and 100.0 µL cold 1 × binding buffer was added followed by 5 µL of FITC annexin V and 5 µL propidium iodide. The samples were gently vortexed and incubated for 15 min at room temperature in the dark. Another 400.0 µl of 1 × binding buffer was added to each sample and signals were detected from 1.0×10^4 cell population using the BD FACSCanto™ II flow cytometer (BD Biosciences, USA) and examined on the BD FACSDiva™ (BD Biosciences, USA) software.

3.9 Detection of caspase 3/7 activation

The Caspase-Glo® 3/7 assay (Promega, USA) is a homogeneous, luminescent assay that measures the activities of caspase 3 and 7, which play key effector roles in apoptosis. The assay contains two components, the Caspase-Glo® 3/7 buffer and the Caspase-Glo® 3/7 substrate (lyophilized). Prior to starting the experiment, the Caspase-Glo® 3/7 buffer and Caspase-Glo® 3/7 substrate was equilibrated to room temperature and the contents of the Caspase-Glo® buffer bottle was transferred to the amber bottle containing Caspase-Glo® 3/7 substrate. The contents were mixed by swirling and inverting until the substrate is thoroughly dissolved to form Caspase-Glo® 3/7 reagent.

48 h post-transfection cells were harvested by trypsinization and centrifugation, and then re-suspended in a 1:1 ratio of 50.0 µl 1 × PBS and 50 µl of Caspase-Glo® 3/7 reagent. Samples were incubated at room temperature for 1 h in the dark and luminescence was then detected using the GloMax Multi Luminescence Multimode Reader (Promega, USA).

3.10 Cell cycle analysis

Cell-cycle analysis was performed by flow cytometry using the BD Cycletest™ Plus DNA Kit Assay (BD Biosciences, USA) 48 h post-transfection. This kit contains 3 solutions: Solution A, which contains trypsin in a spermine tetrahydrochloride detergent buffer for the enzymatic disaggregation of solid tissue fragments and digestion of cell membranes and cytoskeletons; Solution B, which contains trypsin inhibitor and ribonuclease A in citrate-stabilizing buffer with spermine tetrahydrochloride to inhibit trypsin activity and to digest RNA; and Solution C which contains PI and spermine tetrahydrochloride in citrate stabilizing buffer.

48 h post-transfection cells were harvested by trypsinization and centrifugation, and then resuspended in 1.0 ml 1 × PBS before being centrifuged again at 400 × *g* for 5 min. The supernatant was decanted and 250.0 µL Solution A was added and gently mixed by tapping. Samples were incubated at room temperature for 10 min, followed by addition of 200.0 µL of Solution B and incubated a further 10 min at room temperature. Lastly, 200.0 µL of cold Solution C was added and samples were incubated on ice for 10 min. Signals were detected from 1.0×10^4 cell population using the BD FACSCanto™ II flow cytometer (BD Biosciences, USA) and examined on the BD FACSDiva™ (BD Biosciences, USA) software. Results were analyzed using the ModFit LT v3.2.1 (Verity Software House, USA) and the percentage of cells in G_0/G_1, S, and G_2/M phase were counted and compared.

3.11 Quantification of miRNA expression using reverse transcription-quantitative real-time polymerase chain reaction (RT-qPCR) using TaqMan® MicroRNA Assays

The primers used for RTq-PCR was obtained from Applied Biosystems, USA (Table 3.9).

Table 3.9: TaqMan® MicroRNA Assays used for qRT-PCR

Assay ID	Accession Number	Assay Name
000480	MIMAT0000256	hsa-miR-181a
001998	MIMAT0003886	hsa-miR-769-5p
000554	MIMAT0000703	hsa-miR-361-5p
002874	MIMAT0005892	hsa-miR-1304-5p
001571	MIMAT0003276	hsa-miR-608
001093	-	U6

3.11.1 Reverse transcription polymerase chain reaction (RT-PCR)

RT-PCR was performed using the TaqMan® MicroRNA Reverse Transcription Kit (Applied Biosystems, USA) according to a modified version of the manufacturer's protocol. The components of the kit were first allowed to thaw on ice. The RT master mix was then prepared by combining the components listed in Table 3.10.

Table 3.10: Kit components used to prepare RT master mix

Component	Master mix volume per 10 µL reaction*
100 nM dNTPs (with dTTP)	0.10 µL
MultiScribe™ Reverse Transcriptase, 50 U/µL	0.67 µL
10× Reverse Transcription Buffer	1.00 µL
RNase Inhibitor 20 U/ µL	0.13 µL
Nuclease-free water	2.78 µL
Total Volume	**4.68 µL**

* Each 10 µL RT reaction consists of 4.68 µL master mix, 2.00 µL of 5× RT primer, and 3.30 µL RNA samples.

The components were mixed gently and centrifuged to bring solution to the bottom of the tube. The RT master mix was then placed on ice until the RNA reaction was prepared.

The 5 × RT primer and RNA template was thawed on ice. The RT primer tubes were then vortexed to mix and then briefly centrifuged. For each 10.0 µL RT reaction, the RT master mix was combined with 10.0 ng of total RNA in the ratio of 4.68 µL RT master mix : 3.30 µL total RNA. The mixture was mixed gently, and centrifuged briefly to bring the solution to the bottom of the tube. 2.0 µL RT primer from each assay set was added to the corresponding RT reaction tube. The reaction tube was sealed and mixed gently, followed by a brief centrifugation. The reactions were incubated on ice for 5 minutes and then loaded into the thermal cycler, and run according to the following conditions (Table 3.11):

Table 3.11: Thermal cycler conditions for cDNA synthesis

Time	Temperature
30 minutes	16°C
30 minutes	42°C
5 minutes	85°C
∞	4°C

3.11.2 Quantitative real-time PCR (qPCR)

The following components (Table 3.12) were placed on ice and gently mixed. The volumes required, based upon the number of reactions and a reaction volume of 10 µL was calculated.

Table 3.12: Components used to prepare qPCR master mix

Component	Master mix volume per 10 µL reaction
TaqMan® Fast Advanced PCR Master Mix	5.00 µL
Nuclease-free water	3.84 µL
TaqMan® MicroRNA Assay (20)	0.50 µL
Product from RT reaction	0.67 µL
Total Volume	**10.01 µL**

The reaction components were combined in a microcentrifuge tube and gently mixed by inversion and then centrifugation. 10.0 µL was transferred into low-profile microcentrifuge tubes and the tubes were sealed and briefly centrifuged. The reactions

were then loaded into the real-time PCR instrument, and run according to the following conditions (Table 3.13).

Table 3.13: Real-time PCR instrument conditions for qPCR

Step	Optional AmpErase UNG Activity	Enzyme Activation	PCR	
	HOLD	HOLD	CYCLE (40 Cycles)	
			Denature	Anneal/Extend
Temperature	50°C	95°C	95°C	60°C
Time	2 min	10 min	15 sec	60 sec

3.12 Transfection of mimics/ hairpin inhibitors

miRIDIAN miRNA mimics and hairpin inhibitors were purchased from GE Healthcare Dharmacon, USA (Table 3.14). MiRNA mimics were designed as double-stranded oligonucleotides to mimic the function of endogenous mature miRNA, whereas miRNA hairpin inhibitors are RNA oligonucleotides with novel secondary structures that are designed to inhibit the function of endogenous miRNA. Negative control sequences were based on *Caenorhabditis elegans* (*C. elegans*) miRNA (cel-miR-67) and have minimal sequence identity in humans, mouse and rats. The miRIDIAN microRNA mimic and inhibitor transfection control with Dy547 are also based on *C. elegans* miRNA cel-miR-67, and were used as a transfection control for monitoring delivery into the cells.

Table 3.14: Mature miRNA accession number and sequences

ID	Accession Number	Sequence
Hsa-miR-769-5p	MIMAT0003886	UGAGACCUCUGGGUUCUGAGCU
Hsa-miR-361-5p	MIMAT0000703	UUAUCAGAAUCUCCAGGGGUAC
Hsa-miR-1304-5p	MIMAT0005892	UUUGAGGCUACAGUGAGAUGUG
Hsa miR-608	MIMAT0003276	AGGGGUGGUGUUGGGACAGCUCCGU
Cel-miR-67	MIMAT0000039	UCACAACCUCCUAGAAAGAGUAGA

One day prior to transfection, 1.0×10^6 cells were plated in 5.0 ml of appropriate medium, without antibodies, in a T-25 cm^2 culture flask. A 20.0 μM miRNA stock solution in 1 × siRNA buffer (GE Healthcare Dharmacon, USA) was prepared. In separate tubes, 20.0 μL of 20.0 μM miRNA was diluted in 480.0 μL serum-free medium (Tube 1) to prepare the final concentration of 80.0 nM, and 6.0 μL DharmaFECT 1 Transfection Reagent (GE Healthcare Dharmacon, USA) was diluted in 494.0 μL serum free medium (Tube 2). The contents of each tube was gently mixed by pipetting carefully up and down, and incubated for 5 min at room temperature. After incubation, the contents of Tube 1 was added to Tube 2 and mixed gently by pipetting up and down. The combined solution was incubated for 20 min at room temperature to form the transfection mix. 4.0 ml complete medium was added to the transfection mix for the desired transfection volume. The culture medium from the T-25 cm^2 culture flask was removed and 5.0 ml of the appropriate transfection mix was added to the flask. The flask was then incubated at 37°C in 5% CO_2 for 24 h. If cell toxicity was observed after 24 h, the transfection medium was replaced with complete medium and incubation continued. Transfection efficiencies were assessed 24 h post-transfection by visualizing uptake of miRIDIAN MicroRNA Mimic/ Hairpin Inhibitor Transfection Control with Dy547 using fluorescence microscopy. For mRNA analysis, 24 h post-transfection, total RNA was isolated using miRNeasy® Mini Kit (Section 3.3.2) and analyzed using the ScreenTape R6K on the Agilent 2200 TapeStation (Section 3.4.2). RT-qPCR analysis of miRNA expression was carried out using TaqMan® MicroRNA Assays (Section 3.11). Expressions of miRNAs were normalized to the expression of the U6 small nuclear RNA. The $2^{-\Delta\Delta Ct}$ method was used to determine relative quantitation of miRNA, and fold difference relative to scrambled negative controls was determined as Log2 ($2^{-\Delta\Delta Ct}$). The detection of caspase 3/7 activity was performed 48 h post-transfection using the Caspase-Glo® 3/7 assay (Section 3.9) while apoptosis was detected 72 h post-

transfection using the FITC annexin V apoptosis detection kit (Section 3.8), as described previously. Cell cycle analysis was also carried out 48 h post-transfection using the BD Cycletest^{TM} Plus DNA Kit Assay (Section 3.10).

3.13 Combined transfection with si*BCL-XL* and miR-608 inhibitors or miR-361-5p mimics

To observe the connection between *BCL-XL*, miR-608, miR-361-5p and cell death, cells were plated for 24 h prior to transfection with 100.0 nM siRNA 1, as described in Section 3.2. 24 h post-transfection, spent media was removed and cells were transfected with 80.0 nM of either miR-608 hairpin inhibitor, miR-361-5p mimic, or their appropriate negative controls, as described in Section 3.12. The detection of caspase 3/7 activity was performed 48 h post-transfection using the Caspase-Glo® 3/7 assay (Section 3.9), while apoptosis was detected 72 h post-transfection using the FITC annexin V apoptosis detection kit (Section 3.8) as described previously.

3.14 Zebrafish care and use

Experiments involving zebrafish were approved by the University of Malaya, Faculty of Medicine, Institutional Care of Use Committee (FOM, IACUC) (Ethics reference number: 2015-181006/IBS/R/NO) and complied with all relevant animal welfare laws, guidelines and policies. Wild-type *Danio rerio* zebrafish adults were cared for and maintained in the Zebrafish Laboratory (Association for Assessment and Accreditation of Laboratory Animal Care (AAALAC) accredited), Department of Biomedical Science, Faculty of Medicine, University of Malaya, using standard husbandry conditions: 14 hours:10 hours light:dark cycle, regulated conductivity (500.0 μS), pH (7.0) and temperature (28°C), in a ZebTEC zebrafish housing system (Tecniplast, Italy). Adult zebrafish were fed daily, twice with Hikari dry food pellets and once with live *Artemia salina* (brine shrimp).

3.14.1 Zebrafish breeding

The evening prior to collection of eggs, random pairwise mating of zebrafish was performed. At a ratio of 2:1 female:male adult zebrafish were placed in a plastic tank with a breeding insert (Tecniplast, Italy) that has been marbled. Marbles are used to cover the bottom of the tank to prevent breeding fish from eating freshly laid eggs that sink between the marbles to safety. Adult zebrafish will initiate breeding behavior that results in the laying and fertilization of eggs, at the onset of the light cycle.

An hour after the onset of the light cycle, eggs were harvested and transferred to a clean 60 mm × 15 mm petri dish (Corning, NY, USA) containing system water. The eggs were rinsed with clean system water 3 to 6 times to remove any debris. Alternatively, the eggs are swirled around the petri dish and a Pasteur pipette was used to remove any remaining debris, as it swirls for a longer time around the dish. Once the eggs are cleaned, they were transferred into a clean petri dish filled with system water and incubated at 28.5°C. At 3.5 h post-fertilization (hpf), embryos were observed under a Leica EZ4 dissecting microscope (Leica Microsystems, Germany) for any dead or unhealthy embryos to be removed. Embryos were left to incubate and develop in system water containing methylene blue (Sigma Aldrich, USA), and transferred into system water with 75 µM 1-phenyl 2-thiourea (PTU) (Sigma Aldrich, USA) 1 day post-fertilization (dpf) to inhibit pigment formation. Embryos were again incubated at 28.5°C until they were used for experiments at 2 dpf.

3.15 *In vivo* apoptosis model

3.15.1 Cell staining

One day after A549 cells are transfected with miR-608 mimics / inhibitors, miR-361-5p mimics / inhibitors, and mimic and inhibitor negative controls in a 6-well plate, cells were labeled with 1,1'-Dioctadecyl-3,3,3',3'-Tetramethylindocarbocyanine Perchlorate (Dil) dye, a lipophilic fluorescent tracking dye (red fluorescence; excitation: 549 nm; emission: 565nm) that is stable in live zebrafish for at least 2 weeks. Dil stock solution (20 mg/ml) was diluted at 1:1,000 in Dulbecco's phosphate-buffered saline (DPBS) with calcium and magnesium.

Spent media was removed from the wells and cells were washed with 2.0 ml of 1 × DPBS. 2.0 ml Dil labeling solution was added to the wells and left to incubate for 30 min at 37°C in the dark. Following incubation, the medium containing detached labeled cells was collected and transferred to a 15 ml Falcon tube and centrifuged for 1,000 × *g* for 3 min. Supernatant was discarded and cell pellet resuspended in 2.0 ml 1 × DPBS and centrifuged for 1,000 × *g* for 3 min. This process was repeated one more time. The cell pellet was then resuspended in 2.0 ml fresh complete medium and added back to the wells. The plate was then incubated overnight at 37°C in the CO_2 incubator.

3.15.2 Embryo preparation

Chorions of 2 dpf embryos were removed with sharp microsurgical forceps (Watchmaker #5) (Samco, UK). The embryos were held with one forcep and with the help of another pair of forceps a tear was gently made in the chorion and turned upside down so that the embryos fall out with the help of another pair of forceps. The embryos can be brought to the center of the dish for viewing by gently swirling the medium in a circular motion. The embryos were rinsed thoroughly in system water three times and transferred to fresh PTU water.

3.15.3 Embryo microinjection

Labeled transfected cells were harvested and resuspended in culture medium containing 1.0% FBS, at a density of 1.0×10^5 cells/ml. Cells were kept on ice and in the dark until time of injection. Dechorionated embryos were anaesthetized by transferring them into 10.0% benzocaine (Sigma Aldrich, USA) in system water for 2 min before aligning them onto a 1.0% (w/v) modified agarose gel plate. Excess water was removed with a Pasteur pipette.

A microloader (Eppendorf, Germany) was used to load 10.0 µL cell suspension into a 20 µm TransferTip (Eppendorf, Germany), which was connected to A FemtoJet Microinjector (Eppendorf, Germany). Using the InjectMan NI 2 Micromanipulator (Eppendorf, Germany) and the automated Leica M205 A stereo microscope (Leica Microsystems, Germany), the cell suspension was injected into the middle of the embryonic yolk sac region with constant injection pressure (P_i) (100 hpa), compensation pressure (P_c) (45 hpa) and injection time (t_i) (0.1 sec). The injection volume and cell suspension was calibrated to be approximately 100-200 cells/injection in each embryo. After transplantation, embryos were rinsed with system water and then transferred into fresh PTU water and placed at 37°C overnight.

3.15.4 Whole mount caspase 3 immunofluorescence

At 24 h post-injection (hpi), live zebrafish embryos were rinsed twice with 1 × PBS with 0.1% Tween 20 (PBST, pH 7.0) for 5 min each. PBST was removed leaving liquid just above the embryos, and embryos were euthanized with an overdose of 10.0% benzocaine. Embryos were then fixed in 4.0% (w/v) paraformaldehyde (PFA) (Sigma Aldrich, USA) overnight at 4°C.

The following day, PFA was removed and embryos were washed twice in 1 × PBST, 5 min each. 1.0 ml of ice-cold 100.0% methanol was added drop-wise to permeabilize the embryos, and left to incubate at -20°C for 2 h. Methanol was then removed and 1.0 ml 1 × PBST with 0.3% Triton X (Scharlab, Spain) and 1.0% dimethyl sulfoxide (DMSO) (Merck, USA) (PDT) was added. PDT was removed and 1.0 ml fresh PDT was added and embryos were incubated for 30 min at room temperature, with gentle agitation. This step was repeated once. After the washes, PDT was removed and 500.0 µL of blocking buffer made of 1 × PBST with 10.0% FBS and 2.0% BSA was added and embryos were incubated for 1 h at room temperature, with gentle agitation. Embryos were then stained with purified rabbit anti-active caspase 3 antibody (BD Biosciences, USA) (1:500 dilution) for 2 h at 25°C with gentle agitation, followed by two washes in PDT, 30 min each. Again embryos were incubated with blocking buffer for 1 h at room temperature, then stained with anti-rabbit IgG Fab2 Alexa Fluor 647 Conjugate (Cell Signaling Technologies, USA) (1:500 dilution) overnight at 4°C.

The following day, blocking buffer/antibody solution was removed and embryos were washed twice with PDT, 30 min each wash. Embryos were then visualized and imaged using the Leica confocal laser-scanning microscope SP5 II (Leica Microsystems, Germany), at low magnification (5×) (excitation: 650 nm; emission: 665 nm), and Leica Application Suite (LAS) software v5.0 (Leica Microsystems, Germany). Fluorescence of activated caspase 3 was quantified using ImageJ v1.48 Analyst software. A fluorescence intensity threshold of 130-160 was set to eliminate background fluorescence and the "analyze measurement" tool was used to generate arbitrary fluorescence intensity measurements in the threshold area.

3.16 Bioinformatics analyses of miRNA gene targets

An *in silico* approach was used to identify the putative miRNA targets by using TargetScan Human v6.2 (Lewis *et al.*, 2005) (Whitehead Institute for Biomedical Research, USA), the database of conserved 3'UTR miRNA targets, found at http://www.targetscan.org/. Gene-annotation enrichment analyses of the predicted miRNA targets, with total context scores below 0, were then performed using the web tool Database for Annotation, Visualization and Integrated Discovery (DAVID) v6.7 (Huang *et al.*, 2009) (SAIC-Frederick, Inc., USA) at http://david.abcc.nciferf.gov /summary.jsp using default parameters. Data from TargetScan and DAVID were combined to generate a hypothetical pathway of the relationship between the miRNAs and their gene targets.

3.17 Construction of wild type 3'-UTR dual luciferase reporter plasmid

3.17.1 Preparation of Insert DNA (3'-UTR)

3.17.1.1 Primer design

The miRNA 3'UTR target sites of the gene of interest and the *Homo sapiens* 3'UTR was blasted against National Center for Biotechnology Information (NCBI) RefSeq RNA database using the Nucleotide Basic Local Alignment Search Tool (Blastn Suite) (National Center for Biotechnology Information, USA) to obtain the full length mRNA sequence. Forward and reverse primers were then designed using NCBI Primer-Blast by default parameters (Table 3.15).

Table 3.15: Primers used for PCR amplification of genes

Primer Name		Sequence	Length
AKT2	Forward	5′ – ATA CTC GAG GGG ATT AAA ACC TGA ATC TCC AAC CG – 3′	33
3'UTR	Reverse	5′ – TAC GCT AGC TGT ACT TCG ATG ATG AAT TTA CCG CC – 3′	31
SMAD2	Forward	5′ – ATA TTC TCG AGA CTC GAG CAG AAC AGA CTG GG- 3′	32
3'UTR	Reverse	5′ – TAA TTG CTA GCT GCC CTA AAG TGC CTG GGA TT- 3′	32
Luc_F		GAT CGC CGT GTA ATT CTA GTT GTT T	25
SV40_R		CTT CCT TTC GGG CTT TGT TAG C	22

3.17.1.2 Complementary DNA (cDNA) synthesis

First strand cDNA was synthesized for use in PCR using the RevertAid H Minus First Strand cDNA Synthesis Kit (Thermo Fisher Scientific, USA). After thawing, the components of the kit were mixed, briefly centrifuged and stored on ice. The following reagents were then added into a sterile, nuclease-free tube on ice (Table 3.16). The mixture was incubated at 65.0°C for 5 minutes, centrifuged briefly and placed on ice.

Table 3.16: Kit components used to prepare First Strand cDNA synthesis mix

Component	Volume
Template RNA (Total RNA – 5 µg/ 20µL)	5 µg
Primer (Gene specific primer – 2.0 µm)	4 µL
Nuclease-free H_2O	to 12 ul
Total Volume	12 ul

The following components were then added according to the volumes listed below in Table 3.17. The contents of the tube were gently mixed and centrifuged. The reactions were then loaded into the thermal cycler and run according to the following conditions (Table 3.18).

Table 3.17: Kit components used to prepare First Strand cDNA synthesis mix

Component	Volume
5× Reaction Buffer	4 µL
RiboLock RNase Inhibitor (20 U/µL)	1 µL
10 mM dNTP Mix	2 µL
RevertAid H Minus M-MuLV Reverse Transcriptase (200 U/µL)	1 µL
Total Volume	20 µL

Table 3.18: Thermal cycler conditions for cDNA synthesis

Time	Temperature
60 minutes	42°C
5 minutes	70°C
∞	4°C

3.17.1.3 Amplification by PCR

The product of the first strand cDNA synthesis was used directly in PCR. The Phusion Flash High Fidelity PCR Master Mix (Thermo Fisher Scientific, USA) was used to carry out PCR. For each PCR reaction the following components were added to a 0.2 ml microcentrifuge tube. The volumes for a single 20.0 µL reaction are listed in Table 3.19. For multiple reactions, a master mix of common components was prepared and the appropriate volume added to each tube, and the unique reaction components (eg. template) was then added. The reaction tube was centrifuged briefly and loaded into the thermal cycler using the conditions in Table 3.20.

Table 3.19: Kit components used to prepare PCR samples

Component	Volume
2× Phusion Flash PCR Master Mix	10 µL
Forward Primer (1.0 µM)	0.2 µL
Reverse Primer (1.0 µM)	0.2 µL
Template (cDNA)	2 µL
H_2O (Add up to 20 µL)	12.4 µL
Total Volume	20 µL

Table 3.20: PCR cycling conditions

Cycle Step	Temperature	Time	Cycles
Initial denaturation	98°C	10 sec.	1
Denaturation	98°C	1 sec.	
Annealing	62.5°C	5 sec.	30
Extension	72°C	23 sec.	
Final Extension	72°C	1 min.	1
	4°C	Hold	∞

3.17.1.4 Agarose gel electrophoresis

To prepare 1.0% agarose gel, 1.0 g of agarose powder (Sigma Aldrich, USA) was poured into a microwavable flask along with 100.0 ml of 1 × Tris base/ acetic acid/ EDTA (TAE) buffer (Thermo Fisher Scientific, USA). The flask was microwaved for 3 min (until the agarose is completely dissolved and has a nice rolling boil). The agarose solution was cooled down for 5 min and 1.5 µl of RedSafe Nucleic Acid Staining

Solution (20,000×) (iNtRON Biotechnology, South Korea) was added. Gel was poured into the casting tray with the well comb in place, and left to sit at room temperature for 20-30 min or until it has completely solidified.

10.0 µL of DNA sample was mixed with 1.0 µL of Blue/Orange 6× loading dye (Promega, USA). Once solidified, the gel was placed into the BG-Submidi Submarine Unit (BayGene, China) and the tank filled with 1 × TAE until the gel was covered. 5.0 µL of O'GeneRuler 1 kb DNA ladder (Thermo Fisher Scientific, USA) was loaded into the first lane of the gel and the samples were loaded into the additional wells of the gel (DNA ladder sizes are listed in Appendix B).

After DNA samples were loaded, the lid was assembled onto the electrophoresis chamber so that the DNA can be migrated towards the positive lead. The electric source was provided by Power Supply-PowerPac (Bio-Rad, USA). Gel electrophoresis was run at 80 volts and 400 mA of free running current for approximately 60 min or until the dye line is approximately 75.0-80.0% of the way down the gel. The gel was then visualized under UV transillumination and analyzed by the Imager Kit Digital, AlphaImager™ 2000 (Alpha Innotech, USA) at 302 nm wavelength.

3.17.1.5 DNA purification from gel using QIAquick Gel Extraction Kit (Qiagen, USA)

PCR products were purified from the gel using the QIAquick Gel Extraction Kit. This kit contains three components: Buffer QG, Buffer PE and Buffer EB. The DNA fragment was excised from the agarose gel using a clean, sharp scalpel. The gel slice was weighed in a colourless tube and 3 volumes of Buffer QG was added to 1 volume of gel (100.0 mg gel ~ 100.0 µL). The maximum amount of gel per spin column is 400.0 mg. For > 2% agarose gels, 6 volumes of Buffer QG was added. The tubes were incubated at 50°C for 10 min (or until the gel has completely dissolved). The tubes were

vortexed every 2-3 min to help dissolve the gel. Once the gel slice was dissolved completely, the colour of the mixture was checked to ensure it was yellow. If the colour of the mixture is orange or violet, 10.0 µL of 3 M sodium acetate, pH 5.0, was added to the mix and the mixture would turn yellow. 1 volume of isopropanol was added to the sample and mixed. A QIAquick spin column was placed in a provided 2.0 ml collection tube and 800.0 µL of the sample was applied to the QIAquick column and centrifuged for 1 min to bind the DNA. The flow-through was discarded and the QIAquick column was placed back into the same tube. This step was repeated for the remainder of the sample. 500.0 µL of Buffer QG was added to the column and the tube centrifuged for 1 min. The flow-through was discarded and the QIAquick column placed back into the same tube. To wash the sample, 750.0 µL Buffer PE was added to the QIAquick column, left to stand for 3 min at room temperature and then centrifuged for 1 min. The flow-through was discarded and the QIAquick column placed back into the same tube. The QIAquick column with its 2.0 ml collection tube was then centrifuged at full speed for 2 min to remove residual wash buffer. The QIAquick column was then placed into a clean 1.5 ml microcentrifuge tube and the DNA eluted by adding 50 µL of Buffer EB (10 mM Tris Cl, pH 8.5) to the center of the QIAquick membrane and centrifuged for 1 min. After the addition of elution buffer to the QIAquick membrane, increasing the incubation time up to 4 min can increase the yield of purified DNA. If the purified DNA was to be analyzed on a gel, 1 volume of Loading Dye was added to 5 volumes of purified DNA. The solution was pipetted up and down before loading onto the gel.

3.17.2 Preparation of vector DNA (pmirGLO Dual-Luciferase miRNA Expression Vector (Promega, USA))

3.17.2.1 pmirGLO Dual-Luciferase miRNA Expression Vector propagation in *E. coli* competent cells JM109 (Promega, USA)

Ten 1.0 ml centrifuge tubes were chilled on ice. Frozen competent cells were removed from -80°C and placed on ice for 5 min, or until just thawed. Once thawed, the JM109 competent cells were pipetted quickly to prevent warming above 4°C. The thawed cells were gently mixed by flicking, and 100.0 µL was transferred to each chilled tube. While moving the pipette tip through the competent cells, 50 ng of DNA was dispersed into each tube. Tubes were immediately returned to ice for 10 min, after which the cells were heat shocked at 42°C exactly in a water bath. Following this, tubes were immediately placed back on ice for 10 min. 900 µL of ice-cold lysogeny broth (LB) (Sigma Aldrich, USA)/ampicillin (Thermo Fisher Scientific) medium was added to each transformation reaction and incubated for 1 h at 37°C in an incubator shaker (BioSan, Latvia) (225 RPM). For each transformation reaction the cells were diluted 1:10, 1:100 and 100.0 µL undiluted cells on LB/ampicillin agar plates. The plates were then incubated for 12-24 h at 37°C.

3.17.2.2 Purification of pmirGLO Dual-Luciferase miRNA Target Vector from *E. coli* culture using PureYield Plasmid Miniprep System (Promega, USA)

The PureYield Plasmid Miniprep System contains 5 components: the Cell Lysis Buffer (CLC), Neutralization Solution (NSC), Endotoxin Removal Wash (ERB), Column Wash Solution (CWC) and Elution Buffer (EBB).

A single, well-isolated colony from a fresh LB/ampicillin agar plate was chosen, and used to inoculate 10.0 ml of LB broth containing 10% ampicillin. The inoculated broth was incubated overnight (12-18 h) at 37°C. 3.0 ml of bacterial culture growth in

LB broth was transferred to a 15 ml Falcon tube and spun down. The supernatant was discarded and 600.0 µL Tris/EDTA (TE) buffer was added to the cell pellet and resuspended by vortexing. Contents were transferred to a 1.5 ml centrifuge tube and 100.0 µL CLC was added. The tube was mixed by inverting the tube 6 times. The solution changes from opaque to clear blue, indicating complete lysis. Experiment was proceeded to the next step within 2 min as excessive lysis will result in denatured plasmid DNA. 350.0 µL ice-cold NSC was added, and mixed thoroughly by inverting the tube. The sample will turn yellow when neutralization is complete and a yellow precipitate will form. The tube was inverted an additional 3 times to ensure complete neutralization. The tube was then centrifuged at maximum speed for 3 min. Supernatant (≈ 900.0 µL) was transferred to a PureYield minicolumn placed in a PureYield collection tube. The column was centrifuged at maximum speed for 15 sec. The flow-through was discarded and the minicolumn placed back into the same PureYield collection tube. 200.0 µL ERB was added to the minicolumn and centrifuged at maximum speed for 15 sec. 400.0 µL CWC was then added to the minicolumn and centrifuged at maximum speed for 30 sec. The minicolumn was transferred to a clean 1.5 ml microcentrifuge tube and 30.0 µL EBB was added directly to the minicolumn matrix and left to stand at room temperature for 1 min. The column was then centrifuged at maximum speed for 15 sec. The eluted plasmid DNA was stored at -20°C.

3.17.3 Cloning

The insert DNA (3'UTR) was cloned into 3' end of the pmirGLO Dual-Luciferase miRNA Target Vector using restriction enzyme pairs SacI / SalI by a third party vendor, First BASE Laboratories Sdn Bhd, Malaysia. All constructs were verified by sequencing, also performed by the outside vendor. Sequencing results were analyzed using the chromatogram viewer Geospiza's Finch TV (PerkinElmer, USA) and the full

sequence of the insert DNA and pmirGLO/gene constructs was analyzed and compared to sequences in the Human Standard Nucleotide BLAST (National Center for Biotechnology Information, USA) (Appendix C and Appendix D).

3.18 Construction of mutated 3'-UTR pmirGLO Dual Luciferase Reporter Plasmid

To create mutations in the miRNA binding sequence, the cloned pmiRGLO/gene constructs were submitted to a third party vendor, First BASE Laboratories Sdn. Bhd, Malaysia, to undergo their site-directed mutagenesis service. All mutated constructs were verified by sequencing, also performed by the outside vendor.

3.19 Dual Luciferase Reporter Assay System (Promega, USA)

Luciferase activity, indicative of translation from the plasmid, was assayed using the Dual Luciferase Reporter Assay System. One day prior to transfection, 1.5×10^5 cells were plated in 2.0 ml of appropriate medium in a 6-well plate. Cells were co-transfected with 80.0 nM of miRNA mimics / inhibitors or their corresponding negative controls (as described in Section 3.12) and 40.0 ng of wildtype or mutated 3'UTR plasmids.

For plasmid transfection, in separate tubes, 0.8 µL of 50.0 ng/µL plasmid stock solution was diluted in 199.2 µL serum-free culture medium (Tube 1) to prepare a final concentration of 40.0 ng, and 2.0 µL of DharmaFECT 1 transfection reagent was diluted in 198.0 µL serum-free culture medium (Tube 2). The contents of each tube was gently mixed and incubated for 5 min at room temperature. After the 5 min incubation, the contents of Tube 1 was added to Tube 2 and mixed gently by pipetting up and down. The combined solution was incubated for 20 min at room temperature to form the transfection mix. 1.6 ml of complete medium was added to the mixed solution for the desired transfection volume. The culture medium from the 6-well plate was removed and 2 ml of the appropriate transfection mix was added to the flask.

At 24 h post-transfection spent media was removed, cells washed with PBS, and fresh media added back into the wells. The plates were then placed back into the CO_2 incubator for another 24 h. Luciferase activity was detected 48 h post-transfection using the Dual Luciferase Reporter Assay System according to manufacturer's protocol.

Prior to starting the luciferase assay experiments, the content of Dual-Glo Luciferase Buffer was transferred to the bottle of Dual-Glo Luciferase substrate, to create the Dual-Glo Luciferase Reagent. The contents are mixed by inversion until the substrate was fully dissolved. Cells were harvested by trypsinization and centrifugation, and then resuspended in 50.0 µL 1× PBS and transferred to a 1.5 ml centrifuge tube. 50.0 µL Dual-Glo Luciferase Reagent was added and mixed by pipetting. The sample was left to incubate for 10 min and then firefly luminescence was measured using the Glomax Multi - Luminescence Multimode Reader (Promega, USA). 50.0 µL Dual-Glo Stop & Glo Reagent was then added and mixed by pipetting. The sample was incubated for 10 min and then *Renilla* luminescence was measured. The ratio of luminescence from the firefly luciferase reporter to luminescence from the *Renilla* luciferase reporter was calculated. This ratio was normalized to the ratio of the control samples that are treated consistently. This normalization provides optimal and consistent results from the Dual-Glo Luciferase Assay System. *Renilla* luciferase was used as an internal control due to its constitutive expression.

3.20 Gene rescue experiments

3.20.1 Gene silencing using siRNAs

Silencing of the *AKT2* gene was performed using a set of three unique 27 mer siRNA duplexes purchased from OriGene Technologies Inc., USA (Table 3.21). A universal scrambled negative control siRNA (siRNA NC) was used as a control. SiRNA duplexes, provided as 2.0 nM per vial, were reconstituted by resuspension in 100.0 µl of

1 × siRNA buffer (GE Healthcare Dharmacon, USA), yielding a final concentration of 20.0 μM. The duplex solutions were heated to 95°C for 2 min to ensure fully duplexed contents and allowed to cool to room temperature, prior to being stored at -20°C.

One day prior to transfection 1.0×10^6 cells were plated in 5 ml of appropriate medium, without antibodies, in a T-25 cm^2 culture flask. Cells were then transfected with 80 nM of miR-608 inhibitors or inhibitor NC as described in Section 3.12. 6 h post-transfection, spent media was removed and cells were washed with 1 × PBS before being transfected with 10.0 nM siRNA or siRNA NC.

In separate tubes 2.5 μL of 20.0 μM siRNA stock solution was diluted in 495.0 μL serum-free culture medium (Tube 1) to prepare a final concentration of 10.0 nM, and 6.0 μL of DharmaFECT 1 transfection reagent was diluted in 494.0 μL serum-free culture medium (Tube 2). The contents of each tube was gently mixed and incubated for 5 min at room temperature. After the 5 min incubation, the contents of Tube 1 was added to Tube 2 and mixed gently by pipetting up and down. The combined solution was incubated for 20 min at room temperature to form the transfection mix. 4.0 ml of complete medium was added to the mixed solution for the desired transfection volume. The culture medium from the T-25 cm^2 culture flask was removed and 5.0 ml of the appropriate transfection mix was added to the flask.

Transfected cells were incubated in 37°C in the CO_2 incubator prior to determination of gene rescue effects by functional assays. AKT2 protein levels were determined via western blot 72 h post-transfection (Section 3.6). The detection of caspase 3/7 activity was performed 48 h post-transfection using the Caspase-Glo® 3/7 assay (Section 3.9), while apoptosis was detected 72 h post-transfection using the FITC annexin V apoptosis detection kit (Section 3.8) as described previously.

Table 3.21: siRNA duplexes used for *AKT2* silencing

siRNA	Duplex Sequence
siRNA A	GCAUCAUAAAUUGGUAGUUUCCUGC
siRNA B	AGCGUGGUGAAUACAUCAAGACCTG
siRNA C	ACAGCAAAGCAGGAGUAUAAGAAAG

3.20.2 Gene overexpression using pCMV6 plasmids

The mammalian pCMV6/*SMAD2* plasmid was purchased from OriGene Technologies Inc., USA, and was designed to contain the cDNA open reading frame of *SMAD2* without its 3'UTR. The empty pCMV6 plasmid (OriGene Technologies Inc., USA) was used as a control plasmid. DNA plasmids, provided as dried plasmids, were reconstituted with 100.0 µl nuclease free H_2O, yielding a final concentration of 10.0 µg.

One day prior to transfection 1.0×10^6 cells were plated in 5.0 ml of appropriate medium, without antibodies, in a T-25 cm^2 culture flask. Cells were then transfected with 80.0 nM of miR-608 inhibitors or inhibitor NC as described in Section 3.12. 6 h post-transfection, spent media was removed and cells were washed with 1 × PBS before being transfected with 50.0 ng pCMV/SMAD2 or pCMV6 vectors.

In separate tubes 0.5 µL of 10.0 µg plasmid stock solution was diluted in 499.5 µL serum free culture medium (Tube 1) to prepare a final concentration of 50.0 ng, and 6.0 µL of DharmaFECT 1 transfection reagent was diluted in 494.0 µL serum free culture medium (Tube 2). The contents of each tube was gently mixed and incubated for 5 min at room temperature. After the 5 min incubation, the contents of Tube 1 was added to Tube 2 and mixed gently by pipetting up and down. The combined solution was incubated for 20 min at room temperature to form the transfection mix. 4.0 ml of complete medium was added to the mixed solution for the desired transfection volume. The culture medium from the T-25 cm^2 culture flask was removed and 5.0 ml of the appropriate transfection mix was added to the flask.

Transfected cells were incubated in 37°C in the CO_2 incubator prior to determination of gene rescue effects by functional assays. SMAD2 protein levels were determined via western blot 72 h post-transfection (Section 3.6). The detection of caspase 3/7 activity was performed 48 h post-transfection using the Caspase-Glo® 3/7 assay (Section 3.9), while apoptosis was detected 72 h post-transfection using the FITC annexin V apoptosis detection kit (Section 3.8) as described previously.

3.21 Statistical analysis

All experiments were performed in triplicate independent experiments. All data were presented as mean ± standard deviation. Student's *t*-test was used to determine the statistical significance of the difference between two groups of data, where a *p*-value of ≤ 0.05 was considered statistically significant. Analysis of statistical significance between three or more groups of data was performed using the one-way analysis of variance (ANOVA), followed by *post-hoc* Tukey test, where a *p*-value of ≤ 0.05 was considered statistically significant.

CHAPTER 4: RESULTS

4.1 Silencing of *BCL-XL* using siRNA-based transfection resulted in a reduction of SK-LU-1 cell viability and increased apoptosis

4.1.1 siRNA transfection efficiency in SK-LU-1 cells

To assess whether *BCL-XL* plays a similar role in the apoptotic properties of lung adenocarcinoma SK-LU-1 cells, as observed in the A549 cell line previously reported in my Masters study (Othman, 2012), the expression of *BCL-XL* in SK-LU-1 cells was first transiently silenced via transfection with Stealth RNAi™ siRNA Duplex Oligonucleotides. Visual monitoring of the uptake of 100.0 nM of BLOCK iT™ Alexa Fluor® Red Fluorescent Oligo using fluorescence microscopy showed a satisfactory transfection efficiency of ≥ 80.0% for samples treated with the BLOCK-iT™ Alexa Fluor® Red Fluorescent Oligo (Figure 4.1). The percentage of transfection efficiency shown is representative of mean values from independent triplicate experiments with mean ± SD.

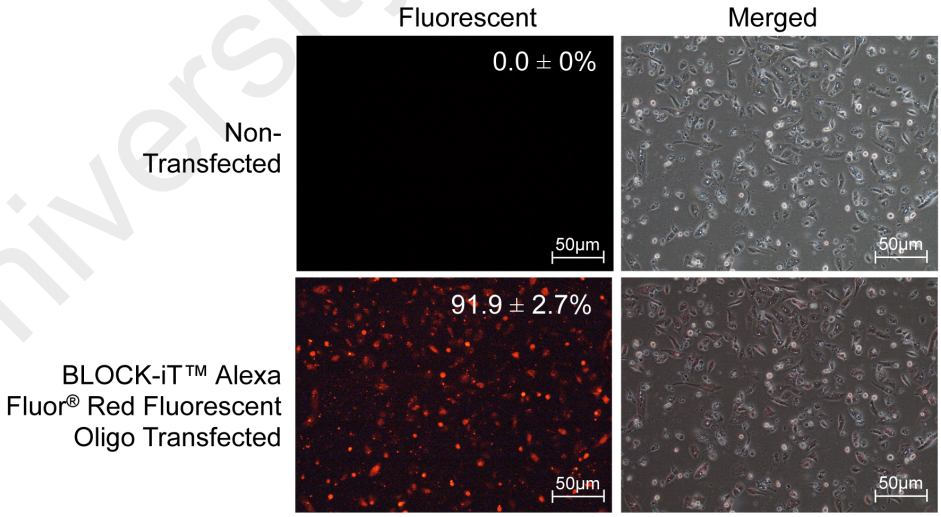

Figure 4.1: Visual monitoring of BLOCK-iT Alexa Fluor Red Fluorescent Oligo transfection efficiency. Fluorescent and merged images of SK-LU-1 cells transfected with 100 nM BLOCK-iT Alexa Fluor Red Fluorescent Oligo. Percentage of mean transfection efficiency ± SD is indicated and all images shown are a representative of triplicate independent experiments.

4.1.2 Determination of siRNA silencing efficiency via qRT-PCR

To evaluate the silencing efficiency of the siRNAs, qRT-PCR was performed to allow for the evaluation of the *BCL-XL* expression in siRNA-transfected and non-transfected cells. Amongst the three siRNAs utilized, silencing efficiency of siRNA 1 indicated the highest negative fold induction of 4.03 ± 0.01 in SK-LU-1 cells (Figure 4.2 and Table 4.1) with a knockdown of 75.16 ± 0.92% in *BCL-XL* expression when compared with non-transfected cells (Table 4.1).

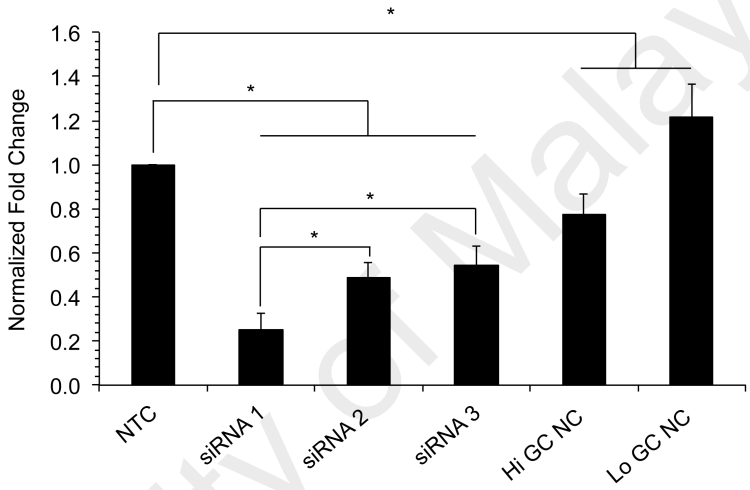

Figure 4.2: qRT-PCR analysis of *BCL-XL* normalized to endogenous *β-actin* expression in siRNA-transfected and non-transfected SK-LU-1 cells. Data presented as mean ± SD, n=3, with significant differences denoted with * *p*-value ≤ 0.05. NTC denotes non-transfected cells. Hi GC NC denotes high GC content scramble RNA negative control-transfected cells. Lo GC NC denotes low GC content scramble RNA negative control-transfected cells.

Table 4.1: Fold change and percentage knockdown of *BCL-XL* gene expression in siRNA-transfected SK-LU-1 cells in comparison to non-transfected cells. Data presented as mean ± SD, n=3, with significant differences between siRNA-transfected cells and non-transfected cells denoted with *p*-value ≤ 0.05. Hi GC NC denotes high GC content scramble RNA negative control-transfected cells. Lo GC NC denotes low GC content scramble RNA negative control-transfected cells.

Sample	Fold Change† ± S.D.	*p*-Value	% Knockdown ± SD	*p*-Value
siRNA 1	-4.03 ± 0.01	0.000	75.16 ± 0.92	0.000
siRNA 2	-2.07 ± 0.05	0.004	51.28 ± 5.43	0.004
siRNA 3	-1.85 ± 0.06	0.005	45.58 ± 5.83	0.005
Hi GC NC	-1.31 ± 0.11	0.047	22.58 ± 11.41	0.047
Lo GC NC	1.22 ± 0.07	0.013	-21.54 ± 6.74	0.013

† Negative values denote down-regulation, while positive values denote up-regulation

4.1.3 Reduced BCL-XL protein levels in response to siRNA silencing

Correspondingly, BCL-XL protein levels were decreased by 98.33 ± 0.50% in siRNA 1-transfected SK-LU-1 cells, as determined by densitometry analysis of western blot bands (Figure 4.3). As siRNA 1 (henceforth referred to as si*BCL-XL*) had the greatest silencing efficiency amongst the three siRNAs, it was selected for further downstream work.

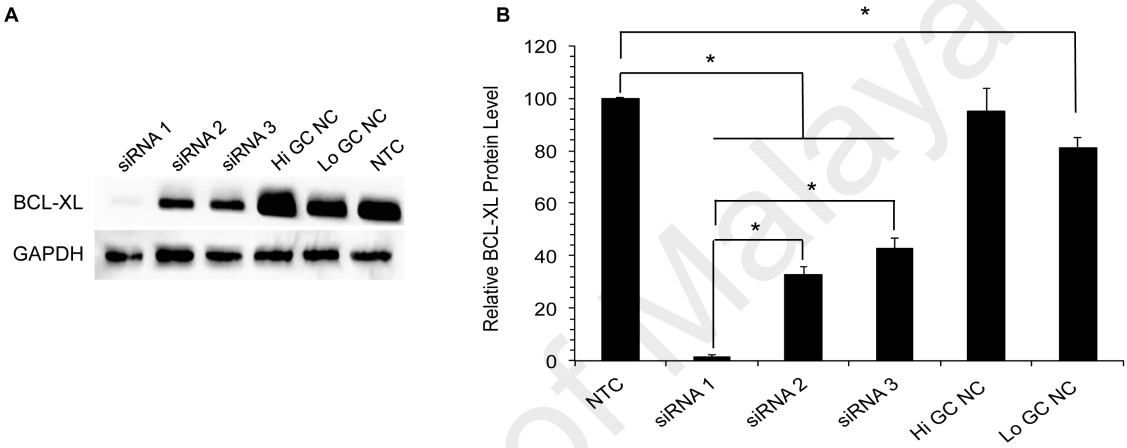

Figure 4.3: Quantification of BCL-XL protein levels in siRNA-transfected SK-LU-1 cells in comparison to non-transfected cells. **(A)** Western blot analysis of BCL-XL protein following siRNA transfection. **(B)** Densitometry analysis of BCL-XL bands using the ImageJ Analyst software. Results were standardized against GAPDH levels and presented as relative protein levels. Data presented as mean ± SD, n=3, with statistically significant differences denoted with * p-value ≤ 0.05. NTC denotes non-transfected cells. Hi GC NC denotes high GC content scramble RNA negative control-transfected cells. Lo GC NC denotes low GC content scramble RNA negative control-transfected cells.

4.1.4 Reduced viability and increased cell death in SK-LU-1 cells in response to *BCL-XL* silencing

To determine the biological effects of *BCL-XL* silencing on SK-LU-1 cells, MTT cell viability assay was performed and revealed that knockdown of *BCL-XL* resulted in a reduction of cell viability, 48 h post-transfection, in comparison to non-transfected SK-LU-1 cells (Figure 4.4). A comparison between non-transfected cells and mock-transfected cells (cells treated with transfection reagent only) did not disclose any changes in viability, hence ruling out toxicity effects of the transfection reagent (Table 4.2). A double fluorescence staining of annexin V-FITC conjugate and propidium iodide was then performed on si*BCL-XL*-transfected cells and non-transfected cells, and analyzed using a flow cytometer to determine if cell death was occurring through the process of apoptosis. After silencing of *BCL-XL* in SK-LU-1 cells, the population of cells indicated a shift from viable cells to early and late stage apoptosis with an increase of apoptosis to 18.54 ± 1.62% (Figure 4.5). Taken together, these results demonstrated that *BCL-XL* plays a similar role in the regulation of apoptosis in both lung adenocarcinoma cells, A549 and SK-LU-1.

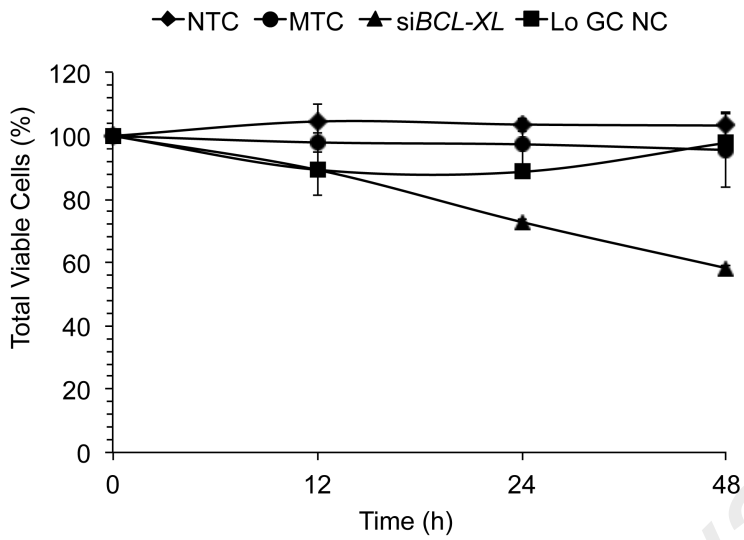

Figure 4.4: Cell viability analysis of *BCL-XL* silencing on SK-LU-1 cells over 48 h as observed using MTT assay. Data presented as mean ± SD, n=3. NTC denotes non-transfected cells. MTC denotes mock-transfected cells. si*BCL-XL* denotes siRNA-transfected cells. Lo GC NC denotes low GC content scramble RNA negative control-transfected cells.

Table 4.2: Total cell viability levels (%) as obtained from MTT assays over 48 h. Data presented as mean ± SD, n=3, with statistically significant differences in comparison to NTC denoted with p-value ≤ 0.05. NTC denotes non-transfected cells. MTC denotes mock-transfected cells. si*BCL-XL* denotes siRNA-transfected cells. Lo GC NC denotes low GC content scramble RNA negative control-transfected cells.

Treatment	Time (h)	Viability (%) ± SD	*p*-Value
NTC	12	104.57 ± 5.61	-
	24	103.61 ± 2.12	-
	48	103.29 ± 3.69	-
MTC	12	97.95 ± 3.03	0.306
	24	97.95 ± 7.56	0.289
	48	95.58 ± 11.97	0.250
si*BCL-XL*	12	89.29 ± 8.06	0.009
	24	72.80 ± 1.15	0.003
	48	58.22 ± 0.98	0.002
Lo GC NC	12	89.31 ± 0.92	0.123
	24	84.65 ± 1.78	0.099
	48	97.81 ± 2.02	0.011

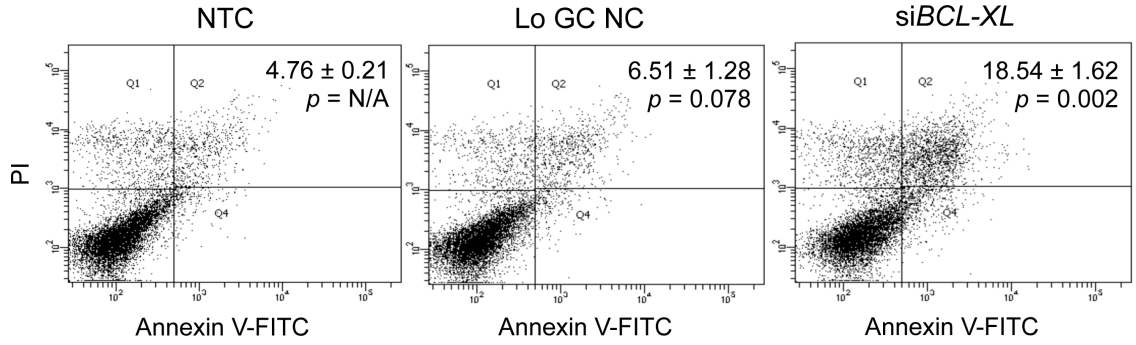

Figure 4.5: Detection of apoptosis 48 h post-si*BCL-XL* transfection using flow cytometry following annexin V-FITC/ propidium iodide (PI) staining. Viable cells are in the lower left quadrant, early apoptotic cells are in the lower right quadrant, late apoptotic cells are in the upper right quadrant and non-viable necrotic cells are in the upper left quadrant. Dot plots are representative of 1.0×10^4 cells from a single replicate with percentage of apoptosis indicated. Data presented as mean ± SD, n=3, with statistically significant differences in comparison to NTC denoted with p-value ≤ 0.05. NTC denotes non-transfected cells. Lo GC NC denotes low GC content scramble RNA negative control-transfected cells. si*BCL-XL* denotes siRNA-transfected cells.

4.2 Validation of candidate miRNA expression levels via RT-qPCR, identified to be dysregulated in A549 cells following *BCL-XL* silencing

In my previous Masters project, a global miRNA expression profile was established using miRNA microarray, which compared total RNA extracted from si*BCL-XL*-transfected and non-transfected A549 cells, and it was determined that miRNA expression changes occur in response to *BCL-XL* silencing. Ten miRNAs were significantly differentially expressed, of which seven miRNAs were down-regulated while three were up-regulated (Othman, 2012). To corroborate whether this dysregulation also occurs in SK-LU-1 cells, five representative differentially expressed miRNAs (miR-181a, miR-769-5p, miR-361-5p, miR-1304, and miR-608) were selected to undergo RT-qPCR validation based on highest fold change as well as putative targets as identified by the TargetScan web tool. RT-qPCR results confirmed that the same pattern of dysregulation was exhibited in both A549 and SK-LU-1 cells following *BCL-XL* silencing, with miR-181a, miR-769-5p, miR-361-5p, and miR-1304 being down-regulated, while miR-608 was up-regulated (Figure 4.6 and Table 4.3).

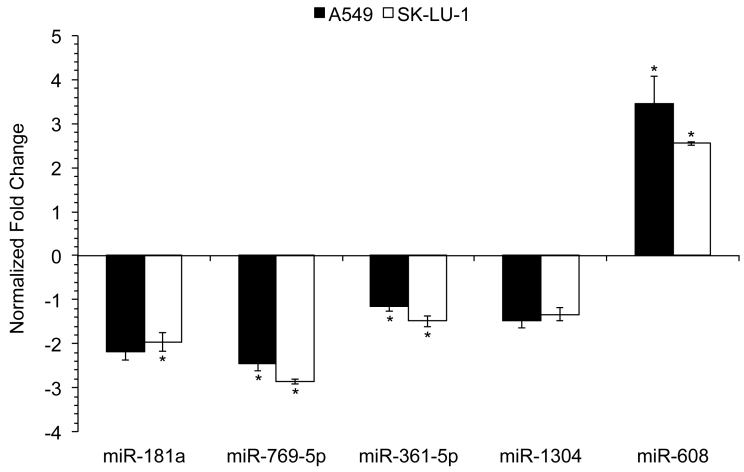

Figure 4.6: RT-qPCR validation of candidate miRNAs. RT-qPCR of the five candidate miRNAs (miR-181a, miR-769-5p, miR-361-5p, miR-1304, and miR-608) validated against A549 results, and presented as normalized fold change. Data presented as mean ± SD, n=3, with statistically significant differences between si*BCL-XL* -transfected cells and non-transfected cells denoted with * p-value ≤ 0.05.

Table 4.3: Fold change of candidate miRNA expression in si*BCL-XL*-transfected cells in comparison to non-transfected cells ($p \leq 0.05$).

MicroRNA	A549		SK-LU-1	
	Fold Change†	***p*-Value**	**Fold Change†**	***p*-Value**
miR-181a	-2.17 ± 0.21	0.051	-1.97 ± 0.21	0.004
miR-769-5p	-2.43 ± 0.18	0.035	-2.84 ± 0.06	0.000
miR-361-5p	-1.16 ± 0.01	0.041	-1.50 ± 0.13	0.007
miR-1304	-1.49 ± 0.16	0.057	-1.33 ± 0.16	0.068
miR-608	3.45 ± 0.62	0.003	2.55 ± 0.04	0.000

† Negative values denote down-regulation, while positive values denote up-regulation

4.3 Up-regulation of miR-608 expression and down-regulation of miR-361-5p expression increases cell death in A549 and SK-LU-1 cells

4.3.1 Determination of miRNA mimic and inhibitor transfection efficiency in A549 and SK-LU-1 cells

Of the five representative dysregulated miRNAs validated, miR-181a was found to be well studied and established to play a role in cancer progression; therefore further downstream work was focused on the four remaining miRNAs: miR-769-5p, miR-361-5p, miR-1304 and miR-608. Overexpression and knockdown studies were performed via transfection of miRNA mimics and inhibitors to determine the biological effects of these miRNAs. Monitoring of miRIDIAN miRNA Mimic and Inhibitor Transfection Control with Dy547 uptake using fluorescence microscopy showed a transfection efficiency of ≥ 80% across all samples (Figure 4.7). Quantification of miRNA overexpression by RT-qPCR, post-transfection, indicated a positive fold change in A549 and SK-LU-1 transfected cells, when compared with cells transfected with scrambled negative controls (Figure 4.8 and Table 4.4), confirming successful transfection of miRNAs.

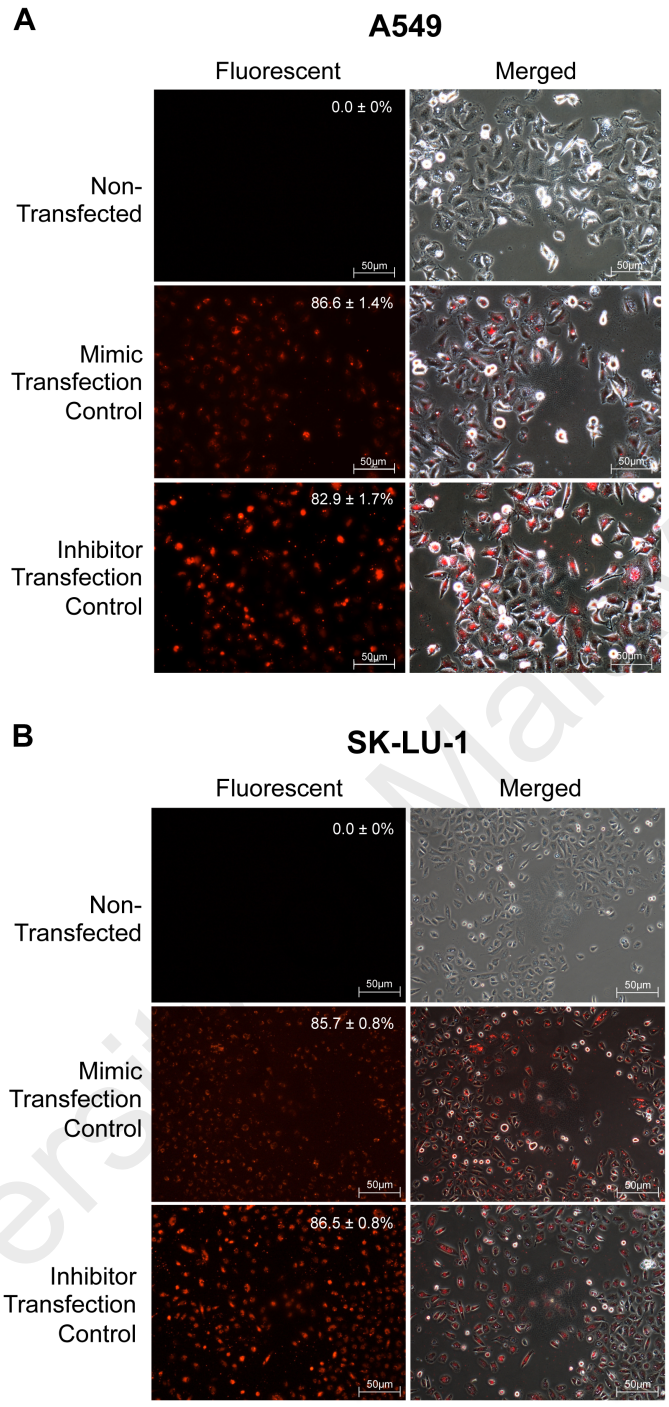

Figure 4.7: Visual monitoring of miRIDIAN microRNA Mimic/Hairpin Inhibitor Transfection Control with Dy547 transfection efficiency. Fluorescent and merged images of **(A)** A549 and **(B)** SK-LU-1 cells transfected with 80.0 nM miRIDIAN microRNA Mimic/Hairpin Inhibitor Transfection Control with Dy547. Percentage of mean transfection efficiency ± SD is indicated, and all images shown are a representative of triplicate independent experiments.

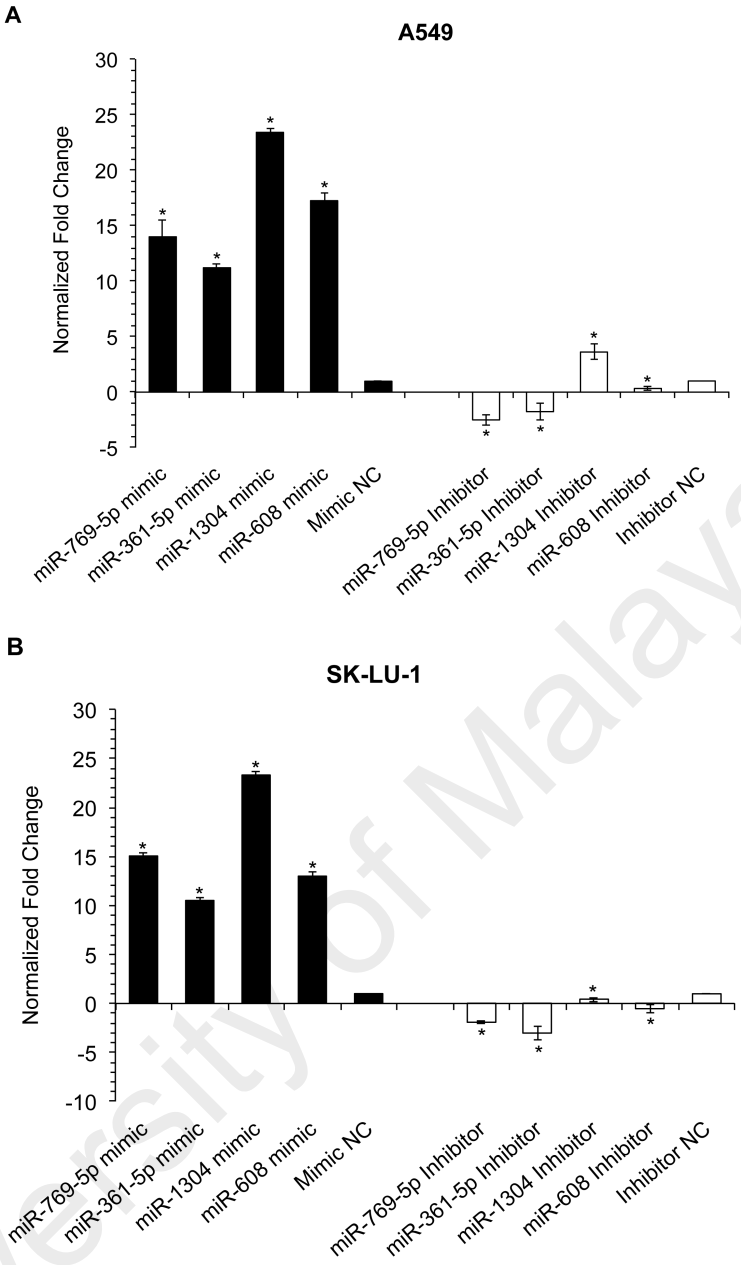

Figure 4.8: Normalized fold change of miR-769-5p, miR-361-5p, miR-1304, and miR-608 mimic/inhibitor-transfected cells. **(A)** A549 and **(B)** SK-LU-1 mimic/inhibitor-transfected cells, in comparison to cells transfected with scrambled negative controls. Samples were normalized to the endogenous control RNU6. Data presented as mean ± SD, n=3, with statistically significant differences between transfected cells and scrambled negative control-transfected cells denoted with * p-value ≤ 0.05. NC denotes cells transfected with scrambled RNA negative control.

Table 4.4: Fold change of miRNA in miRNA-transfected cells in comparison to fold change in scrambled negative control transfected cells. Data presented as mean ± SD, n=3, with statistically significant differences between transfected cells and scrambled negative control-transfected cells denoted with *p*-value ≤ 0.05. NC denotes cells transfected with scrambled RNA negative control.

Treatment	A549		SK-LU-1	
	Fold Change† ± SD	*p*-Value	Fold Change† ± SD	*p*-Value
miR-769-5p Mimic	14.01 ± 1.46	0.0000	15.05 ± 0.36	0.0000
miR-361-5p Mimic	11.26 ± 0.23	0.0000	10.51 ± 0.33	0.0000
miR-1304 Mimic	23.39 ± 0.35	0.0000	23.31 ± 0.40	0.0005
miR-608 Mimic	17.19 ± 0.76	0.0003	12.99 ± 0.46	0.0002
Mimic NC	0.00 ± 0.00	n/a	0.00 ± 0.00	n/a
miR-769-5p Inhibitor	-2.50 ± 0.51	0.0000	-1.93 ± 0.11	0.0000
miR-361-5p Inhibitor	-1.76 ± 0.77	0.0013	-3.04 ± 0.73	0.0000
miR-1304 Inhibitor	3.61 ± 0.69	0.0060	0.39 ± 0.21	0.0420
miR-608 Inhibitor	0.33 ± 0.17	0.0393	-1.81 ± 0.46	0.0872
Inhibitor NC	0.00 ± 0.00	n/a	0.00 ± 0.00	n/a

† Negative values denote down-regulation, while positive values denote up-regulation

4.3.2 Increased apoptosis observed in A549 and SK-LU-1 cells transfected with miR-608 mimics and miR-361-5p inhibitors

Cell death in miRNA mimic and inhibitor transfected cells was detected 72 h post-transfection using flow cytometry after annexin V-FITC/ PI staining in A549 and SK-LU-1 cells. An increase in miR-608 expression and a knockdown of miR-361-5p expression resulted in a significant increase in the apoptotic population of A549 (43.96 ± 0.30 % and 23.10 ± 2.94 %, respectively) and SK-LU-1 cells (15.17 ± 1.27 % and 49.93 ± 6.01 %, respectively) in comparison to total percentage of apoptosis observed in cells transfected with negative controls (Figure 4.9). Correspondingly, an increase in miR-608 and a decrease in miR-361-5p expression resulted in an increase in the relative caspase 3/7 activity in A549 (1.53 ± 0.17 and 1.20 ± 0.17 relative activity, respectively) and SK-LU-1 (1.71 ± 0.31 and 1.67 ± 0.07 relative activity, respectively) cells, indicating cell death was occurring through the mitochondrial apoptotic pathway (Figure 4.10). No significant changes in percentage of apoptosis and caspase 3/7 activity

were detected in cells transfected with miR-769-5p and miR-1304, therefore further downstream work was focused only on miR-608 and miR-361-5p.

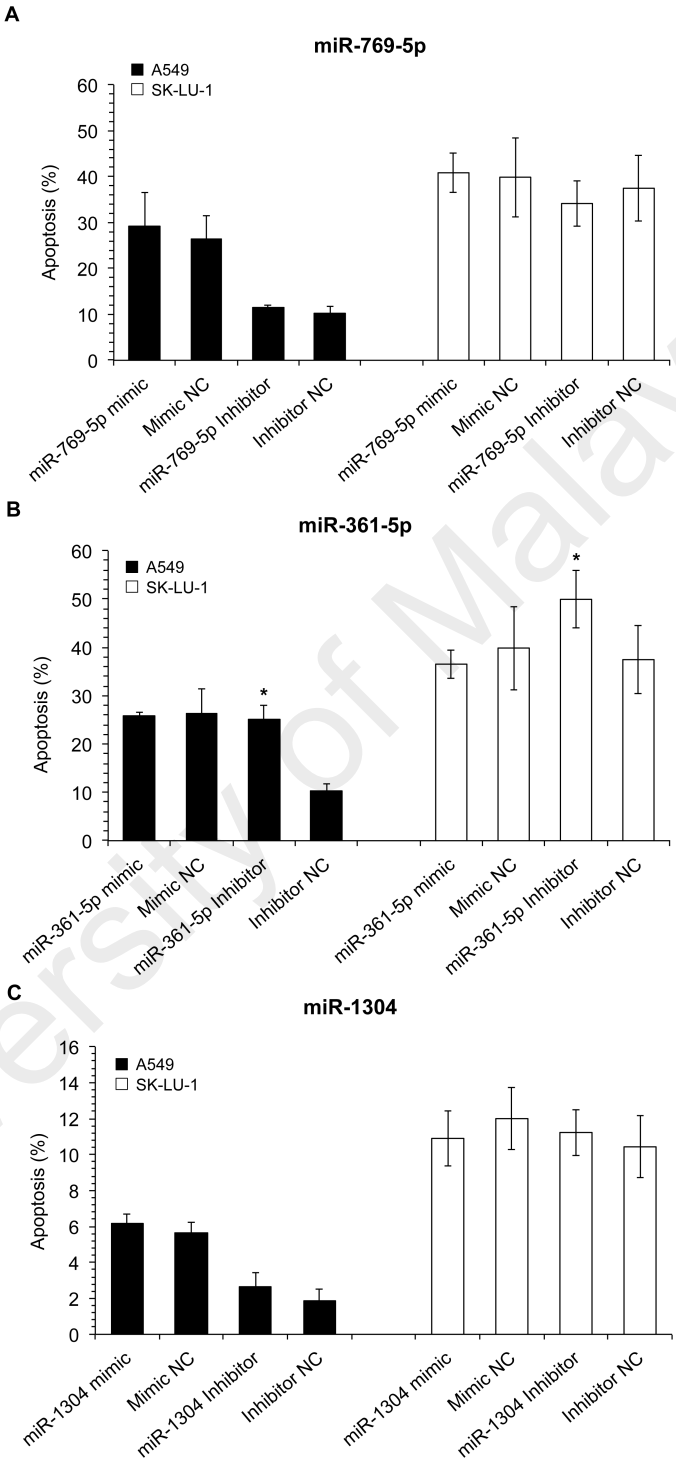

Figure 4.9: Detection of apoptosis 72 h post-transfection with miRNA mimics and inhibitors. **(A)** MiR-769-5p **(B)** miR-361-5p, **(C)** miR-1304, and **(D)** miR-608-induced apoptosis detection using flow cytometry after annexin V-FITC/ PI staining in A549 and SK-LU-1 cells. Data presented as mean ± SD, n=3, with statistically significant differences between miRNA-transfected cells and scrambled negative control-transfected cells denoted with * p-value ≤ 0.05. NC denotes cells transfected with scrambled RNA negative control.

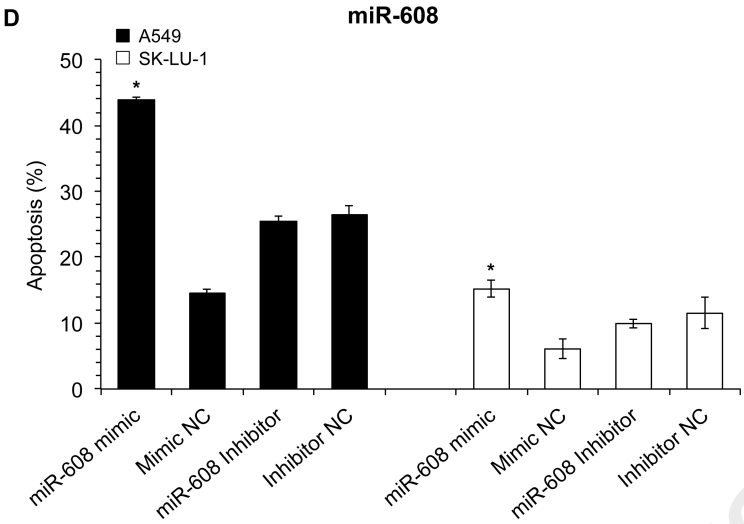

Figure 4.9, continued.

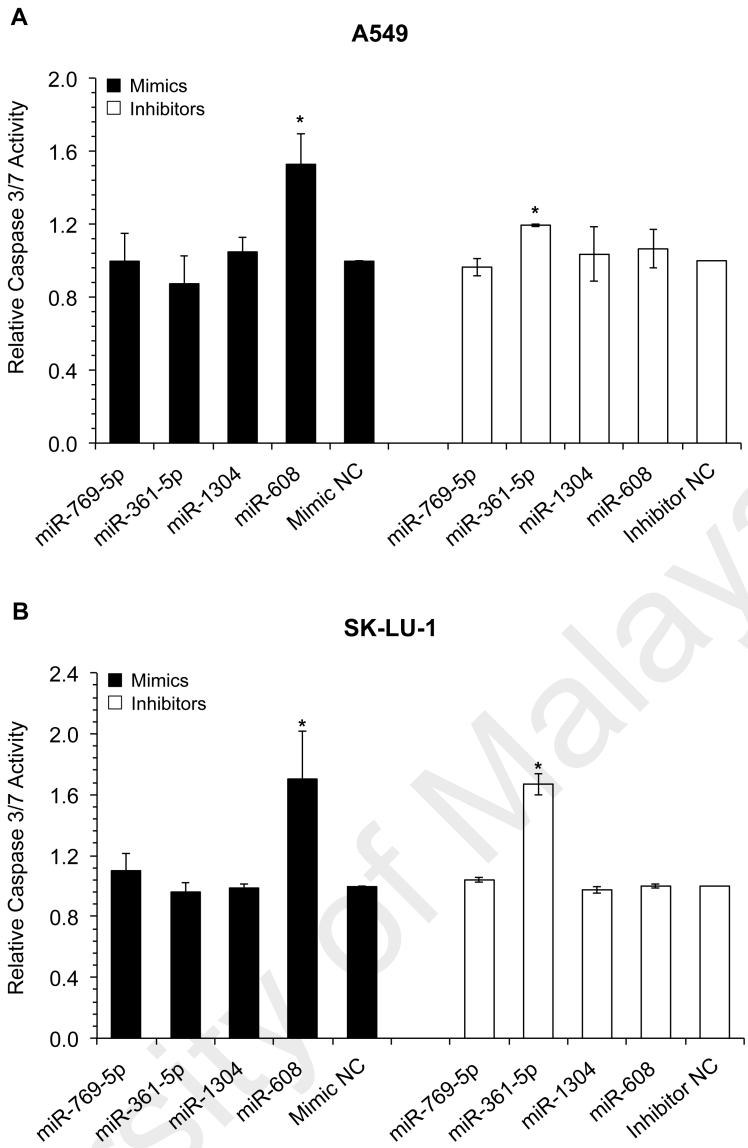

Figure 4.10: Detection of caspase 3/7 activity 48 h post-transfection with miRNA mimics and inhibitors. **(A)** A549 and **(B)** SK-LU-1-miRNA transfected cells detection of caspase 3/7 activity. Data presented as mean ± SD, n=3, with statistically significant differences between transfected cells and scrambled negative control-transfected cells denoted with * p-value ≤ 0.05. NC denotes cells transfected with scrambled RNA negative control.

4.4 Transfection with miR-608 inhibitors and miR-361-5p mimics blocks si*BCL-XL*-induced apoptosis

To determine the relationship between *BCL-XL*, miR-608/miR-361-5p and apoptosis, a combination study was carried out whereby cells were first transfected with si*BCL-XL*, followed by transfection with either miR-608 inhibitors or miR-361-5p mimics. It was found that the apoptotic populations of *BCL-XL*-silenced A549 and SK-LU-1 cells were significantly decreased following miR-608 inhibitors (11.95 ± 1.18% from 22.09 ± 1.47 and 12.36 ± 3.57% from 21.49 ± 3.350% in A549 and SK-LU-1 cells respectively) and miR-361-5p mimic transfection (5.13 ± 0.12% from 11.53 ± 0.83% and 12.03 ± 0.72% from 28.70 ± 0.56% in A549 and SK-LU-1 cells respectively) indicating that antagomiRs of miR-608 and mimics of miR-361-5p were able to block si*BCL-XL*-induced apoptosis (Figure 4.11). Correspondingly, a decrease in caspase 3/7 activation was observed in *BCL-XL*-silenced A549 and SK-LU-1 cells co-transfected with miR-608 inhibitors (0.81 ± 0.10 from 2.64 ± 0.27 and 0.85 ± 0.10 from 3.83 ± 0.45 relative activity, respectively) and miR-361-5p mimics (0.72 ± 0.09 from 2.60 ± 0.72 and 0.85 ± 0.02 from 3.45 ± 0.44 relative activity, respectively) (Figure 4.12), thus suggesting that miR-608 and miR-361-5p plays an important role in the regulation of apoptotic properties.

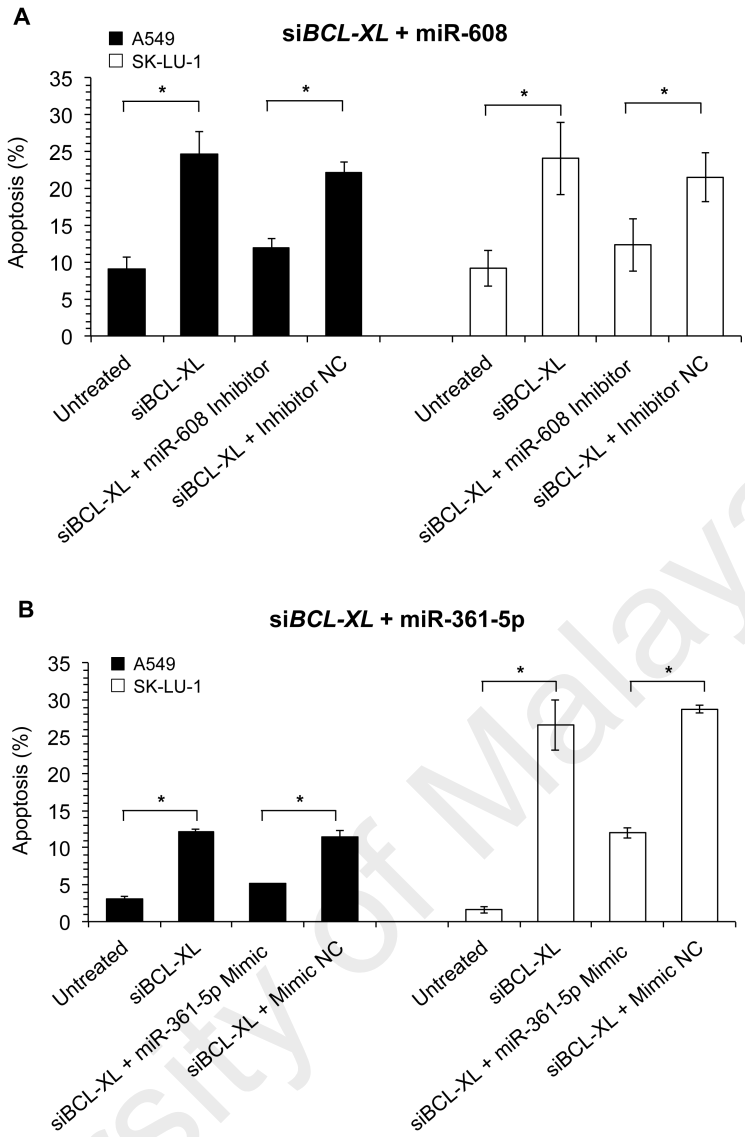

Figure 4.11: Detection of apoptosis 72 h post co-transfection with si*BCL-XL* and miRNAs. **(A)** MiR-608 inhibitors and **(B)** miR-361-5p mimics blocks si*BCL-XL*-induced cell death in A549 cells and SK-LU-1 cells. Data presented as mean ± SD, n=3, * p-value ≤ 0.05. si*BCL-XL* denotes siRNA-transfected cells. NC denotes cells transfected with scrambled RNA negative control.

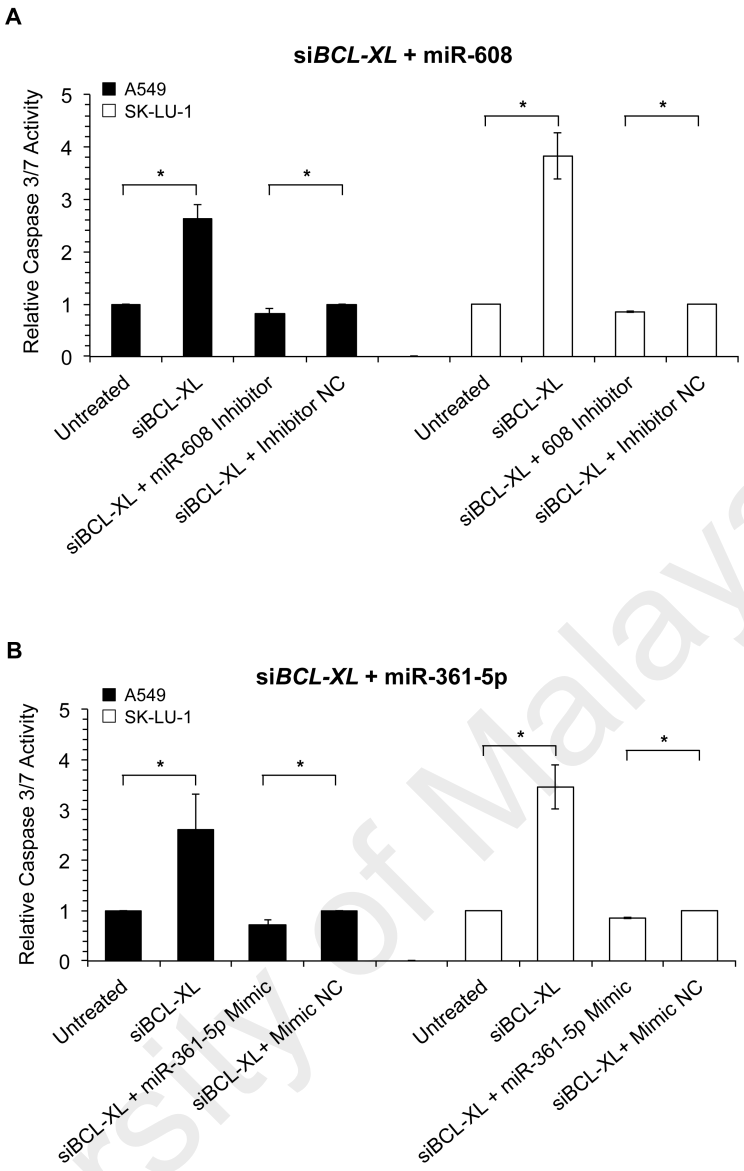

Figure 4.12: Caspase 3/7 activity detection 48 h post co-transfection with si*BCL-XL* and miRNAs. **(A)** MiR-608 inhibitors and **(B)** miR-361-5p mimics blocks si*BCL-XL*-induced caspase 3/7 activation in A549 cells and SK-LU-1 cells. Data presented as mean ± SD, n=3, * p-value ≤ 0.05. NC denotes cells transfected with scrambled RNA negative control. si*BCL-XL* denotes siRNA-transfected cells.

4.5 Up-regulation of miR-608 and down-regulation of miR-361-5p expression induces cell cycle arrest in A549 and SK-LU-1 cells

To examine the effects of miRNA on cell cycle progression, transfected cells were stained with propidium iodide and analyzed using flow cytometry. Results indicate that the number of cells in S phase was substantially increased in cells transfected with miR-608 mimics, in comparison to mimic NC-transfected cells, with a decrease in G_0/G_1 phase cell population, suggesting that miR-608 induced S phase cell cycle arrest (Figure 4.13A – Figure 4.13B). On the other hand, an increase in S phase cell population was seen in miR-361-5p inhibitor-transfected cells (Figure. 4.13C – Figure 4.13D), in comparison to inhibitor NC-transfected cells, thus suggesting that miR-361-5p plays a role in promoting cell cycle progression. Thus far, results have suggested that miR-608 plays a tumour suppressive role in lung cancer progression while miR-361-5p appears to play an oncogenic role.

A

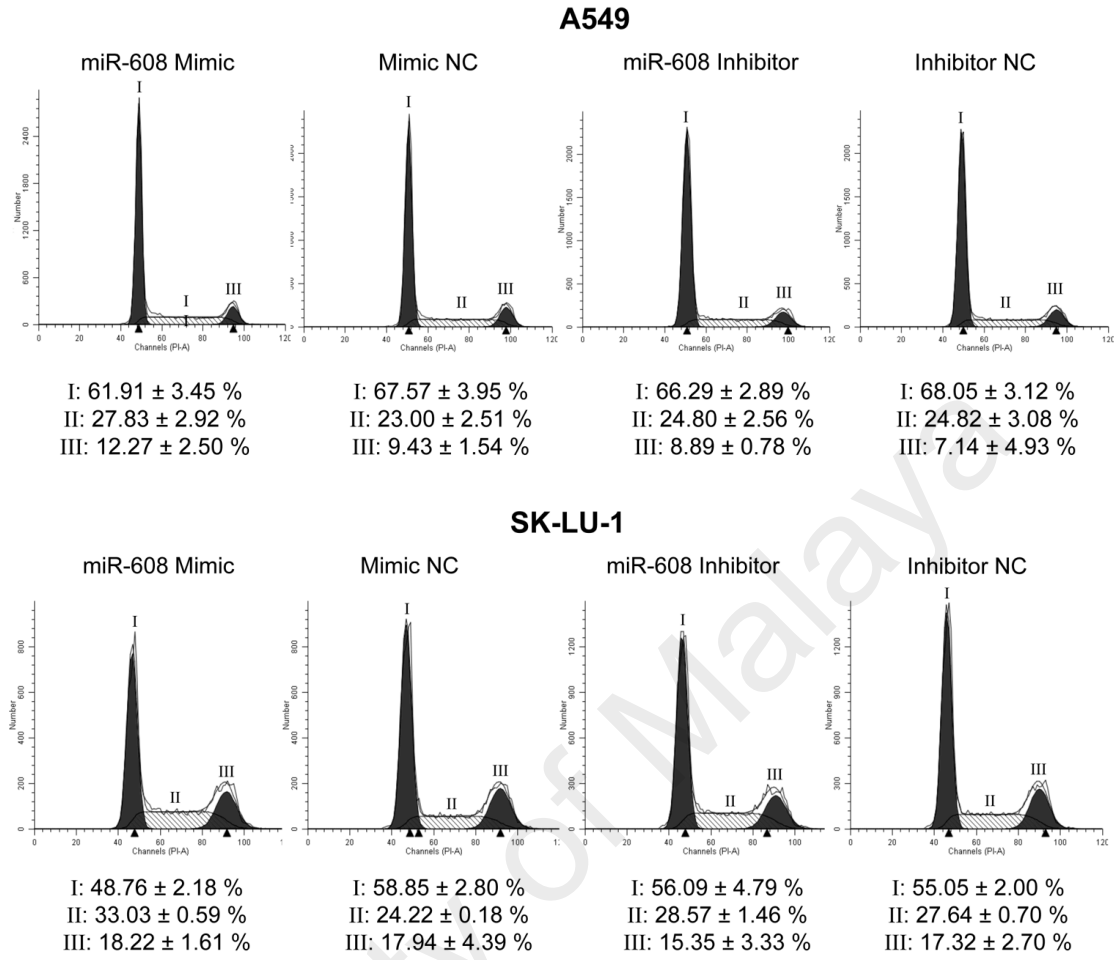

Figure 4.13: Cell cycle analysis 48 h post-transfection with miRNa mimics and inhibitors. Effect of **(A – B)** miR-608 and **(C – D)** miR-361-5p mimics and inhibitors on cell cycle distribution in A549 and SK-LU-1 cells. Data presented as mean ± SD, n=3, * *p*-value ≤ 0.05. NC denotes cells transfected with scrambled RNA negative control. I: G_0/G_1 Phase, II: S Phase, III: G_2/M Phase.

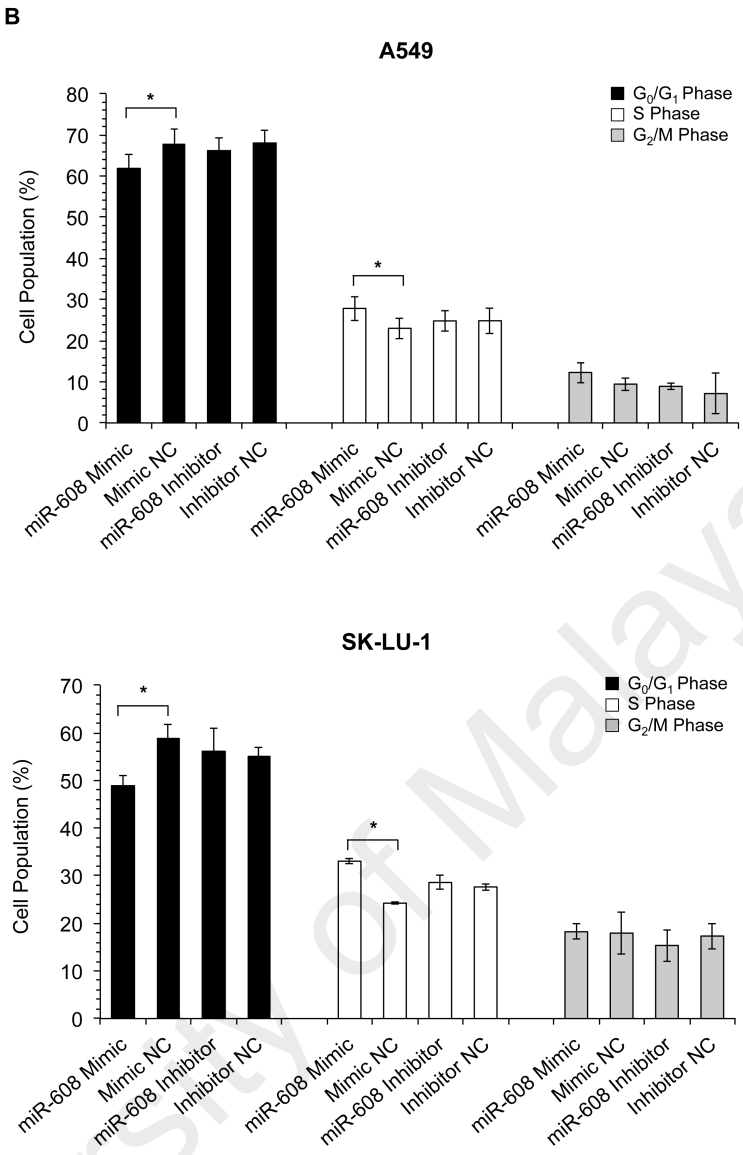

Figure 4.13, continued.

C

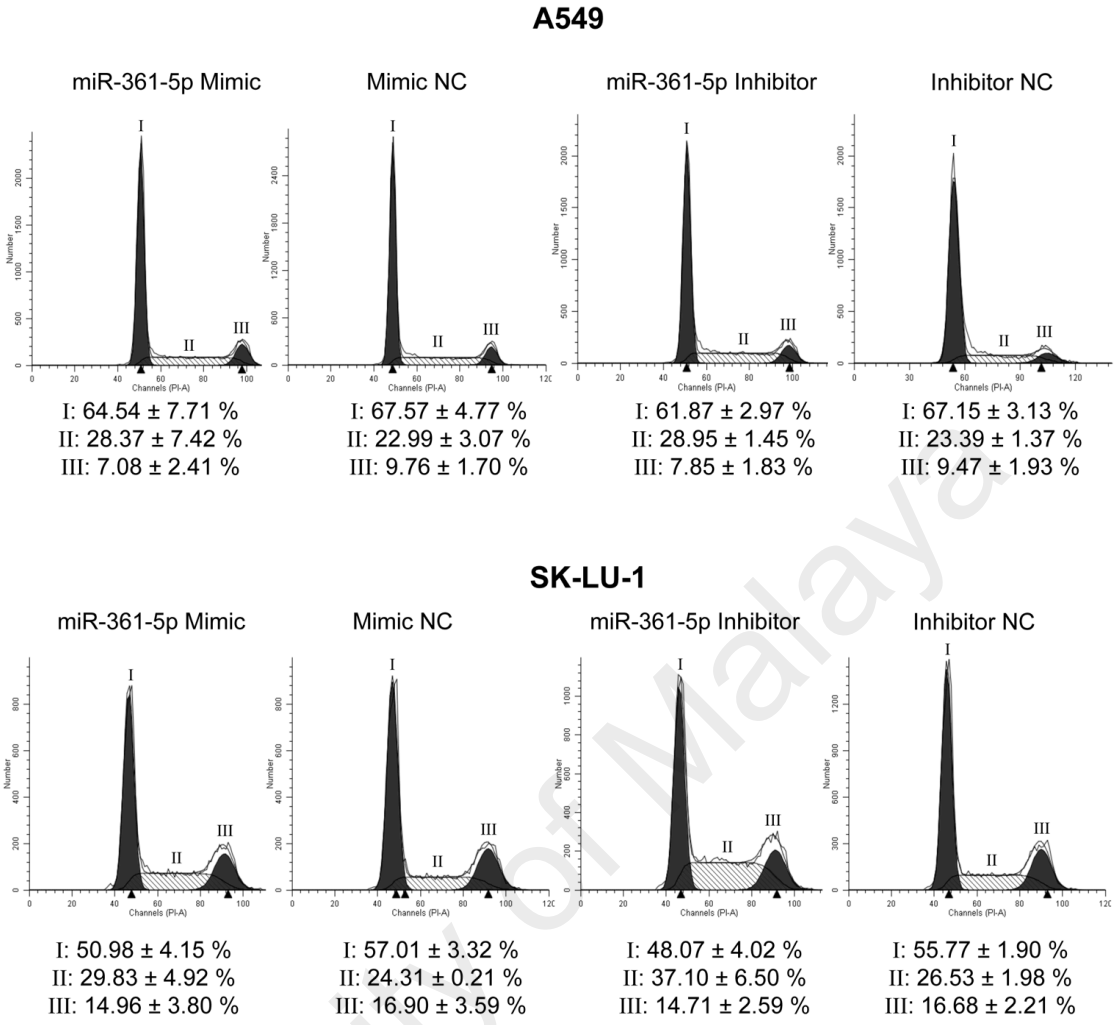

Figure 4.13, continued.

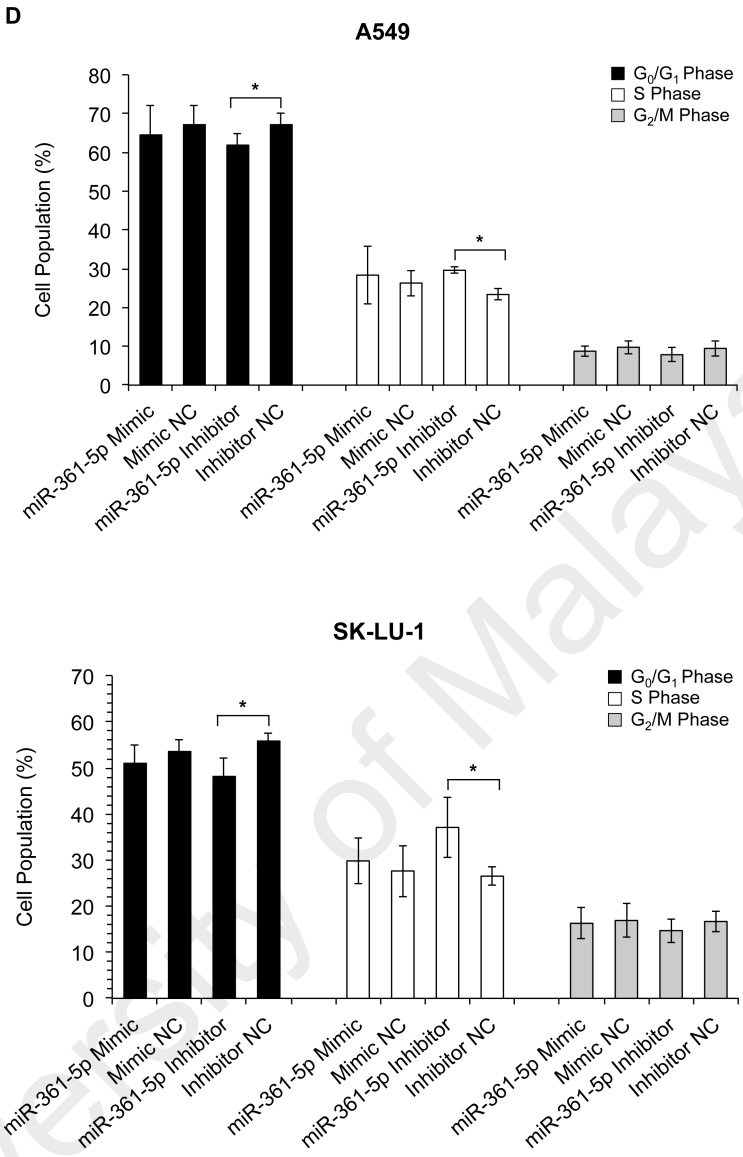

Figure 4.13, continued.

4.6 Up-regulation of miR-608 expression and down-regulation of miR-369-5p expression increases apoptosis *in vivo*

To analyze the *in vivo* apoptotic effects of miR-608 and miR-361-5p, zebrafish were used as an animal model. A549 cells transfected with either miR-608 or miR-361-5p mimics, inhibitors or its corresponding negative controls, were microinjected into zebrafish embryos. Following staining with anti-rabbit fluorophore-conjugated antibodies, embryos were visualized using a Leica confocal microscope (Figure 4.14A

and Figure 4.15A). Analysis of fluorescent images using the ImageJ Analyst software indicated that detection of active caspase 3 was significantly increased by a 6.53 ± 2.08 fold change in zebrafish embryos injected with miR-608 mimics (Figure 4.14B) and 6.41 ± 1.04 fold change in miR-361-5p inhibitor-transfected cells (Figure 4.15B), in comparison to negative control-injected embryos. These results implied that miR-608 mimics and miR-361-5p inhibitors are also able to induce apoptosis *in vivo* via caspase 3 activation.

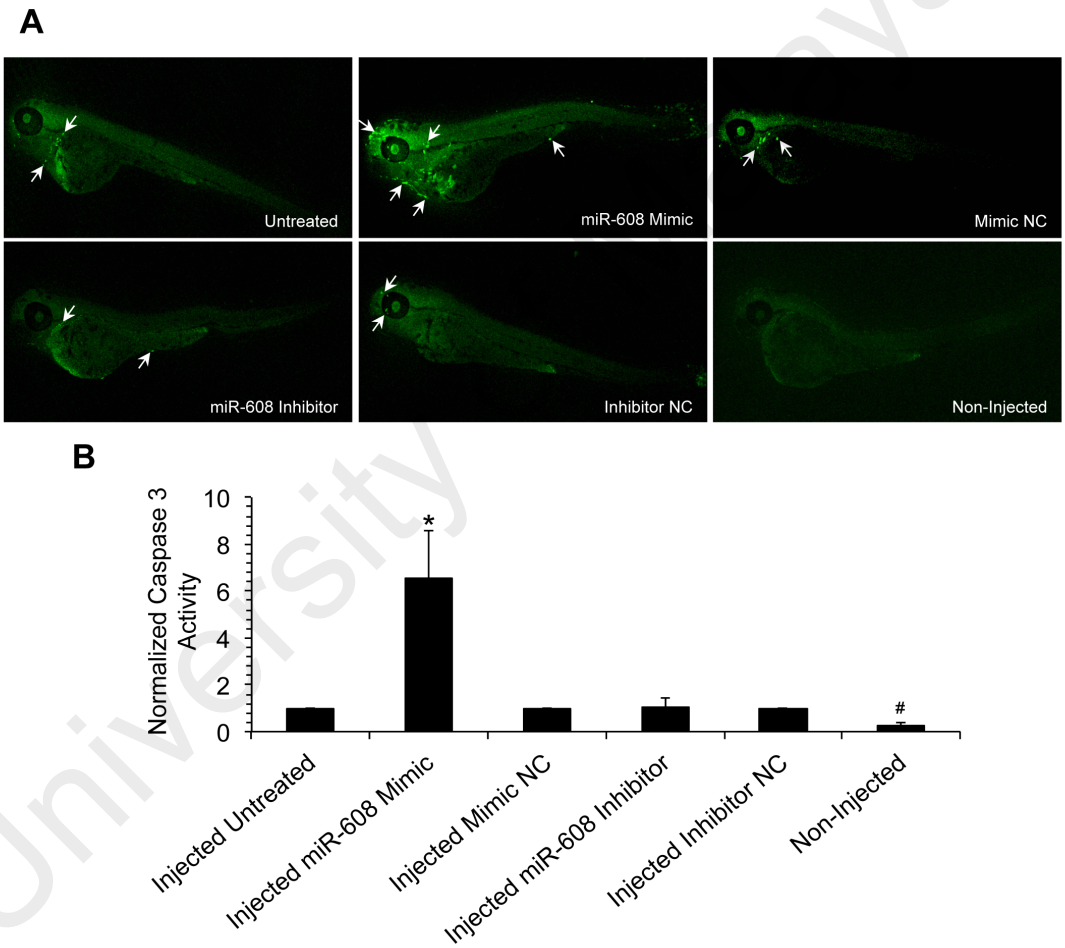

Figure 4.14: Up-regulation of miR-608 induces caspase 3 activation *in vivo*. **(A)** Examination of zebrafish embryos by confocal microscopy following miR-608 injection. Arrows indicate positive active caspase 3 staining. **(B)** Fluorescence was quantified and analyzed using ImageJ Analyst software to generate normalized arbitrary fluorescence units. Data presented as mean ± SD, n=15. Statistically significant differences between mimic-injected groups and mimic NC-injected groups denoted with * p-value ≤ 0.05. Statistically significant differences between non-injected group and injected untreated groups denoted with # p-value ≤ 0.05. NC denotes cells transfected with scrambled RNA negative control.

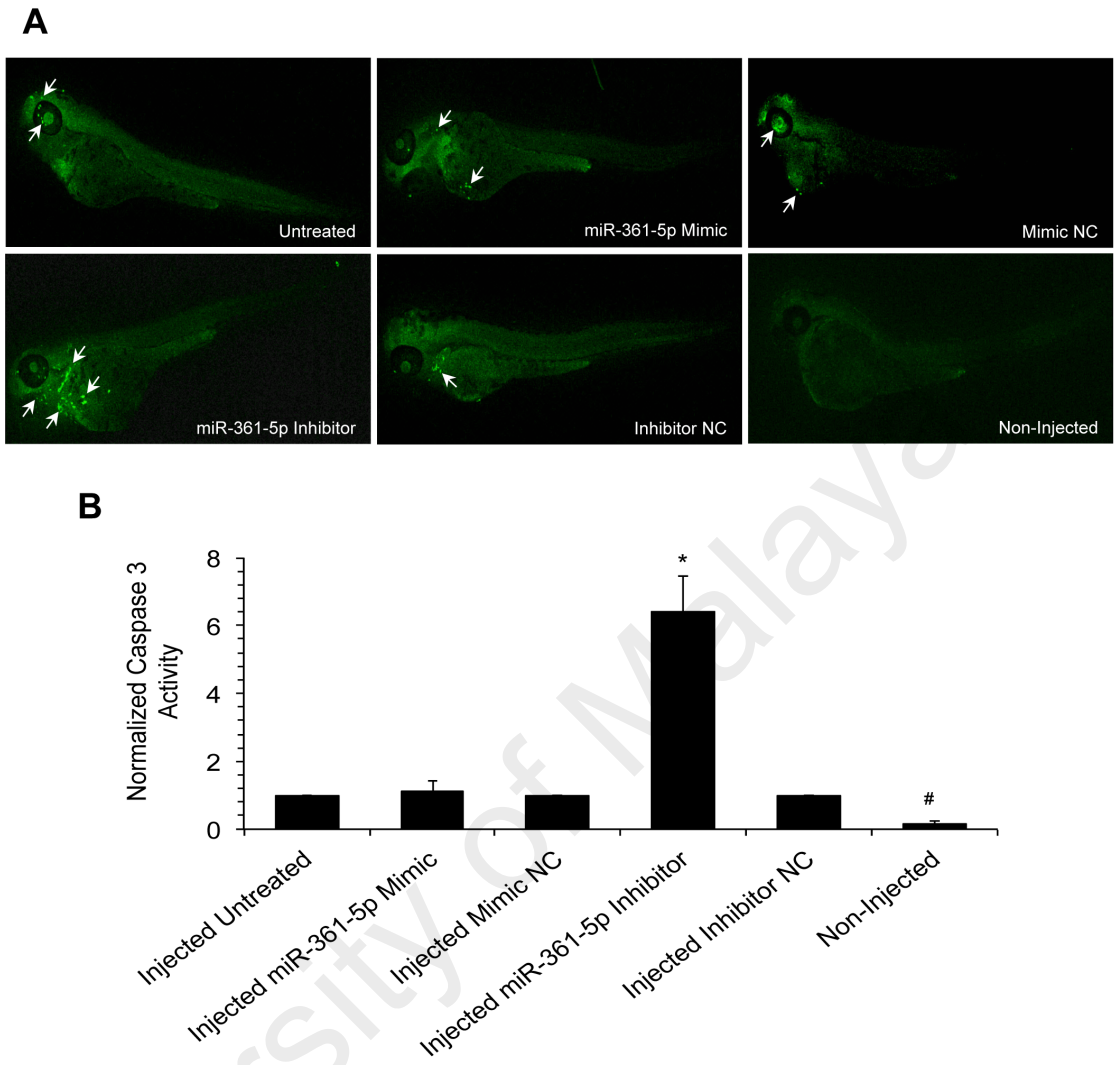

Figure 4.15: Inhibition of miR-361-5p induces caspase 3 activation *in vivo*. **(A)** Examination of zebrafish embryos by confocal microscopy following miR-361-5p injection. Arrows indicate positive active caspase 3 staining. **(B)** Fluorescence was quantified and analyzed using ImageJ Analyst software to generate normalized arbitrary fluorescence units. Data presented as mean ± SD, n=15. Statistically significant differences between inhibitor-injected groups and inhibitor NC-injected groups denoted with * p-value ≤ 0.05. Statistically significant differences between non-injected group and injected untreated groups denoted with # p-value ≤ 0.05. NC denotes cells transfected with scrambled RNA negative control.

4.7 MiR-608 and miR-361-5p-mediated apoptosis in A549 and SK-LU-1 cells is through the regulation of various signaling pathways

4.7.1 MiR-608 and miR-361-5p are predicted to bind to *AKT2* and *SMAD2* 3'UTR, respectively

To understand the underlying molecular mechanism behind miR-608 and miR-361-5p mediated apoptosis, an *in silico* approach was used to identify the putative target genes using the TargetScan Human v5.2 algorithm, followed by gene-annotation enrichment analyses using the web tool DAVID v6.7. Enrichment of genes involved in cancer pathways indicated possible involvement of the TGFβ, PI3K/AKT, MAPK, WNT, and the intrinsic and extrinsic apoptotic pathways (Figure 4.16 and Figure 4.17). The 3'UTR of V-Akt Murine Thymoma Viral Oncogene Homolog 2 (*AKT2*) and Mothers Against Decapentaplegic Homolog 2 (*SMAD2*) contains miR-608 and miR-361-5p binding sites, respectively, and are involved with apoptosis and proliferation and was thus chosen for further validation (Figure 4.18).

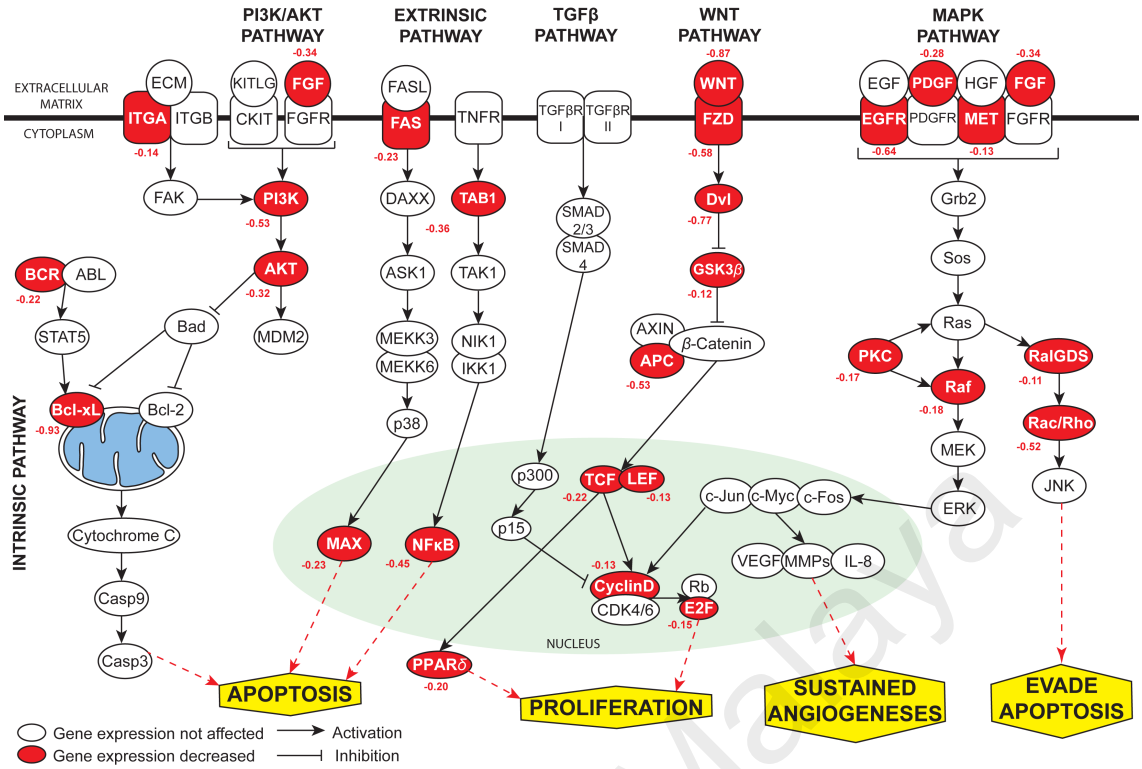

Figure 4.16: Hypothetical signaling network depicting the interactions of up-regulated miR-608 and it's putative targets in various biological pathways including apoptosis, proliferation and angiogenesis. Key signaling pathways were predicted to include the TGFβ, PI3K/AKT, MAPK, WNT, and the intrinsic and extrinsic pathway. Genes in red indicate those predicted to be targets of miR-608. Numbers in red indicate total context score for that specific target with miR-608.

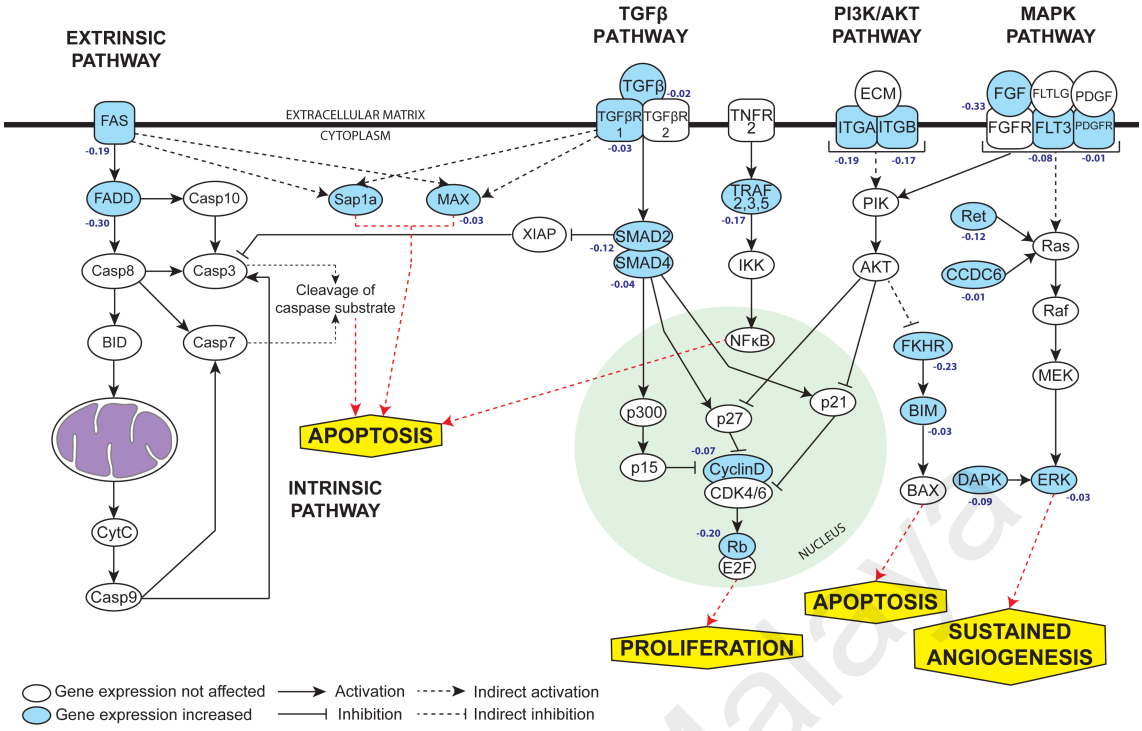

Figure 4.17: Hypothetical signaling network showing the interaction of down-regulated miR-361-5p and it's putative targets in various biological pathways including apoptosis, proliferation and angiogenesis. Key signaling pathways of apoptosis regulation were predicted to include the TGFβ, PI3K/AKT, MAPK, and the intrinsic and extrinsic pathway. Genes in blue indicate those predicted to be targets of miR-361-5p. Numbers in dark blue indicate total context score for that specific target with miR-361-5p.

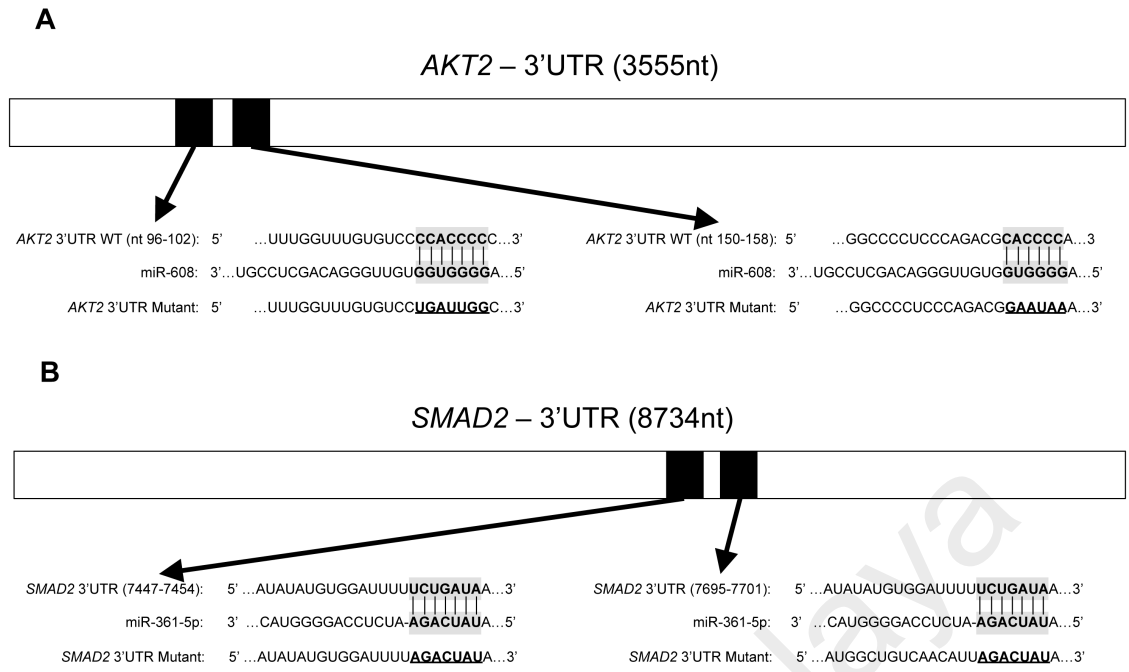

Figure 4.18: MiR-608 and miR-361-5p are predicted to target *AKT2* and *SMAD2* 3'UTR, respectively. **(A)** Sequence alignment of miR-608 and *AKT2* 3'UTR. *AKT2* 3'UTR contains two predicted miR-608 binding sites at nucleotide 96 – 102 and 150 – 158. **(B)** Sequence alignment of miR-361-5p and *SMAD2* 3'UTR. *SMAD2* 3'UTR contains two predicted miR-361-5p binding sites at nucleotide 7447 – 7454 and 7695 – 7701. The seed-recognizing sites in the 3'UTR and the seed regions of the miRNA are highlighted in grey, while the mutated 3'UTR sequences are indicated in bold underlined font.

4.7.2 MiR-608 and miR-361-5p directly binds to *AKT2* and *SMAD2* 3'UTR, respectively, subsequently decreasing its protein expression

To verify the interaction between miRNAs and their putative gene targets, *AKT2* and *SMAD2* 3'UTR and their corresponding mutant counterparts, were cloned into the 3' end of the pmirGLO Dual-Luciferase miRNA Target Expression Vector and the constructs verified by sequencing. Relative firefly luciferase activity, indicative of translation from the plasmid, was then assayed using the Dual Luciferase Reporter Assay System and measured in the presence of miR-608 or miR-361-5p mimics, or mimic negative control, and normalized using *Renilla* luciferase activity. Luciferase reporter assay confirmed that miR-608 and miR-361-5p mimics had a significant inhibitory effect on wild-type 3'UTR of *AKT2* and *SMAD2*, (0.73 ± 0.05 and 0.35 ±

0.05 relative luciferase activity, respectively) but not on mutant 3'UTR (Figure 4.19). It was further demonstrated that mimic negative controls had no effect on either wild-type or mutant luciferase activity. In line with these results no significant difference in the wild-type or mutant luciferase activities was observed in cells transfected with miR-608 and miR-361 inhibitors and inhibitor negative controls. This observation indicates that miR-608 and miR-361-5p can directly bind to the binding sites in *AKT2* and *SMAD2* respectively; and this was further verified by a decrease in AKT2 and SMAD2 protein levels as analyzed by western blot (Figure 4.20 and Figure 4.21).

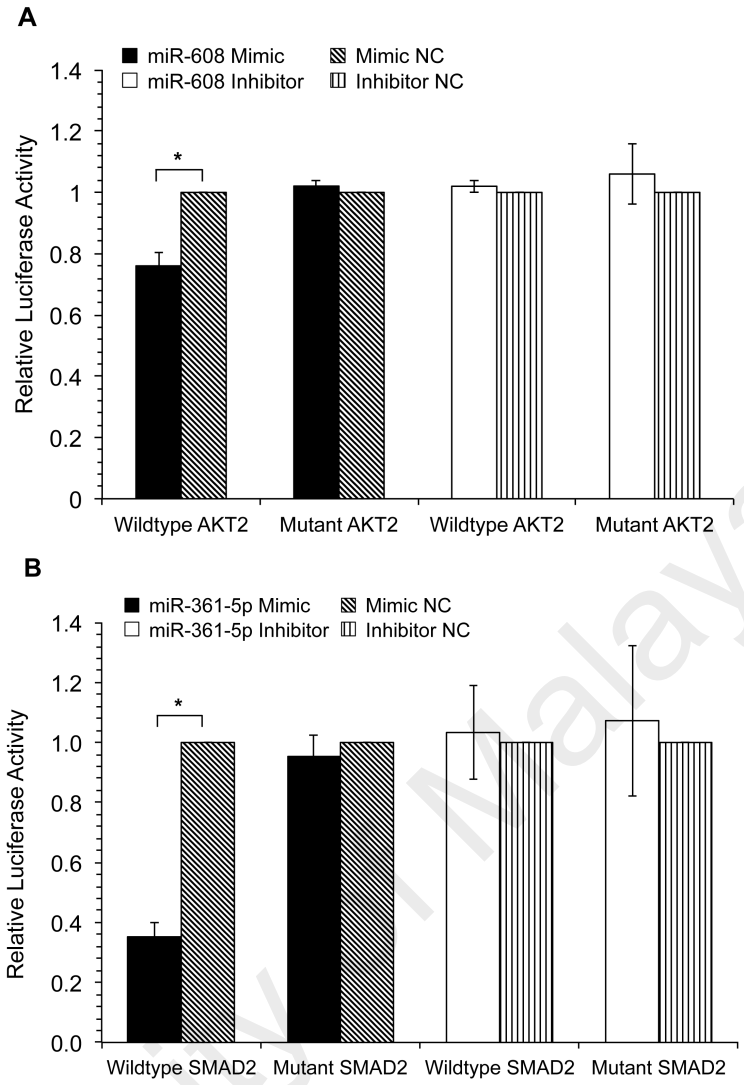

Figure 4.19: Dual luciferase reporter assay on miR-608 and miR-361-5p interaction with *AKT2* and *SMAD2* 3'UTR, respectively. Normalized relative luciferase activity in **(A)** wildtype and mutant pmirGLO/*AKT2* constructs in response to transfection with miR-608 mimic, inhibitor or their respective negative controls in A549 cells; **(B)** wildtype and mutant pmirGLO/*SMAD2* constructs in response to transfection with miR-361-5p mimic, inhibitor or their respective negative controls in A549 cells. Samples were normalized to *Renilla* luciferase activity. Data presented as mean ± SD, n=3, * *p*-value ≤ 0.05. NC denotes cells transfected with scrambled RNA negative control.

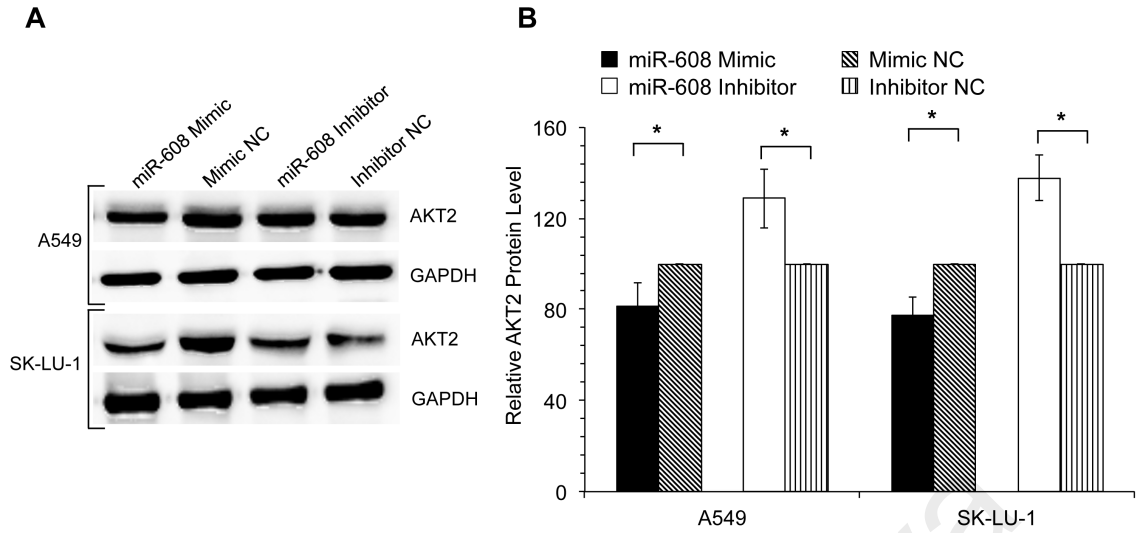

Figure 4.20: Validation of interaction between miR-608 and AKT2 via western blot analysis. **(A)** Western blot bands of AKT2 protein following miR-608 transfection. **(B)** Densitometry analysis of AKT2 protein bands using the ImageJ Analyst software. Results were standardized against GAPDH levels and presented as relative protein levels. Data presented as mean ± SD, n=3, * *p*-value ≤ 0.05. NC denotes cells transfected with scrambled RNA negative control.

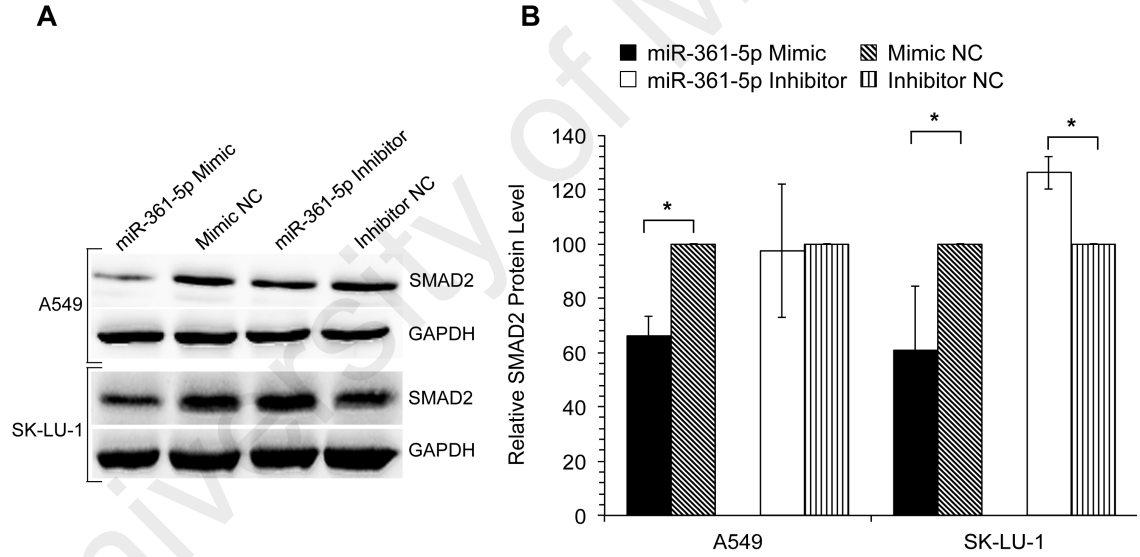

Figure 4.21: Validation of interaction between miR-361-5p and SMAD2 via western blot analysis. **(A)** Western blot bands of SMAD2 protein following miR-361-5p transfection. **(B)** Densitometry analysis of SMAD2 protein bands using the ImageJ Analyst software. Results were standardized against GAPDH levels and presented as relative protein levels. Data presented as mean ± SD, n=3, * *p*-value ≤ 0.05. NC denotes cells transfected with scrambled RNA negative control.

4.8 MiR-608 and miR-361-5p regulate apoptosis in A549 and SK-LU-1 cells through the manipulation of *AKT2* and *SMAD2* expression, respectively

4.8.1 siRNA-mediated silencing of *AKT2* restores miR-608-induced effects in A549 and SK-LU-1 cells

Together, results have demonstrated that miR-608 plays an important role in the regulation of apoptosis, and miR-608 has been identified as direct a regulator of *AKT2*. It can be hypothesized that low expression of miR-608 in NSCLC may inhibit its suppressive effects towards *AKT2*, thus causing *AKT2* expression to be up-regulated, which in turn blocks apoptosis. To investigate this hypothesis, co-transfection of miR-608 inhibitors and siRNA inhibiting *AKT2* was performed in A549 and SK-LU-1 cells. SiRNAs were provided as a set of three siRNA duplexes, therefore to evaluate the silencing efficiency of the siRNAs, densitometry analysis of western blot bands was performed to evaluate the AKT2 protein expression in siRNA-transfected cells in comparison to siRNA NC transfected cells. Amongst the three siRNAs utilized, siRNA C was able to significantly decrease AKT2 protein levels to 72.86 ± 17.85% and 72.52 ± 17.83% in A549 and SK-LU-1 cells, respectively (Figure 4.22). As siRNA C (referred to as si*AKT2* henceforth) had the greatest silencing efficiency amongst the three siRNAs, it was selected for further downstream work.

Cells transfected with miR-608 inhibitors alone led to an increased AKT2 protein expression, while co-transfection of miR-608 inhibitors with si*AKT2* was able to reverse this observation (Figure 4.23). Furthermore, si*AKT2* was able to partially rescue the inhibition of apoptosis and caspase 3/7 activation induced by miR-608 inhibitors (Figure 4.24 and Figure 4.25), leading to a significant increase in apoptosis. Collectively, these results demonstrate the miR-608 plays a tumour suppressive role in NSCLC and this is at least partially through its inhibition of *AKT2*.

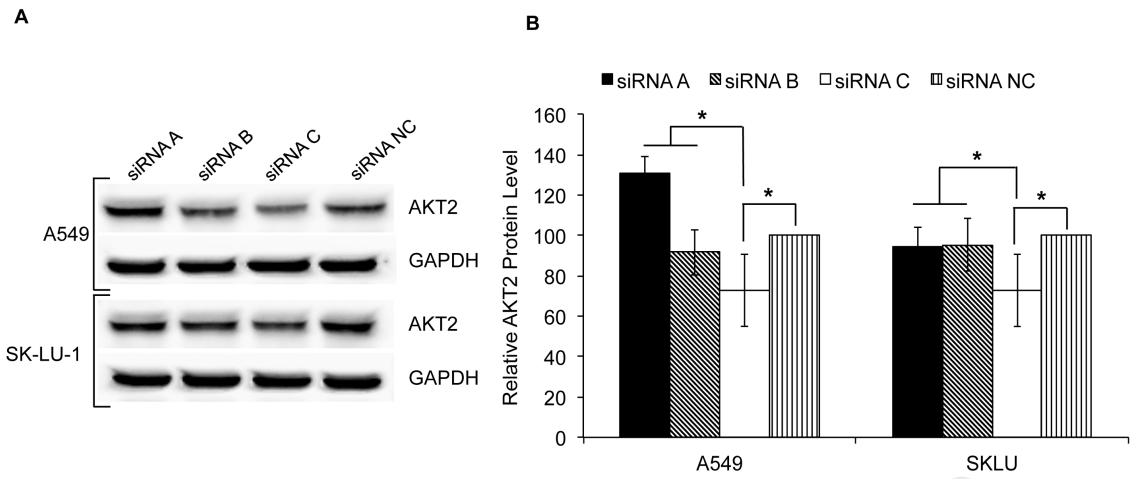

Figure 4.22: Quantitation of AKT2 bands following siRNA-based silencing of *AKT2*. **(A)** Western blot bands of AKT2 protein following transfection with siRNA duplexes used for *AKT2* silencing. **(B)** Densitometry analysis of AKT2 protein bands using the ImageJ Analyst software. Results were standardized against the levels of GAPDH and presented as relative protein levels. Data presented as mean ± SD, n=3, with statistically significant differences denoted with * *p*-value ≤ 0.05. siRNA denotes siRNA-transfected cells. siRNA NC denotes universal scrambled negative control siRNA-transfected cells.

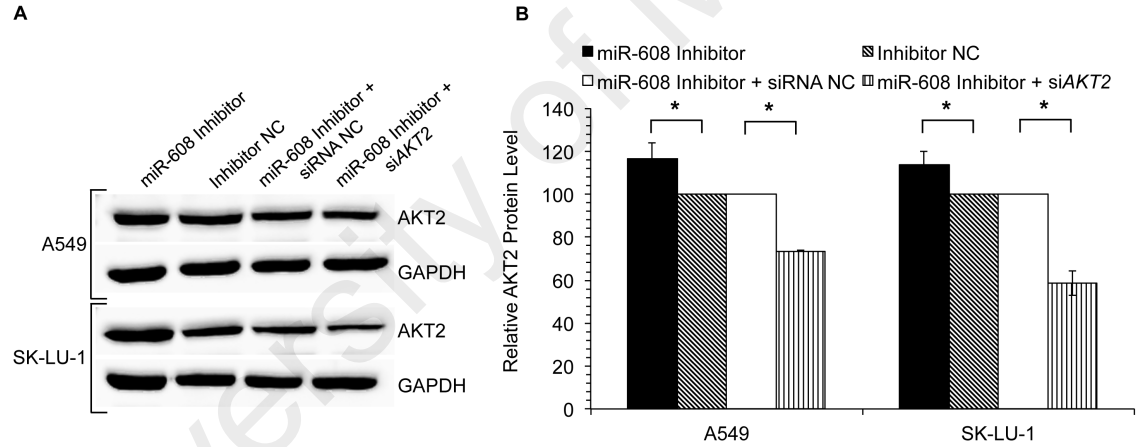

Figure 4.23: Silencing of *AKT2* decreased AKT2 protein levels. **(A)** Western blot analysis of AKT2 protein expression following co-transfection of miR-608 inhibitors and si*AKT2*. **(B)** Densitometry analysis of AKT2 protein bands using the ImageJ Analyst software. Results were standardized against the levels of GAPDH and presented as relative expression. Data presented as mean ± SD, n=3, * *p*-value ≤ 0.05. NC denotes cells transfected with scrambled RNA negative control. si*AKT2* denotes siRNA-transfected cells. siRNA NC denotes universal scrambled negative control siRNA-transfected cells.

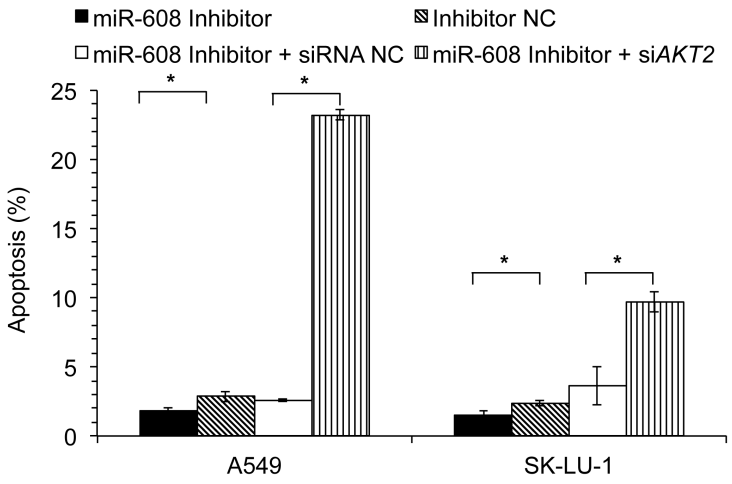

Figure 4.24: Detection of apoptosis 48 h post co-transfection with miR-608 inhibitors and si*AKT2*. Data presented as mean ± SD, n=3, * *p*-value ≤ 0.05. Inhibitor NC and siRNA NC were used as negative controls. NC denotes cells transfected with scrambled RNA negative control. si*AKT2* denotes siRNA-transfected cells. siRNA NC denotes universal scrambled negative control siRNA-transfected cells.

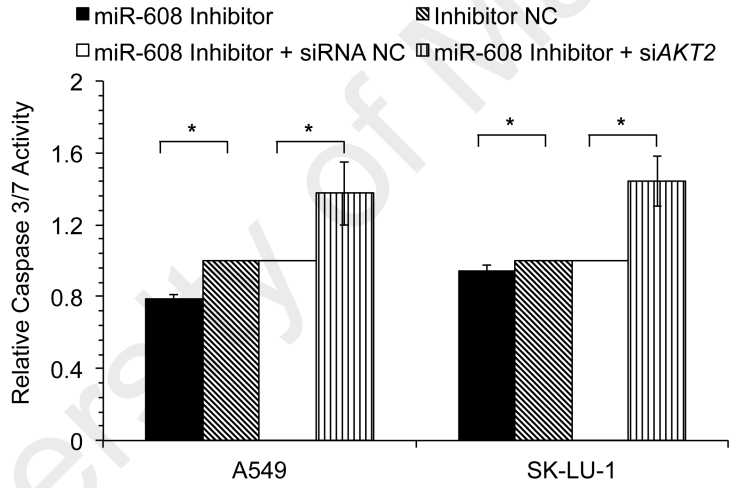

Figure 4.25: Detection of caspase 3/7 activity 48 h post co-transfection with miR-608 inhibitors and si*AKT2*. Data presented as mean ± SD, n=3, * *p*-value ≤ 0.05. NC denotes cells transfected with scrambled RNA negative control. Inhibitor NC and siRNA NC were used as negative controls. si*AKT2* denotes siRNA-transfected cells. siRNA NC denotes universal scrambled negative control siRNA-transfected cells.

4.8.2 Ectopic overexpression of *SMAD2*, without 3'UTR, restores miR-361-5p induced effects in A549 and SK-LU-1 cells

Results have indicated that miR-361-5p suppresses apoptosis in A549 and SK-LU-1 cells, and inhibits *SMAD2* expression. It was thus predicted that miR-361-5p-mediated apoptosis inhibition could in part be credited to the *SMAD2* gene. To further validate that the effect of miR-361-5p on apoptosis is mediated by *SMAD2*, gene rescue experiments were performed whereby *SMAD2* overexpression vector (pCMV6/*SMAD2*), lacking its 3'UTR, was co-transfected into A549 and SK-LU-1 cells along with miR-361-5p mimic. SMAD2 protein expression levels were measured 48 h post transfection, and it was found that pCMV6/*SMAD2* rescued the decreased protein expression that was observed in cells transfected with miR-361-5p mimics only (Figure 4.26). Furthermore, pCMV6/*SMAD2* was able to partially reverse the apoptosis inhibition caused by miR-361-5p (Figure 4.27 and Figure 4.28). Taken together, these observations suggest that the oncogenic role of miR-361-5p in lung adenocarcinoma cells is at least partially by inhibiting its target gene *SMAD2*.

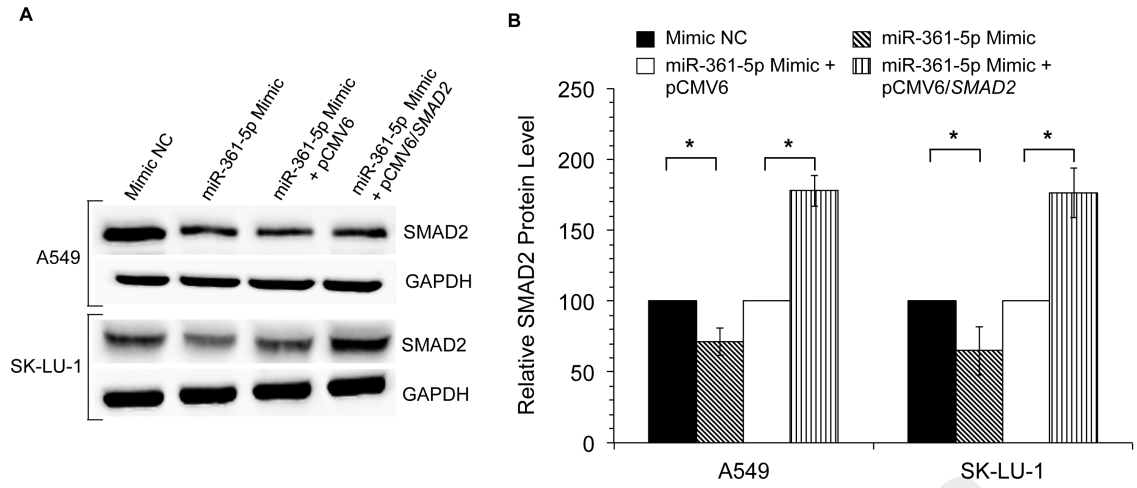

Figure 4.26: Overexpression vector pCMV/*SMAD2* increased SMAD2 protein levels. **(A)** Western blot analysis of SMAD2 protein expression following co-transfection of miR-361-5p mimics and pCMV6/*SMAD2*. **(B)** Densitometry analysis of SMAD2 protein bands using the ImageJ Analyst software. Results were standardized against the levels of GAPDH and presented as relative protein levels. Data presented as mean ± SD, n=3, * *p*-value ≤ 0.05. NC denotes cells transfected with scrambled RNA negative control. pCMV6/*SMAD2* denotes *SMAD2* overexpression vector. pCMV6 denotes empty vectors.

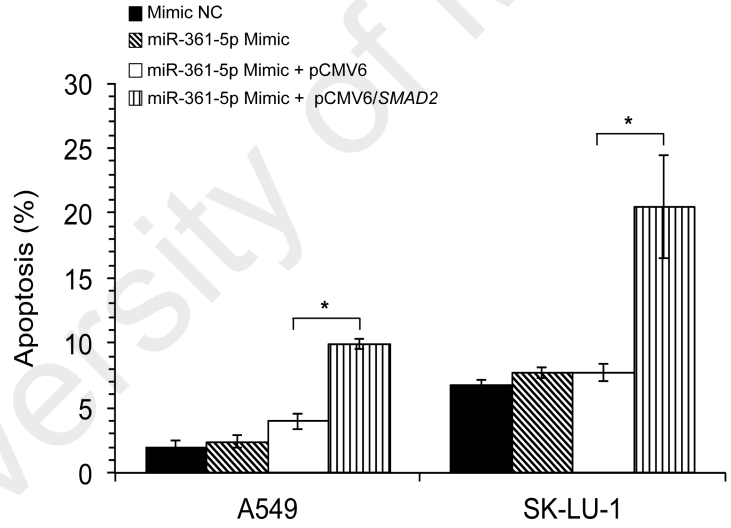

Figure 4.27: Detection of apoptosis 48 h post co-transfection with miR-361-5p mimics and pCMV6/*SMAD2* vectors. Data presented as mean ± SD, n=3, * *p*-value ≤ 0.05. Mimic NC and pCMV6 were used as negative controls. NC denotes cells transfected with scrambled RNA negative control. pCMV6/*SMAD2* denotes *SMAD2* overexpression vector. pCMV6 denotes empty vectors.

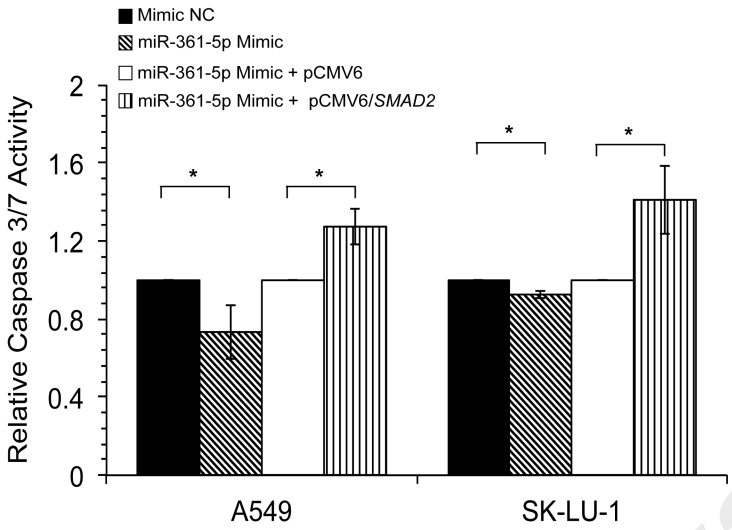

Figure 4.28: Detection of caspase 3/7 activity 48 h post co-transfection with miR-361-5p mimics and pCMV6/*SMAD2* vectors. Data presented as mean ± SD, n=3, * *p*-value ≤ 0.05. Mimic NC and pCMV6 were used as negative controls. NC denotes cells transfected with scrambled RNA negative control. pCMV6/*SMAD2* denotes *SMAD2* overexpression vector. pCMV6 denotes empty vectors.

CHAPTER 5: DISCUSSION

5.1 *BCL-XL* silencing induces a decrease in cell viability and an increase in apoptosis in A549 and SK-LU-1 cells

BCL-XL expression is generally found to be significantly increased in human cancers. Analysis of *BCL-XL* expression using immunohistochemistry, reverse transcription PCR or western blotting has revealed that *BCL-XL* is positively expressed in invasive ductal adenocarcinomas (Miyamoto *et al.*, 1999), squamous cell carcinoma of the head and neck (Pena *et al.*, 1999) and ovarian tumours (Marone *et al.*, 1998) in comparison to neighboring normal tissues. Therefore, *BCL-XL* can be used as an important marker for various cancers. Reports have also indicated that up-regulation of *BCL-XL* contributes to protection of cancer cell lines from apoptosis stimulated by a wide array of chemotherapeutic agents including teniposide, etoposide, methotrexate, fluorouracil, hydroxyurea and cisplatin (Simonian *et al.*, 1997). In metastatic malignant melanoma, high levels of *BCL-XL* lead to avoidance of the normal cell death pathway, and may contribute to melanoma progression and chemotherapy resistance (Tang *et al.*, 1998). Similarly an increased expression of *BCL-XL* in ovarian cancer cell lines contributes to chemoresistance against cisplatin through the blockage of caspase 3 activity and Poly (ADP-ribose) polymerase (PARP) cleavage (Yang *et al.*, 2004). High expression of *BCL-XL* in diffuse large B cell non-Hodgkin's lymphoma was also demonstrated to be associated with chemoresistance in short survival group of patients (Bairey *et al.*, 1999). Other studies have reported that *BCL-XL* plays a critical role in the development of tumours and malignant transformation. *BCL-XL* expression is significantly higher in tongue carcinoma tissues than in normal tongue tissues, with a higher expression found in oral tongue squamous cell carcinoma (OTSCC) tissues in comparison to oral tongue adenocarcinoma (OTA) tissues (Zhang *et al.*, 2014a). Zhang *et al*. (2014) also discovered that expression of *BCL-XL* was considerably higher in

tissues with lymph node metastasis than in those without lymph node metastasis. Up-regulation of *BCL-XL* in squamous cell carcinoma of the tongue was thus concluded to be associated with the early progression of this disease but also inhibits the differentiation of the cancer (Zhang *et al.*, 2014a). Similarly, two studies have shown that in human colon cancer, *BCL-XL* was found to be overexpressed, and was strongly correlated with the pathological grade, lymph node metastasis and Duke's stage of colorectal carcinoma (Krajewska *et al.*, 1996; Biroccio *et al.*, 2001; Zhang *et al.*, 2008), suggesting that overexpression of *BCL-XL* was associated with the progression and invasion of this cancer. Together these results indicate the usefulness of *BCL-XL* expression as a prognostic marker in cancers.

Correspondingly, expression of *BCL-XL* was found to be frequently up-regulated significantly in NSCLC (Groeger *et al.*, 2004; Karczmarek-Borowska *et al.*, 2006; Sanchez-Ceja *et al.*, 2006). Interestingly, high expression of *BCL-XL* in NSCLC cells, specifically in the lung adenocarcinoma subgroup, is usually accompanied with a low expression or non-detectable levels of *BCL-2*, suggesting that *BCL-XL* is the major apoptosis-repressor protein in these cells (Reeve *et al.*, 1996; Koty *et al.*, 2002; Berrieman *et al.*, 2005). Various studies have shown that anti-sense treatment of *BCL-XL* induces a strong apoptotic response and increased chemosensitivity in lung adenocarcinoma cells that lack significant levels of *BCL-2*, while the same response was not observed in SCLC cells most probably due to protection by increased levels of *BCL-2* that are also expressed in these cells (Leech *et al.*, 2000; Lei *et al.*, 2007; Park *et al.*, 2013). Together, these results suggest that *BCL-XL* may be a useful diagnostic marker and can be a potential specific therapeutic target.

In this present study, *BCL-XL* expression in SK-LU-1 lung adenocarcinoma cells was silenced via siRNA transfection to corroborate the findings in A549 lung adenocarcinoma cells previously reported in my Masters study (Othman, 2012). A set of three siRNAs were utilized, and since the siRNAs do not fluoresce, visual monitoring of transfection efficiency was first determined using the BLOCK-iT™ Alexa Fluor® Red Fluorescent Oligo, which is a highly stable, fluorescein-labeled, non-targeted dsRNA compound. As seen in Figure 4.1, results indicated that a satisfactory transfection efficiency of greater than 80.0% was obtained 24 h post-transfection, thus allowing for silencing efficiency of the three siRNAs to be determined using qRT-PCR.

qRT-PCR results revealed that *BCL-XL* expression levels were significantly decreased for all siRNA-transfected SK-LU-1 cells, in comparison to non-transfected cells (Figure 4.2). Amongst the three siRNAs utilized, siRNA 1 had a greatest negative fold change of -4.03 ± 0.01 with a percentage *BCL-XL* gene knockdown of 75.16 ± 0.92% (Table 4.1). Western blot analysis was then performed to confirm successful silencing of *BCL-XL*, and correspondingly, siRNA 1 was demonstrated to induce the greatest decrease in BCL-XL protein levels with a 98.33 ± 0.50% decrease in siRNA 1-transfected SK-LU-1 cells, as determined by densitometry analysis of western blot bands (Figure 4.3). As siRNA 1 (henceforth referred to as si*BCL-XL*) had the greatest silencing efficiency amongst the three siRNAs, it was selected for further downstream work.

MTT viability assay and annexin V-FITC detection was then performed to determine the biological effects of *BCL-XL* silencing in SK-LU-1 cells. Results indicated that a knockdown of *BCL-XL* expression led to a significant decrease in cell viability, 48-h post-transfection, in si*BCL-XL* -transfected cells (58.22 ± 0.98%) in comparison to non-transfected cells (103.29 ± 3.69) (Figure 4.4 and Table 4.2). A shift in population of

cells from viable cells to early and late stage apoptosis was also observed in si*BCL-XL*-transfected cells (Figure 4.5). At this point, the biological effects of *BCL-XL* silencing in SK-LU-1 cells correlate with those observed in A549 cells (Othman, 2012). More importantly, these findings are consistent with other *BCL-XL* antisense treatment studies, as described previously, thus validating that *BCL-XL* may be the critical apoptosis repressor protein in lung adenocarcinoma cell lines.

5.2 *BCL-XL* silencing dysregulates the miRNA expression profile in A549 and SK-LU-1 cells

While silencing of *BCL-XL* leads to an increase of apoptosis mediated cell death as observed through the annexin V-FITC/PI assay, the specific mechanism by which cell death occurs cannot be solely ascribed towards *BCL-XL* inhibition alone. There exists the possibility of rippling effects from miRNA expression alterations towards gene targets associated with other cell death-inducing factors, in response to *BCL-XL* silencing.

The expression of miRNAs can be controlled by various mechanisms which when disrupted can lead to deregulated expression of miRNAs in human diseases including cancer. For example, the expression of miRNAs can be modulated by defects or changes that occur in the activity of important miRNA biogenesis enzymes such as Dicer and Drosha, due to mutations or epigenetic modifications of these enzymes (Thomson *et al.*, 2006; Nakamura *et al.*, 2007; Merritt *et al.*, 2008; Kawahara, 2014). The effects of endogenous (hormones, cytokines) and exogenous (xenobiotics) compounds can also play a role in the regulation of miRNA expression (Chen, 2010; Huumonen *et al.*, 2014; Marrone *et al.*, 2016). Epigenetic changes, such as, DNA hypermethylation has also been reported to cause changes in miRNA expression as many miRNAs are associated with CpG islands (Weber *et al.*, 2007; Lehmann *et al.*,

2008; Toyota *et al.*, 2008). Finally, an important contributor to miRNA expression is alterations in transcription factor activity (Chang *et al.*, 2007; Burk *et al.*, 2008; Mott *et al.*, 2010).

BCL-XL has been reported to play a role in the indirect regulation of an important transcription factor, nuclear factor kappa-light-chain-enhancer of activated B cells (NFκB). In a study by Gabellini and colleagues (2008), up-regulation of *BCL-XL* was found to decrease the cytoplasmic expression of IκBα protein with a corresponding phosphorylation at Ser32 and Ser36 amino acid residues of this protein, leading to its subsequent degradation (Gabellini *et al.*, 2008). Following this, an increase in nuclear p65 protein expression was found in the glioblastoma cell lines overexpressed with *BCL-XL* (Gabellini *et al.*, 2008). In turn, NFκB has been reported to be able to regulate the expression of various miRNAs including miR-9 (Bazzoni *et al.*, 2009), miR-143 (Zhang *et al.*, 2009), miR-146 (Pacifico *et al.*, 2010; Suzuki *et al.*, 2010), miR-21 (Niu *et al.*, 2012), miR-34a (Li *et al.*, 2012b) and miR-224 (Scisciani *et al.*, 2012). With this in mind, it can be assumed that silencing of *BCL-XL* will cause a dysregulation of miRNA expression profiles, whether it is a direct or indirect regulation.

To date, there have been no studies conducted to identify miRNAs regulated or affected by the expression of *BCL-XL*. MiRNAs play an integral role in the regulation of apoptosis in tumourigenesis, and numerous studies have reported dysregulated miRNA expression profiles in cancers. Therefore, profiling of differences in miRNA expression in *BCL-XL*-silenced human lung adenocarcinoma cells and non-silenced cells is useful in identification of specific miRNAs that influence the apoptosis process.

Previously in my Masters project, a global miRNA expression profile was produced detailing the dysregulation of miRNAs between *BCL-XL*-silenced and non-silenced A549 cells. To determine whether the same pattern can be observed in a secondary lung adenocarcinoma cell line, SK-LU-1, the expression of five candidate miRNAs (miR-181a, miR-769-5p, miR-361-5p, miR-1304, and miR-608) were evaluated using RT-qPCR. Results confirmed that the same pattern of dysregulation for these five miRNAs was present in both A549 and SK-LU-1 (Figure 4.6 and Table 4.3), suggesting that these miRNAs may be cancer specific and may be suitable markers for NSCLC.

At the time experimentation was being conducted for this study, there were a number of publications implicating the candidate miRNAs selected for this study in a wide variety of cancers. For example, miR-769-5p expression is reported to be up-regulated in mutated Merkel cell polyomavirus (MCV) positive Merkel cell carcinoma (MCC) (Xie *et al.*, 2014) and in hypoxic lung cancer cells (Geng *et al.*, 2016), where it exhibited its functions in hypoxia-induced lung cancer cells through the regulation of AT-rich interaction domain 1A (*ARID1A*) and *SMAD2* (Geng *et al.*, 2016). On the other hand, miR-1304 is up-regulated in response to paclitaxel treatment in hypopharynx cancer (HPC) cells, Fadu, and can potentially be a biomarker or therapeutic target for paclitaxel-based therapy in HPC patients (Xu *et al.*, 2013). Furthermore, miR-1304 was one amongst four miRNAs that was able to discriminate cases as high or low risk prognosis in lower-grade glioma with isocitrate dehydrogenase (IDH) 1/2 mutations (Cheng *et al.*, 2017).

Expression of miR-361-5p was reported to vary depending on the type of cancer, and it has been shown that this miRNA can function as either a tumour suppressor or an oncomiR. In colorectal and gastric cancer, miR-361-5p plays a tumour suppressive role and inhibits cell proliferation, invasion and metastasis through the direct binding of staphylococcal nuclease domain containing-1 (*SND1*) (Ma *et al.*, 2015). MiR-361-5p also behaves as a tumour suppressor in hepatocellular carcinoma (Sun *et al.*, 2016) and prostate cancer (Liu *et al.*, 2014), inhibiting cell proliferation and inducing apoptosis through direct inhibition of C-X-C chemokine receptor type 6 (*CXCR6*) and signal transducer and activator of transcription 6 (*STAT6*), respectively. In NSCLC, miR-361-5p expression is significantly down-regulated in cancerous tissues and is associated with low survival in NSCLC patients (Zhuang *et al.*, 2016). Conversely, in cervical cancer, miR-361-5p functions as an oncomiR; enhancing cell growth and promoting increased migration and invasion capacity of cervical cells through mediation of the epithelial-to-mesenchymal (EMT) transition (Wu *et al.*, 2013a).

MiR-608 expression is a prognostic marker in carcinogenesis with its expression being down-regulated in various cancers including chordoma cancer (Zhang *et al.*, 2014b), colon cancer (Yang *et al.*, 2016), glioblastoma (Wang *et al.*, 2016), and osteosarcoma (Wu *et al.*, 2016). Single nucleotide polymorphisms (SNPs) rs4919510 of miR-608 is shown to serve as predictors of clinical outcomes in colorectal cancer (Ryan *et al.*, 2012), esophageal squamous cell carcinoma (ESCC), (Yang *et al.*, 2014), breast cancer (Huang *et al.*, 2012; Hashemi *et al.*, 2016b) and bladder cancer (Hashemi, 2016a). MiR-608 is also a marker to predict locoregional recurrence in radiotherapy-treated nasopharyngeal carcinoma (Zheng *et al.*, 2013). rs4919510 SNP in miR-608 has also been reported to influence HER2-positive breast cancer risk and tumour proliferation (Huang *et al.*, 2012). In chordoma cancer, miR-608 induces apoptosis and hinders cell proliferation via regulation of epidermal growth factor

receptor (*EGFR*) and *BCL-XL* (Zhang *et al.*, 2014b). MiR-608 has also been shown to directly target macrophage migration inhibitory factor (*MIF*), inhibiting proliferation, migration and invasion, and inducing apoptosis in both osteosarcoma cell lines (Wu *et al.*, 2016) and glioma stem cells (Wang *et al.*, 2016). Furthermore, miR-608 has been demonstrated to repress tumourigenesis of colon cancer cells both *in vitro* and *in vivo* through the regulation of N-a-acetyltransferase 10 protein (*NAA10*) (Yang *et al.*, 2016).

Out of the five candidate miRNAs dysregulated by *BCL-XL* silencing, miR-181a was the most extensively studied. The altered expression of miR-181a has been discovered in various cancers, with its expression significantly up-regulated in thyroid cancer (He *et al.*, 2005), esophageal squamous cell carcinoma (Xiang *et al.*, 2014), hepatocellular carcinoma (Zhang *et al.*, 2011), breast cancer (Ouyang *et al.*, 2014), colon cancer (Wei *et al.*, 2014), and cutaneous T-cell lymphoma (Sandoval *et al.*, 2015). Up-regulation of miR-181a in gastric cancer promotes cell proliferation (Chen *et al.*, 2013), while increased levels in ovarian cancer induces increased cellular survival, migration, invasion and drug resistance (Parikh *et al.*, 2014). MiR-181a is elevated in colorectal cancer with metastasis, with increased expressions promoting cell motility and invasion as well as tumour growth and liver metastasis, through the inhibition of WNT inhibitory factor 1 (*WIF-1*) (Ji *et al.*, 2014). However, in glioblastoma multiforme, the most malignant type of brain tumour, expression of miR-181a is down-regulated and ectopic overexpression was able to inhibit invasive proliferation of glioblastoma cells (She *et al.*, 2014). MiR-181a has also been reported to be down-regulated in oral squamous cell carcinoma (OSCC), with ectopic overexpression suppressing proliferation and anchorage independent growth ability of OSCC (Shin *et al.*, 2011). MiR-181a was discovered to play a tumour suppressive role in OSCC partially through the regulation of the *KRAS* gene (Shin *et al.*, 2011). As miR-181a was already well studied, the functional roles of miR-181a were not further evaluated in this study.

5.3 MiR-608 and miR-361-5p plays a significant role in the apoptotic properties of A549 and SK-LU-1 cells

The function of miRNAs dysregulated in response to *BCL-XL* silencing was then elucidated via gain-of-function and loss-of-function studies. Overexpression of miRNA using transfectable synthetic miRNA mimics was performed to supplement endogenous miRNA activity to determine the functional roles, whereas knockdown or down-regulation of miRNAs using miRNA hairpin inhibitors was intended to suppress endogenous miRNAs. A combination of up-regulation and down-regulation of miRNAs can aid in the identification of genes and cellular processes regulated by specific miRNAs.

Transfection efficiency was first evaluated through the visual monitoring of the Transfection Controls with Dy547 using fluorescence microscopy (Figure 4.7), to ensure an ≥ 80.0% transfection efficiency was achieved when transfecting a final concentration of 80.0 nM into the cells. Following this, the degree of amplification and suppression of miRNA levels achieved by transfection of 80.0 nM mimics and/or inhibitors were quantified using RT-qPCR. MiRNA mimics were able to induce at least a 10-fold increase in expression; while miRNA inhibitors were able to silence endogenous miRNA levels to a smaller extent (Figure 4.8 and Table 4.4). This subtle decrease in miRNA expression may be explained by the mechanism by which miRNA inhibitors function in the cells, as they are required to compete with cellular target mRNAs to sequester mature miRNA. A smaller decrease in fold change of miRNA expression may thus indicate unsuccessful competition of the miRNA inhibitors with mRNAs.

The functional roles miRNAs play in apoptosis was then assessed using the FITC annexin V apoptosis detection kit. An early feature of apoptosis is the loss of plasma membrane asymmetry, in which case the membrane phospholipid phosphatidylserine (PS) becomes translocated from the inner to the outer leaflet of the plasma membrane (Fadok *et al.*, 1992). Exposure of the PS to the external cellular environment allows for binding to a fluorochrome-tagged protein annexin V, which has a high affinity for PS, thus enabling detection by flow cytometry of cells undergoing apoptosis (Koopman *et al.*, 1994; van Engeland *et al.*, 1998). In the later stages of cell death, when loss of membrane integrity has occurred, staining with annexin V in conjunction with a vital dye, such as, PI allows for discrimination of early and late apoptotic cells, as viable cells exclude PI due to their intact membranes whereas damaged or dead cells are permeable to PI (Nicoletti *et al.*, 1991). Therefore, viable live cells will have minimal annexin V and PI fluorescence, cells in early stage of apoptosis will have bright annexin V fluorescence but still exclude PI, and advance to late stage of apoptosis and secondary necrotic cells will stain strongly with both annexin V and PI.

Of the four miRNAs evaluated, only miR-608 and miR-361-5p were able to elicit significant changes in apoptosis. Overexpression of miR-608 expression via mimics and a down-regulation of miR-361-5p through miRNA inhibitors were able to significantly increase the apoptotic population in both A549 and SK-LU-1 as demonstrated via flow cytometry analysis of annexin V (Figure 4.9). No significant changes in apoptosis were observed with the transfection of either miR-769-5p or miR-1304, indicating that they may not play critical roles in the apoptotic properties of lung adenocarcinoma.

To confirm the presence of an apoptosis process, activation of caspase 3 and 7 were analyzed using the Caspase-Glo® 3/7 assay. As previously described in Chapter 2, caspases are a large protein family that maintains homeostasis through the regulation of cell death and inflammation (Thornberry & Lazebnik, 1998). The activation of effector caspase 3 and caspase 7 cleaves downstream targets that result in the irreversible commitment of cells to apoptotic death, thus making them reliable markers for apoptosis. The Caspase-Glo® 3/7 assay is a homogenous, luminescent assay that measures the activities of caspase 3 and 7, whereby the amount of luminescence measured is proportional to the amount of caspase activity present. Corresponding to flow cytometry analysis of annexin V, caspase 3/7 activity in A549 and SK-LU-1 was significantly increased following transfection with miR-608 mimics and miR-361-5p inhibitors (Figure 4.10). Similarly, no significant changes in caspase 3/7 activity were detected in cells transfected with miR-769-5p and miR-1304.

Thus far, two independent results were observed in the form that *BCL-XL* regulates the expression profile of miRNAs, and miRNAs in turn regulate the apoptotic properties of lung adenocarcinoma cells. To confirm the association between *BCL-XL*, miRNA and cell death, a combination study was performed whereby cells were first transfected with si*BCL-XL*, followed by transfection with either miR-608 inhibitors or miR-361-5p mimics. Results revealed that the increased apoptotic population seen in *BCL-XL* silenced cells was significantly decreased following miR-608 inhibitor and miR-361-5p mimic transfection as determined through flow cytometric analysis of annexin V (Figure 4.11) and luminescence analysis of caspase 3/7 activation (Figure 4.12). This suggests that miR-608 and miR-361-5p play a significant role in blocking *BCL-XL* induced cell death.

Taken together, results have shown the ability of miR-608 and miR-361-5p to play a role in the regulation of apoptosis in lung adenocarcinoma cells and at this point provide the first indication that miR-608 may play a tumour suppressive role while miR-361-5p may play an oncogenic role in lung adenocarcinoma.

As mentioned previously in Section 5.2, previous studies in NSCLC have described miR-361-5p as a tumour suppressor, however opposing results were obtained in this present study. Results from this study have demonstrated that inhibition of miR-361-5p increases apoptosis and caspase 3/7 activation, suggesting that miR-361-5p may also play an oncogenic role in the regulation of apoptosis in NSCLC. The opposing roles of miR-361-5p in different cancers is still not well understood, however it can be hypothesized that the specific functions of miR-36-5p may be tissue- or cell-specific and strongly depends upon their downstream targets. The previous findings of miR-361-5p have been obtained from studies using tissue samples (Zhuang *et al.*, 2016) or the H23 lung adenocarcinoma cell line (Ma *et al.*, 2015). Meanwhile results of this study examine the expression of miR-361-5p in response to *BCL-XL* silencing and in two different cell lines, A549 and SK-LU-1. Therefore, further experiments should be conducted to further understand the roles miR-361-5p play in various cancers and cell lines.

5.4 MiR-608 and miR-361-5p induces cell cycle arrest at the S phase in A549 and SK-LU-1 cells

The balance between cell proliferation and cell death must be regulated in order to maintain tissue homeostasis. The connection between the two processes can be achieved through coupling of cell cycle and cell death through the use, or control, of a shared set of key factors (King & Cidlowski, 1995). Accumulating evidence has shown that in certain situations, deregulation of cell cycle components can prevent or induce apoptotic

responses (Fotedar *et al.*, 1996), involving key proteins, such as, v-Myc avian myelocytomatosis viral oncogene homolog (c-MYC) (Amati *et al.*, 1993), tumour protein p53 (Levine, 1997), and retinoblastoma protein, pRB (Haas-Kogan *et al.*, 1995) in the regulation of both apoptosis and cell cycle (Alenzi, 2004).

The BCL-2 family of proteins has also been associated in the control of apoptosis and cell proliferation. The most prominent effect on cell cycle exhibited by BCL-2 and BCL-XL is the delay of cell progression into the S phase from quiescence, through the inhibition of MYC activation by elevating expression of the cell cycle inhibitor, p27 (Huang *et al.*, 1997; Greider *et al.*, 2002). Furthermore, it was found that a mutation of the conserved residue tyrosine 22 (Y22) in the BH4 domain of *BCL-XL* removed their capability to delay entry into S phase, without affecting their ability to inhibit apoptosis, suggesting that the regulation of anti-apoptosis and cell proliferation by *BCL-XL* is genetically separate (Huang *et al.*, 1997). With this knowledge, it was therefore of interest to determine whether miRNAs dysregulated by the silencing of *BCL-XL*, can also be involved in the progression of cell cycle in lung adenocarcinoma cells.

Analysis of PI stained miR-608 and miR-361-5p-transfected cells via flow cytometry revealed the ability of these miRNAs to regulate cell cycle. Ectopic expression of miR-608 and silencing of miR-361-5p was shown to induce a cell cycle arrest in both A549 and SK-LU-1 cells, with an increase in cell population in the S phase and a decrease in the G_0/G_1 phase (Figure 4.13). Bioinformatics analysis of putative miRNA gene targets identified retinoblastoma-associated protein, E2F, as a target of miR-608 and pRB as a target of miR-361-5p. As miRNAs are negative regulators, overexpression of miR-608 may lead to a decrease in E2F, which is a positive regulator of genes required for transition from G_0 to S phase (Dyson, 1998; Nevins, 1998). On the other hand, inhibition of miR-361-5p may lead to an increase in its target gene pRB, which is a

negative regulator of cell growth, blocking transcription of S phase genes (Weintraub *et al.*, 1995). However, these conclusions are only speculative and further experimental work would have to be performed to confirm direct regulation of E2F and pRB by miR-608 and miR-361-5p, respectively.

5.5 MiR-608 and miR-361-5p induces caspase 3 activation *in vivo*

In vitro assays are only approximate reconstitutions of biological processes occurring under controlled conditions, it is therefore advantageous to validate the results of *in vitro* experimentations in an *in vivo* model. Zebrafish (*Danio rerio*) have been widely used in cancer research. An evaluation of the zebrafish genome with the human genome sequence demonstrates many human cancer genes are structurally and functionally conserved in zebrafish (Amatruda *et al.*, 2002; Stoletov & Klemke, 2008). Certain advantages, such as, rapid generation time, transparent embryos, large clutch size, *ex utero* development of the embryo, and lower maintenance costs make the use of zebrafish, over traditional vertebrate models, very appealing (Lieschke & Currie, 2007; Feitsma & Cuppen, 2008; Shive, 2013).

Another benefit of using zebrafish embryos is that xenotransplantation in the early life-stages of zebrafish do not require immunosuppression as their adaptive immune system only matures at 3-4 weeks after fertilization (Willett *et al.*, 1999; Lam *et al.*, 2004). The first report of successful xenotransplantation of human cancer cells into zebrafish was in 2005, whereby Lee and colleagues transplanted zebrafish embryos with human metastatic melanoma cells and discovered that the cells were able to survive, divide and migrate (Lee *et al.*, 2005). Since then there have been many reports of successful xenotransplantation, by microinjection, of human cancer cells into zebrafish embryo (Haldi *et al.*, 2006; Nicoli *et al.*, 2007; Marques *et al.*, 2009; Pruvot *et al.*, 2011; Yang *et al.*, 2013). Zebrafish embryos have thus been used to study the behavior of

xenografted cells in regards to various biological pathways including metastasis (Marques *et al.*, 2009), invasion (Yang *et al.*, 2013), angiogenesis (Lee *et al.*, 2009), as well as for the screening of various anti-cancer agents (Pruvot *et al.*, 2011; Jung *et al.*, 2012).

The yolk is the ideal location for injection, as it provides a nutrient rich environment for injected cells allowing for cell growth and migration (Haldi *et al.*, 2006). The yolk sac is also able to retain a large number of injected cells, approximately 50-100 cells, without expulsion into the embryo media (Haldi *et al.*, 2006). Furthermore, successful engraftment in zebrafish can be achieved from fewer cells in comparison to xenotransplantation in immunosuppressive mouse strains; therefore host numbers can be scaled up easily, which improves the validity of statistical analyses (Veinotte *et al.*, 2014).

Another advantage of using zebrafish embryo is its optical transparency which allows for the real-time observation of tumour mass formation of fluorescently labeled cancer cells (Haldi *et al.*, 2006; Eguiara *et al.*, 2011; Zhao *et al.*, 2011), as well as allowing the possibility to perform immunostaining and *in situ* hybridization on whole embryos without the need for xenograft biopsies (Veinotte *et al.*, 2014). The pigment formation in zebrafish develop rapidly, so to increase signal detection by whole mount in situ hybridization and confocal microscopy, embryos are treated with 1-phenyl 2-thiourea (PTU) during embryogenesis which help to inhibit melanogenesis (Whittaker, 1966; Eppig, 1970). In this study zebrafish embryos were maintained in system water containing PTU 24 h prior to microinjection with transfected A549 cells. Optical transparency achieved by PTU treatment then allowed for visualization of fluorophore-conjugated active caspase 3 antibodies using a confocal microscope. Analysis of fluorescent images using the ImageJ Analyst software demonstrated that zebrafish

embryos injected with miR-608 mimic and miR-361-5p inhibitor-transfected cells led to a significant increase in active caspase 3 detection in comparison to negative control injected zebrafish (Figure 4.14 and 4.15). These results were in accordance with the miRNA's *in vitro* ability to induce apoptosis via caspase 3 activation.

5.6 MiR-608 and miR-361-5p are predicted to target signaling pathways associated with NSCLC apoptosis and proliferation

Mature miRNAs recognize their target mRNA through base-pairing interactions at a seed region of 2-8 nucleotides on the miRNA and complementary nucleotides in the 3'UTR of mRNAs. Gene expressions of the mRNAs are then inhibited by translational repression or cleavage (Bartel, 2004; Zamore & Haley, 2005). Each individual miRNA has hundreds of evolutionarily conserved targets (Bentwich *et al.*, 2005) and it is estimated that miRNAs may regulate approximately 60% of all human genes (Lewis *et al.*, 2005). For this reason, it is a challenge to identify the gene targets of miRNA; and sophisticated computational algorithms thus play a central role to aid in prediction of miRNA targets (Bentwich, 2005; Rajewsky, 2006; Doran & Strauss, 2007; Maziere & Enright, 2007). In this study, the TargetScan algorithm was utilized which predicts miRNA targets conserved across various genomes through the combination of thermodynamics-based modeling of RNA:RNA duplex interactions and comparative sequence analysis (Grimson *et al.*, 2007). The list of putative miRNA targets obtained from TargetScan were then subjected to gene annotation enrichment using the DAVID software which is a bioinformatics resource that consists of an integrated biological knowledge-base and analytical tools that allow for extraction of biological meaning from large gene lists (Huang da *et al.*, 2009). Results of the bioinformatics analysis in this study implicated various signaling pathways to be targeted by miR-608 and miR-361-5p, which included the TGFβ, PI3K/AKT, MAPK, WNT, and the intrinsic and extrinsic pathways (Figure 4.16 and Figure 4.17). As discussed in Chapter 2, all six of

these pathways play a significant role in the regulation of apoptosis and cell proliferation.

5.6.1 Targeting of the TGFβ signaling pathway

MiR-608 and miR-361-5p were found to target various genes in the TGFβ signaling pathway, which is essential for the regulation of numerous cellular processes including differentiation, motility, lineage determination, cell proliferation, adhesion, and cell death (Massagué, 2008; Jeon & Jen, 2010). *In silico* analysis identified *TGFβ*, *TGFβR1* and *SMAD2/4* as targets of down-regulated miR-361-5p indicating an increase of gene expression allowing them to perform their tumour suppressive activities. An increase in *SMAD2* and *SMAD4* levels will result in a decrease of X-linked inhibitor of apoptosis protein (*XIAP*) expression (Van Themsche *et al.*, 2010), which in turn releases caspase 3 allowing it to induce apoptosis. Furthermore, activation of *SMAD2/4* will induce the transcription of *p15*, a cylin-dependent kinase inhibitor, leading to growth arrest (Feng *et al.*, 2000). On the other hand, cyclin D and *E2F* are positive regulators of cell cycle progression and they are predicted to be targeted by up-regulated miR-608, leading to cyclin dependent kinase (*CDK*) inhibition and accumulation of hypo-phosphorylated *pRB*, which in turn induces cell cycle arrest (Reynisdottir *et al.*, 1995; Hanahan & Weinberg, 2000).

5.6.2 Targeting of the PI3K/AKT signaling pathway

The PI3K/AKT pathway is an important regulator of cell survival and proliferation in lung cancer (Vivanco & Sawyers, 2002), and various members of this pathway were targeted by miR-608 and miR-361-5p. AKT plays a critical role in the activation of numerous biological processes imperative for tumourigenesis including inhibition of apoptosis, angiogenesis, cell proliferation, and tumour cell invasiveness (Testa & Bellacosa, 2001), and this study identified *AKT* as a putative target of up-regulated miR-608. *PI3K*, which phosphorylates *AKT*, was also a target of miR-608, further reducing expression of *AKT*. As *AKT* is imperative for the regulation of many downstream transcription factors that control cell death genes (Brunet *et al.*, 1999), inhibition of this survival factor would cause a subsequent increase in apoptosis. Forkhead transcription factor (FKHR) is a downstream protein inhibited by AKT, and pathway analysis predicted *FKHR* to be a target of miR-361-5p. Therefore, release of inhibition of FKHR by a decreased AKT and miR-361-5p expression would allow translocation of FKHR into the nucleus to induce target genes including pro-apoptotic BIM and FAS ligand to further trigger apoptosis (Brunet *et al.*, 1999).

5.6.3 Targeting of the MAPK signaling pathway

The MAPK signaling pathway, specifically the ERK pathway, was also predicted to be targeted by miR-608 and miR-361-5p. *RET* proto-oncogene and coiled-coil domain containing 6 (*CCDC6*) are both targets of down-regulated miR-361-5p. An increase in the expression of RET and CCDC6 can lead to the formation of a CCDC6-Ret fusion protein (Matsubara *et al.*, 2012), which will allow RET to be constitutively active resulting in increased activation of RAS (Plaza-Menacho *et al.*, 2007). Activation of RAS leads to stimulation of various pathways, including the RAF-MEK-ERK pathway, which subsequently results in tumour cell metastasis, apoptosis, growth, proliferation, invasion and angiogenesis (Slebos *et al.*, 1990; Aviel-Ronen *et al.*, 2006). However

pathway analysis also predicted *EGFR* and hepatocyte growth factor receptor (*MET*) to be targets of miR-608. Both *EGFR* and *MET* had a higher TargetScan context score of -0.64 and -0.13, respectively, then that of *RET* (-0.23) and CCDC6 (-0.01), indicating that *EGFR* and *MET* may be a more positive predicted target. Therefore, decrease in EGFR and MET will indirectly lead to a decreased activation of RAS. Furthermore, *RAF* a proto-oncogene serine/threonine-protein kinase, found downstream of RAS, is also a target of miR-608. Inhibition of *RAF* will prevent phosphorylation of MEK and ERK. Therefore, even though MEK and ERK were targets of miR-361-5p, they would not be able to perform their tumourigenic functions, as upstream proteins would not be able to phosphorylate and activate them. Together up-regulation of miR-608 and down-regulation of miR-361-5p could hypothetically work together to inhibit angiogenesis in lung adenocarcinoma cells.

5.6.4 Targeting of the WNT signaling pathway

Members of the WNT signaling pathway were also predicted to be targets of up-regulated miR-608. Cell proliferation of A549 and SK-LU-1 can hypothetically be inhibited through the suppression of disheveled (DSH) and adenomatous polyposis coli (APC). Decreased expression of DSH and APC will result in the prevention of glycogen synthase-kinase-3-beta (GSK-3β)/APC/Axin complex activation and subsequent phosphorylation of β-catenin. Furthermore, inhibition of DSH will block survivin activation, via inhibition of T-cell factor/lymphoid enhancer factor (TCF/LEF), resulting in caspase activation and reinstating the cell's ability to perform apoptosis (Uematsu *et al.*, 2003; Mazieres *et al.*, 2005; Van Scoyk *et al.*, 2008). Downstream targets of the WNT pathway include *CDK4/6* and cyclin D, which as described previously, will induce cell cycle arrest.

5.6.5 Targeting of the intrinsic and extrinsic signaling pathway

The BCR-ABL fusion protein is a potent anti-apoptotic molecule that is formed when the *ABL* gene from chromosome 9 joins onto the *BCR* gene on chromosome 22 (Prieto *et al.*, 1970). This fusion protein is involved in the activation of various downstream effectors and signal transducers that regulate cell proliferation and apoptosis, including PI3K, AKT, ERK and STAT5 (Lugo *et al.*, 1990; Shuai *et al.*, 1996; Skorski *et al.*, 1997). BCR-ABL has also been found to elicit anti-apoptotic behavior through the induction of *BCL-XL* expression (Gesbert & Griffin, 2000; Horita *et al.*, 2000). In regards to the intrinsic pathway, both *BCR* and *BCL-XL* are putative targets of miR-608, which hypothetically can result in increased apoptosis through cytochrome C release and activation of caspase 3.

In the extrinsic pathway, the cell-surface FAS receptor is predicted to be targeted by both up-regulated miR-608 and down-regulated miR-361-5p. However, the context score for miR-361-5p is lower than that of miR-608, at -0.19, and is thus a more favourable positive target prediction. Activation of FAS receptors will lead to the recruitment of intracellular adaptor proteins, such as, Fas-associated death domains (FADD) to form scaffolding complexes (Strasser *et al.*, 2009). These complexes will in turn recruit caspase 8, a member of the caspase family of cell death proteases, to be cleaved into an active enzyme. Pathway analysis indicate that activation of caspase 8 is not inhibited by the actions of either miR-608 or miR-361-5p, which will thus allow for pro-caspase 3 to be directly activated by pro-caspase 8 (Garrido *et al.*, 2006), enabling an alternative pathway for apoptosis to be initiated in lung adenocarcinoma cells.

5.7 MiR-608 and miR-361-5p directly target *AKT2* and *SMAD2*, respectively

In silico analysis predicted many genes as targets of miR-608 and miR-361-5p. A reporter system was utilized to experimentally validate the direct binding of miRNA to specific mRNA targets. The rationale for using such an assay was that the binding of miRNA to the mRNA target site would inhibit the production of a reporter protein, leading to a decreased activity that can be measured and compared to a control (Kuhn *et al.*, 2008). MiR-608 has sequence complementary to two regions in the 3'UTR of v-Akt Murine Thymoma Viral Oncogene Homolog 2 (*AKT2*) at bases 96 to 102 and 150 to 158, while miR-361-5p has sequence complementary to two regions in the 3'UTR of Mothers Against Decapentaplegic Homolog 2 (*SMAD2*) at bases 7447 to 7454 and 7695 to 7701 (Figure. 4.18). In this study, a fragment of the 3'UTR of the target gene of interest was cloned downstream of the luciferase open reading frame sequence contained in the pmirGLO reporter plasmid. Co-transfection of miR-608 and miR-361-5p mimics with their respective wild-type 3'UTR plasmid constructs produced a decreased luciferase signal in comparison to the control (Figure 4.19). This signifies that the miRNA was able to directly bind to the regions of sequence complementary in the gene of interest, leading to its mRNA being destabilized and repression of luciferase reporter gene translation. On the other hand, co-transfection of miRNA inhibitors with the wild-type 3'UTR plasmid constructs resulted in a slight increase in luciferase activity. In this situation, it can be hypothesized that introduction of miRNA inhibitors prevents endogenous miRNAs from binding to wild-type 3'UTR plasmids, thus leading to increased translation and detection of luciferase, in comparison to cells transfected with the inhibitor negative control.

To validate whether the gene of interest is a true target of the miRNA, changes in the miRNA expression should correspond to a predictable change in the protein levels encoded by the target mRNA (Kuhn *et al.*, 2008). Overexpression and silencing of miRNA expression using miRNA mimics and inhibitors was thus performed and western blot analysis was carried out using specific antibodies against AKT2 and SMAD2. Corresponding to the results obtained in the luciferase assay, a significant decrease was seen in the protein levels following transfection with miRNA mimics, whereby a significant increase in protein levels was seen in cells transfected with miRNA inhibitors (Figure 4.20 and Figure 4.21). Together, results have identified and confirmed *AKT2* and *SMAD2* to be novel targets of miR-608 and miR-361-5p, respectively.

5.8 Regulatory mechanism of miR-608 and miR-361-5p-induced NSCLC apoptosis

Thus far, results of this study have revealed that both miR-608 and miR-361-5p is critical for the regulation of apoptosis in lung adenocarcinoma cells. In addition, miR-608 was shown to directly target *AKT2* whereas miR-361-5p binds directly to *SMAD2* 3'UTR. However the association of *AKT2* and *SMAD2* with NSCLC apoptotic properties had to be further elucidated, and this was evaluated through gene rescue studies utilizing siRNAs and overexpression plasmids.

AKT2 is a serine/threonine protein kinase that contributes significantly in regulation of numerous biological pathways including angiogenesis, proliferation, metabolism, cell survival, and growth (Testa & Bellacosa, 2001; Martelli *et al.*, 2012). Hyperactivation of AKT2 has been reported widely to play a role in human malignancy, with overexpression being reported in many cancers including ovarian (Cheng *et al.*, 1992; Yuan *et al.*, 2000), thyroid (Ringel *et al.*, 2001), pancreatic (Altomare *et al.*, 2002), colorectal (Itoh *et al.*, 2002), breast (Arboleda *et al.*, 2003; Santi & Lee, 2011), glioma (Mure *et al.*, 2010; Cui *et al.*, 2012) and lung cancer (Balsara *et al.*, 2004; Lee *et al.*, 2011; Attoub *et al.*, 2015).

Frequent activation of AKT is an early and important event in the progression of lung cancer (Balsara *et al.*, 2004) and its constitutive activation has been demonstrated in cell lines originating from premalignant and malignant human bronchial epithelial cells, but is not present in normal bronchial cells (West, 2003). AKT also plays a significant role in invasiveness; therefore frequent activation of AKT may potentially be important in the transformation of a precursor lung lesion to a malignant carcinoma (Balsara *et al.*, 2004). In lung cancer, AKT has also been shown to contribute resistance towards chemotherapy, radiation and tyrosine kinase inhibitors through the regulation of survival signals that protect cells from undergoing apoptosis (Brognard; Nakashio *et al.*, 2000). Activated AKT overexpression in lung cancer has also been positively correlated with reduced patient survival (David *et al.*, 2004). Furthermore, down-regulation of AKT2 in NSCLC cells resulted in cleavage of anti-apoptotic BCL-2 family protein, MCL-1, disruption of mitochondrial membrane potential, cytochrome c release and caspase cascade activation (Lee *et al.*, 2011).

In this study, *AKT2* was identified as a novel direct target of miR-608, and the pro-apoptotic effects exhibited by inhibitors of miR-608 was reversed by the silencing of *AKT2* via siRNAs in both A549 and SK-LU-1 cells (Figure 4.23 – Figure 4.25). This finding suggests that targeting of *AKT2* could be the mechanism by which miR-608 functions as a tumour suppressor in NSCLC. These results are in accordance to previous findings of the role AKT2 plays in regulation of apoptosis in NSCLC (Brognard; David *et al.*, 2004).

On the other hand, expression of miR-361-5p is down-regulated in response to silencing of *BCL-XL* and luciferase assay analysis has confirmed that miR-361-5p negatively regulates *SMAD2* levels. Gene rescue studies using *SMAD2* overexpression vectors demonstrated that ectopic up-regulation of *SMAD2* was able to rescue the apoptotic inhibition effect exerted by miR-361-5p (Figure 4.26 – Figure 4.28). Taken together, these observations suggest that the oncogenic role of miR-361-5p in lung adenocarcinoma cells is at least partially by inhibiting its target gene *SMAD2*.

SMADS, a family of structurally related proteins, function as signal transducers of TGFβ family member proteins and are important in the regulation of cell growth inhibition, cellular senescence, differentiation and apoptosis (Derynck *et al.*, 1998; Itoh *et al.*, 2000; Massagué, 2000; Massague & Wotton, 2000; Miyazono *et al.*, 2000). SMAD2, a receptor-regulated SMAD, functions as a tumour suppressor and its expression has been reported to be decreased in various human cancers (Hoot *et al.*, 2008; Munker S, 2012; Samanta & Datta, 2012; Wu *et al.*, 2012). Furthermore, emerging evidence has reported the critical role SMAD2 plays in apoptosis. Yang and colleagues provided one of the first reports of SMAD2 functioning as a tumour suppressor in 2009, whereby SMAD2 was identified to be a critical mediator of TGFβ-induced apoptosis of prostate epithelial cells (Yang, 2009). They later reported that

apoptosis in prostate epithelial cells was induced through the suppression of survivin, an inhibitor of apoptosis, by SMAD2 together with pRB/E2F3 and cell cycle-regulated repressor element (CDE) and cell cycle gene homology region (CHR) (Yang *et al.*, 2008). SMAD2 is also associated with mitochondrial-based pro-apoptotic events through the activation of DAP-kinase promoter (Jang *et al.*, 2002), and various studies have also shown that SMAD2 can down-regulate XIAP to induce caspase 3 activation and TRAIL-induced apoptosis (Wang *et al.*, 2006; Xu *et al.*, 2006; Van Themsche *et al.*, 2010; Xu *et al.*, 2016).

CHAPTER 6: CONCLUSION

In summary, this thesis has provided evidence that miR-608 and miR-361-5p play opposing roles in the regulation of apoptosis in NSCLC. MiR-608 was concluded to play a tumour suppressive role while miR-361-5p functions as an oncogenic miRNA. Ectopic overexpression and inhibition of miR-608 and miR-361-5p, respectively, was able to stimulate cell cycle arrest and promote apoptosis both *in vitro* and *in vivo.* Furthermore, miR-608 and miR-361-5p were found to directly target *AKT2* and *SMAD2*, respectively. Together these findings suggest that down-regulation of *SMAD2* by miR-361-5p is likely to be an authentic mechanism of miR-361-5p-mediated oncogenesis, whereby targeting of *AKT2* could be the mechanism by which miR-608-mediated apoptosis is induced.

This study has demonstrated that miR-608 and miR-361-5p could serve as therapeutic targets for the treatment for lung adenocarcinoma. Studies have shown that there is great potential for the use of miRNAs as targets for cancer treatment, however there are many challenges that must be addressed. Both miR-608 and miR-361-5p are postulated to target many different genes as identified by TargetScan alone, and only a few have been experimentally validated to be genuine targets of these miRNAs. Therefore, more analyses must be performed to assess the biological effects of both miR-608 and miR-361-5p treatment in other normal and neoplastic cell lines *in vitro* and *in vivo.*

Other challenges faced in the development of miRNA-based therapeutics include concerns regarding delivery, potential off-target effects, as well as long-term safety concerns in humans (Garzon *et al*., 2010). Further improvements must be made in terms of the chemical design of miRNA mimics and antagomiRs as well as development of delivery methods to overcome the cellular uptake of synthetic oligonucleotides to attain inhibition of the target. Pharmacokinetic and pharmacodynamics studies must also be performed to warrant that the required miRNA concentrations are attained in tissues and that the targets are down-regulated (Garzon *et al*., 2010). Nevertheless, the notion of miRNA targeting to re-programme miRNA networks in cancer has a strong potential and chance for success.

Furthermore, studies have shown that the effects of individual miRNAs induces only a subtle reduction of protein expression, whereby miRNAs acting in concert have a greater ability to strengthen the functions of individual gene targets and together they can also target numerous genes that are expressed together, or associated with common pathways (Ivanovska & Cleary, 2008). For example, in a study conducted by Krek and colleagues, miR-375, miR-124 and let-7b were found to share a common gene target, *MTPN* (Krek *et al*., 2005). The expression of *MTPN* was found to be significantly decreased in response to co-transfection of miR-124 and let-7b, similar to the effects induced by transfection of miR-375 alone. However, a combined transfection of miR-124 and let-7b together with miR-375 led to a substantially greater target inhibition than effects observed by any other combinations (Krek *et al*., 2005). In another study, Ivanovska and Cleary identified three miRNAs (miR-34a, miR-16 and miR-106b) that regulate networks of genes that are involved in common cellular processes, but through distinct molecular mechanisms (Ivanovska & Cleary, 2008). The possibility of interactions among the miRNAs was investigated, and it was discovered that co-transfection of miR-34a and miR-16 induced a block in the G_1 cell cycle phase that was

greater than that exhibited by each miRNA alone. However, combination of miR-106b with either miR-34a or miR-16, or both together, only induced an intermediate change in phenotype, which reflected the contributions of each miRNA (Ivanovska & Cleary, 2008). These studies suggest that it would be of great interest to look into the effects of co-transfecting miR-608 and miR-361-5p together, on the regulation of apoptotic pathways in NSCLC. Further work on miR-608 and miR-361 may thus provide a platform for anti-sense gene therapy and has the potential to bring them to clinical trails to improve lung adenocarcinoma patient outcomes.

Lastly, while the zebrafish model has many advantages and can serve as invaluable screening tools in early stages of study; they can never replace rodents in the later stages of cancer research. Therefore it would be beneficial to complement these preliminary *in vivo* zebrafish results with further experimentation in mouse models.

REFERENCES

Abramson, J. S., & Shipp, M. A. (2005). Advances in the biology and therapy of diffuse large B-cell lymphoma: Moving toward a molecularly targeted approach. *Blood, 106*(4), 1164-1174.

Alenzi, F. Q. (2004). Links between apoptosis, proliferation and the cell cycle. *British Journal of Biomedical Science, 61*(2), 99-102.

Alessi, D. R., James, S. R., Downes, C. P., Holmes, A. B., Gaffney, P. R., Reese, C. B., & Cohen, P. (1997). Characterization of a 3-phosphoinositide-dependent protein kinase which phosphorylates and activates protein kinase B alpha. *Current Biology, 7*(4), 261-269.

Alexandrow, M. G., & Moses, H. L. (1995). Transforming growth factor beta and cell cycle regulation. *Cancer Research, 55*(7), 1452-1457.

Allan, L. A., Morrice, N., Brady, S., Magee, G., Pathak, S., & Clarke, P. R. (2003). Inhibition of caspase-9 through phosphorylation at Thr 125 by ERK MAPK. *Nature Cell Biology, 5*(7), 647-654.

Altomare, D. A., Tanno, S., De Rienzo, A., Klein-Szanto, A. J., Tanno, S., Skele, K. L., … Testa, J. R. (2002). Frequent activation of AKT2 kinase in human pancreatic carcinomas. *Journal of Cellular Biochemistry, 87*(4), 470-476.

Amati, B., Littlewood, T. D., Evan, G. I., & Land, H. (1993). The c-Myc protein induces cell cycle progression and apoptosis through dimerization with Max. *The EMBO Journal, 12*(13), 5083-5087.

Amatruda, J. F., Shepard, J. L., Stern, H. M., & Zon, L. I. (2002). Zebrafish as a cancer model system. *Cancer Cell, 1*(3), 229-231.

Arboleda, M. J., Lyons, J. F., Kabbinavar, F. F., Bray, M. R., Snow, B. E., Ayala, R., … Slamon, D. J. (2003). Overexpression of AKT2/protein kinase Bbeta leads to up-regulation of beta1 integrins, increased invasion, and metastasis of human breast and ovarian cancer cells. *Cancer Research, 63*(1), 196-206.

Arthur, J. S. C., & Ley, S. C. (2013). Mitogen-activated protein kinases in innate immunity. *Nature Reviews Immunology, 13*(9), 679-692.

Attoub, S., Arafat, K., Hammadi, N. K., Mester, J., & Gaben, A. M. (2015). Akt2 knock-down reveals its contribution to human lung cancer cell proliferation, growth, motility, invasion and endothelial cell tube formation. *Scientific Reports, 5*, 12759.

Aviel-Ronen, S., Blackhall, F. H., Shepherd, F. A., & Tsao, M. S. (2006). K-ras mutations in non-small-cell lung carcinoma: A review. *Clinical Lung Cancer, 8*(1), 30-38.

Bader, A. G., Brown, D., Stoudemire, J., & Lammers, P. (2011). Developing therapeutic microRNAs for cancer. *Gene Therapy, 18*(12), 1121-1126.

Bader, A. G., Brown, D., & Winkler, M. (2010). The promise of microRNA replacement therapy. *Cancer Research, 70*(18), 7027-7030.

Baer, R., Cintas, C., Therville, N., & Guillermet-Guibert, J. (2015). Implication of PI3K/AKT pathway in pancreatic cancer: When PI3K isoforms matter? *Advances in Biological Regulation, 59*, 19-35.

Bailey-Wilson, J. E., Amos, C. I., Pinney, S. M., Petersen, G. M., de Andrade, M., Wiest, J. S., … Anderson, M. W. (2004). A major lung cancer susceptibility locus maps to chromosome 6q23–25. *American Journal of Human Genetics, 75*(3), 460-474.

Bairey, O., Zimra, Y., Shaklai, M., Okon, E., & Rabizadeh, E. (1999). Bcl-2, Bcl-x, Bax, and Bak expression in short- and long-lived patients with diffuse large B-cell lymphomas. *Clinical Cancer Research, 5*(10), 2860-2866.

Balsara, B. R., Pei, J., Mitsuuchi, Y., Page, R., Klein-Szanto, A., Wang, H., … Testa, J. R. (2004). Frequent activation of AKT in non-small cell lung carcinomas and preneoplastic bronchial lesions. *Carcinogenesis, 25*(11), 2053-2059.

Bartel, D. P. (2004). MicroRNAs: Genomics, biogenesis, mechanism, and function. *Cell, 116*(2), 281-297.

Barth, A. I., Nathke, I. S., & Nelson, W. J. (1997). Cadherins, catenins and APC protein: Interplay between cytoskeletal complexes and signaling pathways. *Current Opinion in Cell Biology, 9*(5), 683-690.

Bartling, B., Rehbein, G., Simm, A., Silber, R. E., & Hofmann, H. S. (2010). Porcupine expression is associated with the expression of S100P and other cancer-related molecules in non-small cell lung carcinoma. *International Journal of Oncology, 36*(4), 1015-1021.

Basu, A., & Haldar, S. (2003). Identification of a novel Bcl-xL phosphorylation site regulating the sensitivity of taxol- or 2-methoxyestradiol-induced apoptosis. *FEBS Letters, 538*(1-3), 41-47.

Bazzoni, F., Rossato, M., Fabbri, M., Gaudiosi, D., Mirolo, M., Mori, L., … Locati, M. (2009). Induction and regulatory function of miR-9 in human monocytes and neutrophils exposed to proinflammatory signals. *Proceedings of the National Academy of Sciences USA, 106*(13), 5282-5287.

Bellacosa, A., de Feo, D., Godwin, A. K., Bell, D. W., Cheng, J. Q., Altomare, D. A., … Testa, J. R. (1995). Molecular alterations of the AKT2 oncogene in ovarian and breast carcinomas. *International Journal of Cancer, 64*(4), 280-285.

Bender, H., Wang, Z., Schuster, N., & Krieglstein, K. (2004). TIEG1 facilitates transforming growth factor-beta-mediated apoptosis in the oligodendroglial cell line OLI-neu. *Journal of Neuroscience Research, 75*(3), 344-352.

Bennett, W. P., Hussain, S. P., Vahakangas, K. H., Khan, M. A., Shields, P. G., & Harris, C. C. (1999). Molecular epidemiology of human cancer risk: Gene-environment interactions and p53 mutation spectrum in human lung cancer. *Journal of Pathology, 187*(1), 8-18.

Bentwich, I. (2005). Prediction and validation of microRNAs and their targets. *FEBS Letters, 579*(26), 5904-5910.

Bentwich, I., Avniel, A., Karov, Y., Aharonov, R., Gilad, S., Barad, O., … Bentwich, Z. (2005). Identification of hundreds of conserved and nonconserved human microRNAs. *Nature Genetics, 37*(7), 766-770.

Berrieman, H. K., Smith, L., O'Kane, S. L., Campbell, A., Lind, M. J., & Cawkwell, L. (2005). The expression of Bcl-2 family proteins differs between non-small cell lung carcinoma subtypes. *Cancer, 103*(7), 1415-1419.

Bhatti, I., Lee, A., James, V., Hall, R. I., Lund, J. N., Tufarelli, C., … Larvin, M. (2011). Knockdown of microRNA-21 inhibits proliferation and increases cell death by targeting programmed cell death 4 (PDCD4) in pancreatic ductal adenocarcinoma. *Journal of Gastrointestinal Surgery, 15*(1), 199-208.

Biggs, W. H., Meisenhelder, J., Hunter, T., Cavenee, W. K., & Arden, K. C. (1999). Protein kinase B/Akt-mediated phosphorylation promotes nuclear exclusion of the winged helix transcription factor FKHR1. *Proceedings of the National Academy of Sciences USA, 96*(13), 7421-7426.

Biroccio, A., Benassi, B., D'Agnano, I., D'Angelo, C., Buglioni, S., Mottolese, M., … Zupi, G. (2001). c-Myb and Bcl-x overexpression predicts poor prognosis in colorectal cancer: Clinical and experimental findings. *American Journal of Pathology, 158*(4), 1289-1299.

Blume-Jensen, P., Janknecht, R, & Hunter, T. (1998). The Kit receptor promotes cell survival via activation of PI 3-kinase and subsequent Akt-mediated phosphorylation of Bad on Ser136. *Current Biology, 8*(13), 779-782.

Bonine-Summers, A. R., Law, B. K., & Moses, H. L. (2007). Transforming growth factor-β and cancer. Caligiuri, M. A. & Lotze, M. T. (Eds.), *Cytokines in the Genesis and Treatment of Cancer* (pp. 91-111). Humana Press.

Borchert, G. M., Lanier, W., & Davidson, B. L. (2006). RNA polymerase III transcribes human microRNAs. *Nature Structural & Molecular Biology, 13*(12), 1097-1101.

Bouchie, A. (2013). First microRNA mimic enters clinic. *Nature Biotechnology, 31*(7), 577.

Boulton, T. G., Nye, S. H., Robbins, D. J., Ip, N. Y., Radziejewska, E., Morgenbesser, S. D.,…Yancopoulos, G. D. (1991). ERKs: A family of protein-serine/threonine kinases that are activated and tyrosine phosphorylated in response to insulin and NGF. *Cell, 65*(4), 663-675.

Brambilla, E., Moro, D., Gazzeri, S., & Brambilla, C. (1999). Alterations of expression of Rb, p16(INK4A) and cyclin D1 in non-small cell lung carcinoma and their clinical significance. *Journal of Pathology, 188*(4), 351-360.

Brancho, D., Tanaka, N., Jaeschke, A., Ventura, J. J., Kelkar, N., Tanaka, Y., … Davis, R. J. (2003). Mechanism of p38 MAP kinase activation *in vivo*. *Genes & Development, 17*(16), 1969-1978.

Bravo, D. T., Yang, Y-L, Kuchenbecker, K., Hung, M-S, Xu, Z., Jablons, D. M., & You, L. (2013). Frizzled-8 receptor is activated by the WNT-2 ligand in non-small cell lung cancer. *BMC Cancer, 13*(1), 316.

Brengues, M., Teixeira, D., & Parker, R. (2005). Movement of eukaryotic mRNAs between polysomes and cytoplasmic processing bodies. *Science, 310*(5747), 486-489.

Brennecke, J., Stark, A., Russell, R. B., & Cohen, S. M. (2005). Principles of microRNA-target recognition. *PLoS Biology, 3*(3), e85.

Brocardo, M., & Henderson, B. R. (2008). APC shuttling to the membrane, nucleus and beyond. *Trends in Cell Biology, 18*(12), 587-596.

Brognard, J., Clark, A. S., Ni, Y., & Dennis, P. A. (2001). Akt/protein kinase B is constitutively active in non-small cell lung cancer cells and promotes cellular survival and resistance to chemotherapy and radiation. *Cancer Research, 61*(10), 3986-3997.

Brunet, A., Bonni, A., Zigmond, M. J., Lin, M. Z., Juo, P., Hu, L. S., … Greenberg, M. E. (1999). Akt promotes cell survival by phosphorylating and inhibiting a forkhead transcription factor. *Cell, 96*(6), 857-868.

Burk, U., Schubert, J., Wellner, U, Schmalhofer, O., Vincan, E., Spaderna, S., & Brabletz, T. (2008). A reciprocal repression between ZEB1 and members of the miR-200 family promotes EMT and invasion in cancer cells. *EMBO Reports, 9*(6), 582-589.

Cai, X., Hagedorn, C. H., & Cullen, B. R. (2004). Human microRNAs are processed from capped, polyadenylated transcripts that can also function as mRNAs. *RNA, 10*(12), 1957-1966.

Calin, G. A., Liu, C. G., Sevignani, C., Ferracin, M., Felli, N., Dumitru, C. D., … Croce, C. M. (2004a). MicroRNA profiling reveals distinct signatures in B cell chronic lymphocytic leukemias. *Proceedings of the National Academy of Sciences USA, 101*(32), 11755-11760.

Calin, GA, Sevignani, C, Dumitru, CD, Hyslop, T, Noch, E, Yendamuri, S, … Croce, C. M. (2004b). Human microRNA genes are frequently located at fragile sites and genomic regions involved in cancers. *Proceedings of the National Academy of Sciences USA, 101*(9), 2999-3004.

Campana, D., Coustan-Smith, E., Manabe, A., Buschle, M., Raimondi, S. C., Behm, F. G., … Pui, C. H. (1993). Prolonged survival of B-lineage acute lymphoblastic leukemia cells is accompanied by overexpression of bcl-2 protein. *Blood, 81*(4), 1025-1031.

Cande, C., Vahsen, N., Kouranti, I., Schmitt, E., Daugas, E., Spahr, C., … Kroemer, G. (2004). AIF and cyclophilin A cooperate in apoptosis-associated chromatinolysis. *Oncogene, 23*(8), 1514-1521.

Cano, E., Hazzalin, C. A., & Mahadevan, L. C. (1994). Anisomycin-activated protein kinases p45 and p55 but not mitogen-activated protein kinases ERK-1 and -2 are implicated in the induction of c-fos and c-jun. *Molecular and Cellular Biology, 14*(11), 7352-7362.

Ceppi, P., Mudduluru, G., Kumarswamy, R., Rapa, I., Scagliotti, G. V., Papotti, M., & Allgayer, H. (2010). Loss of miR-200c expression induces an aggressive, invasive, and chemoresistant phenotype in non-small cell lung cancer. *Molecular Cancer Research, 8*(9), 1207-1216.

Cha, S. T., Chen, P. S., Johansson, G., Chu, C. Y., Wang, M. Y., Jeng, Y. M., … Kuo, M. L. (2010). MicroRNA-519c suppresses hypoxia-inducible factor-1alpha expression and tumor angiogenesis. *Cancer Research, 70*(7), 2675-2685.

Chang, L., & Karin, M. (2001). Mammalian MAP kinase signalling cascades. *Nature, 410*(6824), 37-40.

Chang, T. C., Wentzel, E. A., Kent, O. A., Ramachandran, K., Mullendore, M., Lee, K. H., … Mendell, J. T. (2007). Transactivation of miR-34a by p53 broadly influences gene expression and promotes apoptosis. *Molecular Cell, 26*(5), 745-752.

Chen, C., Edelstein, L. C., & Gélinas, C. (2000). The Rel/NF-κB family directly activates expression of the apoptosis inhibitor Bcl-x_L. *Molecular and Cellular Biology, 20*(8), 2687-2695.

Chen, G., Shen, Z. L., Wang, L., Lv, C. Y., Huang, X. E., & Zhou, R. P. (2013). Hsa-miR-181a-5p expression and effects on cell proliferation in gastric cancer. *Asian Pacific Journal of Cancer Prevention, 14*(6), 3871-3875.

Chen, P. Y, Weinmann, L., Gaidatzis, D., Pei, Y., Zavolan, M, Tuschl, T., & Meister, G. (2008). Strand-specific 5'-O-methylation of siRNA duplexes controls guide strand selection and targeting specificity. *RNA, 14*(2), 263-274.

Chen, S., Guttridge, D. C., You, Z., Zhang, Z., Fribley, A., Mayo, M. W., … Wang, C. Y. (2001). WNT-1 signaling inhibits apoptosis by activating beta-catenin/T cell factor-mediated transcription. *The Journal of Cell Biology, 152*(1), 87-96.

Chen, T. (2010). The role of microRNA in chemical carcinogenesis. *Journal of Environmental Science and Health. Part C, Environmental Carcinogenesis & Ecotoxicology Reviews, 28*(2), 89-124.

Chendrimada, T. P., Gregory, R. I., Kumaraswamy, E., Norman, J., Cooch, N., Nishikura, K., & Shiekhattar, R. (2005). TRBP recruits the dicer complex to Ago2 for microRNA processing and gene silencing. *Nature, 436*(7051), 740-744.

Cheng, E. H., Wei, M. C., Weiler, S., Flavell, R. A., Mak, T. W., Lindsten, T., & Korsmeyer, S. J. (2001). BCL-2, BCL-X(L) sequester BH3 domain-only molecules preventing BAX- and BAK-mediated mitochondrial apoptosis. *Molecular Cell, 8*(3), 705-711.

Cheng, H.. L., & Feldman, E. L. (1998). Bidirectional regulation of p38 kinase and c-Jun N-terminal protein kinase by insulin-like growth factor-I. *The Journal of Biological Chemistry, 273*(23), 14560-14565.

Cheng, J. Q., Godwin, A. K., Bellacosa, A., Taguchi, T., Franke, T. F., Hamilton, T. C., … Testa, J. R. (1992). Akt2, a putative oncogene encoding a member of a subfamily of protein-serine/threonine kinases, is amplified in human ovarian carcinomas. *Proceedings of the National Academy of Sciences USA, 89*(19), 9267-9271.

Cheng, W., Ren, X., Zhang, C., Han, S., & Wu, A. (2017). Expression and prognostic value of microRNAs in lower-grade glioma depends on IDH1/2 status. *Journal of Neuro-Oncology*, *132*(2), 207-218.

Chiou, G. Y., Cherng, J. Y., Hsu, H. S., Wang, M. L., Tsai, C. M., Lu, K. H., … Chiou, S. H. (2012). Cationic polyurethanes-short branch PEI-mediated delivery of miR-145 inhibited epithelial-mesenchymal transdifferentiation and cancer stem-like properties and in lung adenocarcinoma. *Journal of Controlled Release, 159*(2), 240-250.

Coller, J., & Parker, R. (2004). Eukaryotic mRNA decapping. *Annual Review of Biochemistry, 73*, 861-890.

Colombel, M., Symmans, F., Gil, S., O'Toole, K. M., Chopin, D., Benson, M., … Buttyan, R. (1993). Detection of the apoptosis-suppressing oncoprotein Bc1-2 in hormone-refractory human prostate cancers. *American Journal of Pathology, 143*(2), 390-400.

Cooper, C. S., Nicholson, A. G., Foster, C., Dodson, A., Edwards, S., Fletcher, A., … Cheng, S. J. (2006). Nuclear overexpression of the E2F3 transcription factor in human lung cancer. *Lung Cancer, 54*(2), 155-162.

Cortez, M. A., Valdecanas, D., Zhang, X., Zhan, Y., Bhardwaj, V., Calin, G. A., … Welsh, J. W. (2014). Therapeutic delivery of miR-200c enhances radiosensitivity in lung cancer. *Molecular Therapy, 22*(8), 1494-1503.

Croce, C. M. (2008). Oncogenes and cancer. *The New England Journal of Medicine, 358*(5), 502-511.

Cui, S. Y., Huang, J. Y., Chen, Y. T., Song, H. Z., Feng, B., Huang, G. C., … De, W. (2013). Let-7c governs the acquisition of chemo- or radioresistance and epithelial-to-mesenchymal transition phenotypes in docetaxel-resistant lung adenocarcinoma. *Molecular Cancer Research, 11*(7), 699-713.

Cui, Y., Wang, Q., Wang, J., Dong, Y., Luo, C., Hu, G., & Lu, Y. (2012). Knockdown of AKT2 expression by RNA interference inhibits proliferation, enhances apoptosis, and increases chemosensitivity to the anticancer drug VM-26 in U87 glioma cells. *Brain Research, 1469*, 1-9.

D'Amico, D., Carbone, D., Mitsudomi, T., Nau, M., Fedorko, J., Russell, E., … Phelps, R. (1992). High frequency of somatically acquired p53 mutations in small-cell lung cancer cell lines and tumors. *Oncogene, 7*(2), 339-346.

Dai, B., Meng, J., Peyton, M., Girard, L., Bornmann, W. G., Ji, L, … Roth, J. A. (2011). STAT3 mediates resistance to MEK inhibitor through microRNA miR-17. *Cancer Research, 71*(10), 3658-3668.

Danial, N. N. (2007). Bcl-2 family proteins: Critical checkpoints of apoptotic cell death. *Clinical Cancer Research, 13*(24), 7254-7263.

Daniel, J. C., & Smythe, W. R. (2004). The role of Bcl-2 family members in non-small cell lung cancer. *Seminars in Thoracic and Cardiovascular Surgery, 16*(1), 19-27.

David, O., Jett, J., LeBeau, H., Dy, G., Hughes, J., Friedman, M., & Brody, A. R.. (2004). Phospho-Akt overexpression in non-small cell lung cancer confers significant stage-independent survival disadvantage. *Clinical Cancer Research, 10*(20), 6865-6871.

Davis, R. J. (2000). Signal transduction by the JNK group of MAP kinases. *Cell, 103*(2), 239-252.

Debatin, K. M. (2004). Apoptosis pathways in cancer and cancer therapy. *Cancer Immunology, Immunotherapy, 53*(3), 153-159.

Degterev, A., Boyce, M., & Yuan, J. (2003). A decade of caspases. *Oncogene, 22*(53), 8543-8567.

Deininger, M. H., Weller, M., Streffer, J., & Meyermann, R. (1999). Antiapoptotic Bcl-2 family protein expression increases with progression of oligodendroglioma. *Cancer, 86*(9), 1832-1839.

del Peso, L., Gonzalez-Garcia, M., Page, C., Herrera, R., & Nunez, G. (1997). Interleukin-3-induced phosphorylation of BAD through the protein kinase Akt. *Science, 278*(5338), 687-689.

Dela Cruz, C. S., Tanoue, L. T., & Matthay, R. A. (2011). Lung cancer: Epidemiology, etiology, and prevention. *Clinics in Chest Medicine, 32*(4), 605-644.

Delbridge, A. R, & Strasser, A. (2015). The BCL-2 protein family, BH3-mimetics and cancer therapy. *Cell Death & Differentiation, 22*(7), 1071-1080.

Derynck, R., Zhang, Y., & Feng, X. H. (1998). Smads: Transcriptional activators of TGF-beta responses. *Cell, 95*(6), 737-740.

Dhanasekaran, D. N., & Reddy, E. P. (2008). JNK signaling in apoptosis. *Oncogene, 27*(48), 6245-6251.

Dhillon, A. S., Hagan, S., Rath, O., & Kolch, W. (2007). MAP kinase signalling pathways in cancer. *Oncogene, 26*(22), 3279-3290.

Domina, A. M., Vrana, J. A., Gregory, M. A., Hann, S. R., & Craig, R. W. (2004). MCL1 is phosphorylated in the PEST region and stabilized upon ERK activation in viable cells, and at additional sites with cytotoxic okadaic acid or taxol. *Oncogene, 23*(31), 5301-5315.

Doran, J., & Strauss, W. M. (2007). Bio-informatic trends for the determination of miRNA-target interactions in mammals. *DNA and Cell Biology, 26*(5), 353-360.

Du, L., Borkowski, R., Zhao, Z., Ma, X., Yu, X., Xie, X. J., & Pertsemlidis, A. (2013). A high-throughput screen identifies miRNA inhibitors regulating lung cancer cell survival and response to paclitaxel. *RNA Biology, 10*(11), 1700-1713.

Duronio, V. (2008). The life of a cell: Apoptosis regulation by the PI3K/PKB pathway. *Biochemical Journal, 415*(3), 333-344.

Dutt, A., Ramos, A. H., Hammerman, P. S., Mermel, C., Cho, J., Sharifnia, T., … Meyerson, M. (2011). Inhibitor-sensitive FGFR1 amplification in human non-small cell lung cancer. *PLoS One, 6*(6), e20351.

Dyson, N. (1998). The regulation of E2F by pRB-family proteins. *Genes & Development, 12*(15), 2245-2262.

Edlind, M. P., & Hsieh, A. C. (2014). PI3K-AKT-mTOR signaling in prostate cancer progression and androgen deprivation therapy resistance. *Asian Journal of Andrology, 16*(3), 378-386.

Eguiara, A., Holgado, O., Beloqui, I., Abalde, L., Sanchez, Y., Callol, C., & Martin, A. G. (2011). Xenografts in zebrafish embryos as a rapid functional assay for breast cancer stem-like cell identification. *Cell Cycle, 10*(21), 3751-3757.

Elmore, S. (2007). Apoptosis: A review of programmed cell death. *Toxicologic Pathology, 35*(4), 495-516.

Eppig, J. J. (1970). Melanogenesis in amphibians. I. A study of the fine structure of the normal and phenylthiourea-treated pigmented epithelium in *Rana pipiens* tadpole eyes. *Zeitschrift Fur Zellforschung Und Mikroskopische Anatomie, 103*(2), 238-246.

Erhardt, P., Schremser, E. J., & Cooper, G. M. (1999). B-Raf inhibits programmed cell death downstream of cytochrome c release from mitochondria by activating the MEK/Erk pathway. *Molecular and Cellular Biology, 19*(8), 5308-5315.

Esquela-Kerscher, A., Trang, P., Wiggins, J. F., Patrawala, L., Cheng, A., Ford, L., … Slack, F. J. (2008). The let-7 microRNA reduces tumor growth in mouse models of lung cancer. *Cell Cycle, 7*(6), 759-764.

Eymin, B., Gazzeri, S., Brambilla, C., & Brambilla, E. (2001). Distinct pattern of E2F1 expression in human lung tumours: E2F1 is upregulated in small cell lung carcinoma. *Oncogene, 20*(14), 1678-1687.

Fadok, V. A., Voelker, D. R., Campbell, P. A., Cohen, J. J., Bratton, D. L., & Henson, P. M. (1992). Exposure of phosphatidylserine on the surface of apoptotic lymphocytes triggers specific recognition and removal by macrophages. *Journal of Immunology, 148*(7), 2207-2216.

Fan, M., & Chambers, T. C. (2001). Role of mitogen-activated protein kinases in the response of tumor cells to chemotherapy. *Drug Resistance Updates, 4*(4), 253-267.

Fan, M., Goodwin, M., Vu, T., Brantley-Finley, C., Gaarde, W. A., & Chambers, T. C. (2000). Vinblastine-induced phosphorylation of Bcl-2 and Bcl-XL is mediated by JNK and occurs in parallel with inactivation of the Raf-1/MEK/ERK cascade. *Journal of Biological Chemistry, 275*(39), 29980-29985.

Feitsma, H., & Cuppen, E. (2008). Zebrafish as a cancer model. *Molecular Cancer Research, 6*(5), 685-694.

Feng, S., Cong, S., Zhang, X, Bao, X., Wang, W., Li, H., … Zhang, B. (2011). MicroRNA-192 targeting retinoblastoma 1 inhibits cell proliferation and induces cell apoptosis in lung cancer cells. *Nucleic Acids Research, 39*(15), 6669-6678.

Feng, X. H., Liang, Y. Y., Liang, M., Zhai, W., & Lin, X. (2002). Direct interaction of c-Myc with Smad2 and Smad3 to inhibit TGF-beta-mediated induction of the CDK inhibitor p15(Ink4B). *Molecular Cell, 9*(1), 133-143.

Feng, X. H., Lin, X., & Derynck, R. (2000). Smad2, Smad3 and Smad4 cooperate with Sp1 to induce p15(Ink4B) transcription in response to TGF-β. *The EMBO Journal, 19*(19), 5178-5193.

Ferlay, J., Soerjomataram, I., Ervik, M., Forman, D., Bray, F., Dikshit R., … Parkin, D.M. (2012). Globocan 2012 v1.0. *Lung cancer. Estimated incidence, mortality and prevalence worldwide in 2012.* Retrieved from http://globocan.iarc.fr.

Ferlay, J., Soerjomataram, I., Ervik, M., Forman, D., Bray, F., Dikshit, R., ... Parkin, D. M. (2013). Globocan 2012 v1.0. *Cancer incidence and mortality worldwide: IARC cancer base no.11.* Retrieved from http://globocan.iarc.fr.

Fernald, K., & Kurokawa, M. (2013). Evading apoptosis in cancer. *Trends in Cell Biology, 23*(12), 620-633.

Fiori, M. E., Barbini, C., Haas, T. L., Marroncelli, N., Patrizii, M., Biffoni, M., & De Maria, R. (2014). Antitumor effect of miR-197 targeting in p53 wild-type lung cancer. *Cell Death & Differentiation, 21*(5), 774-782.

Fleming, Y., Armstrong, C. G., Morrice, N., Paterson, A., Goedert, M., & Cohen, P. (2000). Synergistic activation of stress-activated protein kinase 1/c-Jun N-terminal kinase (SAPK1/JNK) isoforms by mitogen-activated protein kinase kinase 4 (MKK4) and MKK7. *Biochemical Journal, 352*, 145-154.

Foltz, I. N., Lee, J. C., Young, P. R., & Schrader, J. W. (1997). Hemopoietic growth factors with the exception of interleukin-4 activate the p38 mitogen-activated protein kinase pathway. *Journal of Biological Chemistry, 272*(6), 3296-3301.

Fong, K. M., Sekido, Y., & Minna, J. D. (1999). Molecular pathogenesis of lung cancer. *The Journal of Thoracic and Cardiovascular Surgery, 118*(6), 1136-1152.

Fotedar, R., Diederich, L., & Fotedar, A. (1996). Apoptosis and the cell cycle. *Progress in Cell Cycle Research, 2*, 147-163.

Friedman, R. C., Farh, K. K., Burge, C. B., & Bartel, D. P. (2009). Most mammalian mRNAs are conserved targets of microRNAs. *Genome Research, 19*(1), 92-105.

Fujita, Y., Kuwano, K, & Ochiya, T. (2015). Development of small RNA delivery systems for lung cancer therapy. *International Journal of Molecular Sciences, 16*(3), 5254-5270.

Fulda, S. (2009). Caspase-8 in cancer biology and therapy. *Cancer Letters, 281*(2), 128-133.

Fulda, S., & Debatin, K. M. (2004). Targeting apoptosis pathways in cancer therapy. *Current Cancer Drug Targets, 4*(7), 569-576.

Gabellini, C., Castellini, L., Trisciuoglio, D., Kracht, M., Zupi, G., & Del Bufalo, D. (2008). Involvement of nuclear factor-kappa B in bcl-xL-induced interleukin 8 expression in glioblastoma. *Journal of Neurochemistry, 107*(3), 871-882.

Gabrielson, E. (2006). Worldwide trends in lung cancer pathology. *Respirology, 11*(5), 533-538.

Galluzzi, L., Morselli, E., Vitale, I., Kepp, O., Senovilla, L., Criollo, A., … Kroemer, G. (2010). MiR-181a and miR-630 regulate cisplatin-induced cancer cell death. *Cancer Research, 70*(5), 1793-1803.

Garcia, J., Ye, Y., Arranz, V., Letourneux, C., Pezeron, G, & Porteu, F. (2002). IEX-1: A new ERK substrate involved in both ERK survival activity and ERK activation. *The EMBO Journal, 21*(19), 5151-5163.

Gardai, S. J., Hildeman, D. A., Frankel, S. K., Whitlock, B. B., Frasch, S. C., Borregaard, N., … Henson, P. M. (2004). Phosphorylation of Bax Ser184 by Akt regulates its activity and apoptosis in neutrophils. *Journal of Biological Chemistry, 279*(20), 21085-21095.

Garofalo, M., Di Leva, G., Romano, G., Nuovo, G., Suh, S. S., Ngankeu, A., … Croce, C. M. (2009). MiR-221 & 222 regulate TRAIL resistance and enhance tumorigenicity through PTEN and TIMP3 downregulation. *Cancer Cell, 16*(6), 498-509.

Garofalo, M., Jeon, Y. J., Nuovo, G. J., Middleton, J., Secchiero, P., Joshi, P., … Croce, C. M. (2013). MiR-34a/c-dependent PDGFR-α/β downregulation inhibits tumorigenesis and enhances TRAIL-induced apoptosis in lung cancer. *PLoS One, 8*(6), e67581.

Garofalo, M., Quintavalle, C., Di Leva, G., Zanca, C., Romano, G., Taccioli, C., … Condorelli, G. (2008). MicroRNA signatures of trail resistance in human non-small cell lung cancer. *Oncogene, 27*(27), 3845-3855.

Garofalo, M., Romano, G., Di Leva, G., Nuovo, G, Jeon, Y. J., Ngankeu, A., … Croce, C. M. (2011). EGFR and MET receptor tyrosine kinase-altered microRNA expression induces tumorigenesis and gefitinib resistance in lung cancers. *Nature Medicine, 18*(1), 74-82.

Garrido, C., Galluzzi, L., Brunet, M., Puig, P. E., Didelot, C., & Kroemer, G. (2006). Mechanisms of cytochrome c release from mitochondria. *Cell Death & Differentiation, 13*(9), 1423-1433.

Garzon, R., Marcucci, G., & Croce, C. M. (2010). Targeting microRNAs in cancer: Rationale, strategies and challenges. *Nature Reviews Drug Discovery, 9*(10), 775-789.

Gatza, C. E., Oh, S. Y., & Blobe, G. C. (2010). Roles for the type III TGF-beta receptor in human cancer. *Cell Signal, 22*(8), 1163-1174.

Geng, Y., Deng, L., Su, D., Xiao, J., Ge, D., Bao, Y., & Jing, H. (2016). Identification of crucial microRNAs and genes in hypoxia-induced human lung adenocarcinoma cells. *OncoTargets and Therapy, 9*, 4605-4616.

Gesbert, F., & Griffin, J. D. (2000). Bcr/Abl activates transcription of the Bcl-X gene through STAT5. *Blood, 96*(6), 2269-2276.

Giam, M., Huang, D. C., & Bouillet, P. (2008). BH3-only proteins and their roles in programmed cell death. *Oncogene, 27*, S128-136.

Gille, H., Sharrocks, A. D., & Shaw, P. E. (1992). Phosphorylation of transcription factor p62TCF by MAP kinase stimulates ternary complex formation at c-fos promoter. *Nature, 358*(6385), 414-417.

Ginsberg, R. J., Hill, L. D., Eagan, R. T., Thomas, P., Mountain, C. F., Deslauriers, J., … Waters, P. F. (1983). Modern thirty-day operative mortality for surgical resections in lung cancer. *Journal of Thoracic and Cardiovascular Surgery, 86*(5), 654-658.

Gong, J., Zhang, J. P., Li, B., Zeng, C., You, K., Chen, M. X., … Zhuang, S. M. (2013). MicroRNA-125b promotes apoptosis by regulating the expression of Mcl-1, Bcl-w and IL-6R. *Oncogene, 32*(25), 3071-3079.

Gottlieb, E., Vander Heiden, M. G., & Thompson, C. B. (2000). Bcl-x(L) prevents the initial decrease in mitochondrial membrane potential and subsequent reactive oxygen species production during tumor necrosis factor alpha-induced apoptosis. *Molecular and Cellular Biology, 20*(15), 5680-5689.

Grad, J. M., Zeng, X. R., & Boise, L. H. (2000). Regulation of Bcl-xL: A little bit of this and a little bit of STAT. *Current Opinion in Oncology, 12*(6), 543-549.

Granville, D. J., Jiang, H., An, M. T., Levy, J. G., McManus, B. M., & Hunt, D. W. (1999). Bcl-2 overexpression blocks caspase activation and downstream apoptotic events instigated by photodynamic therapy. *British Journal of Cancer, 79*(1), 95-100.

Green, D. R., & Kroemer, G. (2004). The pathophysiology of mitochondrial cell death. *Science, 305*(5684), 626-629.

Greenblatt, M. S., Bennett, W. P., Hollstein, M., & Harris, C. C. (1994). Mutations in the p53 tumor suppressor gene: Clues to cancer etiology and molecular pathogenesis. *Cancer Research, 54*(18), 4855-4878.

Greider, C., Chattopadhyay, A., Parkhurst, C., & Yang, E. (2002). BCL-x(L) and BCL2 delay Myc-induced cell cycle entry through elevation of p27 and inhibition of G1 cyclin-dependent kinases. *Oncogene, 21*(51), 7765-7775.

Grethe, S., Ares, M. P., Andersson, T., & Porn-Ares, M. I. (2004). p38 MAPK mediates TNF-induced apoptosis in endothelial cells via phosphorylation and downregulation of Bcl-x(L). *Experimental Cell Research, 298*(2), 632-642.

Grethe, S., & Porn-Ares, M. I. (2006). p38 MAPK regulates phosphorylation of Bad via PP2A-dependent suppression of the MEK1/2-ERK1/2 survival pathway in TNF-alpha induced endothelial apoptosis. *Cellular Signalling, 18*(4), 531-540.

Grimson, A., Farh, K. K., Johnston, W. K., Garrett-Engele, P., Lim, L. P., & Bartel, D. P. (2007). MicroRNA targeting specificity in mammals: Determinants beyond seed pairing. *Molecular Cell, 27*(1), 91-105.

Groeger, A. M., Esposito, V., De Luca, A., Cassandro, R., Tonini, G., Ambrogi, V., … Wolner, E. (2004). Prognostic value of immunohistochemical expression of p53, bax, Bcl-2 and Bcl-xL in resected non-small-cell lung cancers. *Histopathology, 44*(1), 54-63.

Guicciardi, M. E., & Gores, G. J. (2009). Life and death by death receptors. *The FASEB Journal, 23*(6), 1625-1637.

Guo, S., Rena, G, Cichy, S., He, X, Cohen, P., & Unterman, T. (1999). Phosphorylation of serine 256 by protein kinase B disrupts transactivation by FKHR and mediates effects of insulin on insulin-like growth factor-binding protein-1 promoter activity through a conserved insulin response sequence. *Journal of Biological Chemistry, 274*(24), 17184-17192.

Haas-Kogan, D. A., Kogan, S. C., Levi, D., Dazin, P., T'Ang, A., Fung, Y. K., & Israel, M. A. (1995). Inhibition of apoptosis by the retinoblastoma gene product. *The EMBO Journal, 14*(3), 461-472.

Haase, A. D., Jaskiewicz, L., Zhang, H., Laine, S., Sack, R., Gatignol, A., & Filipowicz, W. (2005). TRBP, a regulator of cellular PKR and HIV-1 virus expression, interacts with Dicer and functions in RNA silencing. *EMBO Reports, 6*(10), 961-967.

Haeusgen, W., Boehm, R., Zhao, Y., Herdegen, T., & Waetzig, V. (2009). Specific activities of individual c-Jun N-terminal kinases in the brain. *Neuroscience, 161*(4), 951-959.

Haldi, M., Ton, C., Seng, W. L., & McGrath, P. (2006). Human melanoma cells transplanted into zebrafish proliferate, migrate, produce melanin, form masses and stimulate angiogenesis in zebrafish. *Angiogenesis, 9*(3), 139-151.

Hammerman, P. S., Sos, M. L., Ramos, A. H., Xu, C., Dutt, A., Zhou, W., … Meyerson, M. (2011). Mutations in the DDR2 kinase gene identify a novel therapeutic target in squamous cell lung cancer. *Cancer Discovery, 1*(1), 78-89.

Han, J., Lee, Y., Yeom, K. H., Kim, Y. K., Jin, H., & Kim, V. N. (2004). The Drosha-DGCR8 complex in primary microRNA processing. *Genes & Development, 18*(24), 3016-3027.

Han, S. W., Hwang, P. G., Chung, D. H., Kim, D. W., Im, S. A., Kim, Y. T., … Kim, N. K. (2005). Epidermal growth factor receptor (EGFR) downstream molecules as response predictive markers for gefitinib (Iressa, ZD1839) in chemotherapy-resistant non-small cell lung cancer. *International Journal of Cancer, 113*(1), 109-115.

Hanahan, D., & Weinberg, R. A. (2000). The hallmarks of cancer. *Cell, 100*(1), 57-70.

Hanahan, D., & Weinberg, R. A. (2011). Hallmarks of cancer: The next generation. *Cell, 144*(5), 646-674.

Hannon, G. J., & Beach, D. (1994). pl5INK4B is a potentia| effector of TGF-β-induced cell cycle arrest. *Nature, 371*(6494), 257-261.

Hashemi, M., Bizhani, F., Danesh Hiva D., Narouie, B., Sotoudeh, M., Radfar, M. H., ... Ghavami, S. (2016a). MiR-608 rs4919510 C>G polymorphism increased the risk of bladder cancer in an Iranian population. *AIMS Genetics, 3*(4), 212-218.

Hashemi, M., Sanaei, S., Rezaei, M., Bahari, G., Hashemi, S. M., Mashhadi, M. A., … Ghavami, S. (2016b). MiR-608 rs4919510 C>G polymorphism decreased the risk of breast cancer in an Iranian subpopulation. *Experimental Oncology, 38*(1), 57-59.

Hata, A. N., Engelman, J. A., & Faber, A. C. (2015). The Bcl-2 family: Key mediators of the apoptotic response to targeted anti-cancer therapeutics. *Cancer Discovery, 5*(5), 475-487.

Hayashita, Y., Osada, H., Tatematsu, Y., Yamada, H., Yanagisawa, K., Tomida, S., … Takahashi, T. (2005). A polycistronic microRNA cluster, miR-17-92, is overexpressed in human lung cancers and enhances cell proliferation. *Cancer Research, 65*(21), 9628-9632.

He, H., Jazdzewski, K., Li, W., Liyanarachchi, S., Nagy, R., Volinia, S., … de la Chapelle, A. (2005). The role of microRNA genes in papillary thyroid carcinoma. *Proceedings of the National Academy of Sciences USA, 102*(52), 19075-19080.

Hecht, S. S. (1999). Tobacco smoke carcinogens and lung cancer. *Journal of the National Cancer Institute, 91*(14), 1194-1210.

Hengartner, M. O. (2000). The biochemistry of apoptosis. *Nature, 407*(6805), 770-776.

Hengartner, M. O. (2001). Apoptosis: Corralling the corpses. *Cell, 104*(3), 325-328.

Hibi, M., Lin, A., Smeal, T., Minden, A., & Karin, M. (1993). Identification of an oncoprotein- and UV-responsive protein kinase that binds and potentiates the c-Jun activation domain. *Genes & Development, 7*(11), 2135-2148.

Hill, M. M., & Hemmings, B. A. (2002). Inhibition of protein kinase B/Akt. Implications for cancer therapy. *Pharmacology & Therapeutics, 93*(2-3), 243-251.

Hockenbery, D. M., Zutter, M., Hickey, W., Nahm, M., & Korsmeyer, S. J. (1991). Bcl2 protein is topographically restricted in tissues characterized by apoptotic cell death. *Proceedings of the National Academy of Sciences USA, 88*(16), 6961-6965.

Hoffmann, D., & Hoffmann, I. (1997). The changing cigarette, 1950-1995. *Journal of Toxicology and Environmental Health, 50*(4), 307-364.

Holmstrom, T. H., Schmitz, I., Soderstrom, T. S., Poukkula, M., Johnson, V. L., Chow, S. C., … Eriksson, J. E. (2000). MAPK/ERK signaling in activated T cells inhibits CD95/Fas-mediated apoptosis downstream of DISC assembly. *The EMBO Journal, 19*(20), 5418-5428.

Hoot, K. E., Lighthall, J., Han, G., Lu, S. L., Li, A., Ju, W., … Wang, X. J. (2008). Keratinocyte-specific Smad2 ablation results in increased epithelial-mesenchymal transition during skin cancer formation and progression. *Journal of Clinical Investigation, 118*(8), 2722-2732.

Hopkins-Donaldson, S., Ziegler, A., Kurtz, S., Bigosch, C., Kandioler, D., Ludwig, C., … Stahel, R. (2003). Silencing of death receptor and caspase-8 expression in small cell lung carcinoma cell lines and tumors by DNA methylation. *Cell Death & Differentiation, 10*(3), 356-364.

Horita, M., Andreu, E. J., Benito, A., Arbona, C., Sanz, C., Benet, I., … Fernandez-Luna, J. L. (2000). Blockade of the Bcr-Abl kinase activity induces apoptosis of chronic myelogenous leukemia cells by suppressing signal transducer and activator of transcription 5-dependent expression of Bcl-xL. *Journal of Experimental Medicine, 191*(6), 977-984.

Howlader, N., Noone, A. M., Krapcho, M., Miller, D., Bishop, K., Altekruse, S. F., … Cronin, K. A. (2017a). *SEER cancer statistics review, 1975-2013.* Retrieved from http://seer.cancer.gov/csr/1975_2013/.

Howlader, N., Noone, A. M., Krapcho, M., Miller, D., Bishop, K., Altekruse, S. F., … Cronin K. A. (2017b). *Cancer stat facts: Lung and bronchus cancer.* Retrieved from https://seer.cancer.gov/statfacts/html/lungb.html.

Hu, P. P., Shen, X., Huang, D., Liu, Y., Counter, C., & Wang, X. F. (1999). The MEK pathway is required for stimulation of p21(WAF1/CIP1) by transforming growth factor-beta. *Journal of Biological Chemistry, 274*(50), 35381-35387.

Huang, A. J., Yu, K. D., Li, J., Fan, L., & Shao, Z. M. (2012). Polymorphism rs4919510:C>G in mature sequence of human microRNA-608 contributes to the risk of HER2-positive breast cancer but not other subtypes. *PLoS One, 7*(5), e35252.

Huang da, W., Sherman, B. T., & Lempicki, R. A. (2009). Systematic and integrative analysis of large gene lists using DAVID bioinformatics resources. *Nature Protocols, 4*(1), 44-57.

Huang, D. C., O'Reilly, L. A., Strasser, A., & Cory, S. (1997). The anti-apoptosis function of Bcl-2 can be genetically separated from its inhibitory effect on cell cycle entry. *The EMBO Journal, 16*(15), 4628-4638.

Huang, G., Shi, L. Z., & Chi, H. (2009). Regulation of JNK and p38 MAPK in the immune system: Signal integration, propagation and termination. *Cytokine, 48*(3), 161-169.

Huumonen, K., Korkalainen, M., Viluksela, M., Lahtinen, T., Naarala, J., & Juutilainen, J. (2014). Role of microRNAs and DNA methyltransferases in transmitting induced genomic instability between cell generations. *Frontiers in Public Health, 2*(139), 1-9.

Hwang, S. J., Cheng, L. S., Lozano, G., Amos, C. I., Gu, X., & Strong, L. C. (2003). Lung cancer risk in germline p53 mutation carriers: Association between an inherited cancer predisposition, cigarette smoking, and cancer risk. *Human Genetics, 113*(3), 238-243.

Inamura, K., & Ishikawa, Y. (2016). MicroRNA in lung cancer: Novel biomarkers and potential tools for treatment. *Journal of Clinical Medicine, 5*(3), 36.

Incoronato, M., Garofalo, M., Urso, L., Romano, G., Quintavalle, C., Zanca, C., … Condorelli, G. (2010). MiR-212 increases tumor necrosis factor-related apoptosis-inducing ligand sensitivity in non-small cell lung cancer by targeting the anti-apoptotic protein PED. *Cancer Research, 70*(9), 3638-3646.

Itoh, N., Semba, S., Ito, M., Takeda, H., Kawata, S., & Yamakawa, M. (2002). Phosphorylation of Akt/PKB is required for suppression of cancer cell apoptosis and tumor progression in human colorectal carcinoma. *Cancer, 94*(12), 3127-3134.

Itoh, S, Itoh, F, Goumans, MJ, & Ten Dijke, P. (2000). Signaling of transforming growth factor-beta family members through Smad proteins. *European Journal of Biochemistry, 267*(24), 6954-6967.

Ivanovska, I., & Cleary, M. A. (2008). Combinatorial microRNAs: Working together to make a difference. *Cell Cycle, 7*(20), 3137-3142.

Jakowlew, S. B. (2008). Transforming growth factor-β in lung cancer, carcinogenesis, and metastasis. In S. B. Jakowlew (Ed.), *Transforming growth factor-beta in cancer therapy* (Vol. 2, pp. 633-671). Humana Press.

Jang, C. W., Chen, C. H., Chen, C. C., Chen, J. Y., Su, Y. H., & Chen, R. H. (2002). TGF-beta induces apoptosis through smad-mediated expression of DAP-kinase. *Nature Cell Biology, 4*(1), 51-58.

Janmaat, M. L., Kruyt, F. A., Rodriguez, J. A., & Giaccone, G. (2003). Response to epidermal growth factor receptor inhibitors in non-small cell lung cancer cells: Limited antiproliferative effects and absence of apoptosis associated with persistent activity of extracellular signal-regulated kinase or Akt kinase pathways. *Clinical Cancer Research, 9*(6), 2316-2326.

Jeon, H. S., & Jen, J. (2010). TGF-beta signaling and the role of inhibitory Smads in non-small cell lung cancer. *Journal of Thoracic Oncology, 5*(4), 417-419.

Jeong, S. Y, Gaume, B., Lee, Y. J., Hsu, Y. T., Ryu, S. W., Yoon, S. H., & Youle, R. J. (2004). Bcl-xL sequesters its C-terminal membrane anchor in soluble, cytosolic homodimers. *The EMBO Journal, 23*(10), 2146-2155.

Ji, D., Chen, Z., Li, M., Zhan, T., Yao, Y., Zhang, Z., … Gu, J. (2014). MicroRNA-181a promotes tumor growth and liver metastasis in colorectal cancer by targeting the tumor suppressor WIF-1. *Molecular Cancer, 13*, 86-104.

Jin, G., Kim, M. J., Jeon, H. S., Choi, J. E., Kim, D. S., Lee, E. B., … Park, J. Y. (2010). PTEN mutations and relationship to EGFR, ERBB2, KRAS, and TP53 mutations in non-small cell lung cancers. *Lung Cancer, 69*(3), 279-283.

Jin, Z., & El-Deiry, W. S. (2005). Overview of cell death signaling pathways. *Cancer Biology & Therapy, 4*(2), 139-163.

Johnson, B. E., Ihde, D. C., Makuch, R. W., Gazdar, A. F., Carney, D. N, Oie, H., … Minna, J. D. (1987). Myc family oncogene amplification in tumor cell lines established from small cell lung cancer patients and its relationship to clinical status and course. *Journal of Clinical Investigation, 79*(6), 1629-1634.

Johnson, B. E., Russell, E., Simmons, A. M., Phelps, R., Steinberg, S. M., Ihde, D. C., & Gazdar, A. F. (1996). MYC family DNA amplification in 126 tumor cell lines from patients with small cell lung cancer. *Journal of Cellular Biochemistry, 24*, 210-217.

Johnson, C. D., Esquela-Kerscher, A., Stefani, G., Byrom, M., Kelnar, K., Ovcharenko, D., … Slack, F. J. (2007). The let-7 microRNA represses cell proliferation pathways in human cells. *Cancer Research, 67*(16), 7713-7722.

Johnson, G. L., & Nakamura, K. (2007). The c-Jun kinase/stress-activated pathway: Regulation, function and role in human disease. *Biochimica et Biophysica Acta, 1773*(8), 1341-1348.

Johnson, S. M., Grosshans, H., Shingara, J., Byrom, M., Jarvis, R., Cheng, A., … Slack, F. J. (2005). Ras is regulated by the let-7 microRNA family. *Cell, 120*(5), 635-647.

Joseph, B., Ekedahl, J., Sirzen, F., Lewensohn, R., & Zhivotovsky, B. (1999). Differences in expression of pro-caspases in small cell and non-small cell lung carcinoma. *Biochemical and Biophysical Research Communications, 262*(2), 381-387.

Jovanovic, M., & Hengartner, M. O. (2006). MiRNAs and apoptosis: RNAs to die for. *Oncogene, 25*(46), 6176-6187.

Jung, D. W., Oh, E. S., Park, S. H., Chang, Y. T., Kim, C. H., Choi, S. Y., & Williams, D. R. (2012). A novel zebrafish human tumor xenograft model validated for anti-cancer drug screening. *Molecular BioSystems, 8*(7), 1930-1939.

Karczmarek-Borowska, B., Filip, A., Wojcierowski, J., Smolen, A., Korobowicz, E., Korszen-Pilecka, I., & Zdunek, M. (2006). Estimation of prognostic value of Bcl-xL gene expression in non-small cell lung cancer. *Lung Cancer, 51*(1), 61-69.

Karin, M., & Ben-Neriah, Y. (2000). Phosphorylation meets ubiquitination: The control of NF-[kappa]B activity. *Annual Review of Immunology, 18*, 621-663.

Kawahara, Y. (2014). Human diseases caused by germline and somatic abnormalities in microRNA and microRNA-related genes. *Congenital Anomalies (Kyoto), 54*(1), 12-21.

Kaye, F. J. (2002). RB and cyclin dependent kinase pathways: Defining a distinction between RB and p16 loss in lung cancer. *Oncogene, 21*(45), 6908-6914.

Kerr, J. F., Wyllie, A. H., & Currie, A. R. (1972). Apoptosis: A basic biological phenomenon with wide-ranging implications in tissue kinetics. *British Journal of Cancer, 26*(4), 239-257.

Kim, D. M., Chung, K. S., Choi, S. J., Jung, Y. J., Park, S. K., Han, G. H., … Seo, Y. S. (2009). RhoB induces apoptosis via direct interaction with TNFAIP1 in HeLa cells. *International Journal of Cancer, 125*(11), 2520-2527.

Kim, E. K., & Choi, E. J. (2010). Pathological roles of MAPK signaling pathways in human diseases. *Biochimica et Biophysica Acta, 1802*(4), 396-405.

Kim, E. K, & Choi, E. J. (2015). Compromised MAPK signaling in human diseases: An update. *Archives of Toxicology, 89*(6), 867-882.

Kim, S. G., Jong, H. S., Kim, T. Y., Lee, J. W., Kim, N. K., Hong, S. H., & Bang, Y. J. (2004). Transforming growth factor-beta 1 induces apoptosis through Fas ligand-independent activation of the Fas death pathway in human gastric SNU-620 carcinoma cells. *Molecular Biology of the Cell, 15*(2), 420-434.

Kim, Y. C., Park, K. O., Kern, J. A., Park, C. S., Lim, S. C., Jang, A. S., & Yang, J. B. (1998). The interactive effect of Ras, HER2, P53 and Bcl-2 expression in predicting the survival of non-small cell lung cancer patients. *Lung Cancer, 22*(3), 181-190.

King, K. L., & Cidlowski, J. A. (1995). Cell cycle and apoptosis: Common pathways to life and death. *Journal of Cellular Biochemistry, 58*(2), 175-180.

Kischkel, F. C., Hellbardt, S., Behrmann, I., Germer, M., Pawlita, M., Krammer, P. H., & Peter, M. E. (1995). Cytotoxicity-dependent APO-1 (Fas/CD95)-associated proteins form a death-inducing signaling complex (DISC) with the receptor. *The EMBO Journal, 14*(22), 5579-5588.

Kitagawa, M., Hatakeyama, S., Shirane, M., Matsumoto, M., Ishida, N., Hattori, K., … Nakayama, K. (1999). An F-box protein, FWD1, mediates ubiquitin-dependent proteolysis of beta-catenin. *The EMBO Journal, 18*(9), 2401-2410.

Kitagawa, Y., Wong, F., Lo, P., Elliott, M., Verburgt, L. M., Hogg, J. C., & Daya, M. (1996). Overexpression of Bcl-2 and mutations in p53 and K-ras in resected human non-small cell lung cancers. *American Journal of Respiratory Cell and Molecular Biology, 15*(1), 45-54.

Kitamura, H., Yazawa, T., Okudela, K., Shimoyamada, H., & Sato, H. (2008). Molecular and genetic pathogenesis of lung cancer: Differences between small-cell and non-small-cell carcinomas. *The Open Pathology Journal, 8*(2), 106-114.

Koopman, G., Reutelingsperger, C. P., Kuijten, G. A., Keehnen, R. M., Pals, S. T., & van Oers, M. H. (1994). Annexin V for flow cytometric detection of phosphatidylserine expression on B cells undergoing apoptosis. *Blood, 84*(5), 1415-1420.

Kops, G. J., de Ruiter, N. D., De Vries-Smits, A. M., Powell, D. R., Bos, J. L., & Burgering, B. M. (1999). Direct control of the forkhead transcription factor AFX by protein kinase B. *Nature, 398*(6728), 630-634.

Kosaka, T., Yatabe, Y., Endoh, H., Kuwano, H., Takahashi, T., & Mitsudomi, T. (2004). Mutations of the epidermal growth factor receptor gene in lung cancer: Biological and clinical implications. *Cancer Research, 64*(24), 8919-8923.

Koty, P. P., Zhang, H., Franklin, W. A., Yousem, S. A., Landreneau, R., & Levitt, M. L. (2002). *In vivo* expression of p53 and Bcl-2 and their role in programmed cell death in premalignant and malignant lung lesions. *Lung Cancer, 35*(2), 155-163.

Koukourakis, M. I., Giatromanolaki, A., O'Byrne, K. J., Cox, J., Krammer, B., Gatter, K. C., & Reed, J. C. (1999). Bcl-2 and c-erbB-2 proteins are involved in the regulation of VEGF and of thymidine phosphorylase angiogenic activity in non-small-cell lung cancer. *Clinical & Experimental Metastasis, 17*(7), 545-554.

Koukourakis, M. I., Giatromanolaki, A., O'Byrne, K. J., Whitehouse, R. M., Talbot, D. C., Gatter, K. C., Harris, A. L. (1997). Potential role of Bcl-2 as a suppressor of tumour angiogenesis in non-small-cell lung cancer. *International Journal of Cancer, 74*(6), 565-570.

Krajewska, M., Moss, S. F., Krajewski, S., Song, K., Holt, P. R., & Reed, J. C. (1996). Elevated expression of Bcl-x and reduced Bak in primary colorectal adenocarcinomas. *Cancer Research, 56*(10), 2422-2427.

Krek, A., Grün, D., Poy, M. N., Wolf, R., Rosenberg, L., Epstein, E. J., … Nikolaus, R. (2005). Combinatorial microRNA target predictions. *Nature Genetics*, *37*(5), 495-500.

Krepela, E., Prochazka, J., Fiala, P., Zatloukal, P., & Selinger, P. (2006). Expression of apoptosome pathway-related transcripts in non-small cell lung cancer. *Journal of Cancer Research and Clinical Oncology, 132*(1), 57-68.

Kreuz, S., Siegmund, D., Scheurich, P., & Wajant, H. (2001). NF-kappaB inducers upregulate cFLIP, a cycloheximide-sensitive inhibitor of death receptor signaling. *Molecular and Cellular Biology, 21*(12), 3964-3973.

Kris, M. G., Natale, R. B., Herbst, R. S., Lynch, T. J., Jr., Prager, D., Belani, C. P., … Kay, A. C. (2003). Efficacy of gefitinib, an inhibitor of the epidermal growth factor receptor tyrosine kinase, in symptomatic patients with non-small cell lung cancer: A randomized trial. *Journal of the American Medical Association, 290*(16), 2149-2158.

Kroemer, G. (2002). Introduction: Mitochondrial control of apoptosis. *Biochimie, 84*(2-3), 103-104.

Kroemer, G., Galluzzi, L., & Brenner, C. (2007). Mitochondrial membrane permeabilization in cell death. *Physiological Reviews, 87*(1), 99-163.

Krutzfeldt, J., Rajewsky, N., Braich, R., Rajeev, K. G., Tuschl, T., Manoharan, M., & Stoffel, M. (2005). Silencing of microRNAs *in vivo* with 'antagomiRs'. *Nature, 438*(7068), 685-689.

Kuhn, D. E., Martin, M. M., Feldman, D. S., Terry, A. V., Nuovo, G. J., & Elton, T. S. (2008). Experimental validation of miRNA targets. *Methods, 44*(1), 47-54.

Kumar, M. S., Erkeland, S. J., Pester, R. E., Chen, C. Y., Ebert, M. S., Sharp, P. A., & Jacks, T. (2008). Suppression of non-small cell lung tumor development by the let-7 microRNA family. *Proceedings of the National Academy of Sciences USA, 105*(10), 3903-3908.

Kumar, M. S., Lu, J., Mercer, K. L., Golub, T. R., & Jacks, T. (2007). Impaired microRNA processing enhances cellular transformation and tumorigenesis. *Nature Genetics, 39*(5), 673-677.

Lagos-Quintana, M., Rauhut, R., Lendeckel, W., & Tuschl, T. (2001). Identification of novel genes coding for small expressed RNAs. *Science, 294*(5543), 853-858.

Lam, S. H., Chua, H. L., Gong, Z., Lam, T. J., & Sin, Y. M. (2004). Development and maturation of the immune system in zebrafish, *Danio rerio*: A gene expression profiling, in situ hybridization and immunological study. *Developmental & Comparative Immunology 28*(1), 9-28.

Lebanony, D., Benjamin, H., Gilad, S., Ezagouri, M, Dov, A., Ashkenazi, K.,…Mansukhani, M. (2009). Diagnostic assay based on hsa-miR-205 expression distinguishes squamous from nonsquamous non-small-cell lung carcinoma. *Journal of Clinical Oncology, 27*(12), 2030-2037.

LeBlanc, H. N., & Ashkenazi, A. (2003). Apo2L/TRAIL and its death and decoy receptors. *Cell Death & Differentiation, 10*(1), 66-75.

Lee, L. M., Seftor, E. A., Bonde, G., Cornell, R. A., & Hendrix, M. J. (2005). The fate of human malignant melanoma cells transplanted into zebrafish embryos: Assessment of migration and cell division in the absence of tumor formation. *Developmental Dynamics, 233*(4), 1560-1570.

Lee, M. W., Kim, D. S., Lee, J. H., Lee, B. S., Lee, S. H., Jung, H. L., … Koo, H. H. (2011). Roles of AKT1 and AKT2 in non-small cell lung cancer cell survival, growth, and migration. *Cancer Science, 102*(10), 1822-1828.

Lee, R. C., Feinbaum, R. L., & Ambros, V. (1993). The C. elegans heterochronic gene *lin-4* encodes small RNAs with antisense complementarity to *lin-14*. *Cell, 75*(5), 843-854.

Lee, S. H., Shin, M. S., Kim, H. S., Lee, H. K., Park, W. S., Kim, S. Y., … Yoo, N. J. (1999). Alterations of the DR5/TRAIL receptor 2 gene in non-small cell lung cancers. *Cancer Research, 59*(22), 5683-5686.

Lee, S. L., Rouhi, P., Dahl Jensen, L., Zhang, D., Ji, H., Hauptmann, G., … Cao, Y. (2009). Hypoxia-induced pathological angiogenesis mediates tumor cell dissemination, invasion, and metastasis in a zebrafish tumor model. *Proceedings of the National Academy of Sciences USA, 106*(46), 19485-19490.

Lee, Y., Ahn, C., Han, J., Choi, H., Kim, J., Yim, J., … Kim, V. N. (2003). The nuclear RNase III Drosha initiates microRNA processing. *Nature, 425*(6956), 415-419.

Lee, Y., Jeon, K., Lee, J. T., Kim, S., & Kim, V. N. (2002). MicroRNA maturation: Stepwise processing and subcellular localization. *The EMBO Journal, 21*(17), 4663-4670.

Lee, Y. S., & Dutta, A. (2007). The tumor suppressor microRNA let-7 represses the HMGA2 oncogene. *Genes & Development 21*(9), 1025-1030.

Leech, S. H., Olie, R. A., Gautschi, O., Simoes-Wust, A. P., Tschopp, S., Haner, R., … Zangemeister-Wittke, U. (2000). Induction of apoptosis in lung-cancer cells following bcl-xL anti-sense treatment. *International Journal of Cancer, 86*(4), 570-576.

Lehmann, U., Hasemeier, B., Christgen, M., Muller, M., Romermann, D., Langer, F., & Kreipe, H. (2008). Epigenetic inactivation of microRNA gene hsa-miR-9-1 in human breast cancer. *Journal of Pathology, 214*(1), 17-24.

Lei, X., Huang, Z., Zhong, M., Zhu, B., Tang, S., & Liao, D. (2007). Bcl-xL small interfering RNA sensitizes cisplatin-resistant human lung adenocarcinoma cells. *Acta Biochimica et Biophysica Sinica (Shanghai), 39*(5), 344-350.

Lemmon, M. A., & Ferguson, K. M. (2000). Signal-dependent membrane targeting by pleckstrin homology (PH) domains. *Biochemical Journal, 350*(Pt 1), 1-18.

Levine, A. J. (1997). p53, the cellular gatekeeper for growth and division. *Cell, 88*(3), 323-331.

Lewis, B. P., Burge, C. B., & Bartel, D. P. (2005). Conserved seed pairing, often flanked by adenosines, indicates that thousands of human genes are microRNA targets. *Cell, 120*(1), 15-20.

Lewis, B. P., Shih, I. H., Jones-Rhoades, M. W., Bartel, D. P., & Burge, C. B. (2003). Prediction of mammalian microRNA targets. *Cell, 115*(7), 787-798.

Li, C., Hashimi, S. M., Good, D. A., Cao, S., Duan, W., Plummer, P. N., … Wei, M. Q. (2012a). Apoptosis and microRNA aberrations in cancer. *Clinical and Experimental Pharmacology and Physiology, 39*(8), 739-746.

Li, F., Chong, Z. Z., & Maiese, K. (2006). Winding through the WNT pathway during cellular development and demise. *Histology and Histopathology, 21*(1), 103-124.

Li, H., Zhu, H., Xu, C. J., & Yuan, J. (1998). Cleavage of BID by caspase 8 mediates the mitochondrial damage in the Fas pathway of apoptosis. *Cell, 94*(4), 491-501.

Li, J., Wang, K., Chen, X., Meng, H., Song, M., Wang, Y., … Bai, Y. (2012b). Transcriptional activation of microRNA-34a by NF-kappa B in human esophageal cancer cells. *BMC Molecular Biology, 13*, 4-14.

Li, J., & Yuan, J. (2008). Caspases in apoptosis and beyond. *Oncogene, 27*(48), 6194-6206.

Li, P., Nijhawan, D., Budihardjo, I., Srinivasula, S. M., Ahmad, M., Alnemri, E. S., & Wang, X. (1997). Cytochrome c and dATP-dependent formation of Apaf-1/caspase-9 complex initiates an apoptotic protease cascade. *Cell, 91*(4), 479-489.

Li, S. P., Junttila, M. R., Han, J., Kahari, V. M., & Westermarck, J. (2003). P38 mitogen-activated protein kinase pathway suppresses cell survival by inducing dephosphorylation of mitogen-activated protein/extracellular signal-regulated kinase kinase1,2. *Cancer Research, 63*(13), 3473-3477.

Li, X., & Hemminki, K.. (2004). Inherited predisposition to early onset lung cancer according to histological type. *International Journal of Cancer, 112*(3), 451-457.

Li, Y. J., Zhang, Y. X., Wang, P. Y., Chi, Y. L., Zhang, C., Ma, Y., … Xie, S. Y. (2012c). Regression of A549 lung cancer tumors by anti-miR-150 vector. *Oncology Reports, 27*(1), 129-134.

Liam, C. K., Pang, Y. K., Leow, C. H., Poosparajah, S., & Menon, A. (2006). Changes in the distribution of lung cancer cell types and patient demography in a developing multiracial asian country: Experience of a university teaching hospital. *Lung Cancer, 53*(1), 23-30.

Licchesi, J. D., Westra, W. H., Hooker, C. M., Machida, E. O., Baylin, S. B., & Herman, J. G. (2008). Epigenetic alteration of WNT pathway antagonists in progressive glandular neoplasia of the lung. *Carcinogenesis, 29*(5), 895-904.

Lieschke, G. J., & Currie, P. D. (2007). Animal models of human disease: Zebrafish swim into view. *Nature Reviews Genetics, 8*(5), 353-367.

Lima, R. T., Busacca, S., Almeida, G. M., Gaudino, G., Fennell, D. A., & Vasconcelos, M. H. (2011). MicroRNA regulation of core apoptosis pathways in cancer. *European Journal of Cancer, 47*(2), 163-174.

Liu, D., Tao, T., Xu, B., Chen, S., Liu, C., Zhang, L., … Chen, M. (2014). MiR-361-5p acts as a tumor suppressor in prostate cancer by targeting signal transducer and activator of transcription-6(Stat6). *Biochemical and Biophysical Research Communications, 445*(1), 151-156.

Liu, J., Rivas, F. V., Wohlschlegel, J., Yates, J. R., Parker, R., & Hannon, G. J. (2005a). A role for the P-body component GW182 in microRNA function. *Nature Cell Biology, 7*(12), 1261-1266.

Liu, J., Valencia-Sanchez, M. A., Hannon, G. J, & Parker, R. (2005b). MicroRNA-dependent localization of targeted mRNAs to mammalian P-bodies. *Nature Cell Biology, 7*(7), 719-723.

Liu, M., Wang, Z., Yang, S., Zhang, W., He, S., Hu, C., … Xu, N. (2011). TNF-α is a novel target of miR-19a. *International Journal of Oncology, 38*(4), 1013-1022.

Liu, X., Zhang, X., Zhan, Q., Brock, M. V., Herman, J. G., & Guo, M. (2012). CDX2 serves as a WNT signaling inhibitor and is frequently methylated in lung cancer. *Cancer Biology & Therapy, 13*(12), 1152-1157.

Lugo, T. G., Pendergast, A. M., Muller, A. J., & Witte, O. N. (1990). Tyrosine kinase activity and transformation potency of BCR-ABL oncogene products. *Science, 247*(4946), 1079-1082.

Lund, E., Guttinger, S., Calado, A., Dahlberg, J. E., & Kutay, U. (2004). Nuclear export of microRNA precursors. *Science, 303*(5654), 95-98.

Luthi, A. U., & Martin, S. J. (2007). The CASBAH: A searchable database of caspase substrates. *Cell Death & Differentiation, 14*(4), 641-650.

Ma, F., Song, H., Guo, B., Zhang, Y., Zheng, Y., Lin, C., … Qiu, X. (2015). MiR-361-5p inhibits colorectal and gastric cancer growth and metastasis by targeting staphylococcal nuclease domain containing-1. *Oncotarget, 6*(19), 17404-17416.

Makin, G., & Dive, C. (2001). Apoptosis and cancer chemotherapy. *Trends in Cell Biology, 11*(11), S22-26.

Malumbres, M., & Barbacid, M. (2003). RAS oncogenes: The first 30 years. *Nature Reviews Cancer, 3*(6), 459-465.

Markowitz, S. D., & Roberts, A. B. (1996). Tumor suppressor activity of the TGF-beta pathway in human cancers. *Cytokine & Growth Factor Reviews, 7*(1), 93-102.

Marone, M., Scambia, G., Mozzetti, S., Ferrandina, G., Iacovella, S., De Pasqua, A., … Mancuso, S. (1998). Bcl-2, bax, bcl-XL, and bcl-XS expression in normal and neoplastic ovarian tissues. *Clinical Cancer Research, 4*(2), 517-524.

Marques, I. J., Weiss, F. U., Vlecken, D. H., Nitsche, C., Bakkers, J., Lagendijk, A. K., … Bagowski, C. P. (2009). Metastatic behaviour of primary human tumours in a zebrafish xenotransplantation model. *BMC Cancer, 9*, 128-142.

Marrone, A. K., Tryndyak, V., Beland, F. A., & Pogribny, I. P. (2016). MicroRNA responses to the genotoxic carcinogens aflatoxin B1 and benzo[a]pyrene in human HepaRG cells. *Toxicological Sciences, 149*(2), 496-502.

Marsit, C. J., Zheng, S., Aldape, K., Hinds, P. W., Nelson, H. H., Wiencke, J. K., & Kelsey, K. T. (2005). PTEN expression in non-small-cell lung cancer: Evaluating its relation to tumor characteristics, allelic loss, and epigenetic alteration. *Human Pathology, 36*(7), 768-776.

Martelli, A. M., Tabellini, G., Bressanin, D., Ognibene, A., Goto, K., Cocco, L., … Evangelisti, C. (2012). The emerging multiple roles of nuclear Akt. *Biochimica et Biophysica Acta, 1823*(12), 2168-2178.

Massagué, J. (1998). TGF-β signal transduction. *Annual Review of Biochemistry, 67*, 753-791.

Massagué, J. (2000). How cells read TGF-β signals. *Nature Reviews Molecular Cell Biology, 1*(3), 169-178.

Massagué, J. (2008). TGF β in cancer. *Cell, 134*(2), 215-230.

Massagué, J, & Wotton, D. (2000). Transcriptional control by the TGF-β/Smad signaling system. *The EMBO Journal, 19*(8), 1745-1754.

Matranga, C., Tomari, Y., Shin, C., Bartel, D. P., & Zamore, P. D. (2005). Passenger-strand cleavage facilitates assembly of siRNA into Ago2-containing RNAi enzyme complexes. *Cell, 123*(4), 607-620.

Matsubara, D., Kanai, Y., Ishikawa, S., Ohara, S., Yoshimoto, T., Sakatani, T., … Niki, T. (2012). Identification of CCDC6-RET fusion in the human lung adenocarcinoma cell line, LC-2/ad. *Journal of Thoracic Oncology, 7*(12), 1872-1876.

Matsubara, H., Takeuchi, T., Nishikawa, E., Yanagisawa, K., Hayashita, Y., Ebi, H., … Takahashi, T. (2007). Apoptosis induction by antisense oligonucleotides against miR-17-5p and miR-20a in lung cancers overexpressing miR-17-92. *Oncogene, 26*(41), 6099-6105.

Mayo, L. D., & Donner, D. B. (2001). A phosphatidylinositol 3-kinase/Akt pathway promotes translocation of Mdm2 from the cytoplasm to the nucleus. *Proceedings of the National Academy of Sciences USA, 98*(20), 11598-11603.

Maziere, P., & Enright, A. J. (2007). Prediction of microRNA targets. *Drug Discovery Today, 12*(11-12), 452-458.

Mazieres, J., He, B., You, L., Xu, Z., & Jablons, D. M. (2005). WNT signaling in lung cancer. *Cancer Letters, 222*(1), 1-10.

McIlwain, D. R., Berger, T., & Mak, T. W. (2013). Caspase functions in cell death and disease. *Cold Spring Harbor Perspectives in Biology, 5*(4), a008656.

Meister, G., Landthaler, M., Dorsett, Y., & Tuschl, T. (2004). Sequence-specific inhibition of microRNA- and siRNA-induced RNA silencing. *RNA, 10*(3), 544-550.

Mendelsohn, J., & Baselga, J. (2003). Status of epidermal growth factor receptor antagonists in the biology and treatment of cancer. *Journal of Clinical Oncology, 21*(14), 2787-2799.

Mercer, B. A., & D'Armiento, J. M. (2006). Emerging role of MAP kinase pathways as therapeutic targets in COPD. *International Journal of Chronic Obstructive Pulmonary Disease, 1*(2), 137-150.

Merritt, W. M., Lin, Y. G., Han, L. Y., Kamat, A. A., Spannuth, W. A., Schmandt, R., … Sood, A. K. (2008). Dicer, Drosha, and outcomes in patients with ovarian cancer. *The New England Journal of Medicine, 359*(25), 2641-2650.

Milne, D. M., Campbell, D. G., Caudwell, F. B., & Meek, D. W. (1994). Phosphorylation of the tumor suppressor protein p53 by mitogen-activated protein kinases. *Journal of Biological Chemistry, 269*(12), 9253-9260.

Miyamoto, Y., Hosotani, R., Wada, M., Lee, J. U., Koshiba, T., Fujimoto, K., … Imamura, M. (1999). Immunohistochemical analysis of Bcl-2, Bax, Bcl-X, and Mcl-1 expression in pancreatic cancers. *Oncology, 56*(1), 73-82.

Miyazono, K., Suzuki, H., & Imamura, T. (2003). Regulation of TGF-beta signaling and its roles in progression of tumors. *Cancer Science, 94*(3), 230-234.

Miyazono, K., ten Dijke, P., & Heldin, C. H. (2000). TGF-beta signaling by Smad proteins. *Advances in Immunology, 75*, 115-157.

Molina, J. R., Yang, P., Cassivi, S. D., Schild, S. E., & Adjei, A. A. (2008). Non–small cell lung cancer: Epidemiology, risk factors, treatment, and survivorship. *Mayo Clinic Proceedings, 83*(5), 584-594.

Mora, A., Komander, D., van Aalten, D. M., & Alessi, D. R. (2004). PDK1, the master regulator of AGC kinase signal transduction. *Seminars in Cell & Developmental Biology, 15*(2), 161-170.

Morton, S., Davis, R. J., McLaren, A., & Cohen, P. (2003). A reinvestigation of the multisite phosphorylation of the transcription factor c-Jun. *The EMBO Journal, 22*(15), 3876-3886.

Mott, J. L., Kobayashi, S., Bronk, S. F., & Gores, G. J. (2007). MiR-29 regulates Mcl-1 protein expression and apoptosis. *Oncogene, 26*(42), 6133-6140.

Mott, J. L., Kurita, S., Cazanave, S. C., Bronk, S. F., Werneburg, N. W., & Fernandez-Zapico, M. E. (2010). Transcriptional suppression of miR-29b-1/miR-29a promoter by c-Myc, hedgehog, and NF-kappaB. *Journal of Cellular Biochemistry, 110*(5), 1155-1164.

Müller, F. H. (1940). Tabakmissbrauch und lungencarcinom. *Zeitschrift für Krebsforschung und klinische Onkologie, 49*, 57-85.

Munker, S., Weng, H. L., Li, Q., Liu, Y., Meyer, C., Dooley, S., & Li, J. (2012). Differential smad expression contributes to severity of cholangiocarcinoma. *Zeitschrift Fur Gastroenterologie,* K102.

Mure, H., Matsuzaki, K., Kitazato, K. T., Mizobuchi, Y., Kuwayama, K., Kageji, T., & Nagahiro, S. (2010). Akt2 and Akt3 play a pivotal role in malignant gliomas. *Neuro-Oncology, 12*(3), 221-232.

Murphy, L. O., Smith, S., Chen, R. H., Fingar, D. C., & Blenis, J. (2002). Molecular interpretation of ERK signal duration by immediate early gene products. *Nature Cell Biology, 4*(8), 556-564.

Muzio, M., Stockwell, B. R., Stennicke, H. R., Salvesen, G. S., & Dixit, V. M. (1998). An induced proximity model for caspase-8 activation. *Journal of Biological Chemistry, 273*(5), 2926-2930.

Na, Y., Lee, S. M., Kim, D. S., & Park, J. Y. (2012). Promoter methylation of WNT antagonist DKK1 gene and prognostic value in Korean patients with non-small cell lung cancers. *Cancer Biomarkers, 12*(2), 73-79.

Nakae, J., Park, B. C., & Accili, D. (1999). Insulin stimulates phosphorylation of the forkhead transcription factor FKHR on serine 253 through a Wortmannin-sensitive pathway. *Journal of Biological Chemistry, 274*(23), 15982-15985.

Nakamura, T., Canaani, E., & Croce, C. M. (2007). Oncogenic All1 fusion proteins target Drosha-mediated microRNA processing. *Proceedings of the National Academy of Sciences USA, 104*(26), 10980-10985.

Nakashio, A., Fujita, N., Rokudai, S., Sato, S., & Tsuruo, T. (2000). Prevention of phosphatidylinositol 3'-kinase-Akt survival signaling pathway during topotecan-induced apoptosis. *Cancer Research, 60*(18), 5303.

Naoki, K., Chen, T. H., Richards, W. G., Sugarbaker, D. J., & Meyerson, M. (2002). Missense mutations of the BRAF gene in human lung adenocarcinoma. *Cancer Research, 62*(23), 7001-7003.

Nasser, M. W., Datta, J., Nuovo, G., Kutay, H., Motiwala, T., Majumder, S., … Ghoshal, K. (2008). Down-regulation of micro-RNA-1 (miR-1) in lung cancer. Suppression of tumorigenic property of lung cancer cells and their sensitization to doxorubicin-induced apoptosis by miR-1. *Journal of Biological Chemistry, 283*(48), 33394-33405.

Nevins, J. R. (1998). Toward an understanding of the functional complexity of the E2F and retinoblastoma families. *Cell Growth & Differentiation, 9*(8), 585-593.

Nicholson, D. W. (1999). Caspase structure, proteolytic substrates, and function during apoptotic cell death. *Cell Growth & Differentiation, 6*(11), 1028-1042.

Nicoletti, I., Migliorati, G., Pagliacci, M. C., Grignani, F., & Riccardi, C. (1991). A rapid and simple method for measuring thymocyte apoptosis by propidium iodide staining and flow cytometry. *Journal of Immunological Methods, 139*(2), 271-279.

Nicoli, S., Ribatti, D., Cotelli, F, & Presta, M. (2007). Mammalian tumor xenografts induce neovascularization in zebrafish embryos. *Cancer Research, 67*(7), 2927-2931.

Niu, J., Shi, Y., Tan, G., Yang, C. H., Fan, M., Pfeffer, L. M., … Wu, Z. H. (2012). DNA damage induces NF-kappaB-dependent microRNA-21 up-regulation and promotes breast cancer cell invasion. *Journal of Biological Chemistry, 287*(26), 21783-21795.

Ohtsuka, K., Ohnishi, H., Fujiwara, M., Kishino, T., Matsushima, S., Furuyashiki, G., … Watanabe, T. (2007). Abnormalities of epidermal growth factor receptor in lung squamous-cell carcinomas, adenosquamous carcinomas, and large-cell carcinomas: Tyrosine kinase domain mutations are not rare in tumors with an adenocarcinoma component. *Cancer, 109*(4), 741-750.

Orrenius, S., Zhivotovsky, B., & Nicotera, P. (2003). Regulation of cell death: The calcium-apoptosis link. *Nature Reviews Molecular Cell Biology, 4*(7), 552-565.

Osada, H., & Takahashi, T. (2011). Let-7 and miR-17-92: Small-sized major players in lung cancer development. *Cancer Science, 102*(1), 9-17.

Othman N. (2012). *Identification of bcl-xl induced microRNAs involved in the apoptotic properties of human lung adenocarcinoma cells, A549.* (Master's Thesis), University of Malaya, Malaysia. Retrieved from http://studentsrepo.um.edu.my/id/eprint/4431.

Othman, N., & Nagoor, N. H. (2014). The role of microRNAs in the regulation of apoptosis in lung cancer and its application in cancer treatment. *BioMed Research International, 2014*(2014), 318030.

Otterson, G. A., Kratzke, R. A., Coxon, A., Kim, Y. W., & Kaye, F. J. (1994). Absence of p16INK4 protein is restricted to the subset of lung cancer lines that retains wildtype RB. *Oncogene, 9*(11), 3375-3378.

Ouyang, M., Li, Y., Ye, S., Ma, J., Lu, L., Lv, W.,…Wang, W. (2014). MicroRNA profiling implies new markers of chemoresistance of triple-negative breast cancer. *PLoS One, 9*(5), e96228.

Ozes, O. N., Mayo, L. D., Gustin, J. A., Pfeffer, S. R., Pfeffer, L. M., & Donner, D.B. (1999). NF-kappaB activation by tumour necrosis factor requires the Akt serine-threonine kinase. *Nature, 401*(6748), 82-85.

Pacifico, F., Crescenzi, E., Mellone, S., Iannetti, A., Porrino, N., Liguoro, D., … Leonardi, A. (2010). Nuclear factor-{kappa}B contributes to anaplastic thyroid carcinomas through up-regulation of miR-146a. *Journal of Clinical Endocrinology & Metabolism, 95*(3), 1421-1430.

Parikh, A., Lee, C., Joseph, P., Marchini, S., Baccarini, A., Kolev, V., … Di Feo, A. (2014). MicroRNA-181a has a critical role in ovarian cancer progression through the regulation of the epithelial-mesenchymal transition. *Nature Communications, 5*, 2977-2993.

Park, D., Magis, A. T., Li, R., Owonikoko, T. K., Sica, G. L., Sun, S. Y., … Deng, X. (2013). Novel small-molecule inhibitors of Bcl-XL to treat lung cancer. *Cancer Research, 73*(17), 5485-5496.

Parker, R., & Song, H. (2004). The enzymes and control of eukaryotic mRNA turnover. *Nature Structural & Molecular Biology, 11*(2), 121-127.

Pećina-Šlaus, N. (2010). WNT signal transduction pathway and apoptosis: A review. *Cancer Cell International, 10*(1), 22-27.

Pellecchia, M., & Reed, J. C.. (2004). Inhibition of anti-apoptotic Bcl-2 family proteins by natural polyphenols: New avenues for cancer chemoprevention and chemotherapy. *Current Pharmaceutical Design, 10*(12), 1387-1398.

Pena, J. C., Thompson, C. B., Recant, W., Vokes, E. E., & Rudin, C. M. (1999). Bcl-xl and Bcl-2 expression in squamous cell carcinoma of the head and neck. *Cancer, 85*(1), 164-170.

Peti, W., & Page, R. (2013). Molecular basis of MAP kinase regulation. *Protein Science, 22*(12), 1698-1710.

Pezzella, F., Turley, H., Kuzu, I., Tungekar, M. F., Dunnill, M. S., Pierce, C. B., … Mason, D. Y. (1993). Bcl-2 protein in non-small-cell lung carcinoma. *New England Journal of Medicine, 329*(10), 690-694.

Pfister, D. G., Johnson, D. H., Azzoli, C. G., Sause, W., Smith, T. J., Baker, S., … Somerfield, M. R. (2004). American society of clinical oncology treatment of unresectable non-small-cell lung cancer guideline: Update 2003. *Journal of Clinical Oncology, 22*(2), 330-353.

Pichler, M., & Calin, G. A. (2015). MicroRNAs in cancer: From developmental genes in worms to their clinical application in patients. *British Journal of Cancer, 113*(4), 569-573.

Pitti, R. M., Marsters, S. A., Lawrence, D. A., Roy, M., Kischkel, F. C., Dowd, P., … Ashkenazi, A. (1998). Genomic amplification of a decoy receptor for Fas ligand in lung and colon cancer. *Nature, 396*(6712), 699-703.

Platanias, L. C. (2003). MAP kinase signaling pathways and hematologic malignancies. *Blood, 101*(12), 4667-4679.

Plaza-Menacho, I., van der Sluis, T., Hollema, H., Gimm, O., Buys, C. H., Magee, A. I., … Eggen, B. J. (2007). Ras/ERK1/2-mediated STAT3 Ser727 phosphorylation by familial medullary thyroid carcinoma-associated RET mutants induces full activation of STAT3 and is required for c-fos promoter activation, cell mitogenicity, and transformation. *Journal of Biological Chemistry, 282*(9), 6415-6424.

Plotnikov, A., Zehorai, E., Procaccia, S., & Seger, R. (2011). The MAPK cascades: Signaling components, nuclear roles and mechanisms of nuclear translocation. *Biochimica et Biophysica Acta, 1813*(9), 1619-1633.

Pop, C., & Salvesen, G. S. (2009). Human caspases: Activation, specificity, and regulation. *Journal of Biological Chemistry, 284*(33), 21777-21781.

Pop, C., Timmer, J., Sperandio, S., & Salvesen, G. S. (2006). The apoptosome activates caspase-9 by dimerization. *Molecular Cell, 22*(2), 269-275.

Prieto, F., Egozcue, J., Forteza, G., & Marco, F. (1970). Identification of the philadelphia (Ph-1) chromosome. *Blood, 35*(1), 23-27.

Pruvot, B., Jacquel, A., Droin, N., Auberger, P., Bouscary, D., Tamburini, J., … Solary, E. (2011). Leukemic cell xenograft in zebrafish embryo for investigating drug efficacy. *Haematologica, 96*(4), 612-616.

Pyne, N. J., & Pyne, S. (1997). Platelet-derived growth factor activates a mammalian Ste20 coupled mitogen-activated protein kinase in airway smooth muscle. *Cellular Signalling, 9*(3-4), 311-317.

Qiao, L., Studer, E., Leach, K., McKinstry, R., Gupta, S., Decker, R., … Dent, P. (2001). Deoxycholic acid (DCA) causes ligand-independent activation of epidermal growth factor receptor (EGFR) and FAS receptor in primary hepatocytes: Inhibition of EGFR/mitogen-activated protein kinase-signaling module enhances DCA-induced apoptosis. *Molecular Biology of the Cell, 12*(9), 2629-2645.

Qiu, T., Zhou, L., Wang, T., Xu, J., Wang, J., Chen, W., … Liu, P. (2013). MiR-503 regulates the resistance of non-small cell lung cancer cells to cisplatin by targeting Bcl-2. *International Journal of Molecular Medicine, 32*(3), 593-598.

Rai, K., Takigawa, N., Ito, S., Kashihara, H., Ichihara, E., Yasuda, T., … Kiura, K. (2011). Liposomal delivery of microRNA-7-expressing plasmid overcomes epidermal growth factor receptor tyrosine kinase inhibitor-resistance in lung cancer cells. *Molecular Cancer Therapeutics, 10*(9), 1720-1727.

Rajewsky, N. (2006). MicroRNA target predictions in animals. *Nature Genetics, 38 Suppl*, S8-13.

Raman, M., Chen, W., & Cobb, M. H. (2007). Differential regulation and properties of MAPKs. *Oncogene, 26*(22), 3100-3112.

Ramsay, J. A., From, L., & Kahn, H. J. (1995). Bcl-2 protein expression in melanocytic neoplasms of the skin. *Modern Pathology, 8*(2), 150-154.

Raponi, M., Dossey, L., Jatkoe, T., Wu, X., Chen, G., Fan, H., & Beer, D. G. (2009). MicroRNA classifiers for predicting prognosis of squamous cell lung cancer. *Cancer Research, 69*(14), 5776-5783.

Reed, J. C. (1999). Dysregulation of apoptosis in cancer. *Journal of Clinical Oncology, 17*(9), 2941-2953.

Reed, J. C. (2008). Bcl-2-family proteins and hematologic malignancies: History and future prospects. *Blood, 111*(7), 3322-3330.

Reeve, J. G., Xiong, J., Morgan, J., & Bleehen, N. M. (1996). Expression of apoptosis-regulatory genes in lung tumour cell lines: Relationship to p53 expression and relevance to acquired drug resistance. *British Journal of Cancer, 73*(10), 1193-1200.

Reinhart, B. J., Slack, F. J., Basson, M., Pasquinelli, A. E., Bettinger, J. C., Rougvie, A. E., … Ruvkun, G. (2000). The 21-nucleotide let-7 RNA regulates developmental timing in Caenorhabditis elegans. *Nature, 403*(6772), 901-906.

Rena, G., Guo, S., Cichy, S. C., Unterman, T. G., & Cohen, P. (1999). Phosphorylation of the transcription factor forkhead family member RKHR by protein kinase B. *Journal of Biological Chemistry, 274*(24), 17179-17183.

Reynisdottir, I., Polyak, K., Iavarone, A., & Massague, J. (1995). Kip/Cip and Ink4 Cdk inhibitors cooperate to induce cell cycle arrest in response to TGF-beta. *Genes & Development, 9*(15), 1831-1845.

Richardson, G. E., & Johnson, B. E. (1993). The biology of lung cancer. *Seminars in Oncology, 20*(2), 105-127.

Riely, G. J., Kris, M. G., Rosenbaum, D., Marks, J., Li, A., Chitale, D. A., … Ladanyi, M. (2008). Frequency and distinctive spectrum of KRAS mutations in never smokers with lung adenocarcinoma. *Clinical Cancer Research, 14*(18), 5731-5734.

Rincon, M., & Davis, R. J. (2009). Regulation of the immune response by stress-activated protein kinases. *Immunological Reviews, 228*(1), 212-224.

Ringel, M. D., Hayre, N., Saito, J., Saunier, B., Schuppert, F, Burch, H., … Saji, M. (2001). Overexpression and overactivation of Akt in thyroid carcinoma. *Cancer Research, 61*(16), 6105-6111.

Robles, A. I., Arai, E., Mathe, E. A., Okayama, H., Schetter, A. J., Brown, D., … Harris, C. C. (2015). An integrated prognostic classifier for stage I lung adenocarcinoma based on mRNA, microRNA, and DNA methylation biomarkers. *Journal of Thoracic Oncology, 10*(7), 1037-1048.

Rodenhuis, S., & Slebos, R. J. (1992). Clinical significance of ras oncogene activation in human lung cancer. *Cancer Research, 52*, 2665s-2669s.

Rodriguez, A., Griffiths-Jones, S. Ashurst, J. L., & Bradley, A. (2004). Identification of mammalian microRNA host genes and transcription units. *Genome Research, 14*(10a), 1902-1910.

Romano, G., Acunzo, M., Garofalo, M., Di Leva, G., Cascione, L., Zanca, C., … Croce, C. M. (2012). MiR-494 is regulated by ERK1/2 and modulates trail-induced apoptosis in non-small-cell lung cancer through Bim down-regulation. *Proceedings of the National Academy of Sciences USA, 109*(41), 16570-16575.

Romashkova, J. A., & Makarov, S. S. (1999). NF-kappa B is a target of AKT in anti-apoptotic PDGF signalling. *Nature, 401*(6748), 86-90.

Roos, W. P., & Kaina, B. (2006). DNA damage-induced cell death by apoptosis. *Trends in Molecular Medicine, 12*(9), 440-450.

Roose, J., & Clevers, H. (1999). TCF transcription factors: Molecular switches in carcinogenesis. *Biochimica et Biophysica Acta, 1424*(2-3), M23-37.

Rousseau, S., Houle, F., Landry, J., & Huot, J. (1997). P38 MAP kinase activation by vascular endothelial growth factor mediates actin reorganization and cell migration in human endothelial cells. *Oncogene, 15*(18), 2169-2177.

Ruan, K., Fang, X., & Ouyang, G. (2009). MicroRNAs: Novel regulators in the hallmarks of human cancer. *Cancer Letters, 285*(2), 116-126.

Ruano-Ravina, A., Figueiras, A., & Barros-Dios, J. M. (2003). Lung cancer and related risk factors: An update of the literature. *Public Health, 117*(3), 149-156.

Rubinfeld, B., Robbins, P., El-Gamil, M., Albert, I., Porfiri, E., & Polakis, P. (1997). Stabilization of beta-catenin by genetic defects in melanoma cell lines. *Science, 275*(5307), 1790-1792.

Ryan, B. M., McClary, A. C., Valeri, N., Robinson, D., Paone, A., Bowman, E. D., … Harris, C. C. (2012). Rs4919510 in hsa-miR-608 is associated with outcome but not risk of colorectal cancer. *PLoS One, 7*(5), e36306.

Saelens, X., Festjens, N., Vande Walle, L., van Gurp, M., van Loo, G., & Vandenabeele, P. (2004). Toxic proteins released from mitochondria in cell death. *Oncogene, 23*(16), 2861-2874.

Sakanaka, C., Weiss, J. B., & Williams, L. T. (1998). Bridging of beta-catenin and glycogen synthase kinase-3beta by axin and inhibition of beta-catenin-mediated transcription. *Proceedings of the National Academy of Sciences USA, 95*(6), 3020-3023.

Samanta, D., & Datta, P. K. (2012). Alterations in the Smad pathway in human cancers. *Frontiers in Bioscience, 17*, 1281-1293.

Samet, J. M., Avila-Tang, E., Boffetta, P., Hannan, L. M., Olivo-Marston, S., Thun, M. J., & Rudin, C. M. (2009). Lung cancer in never smokers: Clinical epidemiology and environmental risk factors. *Clinical Cancer Research, 15*(18), 5626-5645.

Samuels, Y., Wang, Z., Bardelli, A., Silliman, N., Ptak, J., Szabo, S., … Velculescu, V. E. (2004). High frequency of mutations of the PIK3CA gene in human cancers. *Science, 304*(5670), 554.

Sanchez-Ceja, S. G., Reyes-Maldonado, E., Vazquez-Manriquez, M. E, Lopez-Luna, J. J, Belmont, A., & Gutierrez-Castellanos, S. (2006). Differential expression of STAT5 and Bcl-xL, and high expression of Neu and STAT3 in non-small-cell lung carcinoma. *Lung Cancer, 54*(2), 163-168.

Sandler, A. B., Gray, R., Brahmer, J., Dowlati, A., Schiller, J. H., Perry, M. C., & Johnson, D. H. (2005). Randomized phase II/III trial of paclitaxel (P) plus carboplatin (C) with or without bevacizumab (NSC #704865) in patients with advanced non-squamous non-small cell lung cancer (NSCLC): An Eastern Cooperative Oncology Group (ECOG) Trial - e4599. *Journal of Clinical Oncology, 23*, LBA4-LBA4.

Sandoval, J., Diaz-Lagares, A., Salgado, R., Servitje, O., Climent, F., Ortiz-Romero, P. L., … Gallardo, F. (2015). MicroRNA expression profiling and DNA methylation signature for deregulated microRNA in cutaneous T-cell lymphoma. *Journal of Investigative Dermatology, 135*(4), 1128-1137.

Santi, S. A., & Lee, H. (2011). Ablation of Akt2 induces autophagy through cell cycle arrest, the downregulation of p70S6K, and the deregulation of mitochondria in MDA-MB231 cells. *PLoS One, 6*(1), e14614.

Scaffidi, C., Fulda, S., Srinivasan, A., Friesen, C., Li, F., Tomaselli, K. J., … Peter, M. E. (1998). Two CD95 (APO-1/Fas) signaling pathways. *The EMBO Journal, 17*(6), 1675-1687.

Schaeffer, H. J., & Weber, M. J.. (1999). Mitogen-activated protein kinases: Specific messages from ubiquitous messengers. *Molecular and Cellular Biology, 19*(4), 2435-2444.

Schmid, K., Oehl, N., Wrba, F., Pirker, R., Pirker, C., & Filipits, M. (2009). EGFR/KRAS/BRAF mutations in primary lung adenocarcinomas and corresponding locoregional lymph node metastases. *Clinical Cancer Research, 15*(14), 4554-4560.

Schuster, N., & Krieglstein, K. (2002). Mechanisms of TGF-beta-mediated apoptosis. *Cell and Tissue Research, 307*(1), 1-14.

Schwarz, D. S., Hutvagner, G., Du, T., Xu, Z., Aronin, N., & Zamore, P. D. (2003). Asymmetry in the assembly of the RNAi enzyme complex. *Cell, 115*(2), 199-208.

Scisciani, C., Vossio, S., Guerrieri, F., Schinzari, V., De Iaco, R., D'Onorio de Meo, P., … Pediconi, N. (2012). Transcriptional regulation of miR-224 upregulated in human hHCCs by NFκB inflammatory pathways. *Journal of Hepatology, 56*(4), 855-861.

Sebolt-Leopold, J. S., Dudley, D.T., Herrera, R., Van Becelaere, K., Wiland, A., Gowan, R. C., … Saltiel, A. R. (1999). Blockade of the MAP kinase pathway suppresses growth of colon tumors *in vivo. Nature Medicine, 5*(7), 810-816.

Sellers, T. A., & Yang, P. (2002). Familial and genetic influences on risk of lung cancer. In R. King, J. I. Rotter, & A. G. Motulsky (Eds.), *The genetic basis of common diseases,* (Vol. 2, pp. 700-712). New York, NY. Oxford University Press.

Sevilla, L., Zaldumbide, A., Pognonec, P., & Boulukos, K. E. (2001). Transcriptional regulation of the Bcl-X gene encoding the anti-apoptotic Bcl-xLprotein by Ets, Rel/NFkappaB, STAT and AP1 transcription factor families. *Histology and Histopathology, 16*(2), 595-601.

She, Q. B., Ma, W. Y., Zhong, S., & Dong, Z. (2002). Activation of JNK1, RSK2, and MSK1 is involved in serine 112 phosphorylation of Bad by ultraviolet B radiation. *Journal of Biological Chemistry, 277*(27), 24039-24048.

She, X., Yu, Z., Cui, Y., Lei, Q., Wang, Z., Xu, G., … Wu, M. (2014). MiR-181 subunits enhance the chemosensitivity of temozolomide by Rap1B-mediated cytoskeleton remodeling in glioblastoma cells. *Medical Oncology, 31*(4), 892.

Shen, H. W., Gao, S. L., Wu, Y. L., & Peng, S. Y. (2005). Overexpression of decoy receptor 3 in hepatocellular carcinoma and its association with resistance to Fas ligand-mediated apoptosis. *World Journal of Gastroenterology, 11*(38), 5926-5930.

Shepherd, F. A., Pereira, J., Ciuleanu, T. E., Tan, E. H., Hirsh, V., Thongprasert, S., … Seymour, L. (2004). A randomized placebo-controlled trial of erlotinib in patients with advanced non-small cell lung cancer (NSCLC) following failure of 1st line or 2nd line chemotherapy. A National Cancer Institute of Canada Clinical Trials Group (NCIC CTG) Trial. *Journal of Clinical Oncology, 22*, 7022-7022.

Sherr, C. J., & Roberts, J. M. (1999). CDK inhibitors: Positive and negative regulators of G1-phase progression. *Genes & Development, 13*(12), 1501-1512.

Sheth, U., & Parker, R. (2003). Decapping and decay of messenger RNA occur in cytoplasmic processing bodies. *Science, 300*(5620), 805-808.

Shi, Y., & Massagué, J. (2003). Mechanisms of TGF-beta signaling from cell membrane to the nucleus. *Cell, 113*(6), 685-700.

Shigematsu, H., Lin, L., Takahashi, T., Nomura, M., Suzuki, M., Wistuba, I. I., … Gazdar, A. F. (2005). Clinical and biological features associated with epidermal growth factor receptor gene mutations in lung cancers. *Journal of the National Cancer Institute, 97*(5), 339-346.

Shin, K. H., Bae, S. D., Hong, H. S., Kim, R. H., Kang, M. K., & Park, N. H. (2011). MiR-181a shows tumor suppressive effect against oral squamous cell carcinoma cells by downregulating K-ras. *Biochemical and Biophysical Research Communications, 404*(4), 896-902.

Shivdasani, R. A. (2006). MicroRNAs: Regulators of gene expression and cell differentiation. *Blood, 108*(12), 3646-3653.

Shive, H. R. (2013). Zebrafish models for human cancer. *Veterinary Pathology, 50*(3), 468-482.

Shonai, T., Adachi, M., Sakata, K., Takekawa, M., Endo, T., Imai, K., & Hareyama, M. (2002). MEK/ERK pathway protects ionizing radiation-induced loss of mitochondrial membrane potential and cell death in lymphocytic leukemia cells. *Cell Death & Differentiation, 9*(9), 963-971.

Shopland, D. R. (1995). Tobacco use and its contribution to early cancer mortality with a special emphasis on cigarette smoking. *Environmental Health Perspectives, 103*(Suppl 8), 131-142.

Shuai, K., Halpern, J., ten Hoeve, J., Rao, X., & Sawyers, C. L. (1996). Constitutive activation of STAT5 by the BCR-ABL oncogene in chronic myelogenous leukemia. *Oncogene, 13*(2), 247-254.

Simonian, P. L., Grillot, D. A., & Nunez, G. (1997). Bcl-2 and Bcl-XL can differentially block chemotherapy-induced cell death. *Blood, 90*(3), 1208-1216.

Singh, N. (2007). Apoptosis in health and disease and modulation of apoptosis for therapy: An overview. *Indian Journal of Clinical Biochemistry, 22*(2), 6-16.

Skorski, T., Bellacosa, A., Nieborowska-Skorska, M., Majewski, M., Martinez, R., Choi, J. K., … Calabretta, B. (1997). Transformation of hematopoietic cells by BCR/ABL requires activation of a PI-3k/Akt-dependent pathway. *The EMBO Journal, 16*(20), 6151-6161.

Slebos, R. J., Kibbelaar, R. E., Dalesio, O., Kooistra, A., Stam, J., Meijer, C. J., … Mooi, W. J. (1990). K-ras oncogene activation as a prognostic marker in adenocarcinoma of the lung. *New England Journal of Medicine, 323*(9), 561-565.

Soini, Y., Kinnula, V., Kaarteenaho-Wiik, R., Kurttila, E., Linnainmaa, K., & Paakko, P. (1999). Apoptosis and expression of apoptosis regulating proteins bcl-2, mcl-1, bcl-x, and bax in malignant mesothelioma. *Clinical Cancer Research, 5*(11), 3508-3515.

Son, J. W., Kim, Y. J., Cho, H. M., Lee, S. O., Jang, J. S., Choi, J. E., ... Park, J. Y. (2009). MicroRNA expression profiles in Korean non-small cell lung cancer. *Tuberculosis and Respiratory Diseases, 67*, 413-421.

Sordella, R., Bell, D. W., Haber, D. A., & Settleman, J. (2004). Gefitinib-sensitizing EGFR mutations in lung cancer activate anti-apoptotic pathways. *Science, 305*(5687), 1163-1167.

Sorenson, C. M. (2004). Bcl-2 family members and disease. *Biochimica et Biophysica Acta, 1644*(2-3), 169-177.

Soung, Y. H., Lee, J. W., Kim, S. Y., Wang, Y. P., Jo, K. H., Moon, S. W., … Lee, S. H. (2006). Somatic mutations of the ERBB4 kinase domain in human cancers. *International Journal of Cancer, 118*(6), 1426-1429.

Staal, S. P. (1987). Molecular cloning of the akt oncogene and its human homologues ATK1 and AKT2: Amplification of AKT1 in a primary human gastric adenocarcinoma. *Proceedings of the National Academy of Sciences USA, 84*(14), 5034-5037.

Stoletov, K., & Klemke, R. (2008). Catch of the day: Zebrafish as a human cancer model. *Oncogene, 27*(33), 4509-4520.

Strasser, A., Jost, P. J., & Nagata, S. (2009). The many roles of Fas receptor signaling in the immune system. *Immunity, 30*(2), 180-192.

Su, L. K., Vogelstein, B., & Kinzler, K. W. (1993). Association of the APC tumor suppressor protein with catenins. *Science, 262*(5140), 1734-1737.

Sun, J. J., Chen, G. Y., & Xie, Z. T. (2016). MicroRNA-361-5p inhibits cancer cell growth by targeting CXCR6 in hepatocellular carcinoma. *Cellular Physiology and Biochemistry, 38*(2), 777-785.

Sun, S., Schiller, J. H., & Gazdar, A. F. (2007). Lung cancer in never smokers - A different disease. *Nature Reviews Cancer, 7*(10), 778-790.

Suzuki, Y., Kim, H. W., Ashraf, M., & Haider, H. (2010). Diazoxide potentiates mesenchymal stem cell survival via NF-kappaB-dependent miR-146a expression by targeting Fas. *American Journal of Physiology - Heart and Circulatory Physiology, 299*(4), H1077-1082.

Tachibana, I., Imoto, M., Adjei, P. N., Gores, G. J., Subramaniam, M., Spelsberg, T. C., & Urrutia, R. (1997). Overexpression of the TGFbeta-regulated zinc finger encoding gene, TIEG, induces apoptosis in pancreatic epithelial cells. *Journal of Clinical Investigation, 99*(10), 2365-2374.

Takahashi, T., Nau, M. M., Chiba, I., Birrer, M. J., Rosenberg, R. K., Vinocour, M., … Minna, J. D. (1989). P53: A frequent target for genetic abnormalities in lung cancer. *Science, 246*(4929), 491-494.

Takamizawa, J., Konishi, H., Yanagisawa, K., Tomida, S., Osada, H., Endoh, H., … Takahashi, T. (2004). Reduced expression of the let-7 microRNAs in human lung cancers in association with shortened postoperative survival. *Cancer Research, 64*(11), 3753-3756.

Takeyama, Y., Sato, M., Horio, M., Hase, T., Yoshida, K., Yokoyama, T., … Hasegawa, Y. (2010). Knockdown of ZEB1, a master epithelial-to-mesenchymal transition (EMT) gene, suppresses anchorage-independent cell growth of lung cancer cells. *Cancer Letters, 296*(2), 216-224.

Tam, I. Y., Chung, L. P., Suen, W. S., Wang, E., Wong, M. C., Ho, K. K., … Wong, M. P. (2006). Distinct epidermal growth factor receptor and KRAS mutation patterns in non-small cell lung cancer patients with different tobacco exposure and clinicopathologic features. *Clinical Cancer Research, 12*(5), 1647-1653.

Tang, E. D., Nunez, G., Barr, F. G., & Guan, K. L. (1999). Negative regulation of the forkhead transcription factor FKHR by Akt. *Journal of Biological Chemistry, 274*(24), 16741-16746.

Tang, L., Tron, V. A., Reed, J. C., Mah, K. J., Krajewska, M., Li, G., … Trotter, M. J. (1998). Expression of apoptosis regulators in cutaneous malignant melanoma. *Clinical Cancer Research, 4*(8), 1865-1871.

Tang, R. X., Kong, F. Y., Fan, B. F., Liu, X. M., You, H. J., Zhang, P., & Zheng, K. Y. (2012). HBx activates FasL and mediates HepG2 cell apoptosis through MLK3-MKK7-JNKS signal module. *World Journal of Gastroenterology 18*(13), 1485-1495.

Tapia, J. C., Torres, V. A., Rodriguez, D. A., Leyton, L., & Quest, A. F. (2006). Casein kinase 2 (CK2) increases survivin expression via enhanced β-catenin-T cell factor/lymphoid enhancer binding factor-dependent transcription. *Proceedings of the National Academy of Sciences USA, 103*(41), 15079-15084.

Taylor, M. A., & Schiemann, W. P. (2014). Therapeutic opportunities for targeting microRNAs in cancer. *Molecular and Cellular Therapies, 2*(1), 30-43.

Tennis, M., Van Scoyk, M., & Winn, R. A. (2007). Role of the WNT signaling pathway and lung cancer. *Journal of Thoracic Oncology, 2*(10), 889-892.

Testa, J. R., & Bellacosa, A. (2001). Akt plays a central role in tumorigenesis. *Proceedings of the National Academy of Sciences USA, 98*(20), 10983-10985.

Thatcher, N., Chang, A., Parikh, P., Rodrigues Pereira, J., Ciuleanu, T., von Pawel, J., … Carroll, K. (2005). Gefitinib plus best supportive care in previously treated patients with refractory advanced non-small-cell lung cancer: Results from a randomised, placebo-controlled, multicentre study (Iressa survival evaluation in lung cancer). *Lancet, 366*(9496), 1527-1537.

Thomson, J. M., Newman, M., Parker, J. S., Morin-Kensicki, E. M., Wright, T., & Hammond, S. M. (2006). Extensive post-transcriptional regulation of microRNAs and its implications for cancer. *Genes & Development, 20*(16), 2202-2207.

Thornberry, N. A., & Lazebnik, Y. (1998). Caspases: Enemies within. *Science, 281*(5381), 1312-1316.

Thornton, T. M., & Rincon, M. (2009). Non-classical p38 MAP kinase functions: Cell cycle checkpoints and survival. *International Journal of Biological Sciences, 5*(1), 44-52.

Thorsen, S. B., Obad, S., Jensen, N. F., Stenvang, J., & Kauppinen, S. (2012). The therapeutic potential of microRNAs in cancer. *The Cancer Journal, 18*(3), 275-284.

Torii, S., Yamamoto, T., Tsuchiya, Y., & Nishida, E. (2006). ERK MAP kinase in G cell cycle progression and cancer. *Cancer Science, 97*(8), 697-702.

Toyota, M., Suzuki, H., Sasaki, Y., Maruyama, R., Imai, K., Shinomura, Y., … Tokino, T. (2008). Epigenetic silencing of microRNA-34b/c and B-cell translocation gene 4 is associated with CpG island methylation in colorectal cancer. *Cancer Research, 68*(11), 4123-4132.

Tran, S. E., Holmstrom, T. H., Ahonen, M., Kahari, V. M., & Eriksson, J. E. (2001). MAPK/ERK overrides the apoptotic signaling from Fas, TNF, and TRAIL receptors. *Journal of Biological Chemistry, 276*(19), 16484-16490.

Tran, T. N., Selinger, C. I., Kohonen-Corish, M. R., McCaughan, B. C., Kennedy, C. W., O'Toole, S. A., & Cooper, W. A. (2013). Fibroblast growth factor receptor 1 (FGFR1) copy number is an independent prognostic factor in non-small cell lung cancer. *Lung Cancer, 81*(3), 462-467.

Trang, P., Medina, P. P., Wiggins, J. F., Ruffino, L., Kelnar, K., Omotola, M., … Slack, F. J. (2010). Regression of murine lung tumors by the let-7 microRNA. *Oncogene, 29*(11), 1580-1587.

Trang, P., Wiggins, J. F., Daige, C. L., Cho, C., Omotola, M., Brown, D., … Slack, F. J. (2011). Systemic delivery of tumor suppressor microRNA mimics using a neutral lipid emulsion inhibits lung tumors in mice. *Molecular Therapy, 19*(6), 1116-1122.

Tsujimoto, Y., Finger, L. R., Yunis, J., Nowell, P. C., & Croce, C. M. (1984). Cloning of the chromosome breakpoint of neoplastic B cells with the t(14;18) chromosome translocation. *Science, 226*(4678), 1097-1099.

Turjanski, A. G., Vaque, J. P., & Gutkind, J. S. (2007). MAP kinases and the control of nuclear events. *Oncogene, 26*(22), 3240-3253.

Uematsu, K., He, B., You, L., Xu, Z., McCormick, F., & Jablons, D. M. (2003). Activation of the WNT pathway in non small cell lung cancer: Evidence of dishevelled overexpression. *Oncogene, 22*(46), 7218-7221.

Valencia-Sanchez, M. A., Liu, J., Hannon, G. J., & Parker, R. (2006). Control of translation and mRNA degradation by miRNAs and siRNAs. *Genes & Development, 20*(5), 515-524.

van Engeland, M., Nieland, L. J., Ramaekers, F. C., Schutte, B., & Reutelingsperger, C. P. (1998). Annexin V-affinity assay: A review on an apoptosis detection system based on phosphatidylserine exposure. *Cytometry, 31*(1), 1-9.

van Rooij, E., & Kauppinen, S. (2014). Development of microRNA therapeutics is coming of age. *EMBO Molecular Medicine, 6*(7), 851-864.

Van Scoyk, M., Randall, J., Sergew, A., Williams, L. M., Tennis, M., & Winn, R. A. (2008). WNT signaling pathway and lung disease. *Translational Research, 151*(4), 175-180.

Van Themsche, C, Chaudhry, P, Leblanc, V, Parent, S, & Asselin, E. (2010). XIAP gene expression and function is regulated by autocrine and paracrine TGF-beta signaling. *Molecular Cancer, 9*, 216-228.

Veinotte, C. J., Dellaire, G., & Berman, J. N. (2014). Hooking the big one: The potential of zebrafish xenotransplantation to reform cancer drug screening in the genomic era. *Disease Models & Mechanisms, 7*(7), 745-754.

Venditti, A., Del Poeta, G., Maurillo, L., Buccisano, F., Del Principe, M. I., Mazzone, C., … Amadori, S. (2004). Combined analysis of bcl-2 and MDR1 proteins in 256 cases of acute myeloid leukemia. *Haematologica, 89*(8), 934-939.

Vicent, S., Garayoa, M., Lopez-Picazo, J. M., Lozano, M. D., Toledo, G., Thunnissen, F. B., … Montuenga, L. M. (2004). Mitogen-activated protein kinase phosphatase-1 is overexpressed in non-small cell lung cancer and is an independent predictor of outcome in patients. *Clinical Cancer Research, 10*(11), 3639-3649.

Vivanco, I., & Sawyers, C. L. (2002). The phosphatidylinositol 3-kinase Akt pathway in human cancer. *Nature Reviews Cancer, 2*(7), 489-501.

Volinia, S., Calin, G. A., Liu, C. G., Ambs, S., Cimmino, A., Petrocca, F., … Croce, C. M. (2006). A microRNA expression signature of human solid tumors defines cancer gene targets. *Proceedings of the National Academy of Sciences USA, 103*(7), 2257-2261.

Wang, H., Jiang, J. Y., Zhu, C., Peng, C., & Tsang, B. K. (2006). Role and regulation of nodal/activin receptor-like kinase 7 signaling pathway in the control of ovarian follicular atresia. *Molecular Endocrinology, 20*(10), 2469-2482.

Wang, H., Li, M., Zhang, R., Wang, Y., Zang, W., Ma, Y., … Zhang, G. (2013a). Effect of miR-335 upregulation on the apoptosis and invasion of lung cancer cell A549 and H1299. *Tumor Biology, 34*(5), 3101-3109.

Wang, Y., Gu, J., Roth, J. A., Hildebrandt, M. A., Lippman, S. M., Ye, Y., … Wu, X. (2013b). Pathway-based serum microRNA profiling and survival in patients with advanced stage non-small cell lung cancer. *Cancer Research, 73*(15), 4801-4809.

Wang, Y., & Lee, C. G. (2009). MicroRNA and cancer - Focus on apoptosis. *Journal of Cellular and Molecular Medicine, 13*(1), 12-23.

Wang, Z., Xue, Y., Wang, P., Zhu, J., & Ma, J. (2016). MiR-608 inhibits the migration and invasion of glioma stem cells by targeting macrophage migration inhibitory factor. *Oncology Reports, 35*(5), 2733-2742.

Warner, B. J., Blain, S. W., Seoane, J., & Massague, J. (1999). Myc downregulation by transforming growth factor beta required for activation of the p15(Ink4b) G(1) arrest pathway. *Molecular and Cellular Biology, 19*(9), 5913-5922.

Weber, B., Stresemann, C., Brueckner, B., & Lyko, F. (2007). Methylation of human microRNA genes in normal and neoplastic cells. *Cell Cycle, 6*(9), 1001-1005.

Wei, Q., Zhao, Y., Yang, Z. Q., Dong, Q. Z., Dong, X. J., Han, Y., … Wang, E. H. (2008). Dishevelled family proteins are expressed in non-small cell lung cancer and function differentially on tumor progression. *Lung Cancer, 62*(2), 181-192.

Wei, Z., Cui, L., Mei, Z., Liu, M., & Zhang, D. (2014). MiR-181a mediates metabolic shift in colon cancer cells via the PTEN/AKT pathway. *FEBS Letters, 588*(9), 1773-1779.

Weintraub, S. J., Chow, K. N., Luo, R. X., Zhang, S. H., He, S., & Dean, D. C. (1995). Mechanism of active transcriptional repression by the retinoblastoma protein. *Nature, 375*(6534), 812-815.

West, K. A. (2003). Rapid Akt activation by nicotine and a tobacco carcinogen modulates the phenotype of normal human airway epithelial cells. *Journal of Clinical Investigation, 111*(1), 81-90.

Westwick, J. K., Weitzel, C., Minden, A., Karin, M., & Brenner, D. A. (1994). Tumor necrosis factor alpha stimulates AP-1 activity through prolonged activation of the c-Jun kinase. *Journal of Biological Chemistry, 269*(42), 26396-26401.

Whittaker, J. R. (1966). An analysis of melanogenesis in differentiating pigment cells of ascidian embryos. *Developmental Biology, 14*(1), 1-39.

Widelitz, R. (2005). WNT signaling through canonical and non-canonical pathways: Recent progress. *Growth Factors, 23*(2), 111-116.

Wiemer, E. A. (2007). The role of microRNAs in cancer: No small matter. *European Journal of Cancer, 43*(10), 1529-1544.

Wiggins, J. F., Ruffino, L., Kelnar, K., Omotola, M., Patrawala, L., Brown, D., & Bader, A. G. (2010). Development of a lung cancer therapeutic based on the tumor suppressor microRNA-34. *Cancer Research, 70*(14), 5923-5930.

Wightman, B., Ha, I., & Ruvkun, G. (1993). Posttranscriptional regulation of the heterochronic gene lin-14 by lin-4 mediates temporal pattern formation in C. Elegans. *Cell, 75*(5), 855-862.

Wikman, H., & Kettunen, E. (2006). Regulation of the G1/S phase of the cell cycle and alterations in the Rb pathway in human lung cancer. *Expert Review of Anticancer Therapy, 6*(4), 515-530.

Willett, C. E., Cortes, A., Zuasti, A., & Zapata, A. G. (1999). Early hematopoiesis and developing lymphoid organs in the zebrafish. *Developmental Dynamics, 214*(4), 323-336.

Winston, J. T., Strack, P., Beer-Romero, P., Chu, C. Y., Elledge, S. J., & Harper, J. W. (1999). The $SCF^{\beta\text{-}TRCP}$–ubiquitin ligase complex associates specifically with phosphorylated destruction motifs in Iκbα and β-catenin and stimulates Iκbα ubiquitination *in vitro. Genes & Development, 13*(3), 270-283.

Wu, J., Sun, J., Gu, J., Liu, G., & Huizhu, S. (2016). MicroRNA-608 inhibits the cell proliferation in osteosarcoma by macrophage migration inhibitory factor. *International Journal of Clinical and Experimental Pathology, 9*(9), 9166-9174.

Wu, X., & Deng, Y. (2002). Bax and BH3-domain-only proteins in p53-mediated apoptosis. *Frontiers in Bioscience, 7*, 151-156.

Wu, X., Xi, X., Yan, Q., Zhang, Z., Cai, B., Lu, W., & Wan, X. (2013a). MicroRNA-361-5p facilitates cervical cancer progression through mediation of epithelial-to-mesenchymal transition. *Medical Oncology, 30*(4), 751-763.

Wu, Y., Crawford, M., Mao, Y., Lee, R. J., Davis, I. C., Elton, T. S., … Nana-Sinkam, S. P. (2013b). Therapeutic delivery of microRNA-29b by cationic lipoplexes for lung cancer. *Molecular Therapy Nucleic Acids, 2*, e84.

Wu, Y., Li, Q., Zhou, X., Yu, J., Mu, Y., Munker, S., … Weng, H. (2012). Decreased levels of active Smad2 correlate with poor prognosis in gastric cancer. *PLoS One, 7*(4), e35684.

Xiang, Z., Dong, X., Sun, Q., Li, X., & Yan, B. (2014). Clinical significance of up-regulated miR-181a in prognosis and progression of esophageal cancer. *Acta Biochimica et Biophysica Sinica (Shanghai), 46*(11), 1007-1010.

Xie, H., Lee, L., Caramuta, S., Hoog, A., Browaldh, N., Bjornhagen, V., … Lui, W. O. (2014). MicroRNA expression patterns related to merkel cell polyomavirus infection in human merkel cell carcinoma. *Journal of Investigative Dermatology, 134*(2), 507-517.

Xiong, S., Zheng, Y., Jiang, P., Liu, R., Liu, X., & Chu, Y. (2011). MicroRNA-7 inhibits the growth of human non-small cell lung cancer A549 cells through targeting Bcl-2. *International Journal of Biological Sciences, 7*(6), 805-814.

Xu, C. Z., Shi, R. J., Chen, D., Sun, Y. Y., Wu, Q. W., Wang, T., & Wang, P. H. (2013). Potential biomarkers for paclitaxel sensitivity in hypopharynx cancer cell. *International Journal of Clinical and Experimental Pathology, 6*(12), 2745-2756.

Xu, F., Zhou, D., Meng, X., Wang, X., Liu, C., Huang, C., … Zhang, L. (2016). Smad2 increases the apoptosis of activated human hepatic stellate cells induced by TRAIL. *International Immunopharmacology, 32*, 76-86.

Xu, G., Zhou, H., Wang, Q., Auersperg, N., & Peng, C. (2006). Activin receptor-like kinase 7 induces apoptosis through up-regulation of Bax and down-regulation of XIAP in normal and malignant ovarian epithelial cell lines. *Molecular Cancer Research, 4*(4), 235-246.

Xu, H. T., Wei, Q., Liu, Y., Yang, L. H., Dai, S. D., Han, Y., … Wang, E. H. (2007). Overexpression of axin downregulates TCF-4 and inhibits the development of lung cancer. *Annals of Surgical Oncology, 14*(11), 3251-3259.

Yamamoto, H., Shigematsu, H., Nomura, M., Lockwood, W. W., Sato, M., Okumura, N., … Gazdar, A. F. (2008). PIK3CA mutations and copy number gains in human lung cancers. *Cancer Research, 68*(17), 6913-6921.

Yanaihara, N., Caplen, N., Bowman, E., Seike, M., Kumamoto, K., Yi, M., … Harris, C. C. (2006). Unique microRNA molecular profiles in lung cancer diagnosis and prognosis. *Cancer Cell, 9*(3), 189-198.

Yang, B. S., Hauser, C. A., Henkel, G., Colman, M. S., Van Beveren, C., Stacey, K. J., … Ostrowski, M. C. (1996). Ras-mediated phosphorylation of a conserved threonine residue enhances the transactivation activities of c-Ets1 and c-Ets2. *Molecular and Cellular Biology, 16*(2), 538-547.

Yang, H., Li, Q., Niu, J., Li, B., Jiang, D., Wan, Z., … Bai, S. (2016). MicroRNA-342-5p and miR-608 inhibit colon cancer tumorigenesis by targeting NAA10. *Oncotarget, 7*(3), 2709-2720.

Yang, J., Song, K., Krebs, T. L., Jackson, M. W., & Danielpour, D. (2008). Rb/E2F4 and Smad2/3 link survivin to TGF-beta-induced apoptosis and tumor progression. *Oncogene, 27*(40), 5326-5338.

Yang, J., Wahdan-Alaswad, R., & Danielpour, D. (2009). Critical role of Smad2 in tumor suppression and transforming growth factor-beta–induced apoptosis of prostate epithelial cells. *Cancer Research, 69*(6), 2185-2190.

Yang, L., Cao, Z., Yan, H., & Wood, W. C. (2003). Coexistence of high levels of apoptotic signaling and inhibitor of apoptosis proteins in human tumor cells: Implication for cancer specific therapy. *Cancer Research, 63*(20), 6815-6824.

Yang, P. W., Huang, Y. C,. Hsieh, C. Y., Hua, K. T., Huang, Y. T., Chiang, T. H., … Lee, J. M. (2014). Association of miRNA-related genetic polymorphisms and prognosis in patients with esophageal squamous cell carcinoma. *Annals of Surgical Oncology, 21*, S601-609.

Yang, X., Zheng, F., Xing, H., Gao, Q., Wei, W., Lu, Y., … Ma, D. (2004). Resistance to chemotherapy-induced apoptosis via decreased caspase-3 activity and overexpression of antiapoptotic proteins in ovarian cancer. *Journal of Cancer Research and Clinical Oncology, 130*(7), 423-428.

Yang, X. J., Cui, W., Gu, A., Xu, C., Yu, S. C., Li, T. T., … Bian, X. W. (2013). A novel zebrafish xenotransplantation model for study of glioma stem cell invasion. *PLoS One, 8*(4), e61801.

Yarden, Y., & Sliwkowski, M. X. (2001). Untangling the ErbB signalling network. *Nature Reviews Molecular Cell Biology, 2*(2), 127-137.

Yekta, S., Shih, I. H., & Bartel, D. P. (2004). MicroRNA-directed cleavage of HOXB8 mRNA. *Science, 304*(5670), 594-596.

Yu, L., Todd, N. W., Xing, L., Xie, Y., Zhang, H., Liu, Z., … Jiang, F. (2010). Early detection of lung adenocarcinoma in sputum by a panel of microRNA markers. *International Journal of Cancer, 127*(12), 2870-2878.

Yu, S. L., Chen, H. Y., Chang, G. C., Chen, C. Y., Chen, H. W., Singh, S., … Yang, P. C. (2008). MicroRNA signature predicts survival and relapse in lung cancer. *Cancer Cell, 13*(1), 48-57.

Yuan, Z. Q., Sun, M., Feldman, R. I., Wang, G., Ma, X., Jiang, C., … Cheng, J. Q. (2000). Frequent activation of AKT2 and induction of apoptosis by inhibition of phosphoinositide-3-OH kinase/Akt pathway in human ovarian cancer. *Oncogene, 19*(19), 2324-2330.

Zamore, P. D., & Haley, B. (2005). Ribo-gnome: The big world of small RNAs. *Science, 309*(5740), 1519-1524.

Zang, Y. S., Zhong, Y. F., Fang, Z., Li, B., & An, J. (2012). MiR-155 inhibits the sensitivity of lung cancer cells to cisplatin via negative regulation of Apaf-1 expression. *Cancer Gene Therapy, 19*(11), 773-778.

Zha, J., Harada, H., Yang, E., Jockel, J., & Korsmeyer, S. J. (1996). Serine phosphorylation of death agonist BAD in response to survival factor results in binding to 14-3-3 not BCL-X(L). *Cell, 87*(4), 619-628.

Zhang, B., Pan, X., Cobb, G. P., & Anderson, T. A. (2007). MicroRNAs as oncogenes and tumor suppressors. *Developmental Biology, 302*(1), 1-12.

Zhang, C., Zhang, J., Zhang, A., Wang, Y., Han, L., You, Y., … Kang, C. (2010a). Puma is a novel target of miR-221/222 in human epithelial cancers. *International Journal of Oncology, 37*(6), 1621-1626.

Zhang, J. G., Wang, J. J., Zhao, F., Liu, Q., Jiang, K., & Yang, G. H. (2010b). MicroRNA-21 (miR-21) represses tumor suppressor PTEN and promotes growth and invasion in non-small cell lung cancer (NSCLC). *Clinica Chimica Acta, 411*(11-12), 846-852.

Zhang, K., Jiao, K., Xing, Z., Zhang, L., Yang, J., Xie, X., & Yang, L. (2014a). Bcl-xL overexpression and its association with the progress of tongue carcinoma. *International Journal of Clinical and Experimental Pathology, 7*(11), 7360-7377.

Zhang, X., Liu, S., Hu, T., Liu, S., He, Y., & Sun, S. (2009). Up-regulated microRNA-143 transcribed by nuclear factor kappa B enhances hepatocarcinoma metastasis by repressing fibronectin expression. *Hepatology, 50*(2), 490-499.

Zhang, Y., Schiff, D., Park, D., & Abounader, R. (2014b). MicroRNA-608 and microRNA-34a regulate chordoma malignancy by targeting EGFR, Bcl-xL and MET. *PLoS One, 9*(3), e91546.

Zhang, Y. L., Pang, L. Q., Wu, Y., Wang, X. Y., Wang, C. Q., & Fan, Y. (2008). Significance of Bcl-xL in human colon carcinoma. *World Journal of Gastroenterology, 14*(19), 3069-3073.

Zhang, Z. Z., Liu, X., Wang, D. Q., Teng, M. K., Niu, L. W., Huang, A. L., & Liang, Z. (2011). Hepatitis B virus and hepatocellular carcinoma at the miRNA level. *World Journal of Gastroenterology, 17*(28), 3353-3358.

Zhao, C., Wang, X., Zhao, Y., Li, Z., Lin, S., Wei, Y., & Yang, H. (2011). A novel xenograft model in zebrafish for high-resolution investigating dynamics of neovascularization in tumors. *PLoS One, 6*(7), e21768.

Zheng, J., Deng, J., Xiao, M., Yang, L., Zhang, L., You, Y., … Tong, Q. (2013). A sequence polymorphism in miR-608 predicts recurrence after radiotherapy for nasopharyngeal carcinoma. *Cancer Research, 73*(16), 5151-5162.

Zhu, S., Wu, H., Wu, F., Nie, D., Sheng, S., & Mo, Y. Y. (2008). MicroRNA-21 targets tumor suppressor genes in invasion and metastasis. *Cell Research, 18*(3), 350-359.

Zhu, W., Shan, X., Wang, T., Shu, Y., & Liu, P. (2010). MiR-181b modulates multidrug resistance by targeting BCL2 in human cancer cell lines. *International Journal of Cancer, 127*(11), 2520-2529.

Zhu, W., Xu, H., Zhu, D., Zhi, H., Wang, T., Wang, J., … Liu, P. (2012a). MiR-200bc/429 cluster modulates multidrug resistance of human cancer cell lines by targeting BCL2 and XIAP. *Cancer Chemotherapy and Pharmacology, 69*(3), 723-731.

Zhu, W., Zhu, D., Lu, S., Wang, T., Wang, J., Jiang, B., … Liu, P. (2012b). MiR-497 modulates multidrug resistance of human cancer cell lines by targeting BCL2. *Medical Oncology, 29*(1), 384-391.

Zhuang, Z. L., Tian, F. M., & Sun, C. L. (2016). Downregulation of miR-361-5p associates with aggressive clinicopathological features and unfavorable prognosis in non-small cell lung cancer. *European Review for Medical and Pharmacological Sciences, 20*(24), 5132-5136.

Zou, H., Li, Y., Liu, X. & Wang, X. (1999). An APAF-1.cytochrome c multimeric complex is a functional apoptosome that activates procaspase-9. *Journal of Biological Chemistry, 274*(17), 11549-11556.

LIST OF PUBLICATIONS AND PAPERS PRESENTED

PUBLICATIONS

1. Othman, N., In, L. L. A., Harikrishna, J. A., & Hasima N. (2013). *Bcl-xL* Silencing Induces Alterations in hsa-miR-608 Expression and Subsequent Cell Death in A549 and SKLU1 Human Lung Adenocarcinoma Cells. *PLoS One, 8*(12), e81735.

2. Othman, N. & Hasima, N. (2014). The Role of microRNAs in the Regulation of Apoptosis in Lung Cancer and Its Application in Cancer Treatment. *Biomed Research International*, *2014*(2014), 318030.

3. Othman, N. & Hasima, N. (2017). miR-608 regulates apoptosis in human lung adenocarcinoma via regulation of *AKT2*. *International Journal of Oncology*. (ACCEPTED)

CONFERENCE PROCEEDINGS

1. Othman N. & Hasima N. (2013). Bcl-xL silencing induces alterations in hsa-miR-608 expression and subsequent cell death in A549 and SK-LU1 human lung adenocarcinoma cells. 1st National Conference for Cancer Research in Conjunction with 5th Regional Conference in Molecular Medicine (RCMM). Kuala Lumpur, Malaysia. (Poster – 2nd Prize Poster Award in Cancer)
2. Othman N. & Hasima N. (2014). Up-regulation of hsa-miR-608 expression, in response to Bcl-xL silencing, increases cell death in A549 and SK-LU1 human lung adenocarcinoma cells. 21st MSMBB Annual Scientific Meeting. Kuala Lumpur, Malaysia. (Poster)
3. Othman N. & Hasima N. (2015). Up-regulation of hsa-miR-608 expression, in response to Bcl-xL silencing, increases cell death in A549 and SK-LU1 human lung adenocarcinoma cell. Golden Helix Symposia 2015: Next Generation Pharmacogenomics. Kuala Lumpur, Malaysia. (Poster)